Durham E-Theses

Overpressure and Lateral Drainage in the Palaeogene Strata of the Central North Sea

JENNA ROBERTSON

How to cite:

ROBERTSON, JENNA (2013) *Overpressure and Lateral Drainage in the Palaeogene Strata of the Central North Sea.* Doctoral thesis, Durham University.

Overpressure and Lateral Drainage in the Palaeogene Strata of the Central North Sea

By Jenna Robertson

Department of Earth Sciences

Durham University

September 2013

This thesis was submitted to the University of Durham in partial fulfilment of the requirements for the degree of Doctor of Philosophy

ABSTRACT

Knowledge of subsurface pressures within the Palaeogene strata of the Central North Sea is an important aspect of the petroleum geology of the basin, enabling a better understanding of migration pathways, the potential for hydrodynamic trapping with tilted fluid contacts, and better assurance that drilling is carried out both safely and efficiently.

In this thesis, Palaeogene pressure data collected from over 300 offshore wells in the UK, Norwegian and Danish sectors of the North Sea are analysed. Regional overpressure distributions within individual Palaeocene and Eocene sandstone members are mapped across the Central North Sea, and lateral fluid flow pathways are interpreted within each individual sandstone member. Drainage within the older Maureen, Mey and Forties sandstone members is found to be predominantly south-east to north-west, with additional westwards drainage observed within the Mey and Forties sands, where smaller lateral fans fed into the basin from the Western Platform. Overpressure distributions within the Cromarty and Tay sandstone members indicate drainage westwards, where fluids probably escape through shelfal sandstones of the Mousa and Dornoch formations.

Locations of vertical drainage pathways between sandstone members were interpreted using local anomalies in the overpressure distributions and shared hydrocarbon accumulations, with vertical fluid flow found to be facilitated most commonly via areas of direct contact between sands, salt diapir structures, remobilised sands, and non-sealing graben-bounding faults. Areas with the greatest potential of hydrodynamic trapping were identified, although more accurate assessment of the prospectivity of such areas is required on a local scale.

Attempts at establishing the source of fluids entering into the Palaeogene system were made using 1D and 3D basin modelling. The results indicate a larger influx of fluid derived from the underlying pre-Cretaceous strata than from the overlying Tertiary mudrocks. These results, however, provide little quantification, and there is considerable scope for further work on 3D basin modelling.

Overpressure and Lateral Drainage in the Palaeogene Strata of the Central North Sea

By Jenna Robertson

Department of Earth Sciences

Durham University

September 2013

This thesis was submitted to the University of Durham in partial fulfilment
of the requirements for the degree of Doctor of Philosophy

CONTENTS

LIST OF FIGURES

and those supplied to the study by Ternan Ltd (2010), based on analysis of well data available within the study region. The Siri Sandstone is situated in the Norwegian and Danish sectors.

from 3D seismic data at Maersk Oil UK Ltd Aberdeen.

representative overpressure of 30 psi. Composite log confirms that the measurement was recorded in a water column. Although IHS quality of the data point is 'unknown' the composite log does not indicate there is anything wrong with the test. Since the overpressure value calculated appears to fit well with surrounding (higher category) values for the Forties reservoir, this overpressure value was deemed suitable to contour the overpressure distribution for the Forties Sandstone Member.

not shown. Hydrocarbon fields reservoired in the Mey and Heimdal sandstone members are shown in outline.

Tay sands are situated on average ~260 ft (80 m) above the top Balder, although areas of direct contact exist locally. The purple dashed line is the line of section for **Figure 5.24**.

Values of overpressure differences (in psi) are also shown.

Wood (2011).

purposes. Direct pore pressure measurements recorded within the Jurassic Fulmar Sandstone Member of the modelled well are not shown in the figure due to scale; however, overpressures of approximately 5915 psi (40.8 MPa) were calculated between depths of 14946 ft (4560 m) and 15077 ft (4600 m) TVDSS.

LIST OF TABLES

LIST OF ABBREVIATIONS

atm: atmosphere

psi: pounds per square inch (lb/in^2)

psi ft $^{-1}$: pounds per square inch per foot

psia: pounds per square inch absolute

psig: pounds per square inch gauge

MPa: megapascal

MPa m $^{-1}$: megapascals per metre

kPa: kilopascal

kPa m $^{-1}$: kilopascals per metre

GOC: gas-oil contact

GWC: gas-water contact

OWC: oil-water contact

FWL: free-water level

ODT: oil down to

WUT: water up to

TVDSS: true vertical depth sub sea

LWD: Logging while drilling

MWD: Measuring while drilling

mD: millidarcy

nD: nanodarcy

USEFUL CONVERSIONS

Length

SI unit = metres (m)

1 m = 3.2808 ft

1 ft = 0.3048 m

Pressure

SI unit = Pascal (Pa) or Newton per square metre (N m^{-2})

1 Pa = 1 N m^{-2}	1 MPa = 145.03774 psi	1 psi = 0.0681 atm
1 Pa = 1 x 10^{-6} MPa	1 psi = 6894.757 Pa	1 psi = 0.070306 kg cm^{-2}
1 MPa = 1000 kPa	1 psi = 0.0689475 bar	1 atm = 101325 Pa

Pressure gradients

1.0 psi ft^{-1} = 22.621 MPa km^{-1}	1.0 psi ft^{-1} = 19.25 ppg	1 g/cc = 8.3454 ppg
1.0 psi ft^{-1} = 0.226206 bar m^{-1}	1.0 psi ft^{-1} = 2.30666 g/cc	

Typical water gradients

Fresh water pressure gradient	0.434 psi ft^{-1} or 8.345 ppg or 1.0 g/cc
Saturated brine pressure gradient	0.519 psi ft^{-1} or 9.991 ppg or 1.2 g/cc
CNS average regional water gradient	0.445 psi ft^{-1} or 8.566 ppg or 1.03 g/cc

Typical hydrocarbon gradients

(Gradients are given at surface conditions)

< 10° API gravity oil	< 0.433 psi ft$^{`}$ or < 8.34 ppg or < 0.99 g/cc
20° API gravity oil	0.404 psi ft^{-1} or 7.778 ppg or 0.93 g/cc
40° API gravity oil	0.357 psi ft^{-1} or 6.872 ppg or 0.82 g/cc
60° API gravity oil	0.320 psi ft^{-1} or 6.160 ppg or 0.74 g/cc

DECLARATION

The content of this thesis is the original work of the author and is not based on joint research (other people's work, where included, is acknowledged by reference). The materials contained within have not been previously submitted for a degree at this or any other university.

Jenna Robertson

Durham

September 2013

Copyright

ACKNOWLEDGEMENTS

Well I finally made it... the work has been done and the thesis is written. I hope you enjoy the read and that you learn something useful along the way. Bear in mind when you read this research that several people have contributed in some way to its completion.

Firstly I would like to thank my supervisor Neil Goulty, who has always been there to provide guidance, encouragement and support throughout the project. I have learnt so much from you over these past years and I am extremely grateful for your patience, as well as your corrections, edits and feedback. It has been a pleasure working with you Neil.

Huge thanks must be given to everyone in the Exploration and New Business team at Maersk Oil UK, based in Aberdeen. In addition to providing funding to this project, you are all amazing people. I'd like to thank all of my friends there especially Gareth Yardley for all of his help and assistance. You rescued me from despair Gareth many a time and greatly aided my understanding to the basin modelling work. To Neville Brookes, John Colleran, Matt Farris and Ben Frizzell who were always willing to help. Time that I spent in Aberdeen working at Maersk away from home, passed so much faster when you were around to make me laugh. My one desire is that this work proves useful to you all over time. Nothing would make me happier than to see Gareth reaching for my PhD thesis off his bookshelf!

Thanks must be given to my secondary supervisor Richard Swarbrick, along with the IkonGeopressure team; Phil, Sam, Alex, Dave, Ed, Patricia and Janie. Special thanks to Ikon Science and the UK Government Department of Energy and Climate Change who also provided funding to the research.

During the earlier stages of the project, Binh you provided much needed help and also to everyone at Temis, the trip to Paris was amazing. Additionally, Ternan Ltd must be thanked for supplying play distribution maps for the Palaeocene strata of the Central North Sea basin, IHS for supplying the vast amounts of well data to the study (Mark Diaz, you were a great help at times) and the guys at EnCore Oil, thanks for letting me visit your offices. Furthermore, Maggie Evans at Ikon Science, thank you for providing me with the numerous RokDoc software licences over the years.

To Sharon and Gary Robertson

1 | Introduction

"The journey of a thousand miles begins with one step"

Lao Tzu (604 BC-531 BC) [Chinese philosopher]

1. Introduction

The research presented within this thesis provides an in depth examination of the regional present-day overpressure distributions within the Palaeogene strata of the Central North Sea Basin. Using pressure data collected from a total of 286 wells, overpressure distributions are mapped for each Palaeogene sandstone member. Lateral and vertical fluid flow pathways are analysed, using these mapped overpressure distributions, and likely migration routes for hydrocarbons are determined.

1.1. Rationale

Knowledge of subsurface pressures is fundamental to petroleum geology and can have major significance during stages of exploration, drilling, appraisal and production (Lindberg *et al.*, 1980). Detection and evaluation of abnormal subsurface pressures is necessary to ensure that drilling is carried out both safely and efficiently (Ecclestone-Brown, 2002). If subsurface pressures are not fully understood at the time of drilling, they can result in unnecessary mud losses or blow-outs, both of which can prove costly and in the case of blow-outs can endanger people's lives.

From an exploration viewpoint, the increased understanding of present-day pressure variations on a regional scale is of growing importance (Law and Spencer, 1998). Such work can assist with the search for petroleum by highlighting directions of fluid flow and possible migration pathways, as well as providing a more accurate indication of basin hydrodynamics and potential areas of hydrodynamic trapping (O'Connor *et al.*, 2008). Hydrodynamic trapping can result in tilted hydrocarbon-water contacts which may act to increase or reduce the estimated hydrocarbon in place and potentially cause hydrocarbon accumulations to move off structure. Consequently, a full understanding of aquifer fluid flow is necessary to ensure that accurate reserve estimates can be made, in addition to the accurate planning and placement of wells.

1.1.1. Why the Palaeogene strata?

Emphasis is placed largely on the Palaeogene petroleum system of the Central North Sea, primarily since the majority of pressure data made available to the study were recorded within the Palaeogene reservoir members, but equally since the Palaeogene system forms a major exploration target that continues to be of great economic importance today. Reservoirs of Palaeogene age have produced significant amounts of hydrocarbons in the Central North Sea since the late 1960s (Den Hartog Jager *et al.*, 1993; Ahmadi *et* al., 2003). The Palaeogene system accounts for approximately 14% of all North Sea Basin total discovered reserves, making it the third most economically successful petroleum play after the Lower/ Middle Jurassic and Upper Jurassic systems.

Understanding migration pathways within the Palaeogene strata has never been more important than at the present, with the recent discoveries of light oil along the western margins of the basin in UK block 28/9. It was once assumed that the hydrocarbon deposits in this area of the basin would be heavily biodegraded as was found to be the case further northwards in the Elke (UK 28/03), Narwhal (UK 28/02) and Pilot (UK 21/27) fields, owing to the shallow depth of reservoir burial, lower temperature and potential influx of fresher waters. However, the discoveries of Catcher (in 2010), hailed as one of the biggest oil finds in the North Sea since the Buzzard discovery over 12 years ago, Varadero (in 2011) and Burgman (in 2012) are of higher quality, lower API oil, showing signs of only low to moderate biodegradation. The better quality oil within UK 28/9 may indicate shorter migration pathways from the source rock to this area of the basin and more recent migration, highlighting the need to better understand regional migration pathways and consequently pressure variations within and between the Palaeogene sand units.

1.2. Study region

The study region covers the vast majority of the Central North Sea Basin, encapsulating the entire Central Graben, Witch Ground Graben and Fisher Bank Basin areas of the Outer Moray Firth (**Figure 1.1**). The region covers an area of approximately 55,000 km^2 lying between latitudes 55° 20'N to 58° 20'N and extending west to east between longitudes of 0° to 5°E.
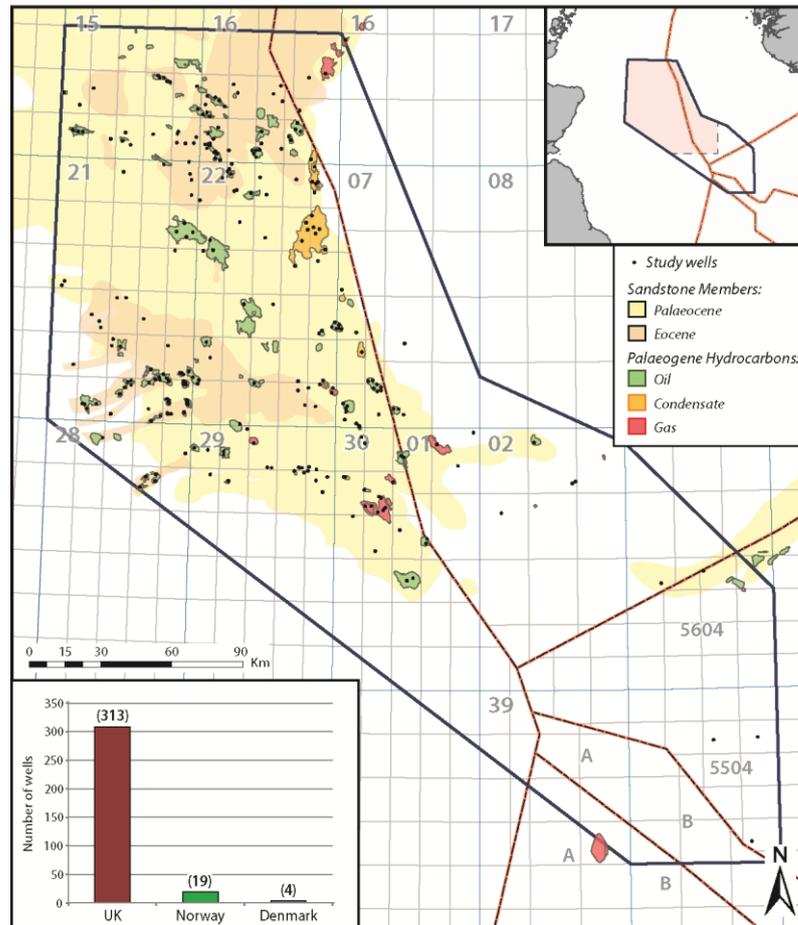
Figure 1.1 - The Central North Sea study region used throughout this research. The vast majority of the data have been collected from the UK sectors, where the reservoir sandstone members are located (adapted from Ahmadi *et* al., 2003).

Pressure data were collected from a total of 327 wells sampling the Palaeogene and Neogene successions of this region, anywhere from the sea bed down to the top of the Ekofisk Formation. Due to the lack of sampling which is carried out at shallow depths in the hydrocarbon industry, a total of only six pressure points could be used to represent the Neogene and consequently the main focus of this study is the Palaeogene strata, excluding the Ekofisk Chalk. Although the study region encapsulates the Norwegian and Danish sectors of the North Sea, it can be seen that the vast majority of well data falls within the UK sector only, corresponding largely with the occurrence of the Palaeogene reservoir sandstone members. Consequently, it may be seen throughout the thesis that the large majority of analysis and discussion regards the UK sector and Norwegian quadrants directly east of the median line.

1.3. Objectives

The objectives of this research are:-

1) Determine lateral drainage and migration pathways within the Palaeogene strata.

2) Determine vertical drainage and migration pathways within the Palaeogene strata; understanding which features are most likely to facilitate fluid flow, i.e. salt diapirs, faults, areas of sandstone connectivity.

3) Locate areas of the basin with the potential for hydrodynamic trapping.

4) Assess the relative contributions from Tertiary and Mesozoic strata into the presently draining Palaeocene sands.

In fulfilling the above objectives, the overall aim is to gain a regional understanding of overpressure and fluid flow within the Palaeogene system of the Central North Sea. Working on a regional scale is important since a better understanding of the source of draining fluids passing through the Palaeogene system can be achieved.

A greater understanding of the Central North Sea Palaeogene pressure system will enable better comparisons to be made with other abnormally pressured systems globally. Overpressure is a worldwide occurrence having been recorded in almost every geological environment and in strata of all ages (Mouchet and Mitchell, 1989; Swarbrick and Osborne, 1998). Improved understanding of lateral drainage and its effects on the pressure distribution within the Palaeogene strata of the Central North Sea may assist with a better understanding of other actively draining basins which have significant hydrocarbon potential, such as the South Caspian Sea (Bredhoeft *et al.*, 1988), the Mahakam Delta, Indonesia (Grosjean *et al.*, 1994; Ramdhan, 2010), Beaufort Basin, Canada (Magara, 1978), and the Plio-Pleistocene strata of the US Gulf of Mexico (Schmidt, 1973).

1.4. Thesis synopsis

In this first chapter, the main research problems are discussed and the objectives of this thesis are stated. The importance of this research with regards to petroleum exploration is also briefly highlighted.

In Chapter 2, the geology and petroleum system of the Central North Sea are described with main emphasis on the Palaeogene strata. The bulk of Chapter 2 is based on previously published data, although the regional distribution maps presented for each individual Palaeogene reservoir have been generated as part of the present study.

The theoretical background and basic concepts of overpressure and fluid flow are described in Chapter 3, followed by a discussion specific to the Central North Sea; detailing current understanding of the main overpressure generating mechanisms and of the overpressure distribution, both vertically and laterally.

The methodologies which were used to build a regional pressure database for the Central North Sea are discussed in Chapter 4, along with the methodologies used to generate regional overpressure distribution maps for each Palaeogene sandstone member.

In Chapter 5, the regional overpressure distribution maps for each individual Palaeogene sandstone member are presented and lateral fluid flow pathways are interpreted. Areas of vertical drainage are interpreted from local anomalies observed within the overpressure distributions, good hydraulic connectivity being indicated where equal overpressures are encountered within different sandstone members and where water gradients are shared between units. Areas with the potential for hydrodynamic trapping are also identified within this chapter and the level of tilt experienced at hydrocarbon-water contacts is calculated. The content of Chapter 5 regarding the Forties, Cromarty and Tay sandstone members was accepted for publication in Petroleum Geoscience (Robertson *et al.*, 2013).

Chapter 6 examines fifteen direct pore pressure measurements that are thought to reflect pressures attained within the lower permeability muds which surround the Palaeogene sandstone members. Such values are typically recorded within thin isolated bodies of sand encased by mudstone. Analysis of these values provides insight into the magnitudes of overpressure which may be reached within the muds and further aids

understanding of the pressure profile through the muds and fluid drainage out from the muds into nearby Palaeogene fan sands.

In Chapter 7, attempts are made to establish the source of fluids entering the Palaeogene system, i.e. whether the fluids which feed the laterally draining Palaeogene system are sourced predominantly from above or below. Generation of a 1D basin model for UK well 30/11b-3 is documented and the results analysed. Wireline log data for UK well 30/11b-3 are used to estimate present-day porosity down hole, and a brief description of the various methods used to derive porosity is provided. An early attempt at producing a simple 3D basin model is documented towards the end of Chapter 7, leading onto a discussion of the modelled results and the limitations of the model produced.

In Chapter 8 conclusions drawn from the preceding chapters of the thesis are summarized and areas of possible future research are identified and discussed.

2 | The Central North Sea

"There is no great writing, only great rewriting" Louis Brandeis (1856-1941) [American Associate Justice of the Supreme Court]

2. The Central North Sea

The geological history, stratigraphy, basin structure and petroleum system of the Central North Sea are all discussed within this chapter. Emphasis is placed largely on the Palaeogene strata since they form the main focus of the pressure research.

2.1. Geological history

The North Sea Basin has a complex tectono-sedimentary history which has profoundly influenced its development into the prolific hydrocarbon province it is today. The failed rift system comprises three branches: the Viking Graben, the Inner and Outer Moray Firth, and the Central North Sea Trough (Erratt *et al*., 1999). The Central Graben forms the NW-SE trending branch of this system (**Figure 2.1**).

The onset of extension and rifting across the basin is thought to have commenced during the Triassic, with multiple phases of extension occurring from the Triassic until the Early Cretaceous (Fisher and Mudge, 1990; Bartholomew *et al*., 1993; Cornford, 1994; Erratt *et al*., 1999). The most widespread of these extensional phases is thought to have occurred during the Late Jurassic (Fraser *et al*., 2002). Fault control of sedimentation was important throughout syn-rift deposition and resulted in the development of several fault bounded sub-basins (Erratt *et al*., 1999), most notably the West Central Graben and the East Central Graben.

During the Late Jurassic, sea level rise marked the onset of marine sedimentation across the basin (Holm, 1998) which has persisted until the present day. Following the failed rifting events of the Jurassic period, the Central North Sea basin was in a state of thermal sag. Despite the vast quantities of chalk that had been deposited throughout the Cretaceous and early Palaeocene (Danian stage), the basin remained effectively sediment-starved with rates of thermal and load-induced subsidence surpassing rates of deposition. By the end of the Palaeogene, however, the basin had filled significantly, with more than 1.5 km of Palaeogene sediments being deposited in the centre of the basin.
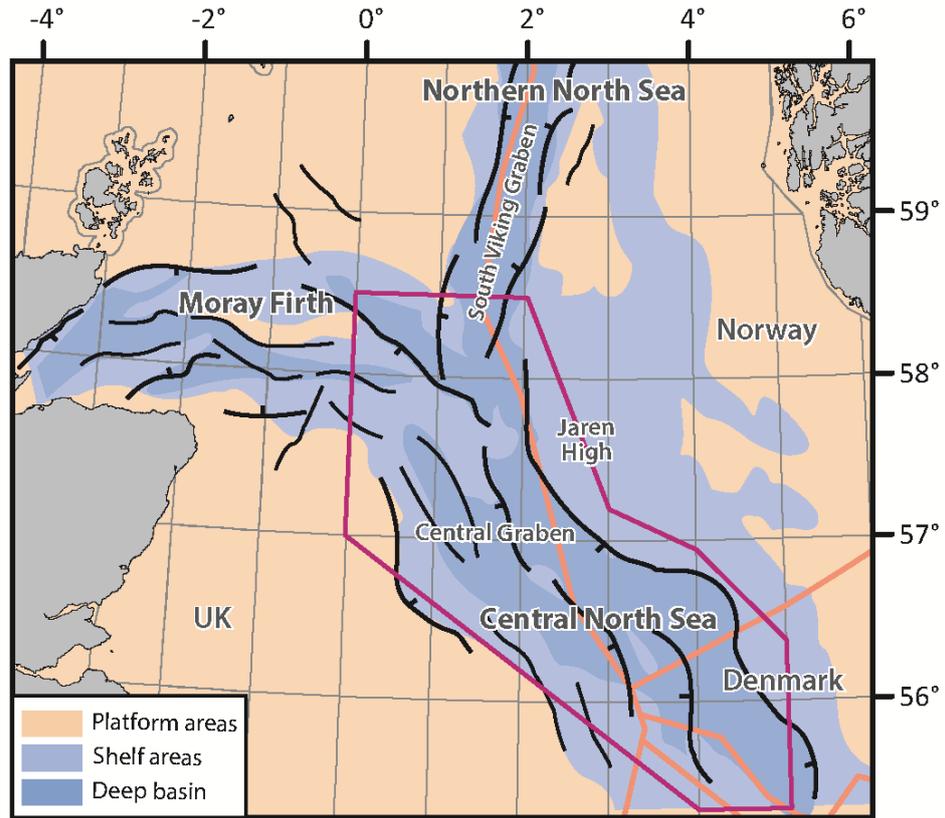
Figure 2.1 - Map showing the principal structure of the North Sea Rift Basin. The study area is outlined in magenta. Modified from Koša (2007).

2.1.1. Late Cretaceous - Present day

The Palaeogene period of the Central North Sea region is characterized by high sediment influx, rapid basin subsidence, and extensive salt movement. At the start of the Palaeocene epoch, sedimentation within the Central North Sea remained similar to that in the Late Cretaceous (Anderton, 2000; Surlyk *et al.*, 2003), with deposition of thick Danian chalks and marls (forming the Ekofisk Formation) continuing to slowly infill and drape the deep water troughs within the Central Graben. It was not until the end of the Danian (early Palaeocene) that deposition of these vast thicknesses of chalks and marls was brought to a close.

Development of a thermal plume situated beneath eastern Greenland, northern Britain and western Norway (Anderton, 1993) marked the beginning of NE Atlantic opening and resulted in large-scale thermal uplift and periodic south-easterly tilting of the northern British Isles (Den Hartog Jager *et al.*, 1993; Mudge and Bujak, 1996*a*;

10

Ahmadi *et al.*, 2003). Onset of uplift is thought to have occurred during the Danian (Ahmadi *et al.*, 2003), or even as early as the Campanian (80 Ma) (Den Hartog Jager *et al.*, 1993), with maximum uplift reaching its peak during the mid-Thanetian (Late Palaeocene) (Anderton, 1993, 2000; Ahmadi *et al.*, 2003).

Erosion of the newly exposed landmass, along with contemporaneous eustatic sea-level fall (Den Hartog Jager *et al.*, 1993; Anderton, 2000), led to regular influx of siliciclastic material into the basin, building outwards towards the Outer Moray Firth as a sequence of delta fronts (Gatliff *et al.*, 1994). Increased sediment loading, along with high rates of thermally induced basin subsidence, eventually led to instability of the delta front and consequent slope failure, with mass transport of clastic turbidites south-eastwards into the deeper parts of the basin (Ahmadi *et al.*, 2003). Intermittent delivery of coarse siliciclastics into the basin throughout the remainder of the Palaeocene and Eocene epochs resulted in a series of deep marine sandstone units which progressively thin south-eastwards, away from the Scotland–Shetland land mass, becoming increasingly buried and encased by pelagic muds. As Mudge and Bujak (1996*a*) emphasized, this thinning suggests there was little sediment input derived from the Norwegian land mass during the Palaeocene, since it had experienced less uplift than the British Isles (Ahmadi *et al.*, 2003).

Distribution of the earliest fan members, the Maureen and Mey sandstones, was largely influenced by the seafloor bathymetry, which in turn was largely reflective of the relict topography of the underlying Mesozoic graben (Mudge and Copestake 1992*a*; Kilhams *et al.*, 2012), with thick sands accumulating along pre-existing structural depocentres and remaining thin or absent above positive structures such as the Halibut Horst, J-Ridge and Forties–Montrose High (Mudge and Bujak, 1996*a*). The oldest of these fan units, the Maureen, comprises a mix of sand, reworked chalk and marls, indicating erosion and re-deposition of the underlying Cretaceous carbonates during the earliest stages of uplift of the Scotland-Shetland landmass. Similarly, the largest of the fan units, the Mey Sandstone Member belonging to the Lista Formation, represents the period of greatest clastic input into the basin (Liu and Galloway, 1997), corresponding largely with the time of maximum source uplift (Anderton, 1993; Ahmadi *et al.*, 2003). By late Thanetian times, the relict graben topography had become largely infilled and the basin had considerably shallowed (Anderton 1993), allowing subsequent deposits of the Forties and Cromarty sandstone members to be laid down on a more gentle, easterly

11

dipping slope (Mudge and Copestake, 1992*a*). Such changes in sedimentation pattern enabled deltas to prograde seawards into the basin (Anderton, 1993), introducing the shelfal sands of the Dornoch and Mousa formations into the region.

Continental rupture and initiation of sea floor spreading in the NE Atlantic took place around 55-54 Ma, close to the Palaeocene–Eocene boundary (Knox and Morton, 1988; Anderton, 2000; Ahmadi *et al.*, 2003), and is marked by the extensive ash deposits of the Balder Formation. Rupture signified the re-establishment of post-rift thermal subsidence (Nadin and Kusznir, 1995) across the basin, along with diminishing clastic input from the once uplifted landmasses to the north-west (Liu and Galloway, 1997). Throughout the Eocene epoch, sedimentation patterns changed greatly from the large stacked submarine fan deposits of the Palaeocene to thick prograding delta fronts, such as those represented by the Dornoch and Mousa formations, with small fans restricted to the basin margins (Jones *et al.*, 2003). Such fan units are encased by the thick hemipelagic sediments of the Horda Formation and form important hydrocarbon exploration targets today, i.e. the Tay and Grid sandstone members. The remainder of the Palaeogene sequence is largely mud-prone (Liu and Galloway, 1997; Jones *et al.*, 2003).

Up to 3000 m of sediment have been deposited into the Central North Sea region over the past 34 Ma (Oligocene–Recent) (Fyfe *et al.*, 2003), with burial rates for the past 3 Ma (Pliocene–Recent) estimated at ~ 500 m Ma^{-1} (Swarbrick *et al.*, 2000). Tectonic uplift of Scandinavian source terrain (Liu and Galloway, 1997) meant that directions of sediment supply changed to include the north and east, while supply from the East Shetland Platform to the west was much reduced (Jordt *et al.*, 1995). Rapid sedimentation and load-induced subsidence continued throughout the Oligocene to the present day, and consequently the basin has developed into the overall form of a shallow saucer-shaped depression (Anderton, 2000).

Extensive movement of Permian-aged salt was initiated during Triassic times and is thought to have continued through to the middle Miocene (Davison *et al.*, 2000). Structures associated with salt diapirs host some of the largest hydrocarbon accumulations across the region, with numerous styles of salt-related trap, including salt-induced anticlines, as seen in the Andrew, Mungo and Maureen fields, and salt

abutment traps, as seen in the Banff and Pierce fields (Davison *et al.*, 2000; Ahmadi *et al.*, 2003).

2.2. Stratigraphy

A typical stratigraphic column for the Central North Sea is shown in **Figure 2.2**. In general, the stratigraphic system can be separated into pre-, syn- and post- rift sections (Holm, 1998), although there is still some dispute regarding the timing of rift onset. The pre-rift section comprises largely pre-Jurassic sediments and contains notable reservoir units such as the Triassic Skagerrak Formation and the Devonian Old Red Sandstone. The thick Zechstein evaporite sequence of Late Permian age forms an important interval, since halokinesis has affected deposition of many younger sediments. Within the syn-rift section, the shallow marine Fulmar and Piper sandstone formations of Late Jurassic age form major hydrocarbon reservoirs. The Heather Formation and Kimmeridge Clay Formation, also deposited during the Late Jurassic syn-rift phase, are of critical importance to the petroleum system of the region because they have acted as source rocks for all known hydrocarbon accumulations in the Central North Sea. The post-rift section comprises numerous important reservoir intervals in addition to important sealing lithologies such as the thick Chalk sequence and the Tertiary shales. Glennie (1990) and Evans *et al*. (2003) provide a more detailed review of the entire North Sea stratigraphy. Only the Palaeogene stratigraphy of the Central North Sea is discussed in detail within this thesis.

2.2.1. Palaeogene lithostratigraphy

The Palaeogene lithostratigraphic nomenclature scheme used throughout this thesis is that of Knox and Holloway (1992). This is the most recently published scheme for the Central North Sea. Sand formations originally proposed by Deegan and Scull (1977) are relegated to member status within time-equivalent, shale-dominated formations, i.e. each major submarine fan unit is given member status within its corresponding (encasing) basinal shale formation (**Figure 2.3**). The Palaeocene and Eocene successions are represented by the Montrose, Moray and Stronsay groups together with
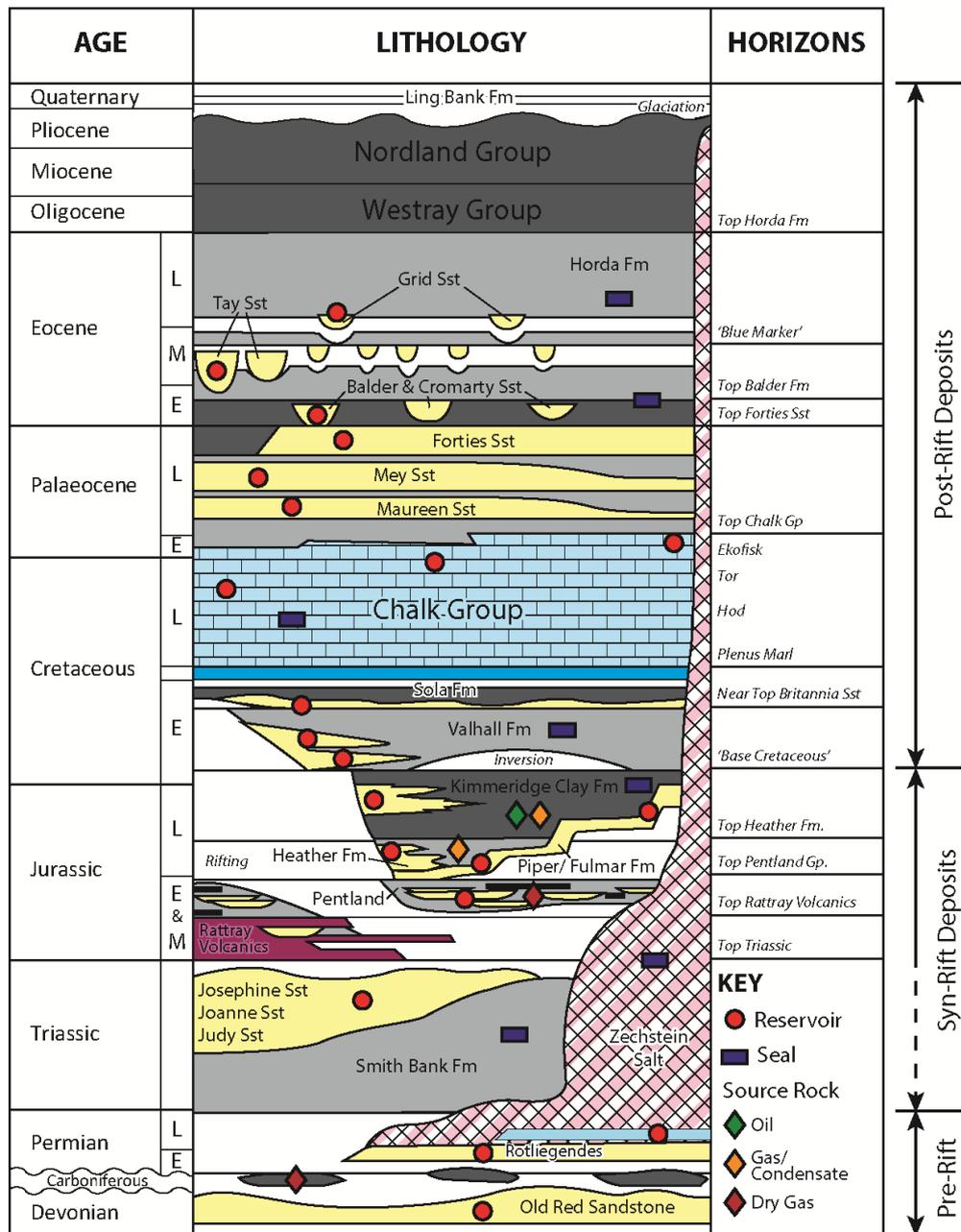
Figure 2.2 - Generalised Central North Sea stratigraphic column showing basin development, common reservoir, seal and source rocks, useful stratigraphic/seismic horizons and the typical stratigraphic section (modified from Brookes, 2012).

the uppermost part of the Lower Palaeocene Ekofisk Chalk Formation. As is common practice in the hydrocarbon industry, the base of the Palaeogene succession is taken to lie at the top of the Ekofisk Formation (mid-late Danian age) (Ahmadi *et al.*, 2003); consequently, the Ekofisk Formation and underlying older formations are not described in detail within this thesis. For a detailed lithological description of the entire Central North Sea stratigraphy, readers are referred to Evans *et al.* (2003). A brief description of

14
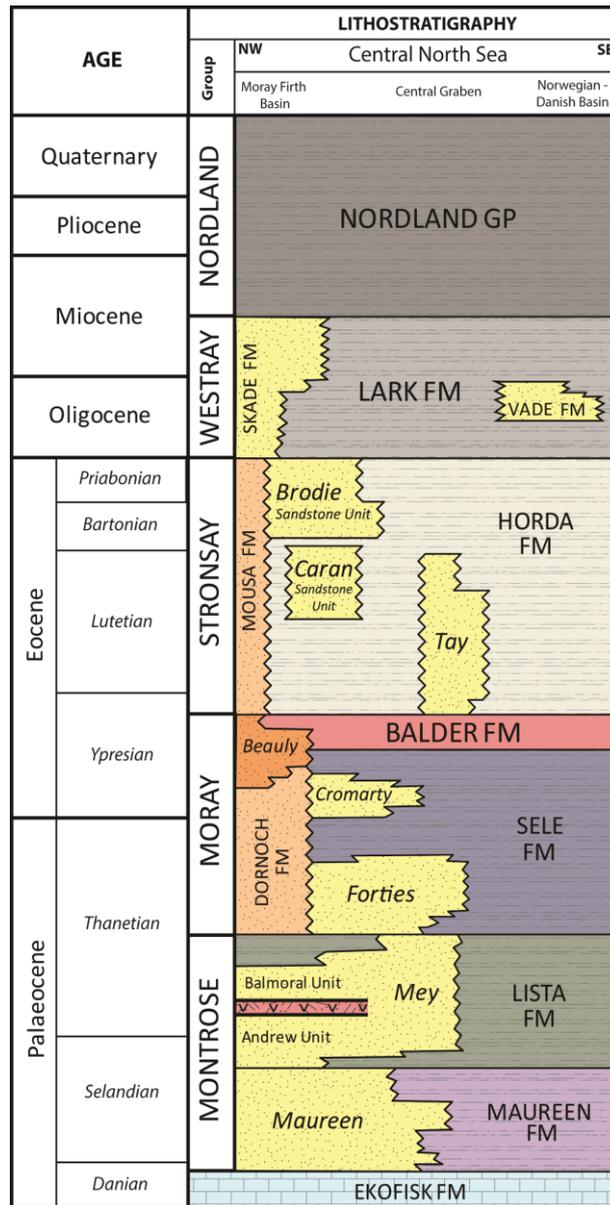
Figure 2.3 - Stratigraphic column showing the lithostratigraphic nomenclature of Knox & Holloway (1992). Each major submarine fan is given member status within the encasing age-equivalent basinal mudrock formation. Main area of interest in this study comprises the Montrose, Moray and Stronsay Groups. Note how the Mey Sandstone Member (belonging to the Montrose Group) comprises the Andrew and Balmoral sandstone units separated by the Balmoral Tuffite Unit. Similarly, the Caran Sandstone Unit and Brodie Sandstone Unit, belonging to the Stronsay Group, form the Grid Sandstone Member (not labelled on the column).

the Palaeogene stratigraphy is provided here, although for a more detailed description readers are referred to the work of Knox and Holloway (1992), Ahmadi *et al*. (2003) and Jones *et al*. (2003).

2.2.1.1. Montrose Group

The Montrose Group of Knox and Holloway (1992) lies between the Chalk and Moray groups and contains the Maureen and Lista formations, which comprise the Maureen Sandstone Member and the Mey/Heimdal Sandstone members, respectively (**Figure 2.3**). The group is present across the entire Central North Sea region, reaching a thickness in excess of 600 m (Knox and Holloway, 1992).

2.2.1.2. Moray Group

The Moray Group comprises the Sele, Dornoch and Balder formations of Knox and Holloway (1992), and is situated between the Palaeocene Montrose Group and the Eocene Stronsay Group (**Figure 2.3**). Sediments of both Palaeocene and early Eocene age are contained within the Moray Group. The group marks a change in depositional environment from the underlying Montrose Group (Mudge and Copestake, 1992*a*), with the introduction of deltaic and shallow marine shelf deposits prograding eastwards into the Central North Sea study region. Knox and Holloway's (1992) naming system for the group classifies all 'deltaic and shelfal' deposits as belonging to the Dornoch Formation, whereas time-equivalent 'basinal' successions may be assigned to the Sele and Balder formations. Basinal sandstones belonging to the Forties and Cromarty sandstone members are encased within the Sele Formation mudstones. The top of the Moray Group is represented by the tuffaceous Balder Formation, which is regionally extensive across the North Sea Basin (Mudge and Copestake, 1992*a*). The Balder Formation forms a good seismic marker horizon, which is consequently often used to represent the top of the Palaeocene (Ahmadi *et al.*, 2003).

2.2.1.3. Stronsay Group

The Stronsay Group of Knox and Holloway (1992) comprises the Mousa and Horda formations and is situated between the underlying Moray Group and the overlying Oligocene Westray Group. Much like the Dornoch/Sele formation naming scheme of the older Moray Group, Knox and Holloway (1992) have divided the Stronsay Group into two formations, based on depositional facies of the sediments. The Mousa

Formation is of shelf facies, containing sands and silts, whilst the time-equivalent Horda Formation is of basinal facies, comprising muds with basinal sands belonging to the Tay and Grid sandstone members.

The Stronsay Group represents a considerable time span from early Eocene to the earliest Oligocene (Knox and Holloway, 1992), i.e. approximately 19 Ma. This is a great contrast to the combined Montrose and Moray groups whose age range is only about 9 Ma, from late Palaeocene to early Eocene. Overall, the group marks a clear change in basin dynamics following on from continental rupture in the North Atlantic, as marked by the Balder Formation at the top of the Moray Group.

2.2.1.4. *Westray and Nordland group sediments*

The remaining sediments of the Central North Sea, aged from early Oligocene to Recent, belong to the Westray and Nordland groups of Knox and Holloway (1992). These deposits are dominantly composed of thick basinal muds and form a broad asymmetric basin fill. The Westray Group comprises shelfal and basinal deposits belonging to the Skade and Lark formations, respectively, with distribution of the Skade Formation being restricted to the western margins of the basin around UK quadrants 14 and 20. The Lark Formation is more extensive across the area, reaching thicknesses of around 1000 m in deeper parts of the Central Graben (Knox and Holloway, 1992). The Nordland Group ranges in age from late mid-Miocene to Holocene and reaches thicknesses of approximately 1500 m in the Central Graben (Knox and Holloway, 1992). At least 500 m of these upper Nordland sediments were deposited over the last ~ 2.5 Ma (Pleistocene to Recent) (Fyfe *et al*., 2003), making a significant contribution to the burial history of underlying sediments in the basin.

2.2.2. *Palaeogene biostratigraphy*

There have been numerous biostratigraphic schemes published for the Palaeogene strata of the Central North Sea which utilize bioevents taken from a range of microfossils (King, 1989; Gradstein *et al*., 1992; Powell, 1992; Mudge and Copestake, 1992*a*; Schröder, 1992; Mudge and Bujak, 1996*a*, *b*; Bujak and Mudge 1994; Joy, 1996). One

17

of the most commonly used zonation schemes for the Central North Sea is that of Bujak and Mudge (1994) and Mudge and Bujak (1996*a, b*), who distinguish 14 zones and 34 subzones of dinocyst within the Palaeocene and Eocene strata of the North Sea. Another commonly used scheme is that of Mudge and Copestake (1992*a, b*), who identified a number of bioevents for the Palaeogene strata using a variety of microfaunal assemblages (foraminifera, dinocyst and radiolarian species). In industry, a particularly common scheme is the PT zonation scheme developed by Shell UK Exploration and Production (Schröder, 1992). Under this scheme, the Palaeocene strata are composed of three zones (PT13, PT15 and PT19) and the Eocene of up to six zones (PT20, PT21, PT22, PT23, PT24, PT27/29). The term PT appropriately stands for 'Palynology/Palaeontology in the Tertiary,' since the biostratigraphic zones which make up the scheme are assessed jointly through a combination or microflora and microfauna.

2.3. Palaeogene reservoir members

A detailed description of each of the Palaeogene reservoir sandstones encountered within the study region is provided within this section. Emphasis is placed solely on reservoir intervals, since these form the intervals for which overpressure was mapped and shall be later discussed in **Chapter 5.**

2.3.1. Maureen Sandstone Member

The term 'Maureen Sandstone Member' is adopted throughout this thesis to describe any basinal submarine sandstone encountered within the Maureen Formation. A large proportion of the Maureen Formation in the Central North Sea is composed of sandstone, with Liu and Galloway (1997) stating that the formation has a 41% net sand volume, making it the most sand-prone depositional system in the Palaeocene (Ahmadi *et al*., 2003).

The distribution of the Maureen Sandstone Member within the study region is shown in **Figure 2.4**. It can be seen that the sandstone distribution crudely reflects the relict topography of the basin, with underlying faults influencing flow direction and deposition of the sands. Overall sandstone thickness decreases south-eastwards with
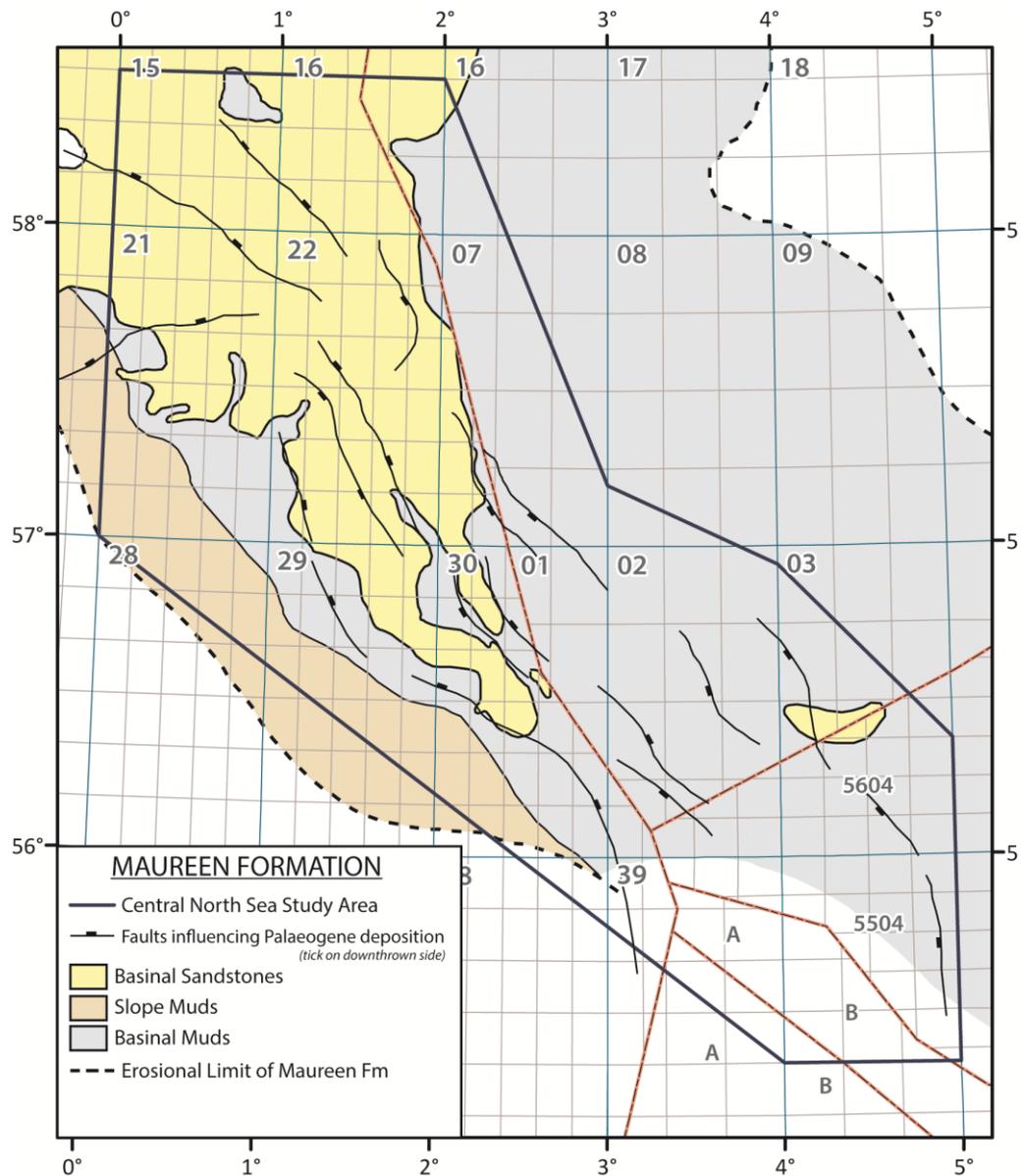
Figure 2.4 - Palaeogeographic map of early Palaeocene during deposition of the Maureen Formation, showing the distribution of the Maureen Sandstone Member along with faults which may have influenced Palaeogene deposition. Basinal sandstone distribution was determined from the analysis of well data. The remainder of map was generated using a combination of previously published maps presented in Ahmadi *et al.* (2003) and those supplied to the study by Ternan Ltd (2010).

decreasing flow from the sediment source. Maureen sands are thickest in north and north-eastern parts of the study region, reaching in excess of 200 m in UK quad 15 and 150 m in the north of UK quad 21. Sandstones are typically medium to fine-grained in this area and comprise thick, clean, poorly unconsolidated units interpreted as stacked,

19

channelized submarine fan deposits (Knox and Holloway, 1992). Towards the distal areas of the fan, in the east and southeast, sandstone thickness decrease to around 60 m in thickness. Numerous thinner sandstone units are more typical in these areas, often surrounded by a chalky matrix. Sands are commonly mixed with reworked limestones to produce varied lithologies which are difficult to identify on the basis on wireline signatures alone (Knox and Holloway, 1992). Thicker Maureen sands are found locally in distal areas. For example, in UK blocks 30/17 and 30/18 sands reach thicknesses greater than 90 m. Such areas of thicker sand are also thought to be related to the infilling of structural lows in the deeper parts of the basin. Sands are thinner above structural highs, such as Forties-Montrose High in UK quad 22.

2.3.2. *Mey Sandstone Member*

The Mey Sandstone Member of Knox and Holloway (1992) encompasses the Andrew, Glamis and Balmoral members of Mudge and Copestake (1992*a*). Where these members could be distinguished, they are referred to herein as the Andrew Sandstone Unit, Balmoral Tuffite Unit and Balmoral Sandstone Unit, respectively, in accordance with the Knox and Holloway (1992) naming scheme (**Figure 2.5**); otherwise pressures have been simply classified as belonging to the Mey Sandstone Member.

The Balmoral Tuffite Unit represents the first phase of Palaeogene pyroclastic sedimentation across the Central North Sea region, relating to the early stages of NE Atlantic opening (Knox and Morton, 1988; Den Hartog Jager *et al.*, 1993). Where the unit is present towards the northern limits of the study region, around UK quads 14, 15, 20 and 21, it forms a useful marker with which to distinguish between the underlying Andrew and overlying Balmoral sandstone units (**Figure 2.6**). Where the Balmoral Tuffite Unit is not present, it is much more difficult to distinguish between individual units of the Mey Sandstone Member, unless biostratigraphic data are available (Knox and Holloway, 1992). Distribution of the Andrew Sandstone Unit is generally confined to the Outer Moray Firth and northern Central Graben around UK quadrants 13, 14, 15 and northern parts of UK quadrants 20, 21 and 22, whereas the younger Balmoral Sandstone Unit is more extensive across the Central Graben and reaches as far south as UK quadrant 30 (Ahmadi *et al.*, 2003).
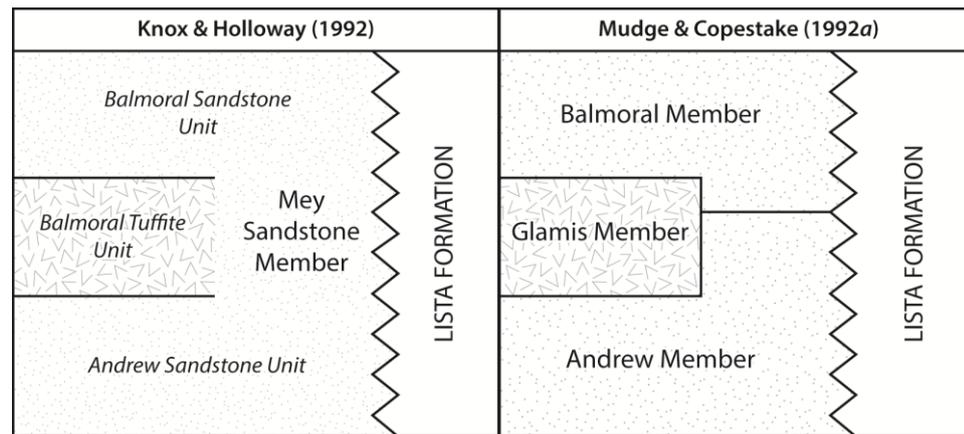
Figure 2.5 - Comparison of the Knox and Holloway (1992) and Mudge and Copestake (1992*a*) lithostratigraphic nomenclature schemes for the Lista Formation.

The Mey Sandstone Member covers a large area of the Central North Sea, reaching thicknesses in excess of 500 m where the Balmoral Tuffite Unit is present in the Outer Moray Firth. Overall, the sandstone is typically fine to medium-grained and commonly contains angular clasts of mudstone and limestone (Knox and Holloway, 1992). Average grain size generally decreases distally within the Mey fan and similar changes can be observed in sandstone porosity (Kilhams *et al.*, 2012). The distribution of the Mey Sandstone Member in the area of this study is shown in **Figure 2.6**. Several authors have published distribution and thickness maps for the Mey Sandstone Member (Knox and Holloway, 1992; Reynolds, 1994; Mudge and Bujak, 1994; Kilhams *et al.*, 2012). The most recent of these by Kilhams *et al*. (2012) provides an in depth analysis of the Mey Sandstone depositional fairways, sandstone thickness and sedimentological facies. Net sand thickness of the Mey Sandstone Member exceeds 75 m in proximal areas around the Outer Moray Firth where both the Andrew and Balmoral sandstone units are present, decreasing in distal areas to less than 15 m around UK quad 30 (Kilhams *et al*., 2012). The Mey deposits, in combination with the laterally equivalent Heimdal Sandstone Member (see *section 2.3.3*), form the most extensive of the Palaeogene sands, with clastic basinal input being at its greatest throughout the deposition of the Lista Formation (Ahmadi *et al.*, 2003).

Both lateral and axial sediment routing systems were active during deposition of the Mey Sandstone Member (Kilhams *et al*., 2012). A large axial NW-SE orientated fan system exists in line with the underlying Central Graben structure, which can be further

21
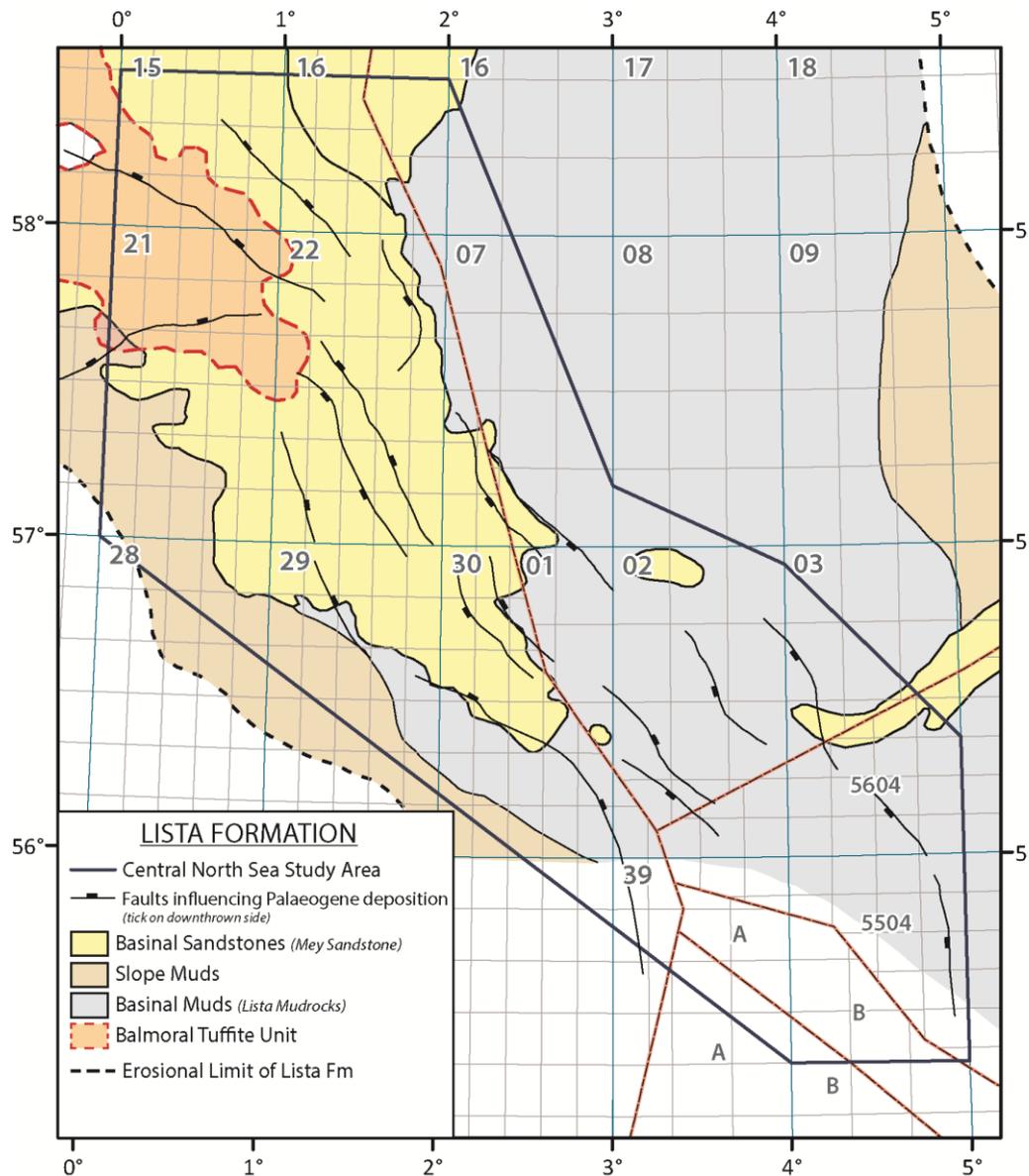
Figure 2.6 - Palaeogeographic map of Lista Formation times, showing the distribution of the combined Mey Sandstone Member along with the Balmoral Tuffite Unit. Faults which may have influenced Palaeogene deposition are also shown. Maps are modified from those presented in Ahmadi *et al* (2003) and those supplied to the study by Ternan Ltd (2010), based on analysis of well data available within the study region. The Siri Sandstone is situated in the Norwegian and Danish sectors.

divided into two coeval western and eastern fairways (Reynolds, 1994; Kilhams *et al.*, 2012, Fig. 3). Pathways of sediment routing within these axial fairways appear to be largely controlled by the underlying Mesozoic graben structure, as was also observed within the older, underlying Maureen Sandstone Member **(Figure 2.4)**. In the northern area of the Mey fan, the Forties-Montrose High acts to separate the two fairways into

22

western and eastern systems, as the Josephine Ridge does in southern areas (Kilhams *et al*., 2012). On its eastern and western limits, the axial fan is constrained by the Jaeren High and graben-bounding faults (O'Connor and Walker, 1993; Kilhams *et al*., 2012). At least two lateral (roughly west-east) fan systems were recognised by Kilhams *et al*. (2012) as belonging to the Mey Sandstone Member, with sediments being fed into the basin from the western margin around the southern and northern parts of UK quadrants 21 and 28, respectively (near to the Gannet Field area). Work carried out by Morton *et al*. (2004) on detrital garnet composition of the Mey Sandstone Member in this area indicates that sediments were sourced from the Dalradian of Scotland located directly to the west. It is likely that sediments would have bypassed the slope margins to be deposited as smaller fan units within the basin. The distal extents of these smaller lateral fans remains unknown, although Kilhams *et al*. (2012) state that amalgamation with the larger western and eastern axial fairway Mey sands is possible. Other areas of lateral sediment input along the western margin may be present potentially around UK blocks 21/16 and 21/22.

Local variations in the thickness of the Mey Sandstone Member may be observed around salt diapiric features, with thickening around the Merganser-Machar salt trend in UK blocks 22/30 and 23/26, and around the Joanne salt stock in UK Quad 30 (Kilhams *et al*., 2012). Such variations may reflect the Palaeocene sea-floor bathymetry, with sediment transport pathways around the then actively growing diapirs (Davison *et al*., 2000), or potentially post-sediment remobilisation caused by slumping (Kilhams *et al*., 2012).

2.3.3. Heimdal Sandstone Member

The Heimdal Sandstone Member is the coeval equivalent in the northern North Sea (Viking Graben) region of the Mey Sandstone Member. The sandstone was fed into the basin west/south-westwards from the East Shetland Platform (Ahmadi *et al*., 2003) and consequently only a small proportion of the Heimdal Sandstone Member is present in the study region, situated in UK blocks 16/22, 16/23, 16/24, 16/28, 16/29 and Norwegian blocks 15/08, 15/09, 15/12. Typically the sand is very fine to medium-grained, moderately sorted and poorly cemented (Mudge and Copestake, 1992*b*; Knox and Holloway, 1992). According to Ahmadi *et al*. (2003) the duration of Heimdal

Sandstone deposition spans the entire Lista Formation and so the sandstone is laterally equivalent to both the Andrew and Balmoral sandstone units belonging to the Mey Sandstone Member. Coalescence of the Mey and Heimdal sandstone members is limited to around the Fladen Ground Spur, located towards the top of the study area in UK quad 16 and Norwegian quad 15 where the sands thin or are locally absent (Knox and Holloway, 1992).

2.3.4. *Forties Sandstone Member*

The Forties Sandstone Member is the oldest of the basinal sandstones belonging to the Sele Formation, being of late Thanetian age (**Figure 2.3**). The sandstone is typically fine to coarse-grained and moderately to poorly sorted, with local pebbly areas (Knox and Holloway, 1992; Ahmadi *et al*., 2003). Sands may appear massively bedded and homogenous, or interbedded with laminated mudstones and siltstones belonging to the surrounding Sele Formation. Soft-sedimentation and dewatering structures are commonly observed within the sands, including dish structures, convolute laminations, microfaulting and sandstone dykes (Knox and Holloway, 1992; Ahmadi *et al*., 2003; Koša, 2007).

Numerous studies have examined the Forties Sandstone Member at field scale (Armstrong *et al*., 1987; Wills, 1991; Whyatt *et al.*, 1992; Birch and Haynes, 2003; Davis *et al*., 2009) and several authors have published distribution and thickness maps for the Forties Sandstone Member and combined Sele Formation sandstones (Knox and Holloway, 1992; Den Hartog Jager *et al.*, 1993; Reynolds, 1994; Mudge and Bujak, 1994; Ahmadi *et al*., 2003; Hempton *et al*., 2005). The palaeogeographic distribution of the Forties Sandstone Member used in this thesis is shown in **Figure 2.7**. As with the older underlying Palaeocene deposits, the majority of Forties sediments were fed into the basin from the NW, reflecting extensive erosion of the Scotland-Shetland landmass (Morton *et al*., 2004; Hempton *et al*., 2005). Sand supply into the basin was, however, not as great as it had been for the previously deposited fans and the total volume of the Forties Sandstone Member is considerably smaller than the underlying Mey (Den Hartog Jager *et al*., 1993), with approximately 28% net sand-grain volume for the combined Sele and Dornoch formations according to Liu and Galloway (1997). Consequently, the Forties Sandstone Member is not as laterally extensive as the
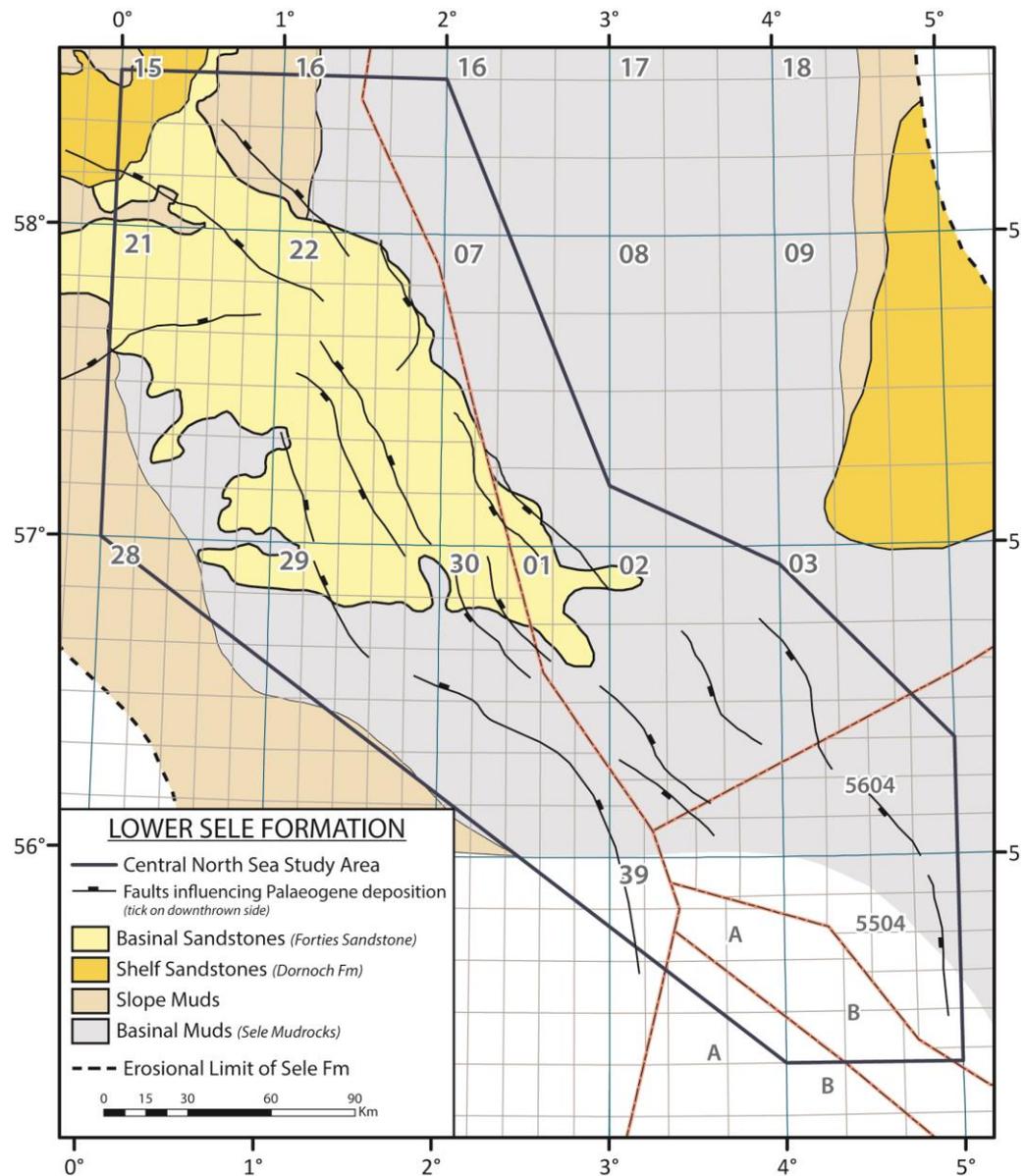
Figure 2.7 - Palaeogeographic map of Lower Sele Formation times, showing the distribution of the Forties Sandstone Member along with faults which may have influenced Palaeogene deposition. Maps are amended from those presented in Ahmadi *et al* (2003) and those supplied to the study by Ternan Ltd (2010). Individual analysis of well data within the study region was also made to accurately assess sandstone distribution. Erosional Limit of Sele Formation used from Ternan Ltd (2010).

underlying sandstones and has its furthest southern occurrence in Norwegian block 1/6 (**Figure 2.7**).

Like the Mey Sandstone Member, both lateral and axial sediment routing systems were active during Forties deposition (Reynolds, 1994; Hempton *et al.*, 2005).

25

A larger Forties axial fan is orientated NNW-SSE and is constrained to the west and east by rapid thinning of sands onto the Forties Platform and Jaeren High, respectively. Net thickness of the sand is greatest in proximal areas, reaching up to 275 m around the Forties Field in UK block 21/15 where the sands appear highly channelized (Hempton *et al.*, 2005), and gradually thins south-eastwards, away from the Scotland-Shetland landmass. Around the Pierce Field in UK block 23/27, net sandstone thickness is approximately 140 m, thinning to less than 15 m further south in UK block 29/10. In these distal areas, the Forties Sandstone Member comprises typically sheet-dominated sands with relatively few channels. Hempton *et al*. (2005) note how such distal sand sheets are interpreted to overlap, thus providing relatively good connectivity.

The sandstone is known to thin locally above structural palaeo-highs, such as the Forties-Montrose High. These variations in thickness are thought mainly to be a result of differential compaction (Den Hartog Jager *et al*., 1993; Koša, 2007), as opposed to changes in sediment routing around topographic features. In contrast, variations in Forties thickness associated with halokinesis are thought to be related to changes in sediment transport pathways, with Forties sands thinning and becoming locally absent above salt diapirs. McCormick and Leisham (2004) note how Forties sediments were re-routed during deposition around an active salt feature within the Chalk of UK block 29/1, which presumably impacted seabed bathymetry. It is likely that the quality of Forties sand deteriorates where there is local thinning associated with such features (Hempton *et al*., 2005).

Sediment was also fed into the Forties Sandstone Member via a series of smaller lateral westerly derived fan systems (Hempton *et al*., 2005) situated around the southern and northern parts of UK quadrants 21 and 28. Deposition in this area of the basin appears to have followed on from the underlying Mey Sandstone, with Forties subsidiary systems continuing to use the underlying Mey channels (McCormick and Leisham, 2004) which had cut into the western basin slope. Sediments deposited in this area were sourced from the Dalradian province of western Scotland (Morton *et al*., 2004). Lateral fans coalesce distally with the larger axial Forties fan system (Reynolds, 1994), potentially as far to the east as the Scoter and Merganser fields in UK block 22/30 (Hempton *et al.*, 2005).

Well data analysis carried out by Hempton *et al*. (2005) shows how numerous reservoir attributes within the Forties Sandstone Member gradually decrease down dip in both the axial and lateral sand fairways. Reductions in thickness, net:gross, sand-bed thickness, degree of channelization, grain size, permeability and porosity are all observed, although the reductions in porosity are only minor. Hempton *et al*. (2005) believe this to be associated with the increasing level of detrital clays down dip, which are effective at occluding smaller pores.

In the northwest of the study area, around UK quadrant 14 and the west of UK quadrant 15, the Forties sands amalgamate with shelf and coastal deposits belonging to the Dornoch Formation.

2.3.5. *Cromarty Sandstone Member*

The term 'Cromarty' was initially proposed by Mudge and Copestake (1992*a*) to refer to sands lying above the Forties Sandstone Member in the Outer Moray Firth region. Knox and Holloway (1992) amended the term with the addition of 'Sandstone Member' and extended its distribution to include those sands within the Sele Formation, lying above the Forties in the northern and western areas of the Central Graben. Despite this, alternative names continue to be applied to the Cromarty Sandstone Member, which is often referred to as the Rogaland sands (Schröder, 1992; Den Hartog Jager *et al*., 1993), upper Sele sands (Hempton *et al*., 2005) and the Bittern Sandstone Member (Hempton *et al*., 2005).

The Cromarty Sandstone Member is of Ypresian (early Eocene) age and comprises a series of small turbidite fan units within the upper Sele Formation. Sands are typically clean, unconsolidated, very fine to fine-grained, and interbedded with grey claystones belonging to the surrounding Sele Formation (Mudge and Copestake, 1992*a*; Ahmadi *et al*., 2003). Usually sands appear massive or thickly bedded, often displaying blocky profiles on wireline logs and sharp contacts with encasing Sele claystones and siltstones (Knox and Holloway, 1992).

The distribution of the Cromarty Sandstone Member used within this study is shown in **Figure 2.8.** Sands are present in the Outer Moray Firth and Central Graben area, across UK quadrants 15, 21, 22, 28 and 29. It can be seen that the Cromarty
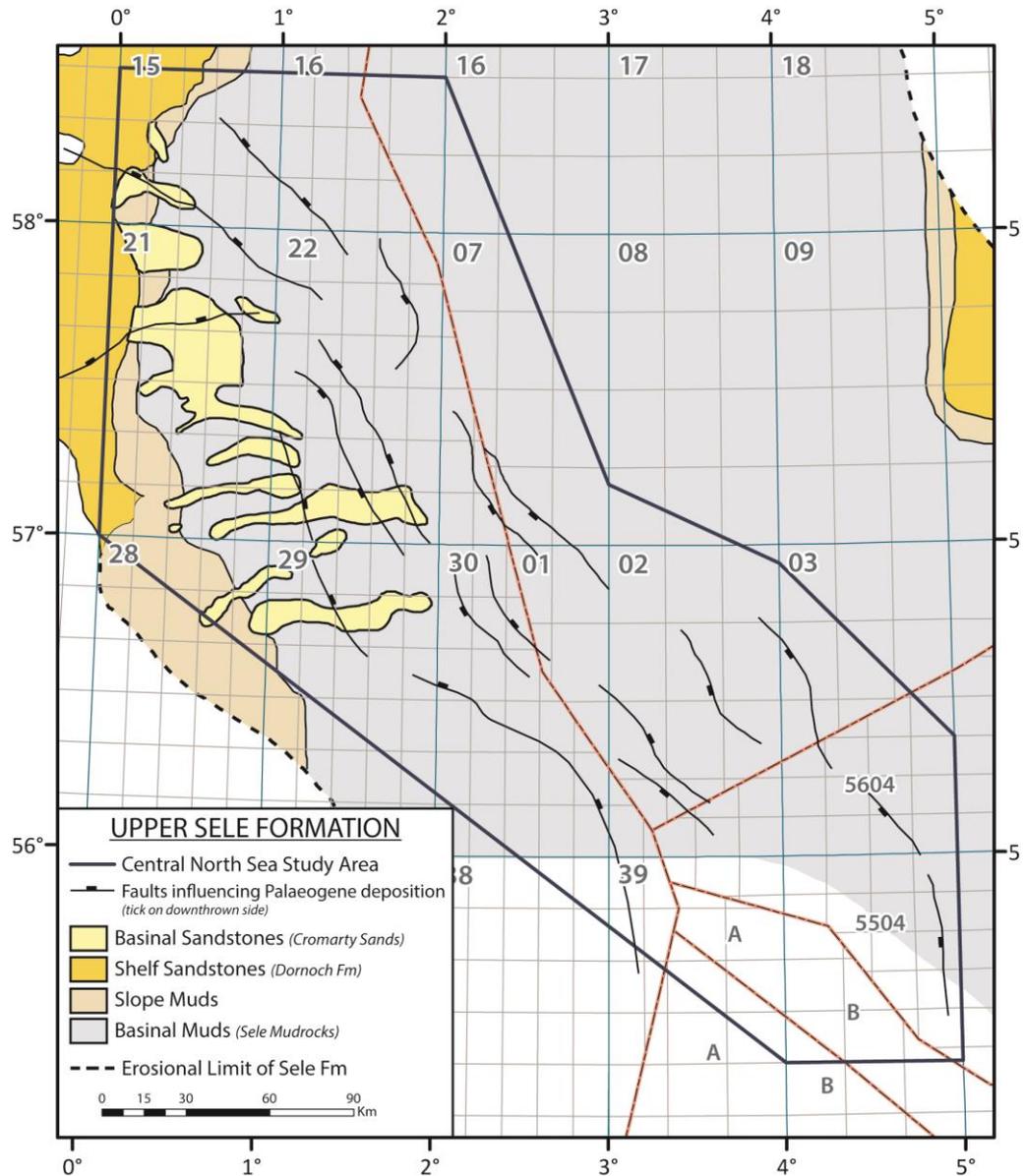
Figure 2.8 - Palaeogeographic map of upper Sele Formation times, showing the distribution of the Cromarty Sandstone Member along with faults which may have influenced Palaeogene deposition. Maps are amended from those presented in Ahmadi *et al* (2003) and those supplied to the study by Ternan Ltd (2010). Individual analysis of well data within the study region was also made to accurately assess sandstone distribution. Erosional Limit of Sele Formation used from Ternan Ltd (2010).

consists of small fans trending approximately west-east to southwest-northeast which have been sourced by feeder channels at various points along the western margin of the Central North Sea Basin (Hempton *et al*., 2005). Sands are thickest in the Outer Moray Firth area, with approximately 120 m of net sand recorded in UK block 21/2 (Knox and Holloway, 1992; Ahmadi *et al*., 2003). In this area, the sands amalgamate with shelfal

28

sediments belonging to the Dornoch Formation. Further south, where the Dornoch sequence is absent along the Western Platform and Western Central Graben (Ahmadi *et al*., 2003), Cromarty sands are present on both the slope and basin floor. Sands in this region, around the southern parts of UK quads 21 and 22 and northern parts of UK quads 28 and 29, are thinner reaching up to approximately 30 m net sand.

Sediment routing pathways of the Cromarty sands are thought to have been controlled by sea floor bathymetry, which was largely influenced by the positioning of underlying Forties and Mey channel complexes as well as salt movement at depth (McCormick and Leisham, 2004). Individual fans exhibit degrading reservoir attributes from proximal to distal areas, similar to what was observed for the underlying Forties Sandstone Member (Hempton *et al*., 2005), although overall reservoir attributes of the Cromarty sandstone are of much higher quality than those of the underlying sandstone members. Hempton *et al*. (2005) note how updip properties for the Cromarty lateral fans are the best in the whole of the Sele Formation, using the Bittern Field area of UK block 29/1 as an example; having higher net:gross (85%), higher porosity (34%) and higher permeabilities (exceeding 1000 mD) than other sands in the Sele Formation.

Unlike the overlapping channel sequences of the underlying Forties Sandstone Member, Den Hartog Jager *et al*. (1993) classify the Cromarty sands as 'isolated channel complexes,' and describe them as having thick massive channels, with linear geometry and limited lateral extent. Additional work carried out by Jennette *et al*. (2000) indicates that the channels are of low sinuosity and that they may display highly mounded geometries. Mounded channels such as those belonging to the Cromarty Sandstone Member are frequently associated with sand remobilisation and dewatering structures (see *section 2.4.4*).

2.3.6. *Tay Sandstone Member*

The Tay Sandstone Member was deposited over a long period of time, from the middle Ypresian (early Eocene) to late Lutetian (middle Eocene) (Den Hartog Jager *et al*., 1993; Jones *et al*., 2003), and represents the amalgamation of several prograding fan deposits comprising both slope and basinal facies (Armstrong *et al*., 1987). Sandstones are typically fine to medium-grained, interbedded with silty, fissile grey-green

mudstones belonging to the surrounding Horda Formation (Knox and Holloway, 1992). Along the slope margin of UK quadrant 28, sands are commonly friable and clean, showing evidence of remobilisation in the form of dish structures and discordant contacts.

Several published papers have described the Tay Sandstone Member on a field scale (Armstrong *et al*., 1987; Banner *et al*., 1992; Jones *et al*., 2003) and rather fewer on a regional scale (Den Hartog Jager *et al*., 1993; Jennette *et al*., 2000). The distribution of the Tay Sandstone Member within the study area is shown in **Figure 2.9.** Tay sands are largely restricted to southern parts of UK quadrants 21 and 22 and northern parts of UK quadrant 28, potentially extending further eastwards into UK quad 29. The Tay Sandstone Member was deposited in a broad WNW-ESE trending topographic low (Den Hartog Jager *et al*., 1993; Jones *et al*., 2003), with the main source of sediment being fed into the basin from the NW according to numerous published sources (Armstrong *et al*., 1987; Den Hartog Jager *et al*., 1993; Jennette *et al*., 2000). Several WSW−ENE orientated feeder channels are present in and around the southern and northern blocks of UK quadrants 21 and 28, where sediment was fed into the basin from various points along the Western Platform. The distribution of these channels can be seen in the general sandstone outline (**Figure 2.9**) and also crudely inferred from the distribution of Tay hydrocarbon accumulations (see **Appendix A**). According to Den Hartog Jager *et al*. (1993), these feeder channels were active at different times throughout the Eocene, with sediments generally by-passing the slope to be deposited as basin-floor fans. Where Tay sands are found along the slope, they comprise either highly channelized features deposited within submarine canyons, as observed in the Pilot Field, UK block 21/27, or as smaller sand bodies which have ponded in accommodation space developed in the hanging walls of slope faults, such as in UK quadrant 28/9 around the Catcher, Varadero and Burgman discoveries. Smaller sand bodies isolated from the main Tay sand body are also present.

The main Tay fan tapers distally towards the SE and NE (Jennette *et al*., 2000), with net sand thickness in these areas being generally less than 15 m. A large build-up of sediment is observed towards the centre of the Tay Sandstone Member, orientated NW-SE and roughly aligned with the base of the slope margin. Net sand thickness is greatest in this area reaching in excess of 150 m in UK blocks 21/17 and 21/23. Within the WSW−ENE orientated feeder channels, the net thickness of the Tay sands is highly
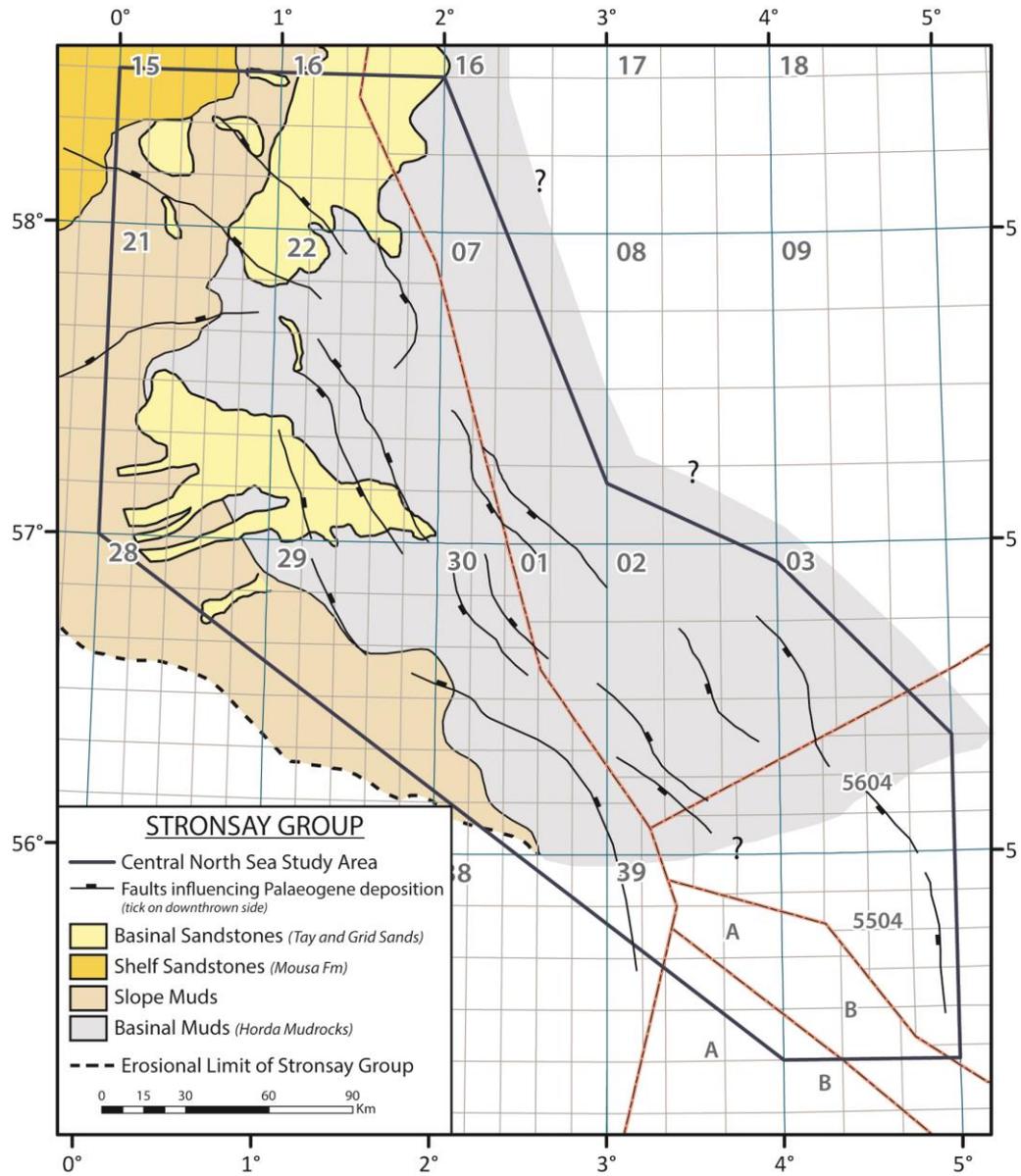
Figure 2.9 - Palaeogeographic map of the Stronsay Group, showing the distribution of the Tay and Grid sandstone members, along with faults which may have influenced Palaeogene deposition. Maps are amended from those presented in Ahmadi *et al* (2003) and those supplied to the study by Ternan Ltd (2010). Individual analysis of well data within the study region was also made to accurately assess sandstone distribution. Erosional limit of the Stronsay Group taken from Ternan Ltd (2010).

variable due to ponding of sediments as well as bypass over the slope. Other variations in Tay sand thickness are related to syn-sedimentary salt movement (Den Hartog Jager *et al.*, 1993), with salt-induced structural highs influencing sediment accumulation and flow pathways over time, as seen at the Gannet B Field (Armstrong *et al.*, 1987). In parts of UK quadrant 21, where the Horda Formation is unconformable over salt-

31

induced highs, the Tay Sandstone Member may variously overlie sediments belonging to the Balder, Sele and Lista formations (Knox and Holloway, 1992).

Work carried out by Den Hartog Jager *et al.* (1993) indicates that the Tay sediments developed from basin-floor fans into slope fans, progressively retreating westwards over time. Furthermore, Tay sediments also appear to have evolved from earlier sheet-like geometries into mounded geometries, becoming increasingly sandier and more channelized (Den Hartog Jager *et al.*, 1993; Jennette *et al.*, 2000).

2.3.7. Grid Sandstone Member

The Grid Sandstone Member of middle Lutetian (Eocene) to late Priabonian (Oligocene) age, is located in the northern part of the study region, around UK quadrants 15, 16 and northern quadrants 21 and 22 (**Figure 2.9**). The member comprises sandstones of combined shallow-water and deep-water origin (Knox and Holloway, 1992; Jones *et al.*, 2003) in addition to remobilised and injected sandstones (Newton and Flanagan, 1993; Huuse *et al.*, 2005). Classification of the Grid sands is therefore complex, made even more so by the fact that all Grid sands are lithologically similar, sharing similar wireline characteristics (Knox and Holloway, 1992; Newton and Flanagan, 1993). Several stratigraphic schemes are in existence for the Eocene sediments of the Central North Sea (Knox and Holloway, 1992; Mattingly and Bretthauer, 1992; Galloway *et al.*, 1993; Mudge and Bujak, 1994). A comparison chart of the most widely used schemes is shown in **Figure 2.10**. Throughout this thesis the Knox and Holloway (1992) nomenclature is adopted for the middle to upper Eocene Sands, although reference is also made to the nomenclature of Mattingly and Bretthauer (1992), where it is thought necessary.

The Grid Sandstone Member of Knox and Holloway (1992) comprises the older Caran Sandstone Unit and the younger Brodie Sandstone Unit (**Figure 2.3** and **Figure 2.10**). In the Central Graben and Outer Moray Firth, distinction of these two sandstone units is relatively easy since a substantial thickness of Horda mudstone separates the two (Knox and Holloway, 1992). Where distinction of these two units is more difficult, the term Grid Sandstone Member is used as an 'umbrella' term to classify the middle to late Eocene sands. A brief description of each reservoir unit is provided below.

Ma	Epoch age			Mudge & Bujak (1994)	Galloway et al. (1993)	Knox & Holloway (1992)		Mattingly & Bretthauer (1992)		Murphy & Wood (2011)
31	Oligocene	Early	Rupelian			Westray Group		Lark		
32										
33										
34	Eocene	Late	Priabonian	II	Thet		Grid Sandstone Member / Brodie Sandstone Unit		Brioc	
35					Belton					
36										
37				Grid						
38		Bartonian			Upper Hordaland			Alba		Brioc Sands
39			I							
40										
41									Nauchlan	
42		Mid		III	Lower Hordaland	Stronsay Group / Mousa Fm (shelf sandstones) Horda Fm (basinal mudstones)		Horda	Nauchlan	Nauchlan
43			Lutetian							
44										
45			II	Alba			Grid Sst Mem. / Caran Sst Unit			
46			I					Lothian	Caran	Caran Injectites
47			III				Tay Sandstone Member			
48				Frigg	Frigg					
49		Early	Ypresian	II				Orkney		
50										
51			I							
52										
53				Balder	Balder	Moray Group / Balder Fm	Rogaland Group	Balder		Cromarty
54	Palaeocene	Late	Thanetian	Dornoch		Sele Fm				Forties
55				Forties		Mont-rose / Lista Fm				Mey
56				Lista						

Figure 2.10 - Stratigraphic comparison chart for Eocene sediments (modified from Jones *et al*, 2003; Murphy and Wood, 2011).

2.3.7.1. *Caran Sandstone Unit*

The Caran Sandstone Unit is the older of the two units comprising the Grid Sandstone Member, and corresponds to the Caran Sandstone Member of Mattingly and Bretthauer (1992) (**Figure 2.10**). There is much ambiguity surrounding the source of the Caran sandstone with some authors favouring a depositional origin (Knox and Holloway, 1992; Mattingly and Bretthauer, 1992; Jones *et al*., 2003) whilst the more recent invoke a wholly injected origin (Huuse *et al.*, 2005; Murphy and Wood, 2011).

33

Knox and Holloway (1992) describe the Caran Sandstone Unit as an isolated deep marine fan sand, whose deposition was restricted to distal areas of the basin focused over the South Viking Graben. They state that sediments which fed the Caran submarine fan were derived exclusively from the East Shetland Platform and the Fladen ground spur. In contrast, Huuse *et al.* (2005) favour a completely injected origin for the Caran Sandstone Unit, suggesting that it was sourced from a pre-Balder parent sand, most likely fed from the underlying Palaeocene sand bodies. Seismic evidence which supports the latter includes: 1) the proximity of Caran injectites to the top Balder (Huuse *et al.*, 2005); 2) common disruption of the top Balder horizon (Molyneux *et al.*, 2002; Murphy and Wood, 2011); and 3) a common relationship between structurally high Balder areas and injected features (Huuse *et al.*, 2005).

Murphy and Wood (2011) thought that the Caran sands were sourced from the underlying Forties Sandstone Member; however, the occurrence of injected sands within UK blocks 16/21 and 16/28 where no underlying Forties sands are present indicates that the Forties Sandstone Member cannot be the sole parent source.

On seismic sections, injected Caran sands appear as cross-cutting, high amplitude reflections with V-shaped, Y-shaped, or even W-shaped geometries (Huuse *et al.*, 2003; Murphy and Wood, 2011). In 3D these geometries comprise large scale sub-circular to conical bodies, commonly 600-1000 m wide with vertical extents of as much as 160 m (Molyneux *et al.*, 2002; Huuse *et al.*, 2005; Murphy and Wood, 2011).

Murphy and Wood (2011) mapped the distribution of Caran sandstone injectites around the Chestnut Field in UK blocks 22/1 and 22/2 and the southern parts of UK blocks 16/26 and 16/27. Their distribution does not correspond to a depositional trend one would expect for a channelized, deep-water turbidite deposit, but consists of clusters of isolated sands which appear to form occasional large injectite complexes. The overall distribution of these injected sands appears confined, with very few mapped Caran sands present to the east of the Chestnut Field (Murphy and Wood, 2011).

2.3.7.2. *Brodie Sandstone Unit*

The Brodie Sandstone Unit of Knox and Holloway (1992) corresponds to the Nauchlan and Brioc sandstone members of Mattingly and Bretthauer (1992) (**Figure 2.10**). Unlike

the underlying Caran Sandstone Unit, the Brodie sediments are thought to be of depositional origin, with accumulation of shallow marine deposits in proximal areas of the basin along the slope margin, as well as in the deeper more distal areas of the basin (Knox and Holloway, 1992; Jones *et al*., 2003). Brodie deposits are extensive across the northern North Sea and much of the Outer Moray Firth region (Knox and Holloway, 1992), with sediments having been sourced from the extensive Mousa Formation shelf system (Jones *et al*., 2003) situated to the west and northwest of the basin (**Figure 2.9**).

The uppermost Brodie sands, largely corresponding to the Brioc Member of Mattingly and Bretthauer (1992) are thinly bedded and pass laterally with little change into shelf sands belonging to the Mousa Formation (Knox and Holloway, 1992; Jones *et al*., 2003). In contrast, the lower Brodie sands corresponding to the Nauchlan Member of Mattingly and Bretthauer (1992) appear thickly bedded and channelized (Newton and Flanagan, 1993).

Water-escape features such as dish and pipe structures are common in both the 'Brioc' and 'Nauchlan' Brodie sands, as are injected sands albeit on a lesser scale than the underlying Caran Sandstone Unit (Newton and Flanagan, 1993). Such structures signify rapid deposition of the sands (Lonergan and Cartwright, 1999; Jones *et al*., 2003). Around the Chestnut and Alba fields, within UK blocks 22/1, 22/2 and 16/26, extensive research has been carried out with regards to the complex geometry and character of the Brodie sandstone bodies (Lonergan and Cartwright, 1999; Duranti *et al*., 2002; Huuse *et al*., 2003; Duranti and Hurst, 2004; Murphy and Wood, 2011) which appear in transverse vertical section as broad, low-sinuosity, lenticular channels with distinctive discordant, wing-like intrusions projecting from the channel sides. Duranti *et al*. (2002) interpreted the Brodie (Brioc) sands to be wholly extensions of the main underlying Brodie (Nauchlan) sand which have formed by upward injection. Huuse *et al*. (2005) hypothesised that the Brodie Sandstone Unit in the Outer Moray Firth may have formed as a seabed extrudite sourced from the underlying injected Caran Sandstone Member, although Murphy and Wood (2011) have disregarded this hypothesis, asserting that Brodie sandstone is geochemically distinct from the underlying Caran. The vast majority of authors favour a post-depositional remobilised channel sand interpretation of the Brodie Nauchlan sands (Huuse *et al*., 2005; Lonergan and Cartwright, 1999; Szarawarska *et al*., 2010; Murphy and Wood, 2011).

2.4. Basin architecture

A depth map for the Top Balder horizon is shown in **Figure 2.11**. Palaeogene sediments are most deeply buried above the Central Graben around UK quadrants 23, 29 and 30 and Norwegian quadrant 1, where the top of the Palaeocene (i.e. top Balder Formation) is situated at depths of approximately 3100 m. Within the Central North Sea study region, the top Balder shallows to approximately 500 m depth along the Western Platform in UK quadrants 28 and 21 south (**Figure 2.11**). Although not seen in **Figure 2.11**, the top Balder Formation surfaces below the seabed around the Inner Moray Firth within UK quadrant 12. The Palaeogene sequence gradually thickens and shallows towards the Moray Firth, as shown in the regional cross-section of **Figure 2.12.**

2.4.1. Burial history

A typical burial history for deeper areas of the Central North Sea region is shown in **Figure 2.13**. Following Early Mesozoic rifting and subsidence, burial was extremely slow across the basin until the Late Cretaceous. According to Swarbrick *et al*. (2004), a hiatus in sedimentation occurred around the Early Cretaceous, the duration of which increased from the centre of the basin towards the edges. During the Late Cretaceous, rates of burial began to increase and rapid continuous deposition of sediment across the basin has persisted through to the present day. According to Fyfe *et al*. (2003) approximately 3000 m of sediment has been deposited since the Oligocene 34 Ma ago. Around 1500 m of this sediment, mainly glacial in origin, was deposited during the Pliocene and Quaternary (Swarbrick *et al*., 2000; Gyllenhammar, 2003). In their study of the Judy Field in UK block 30/7, Swarbrick *et al*. (2000) indicated that rates of burial increased dramatically to approximately 500 m Ma^{-1} over the last 3 Ma alone (late Pliocene to Recent).

2.4.2. Geothermal gradient

Kubala *et al*. (2003) state that the average geothermal gradient for North Sea Basin is 34.6 ^{o}C km^{-1}. In the Central North Sea region geothermal temperature gradients are typically between 35 °C km^{-1} and 41 ^{o}C km^{-1}, reaching in excess of 41 ^{o}C km^{-1} in deep

36
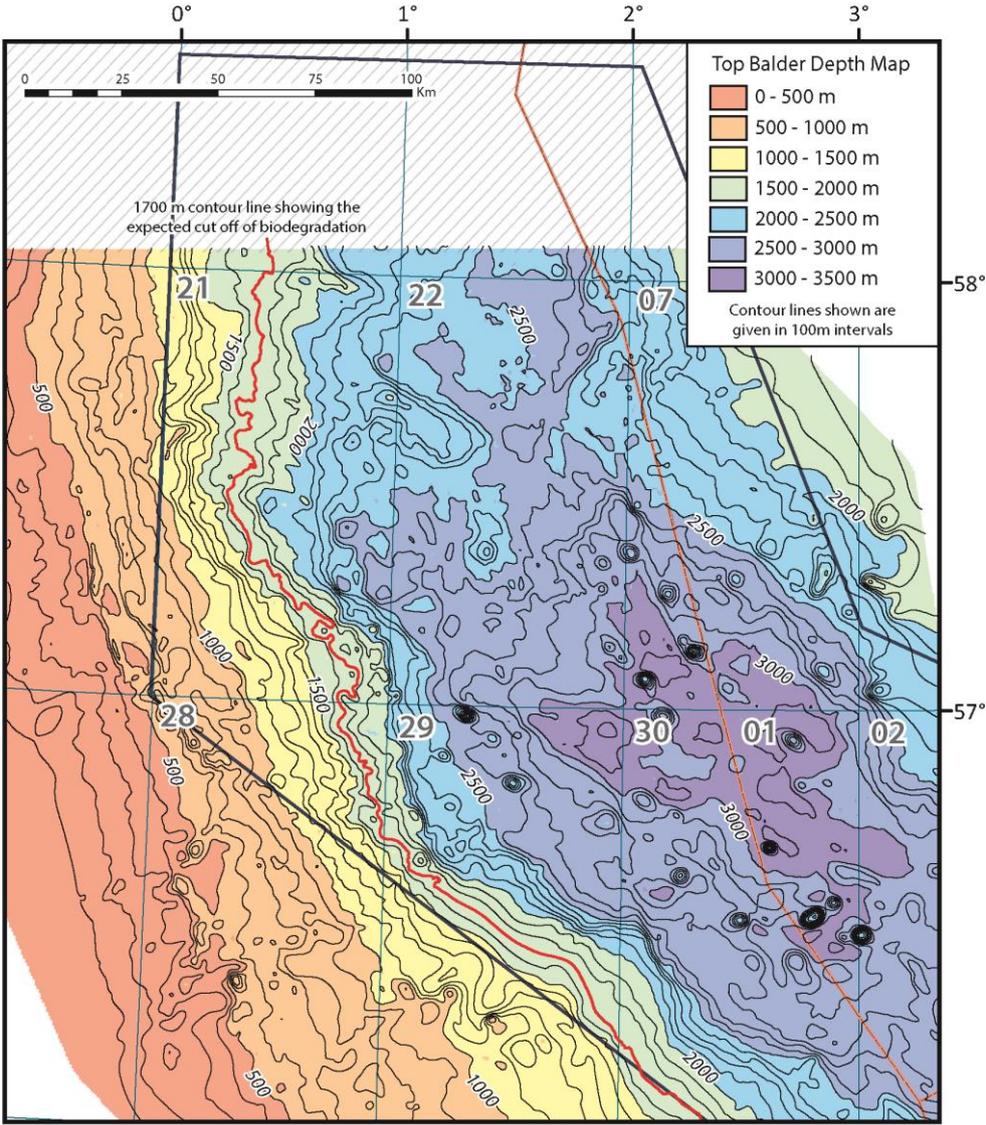
Figure 2.11 - Depth to the top of the Balder Formation, representing the top Palaeocene. Depth is given in metres, with contouring of 100 m intervals. Maximum subsidence of Palaeocene is approximately 3100 m (10170 ft) observed in the Central Graben within UK quadrants 23, 29, 30 and Norwegian quadrant 1. The Palaeocene subcrops beneath the seabed (< 1000 m depth) in UK quadrant 28 and appears to shallow towards the NW. Several bulls-eye contours in and around the deeper areas of burial show influence from salt diapirism; the Palaeocene thins and shallows above such features. Highlighted red contour at 1700 m indicates the depth above which biodegradation is likely to occur. Coverage of the depth map does not extend northwards into UK quadrants 15 and 16. Map was constructed from 3D seismic data at Maersk Oil UK Ltd Aberdeen.
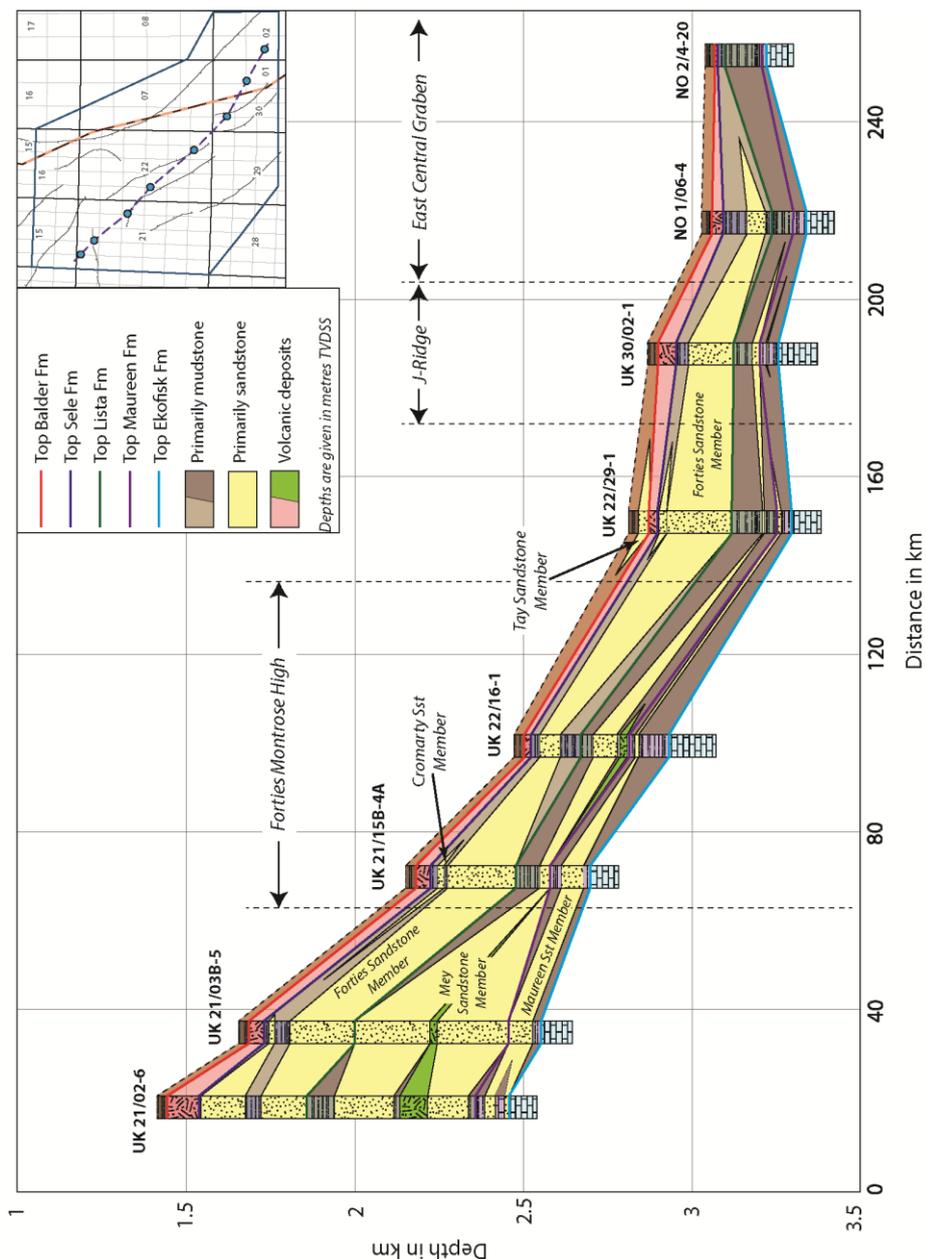
Figure 2.12 - NW-SE cross-section through the Palaeocene section of the Central North Sea study region, showing each Palaeocene sandstone member to thicken and coalesce towards to NW of the area. Line of section is shown in figure inset.

graben areas located towards the SE of the study region. Kubala *et al*. (2003) associate the higher geothermal gradients observed in the Central North Sea with generally higher heat flow, in addition to the rapid rates of burial which occurred during the Late Cenozoic. The latter resulted in higher geothermal gradients associated with the great
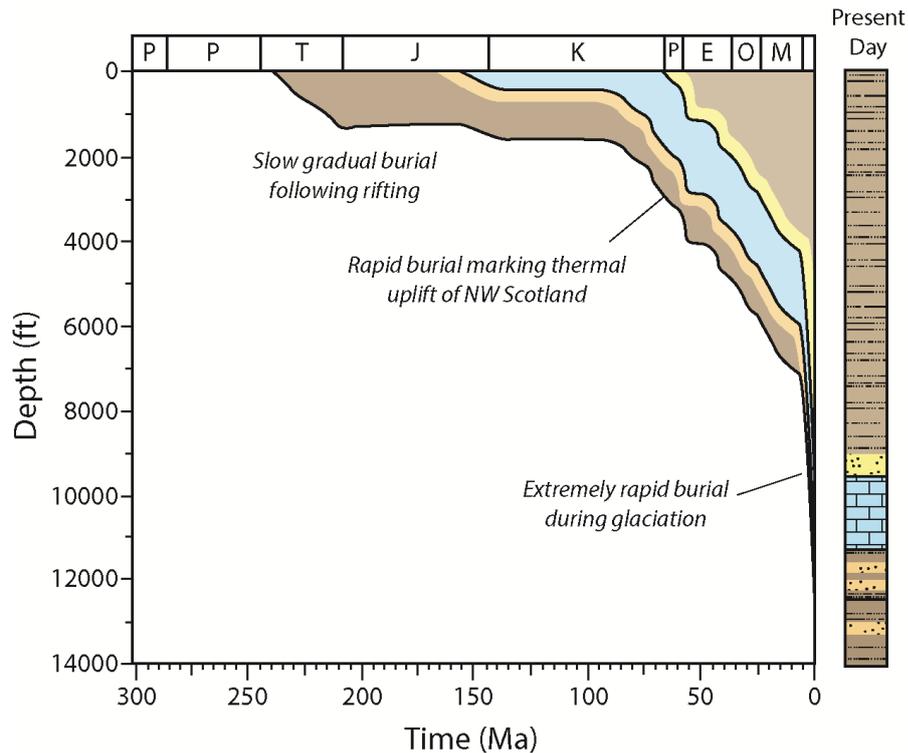
Figure 2.13 – Typical burial history curve for the Central Graben region of the basin based on stratigraphic and depth data recorded within UK well 30/11b-3 (generated using Temis Suite software, 2010).

thicknesses of undercompacted mudrocks with high water content and lower thermal conductivity. High geothermal gradients in the Central North Sea region influence the degree of hydrocarbon maturity experienced within the basin, which in turn can directly impact the generation of overpressure through hydrocarbon generation (see *section 3.3.2.1*).

2.4.3. Salt diapirism

Salt diapir structures host some of the largest hydrocarbon fields in the Central North Sea, with Palaeogene oil columns extending vertically up to heights of 1.3 km in the surrounding reservoir rocks (Hodgson *et al.*, 1992; Davison *et al.*, 2000). The majority of salt diapirs are found above the Central Graben where the Zechstein salt is thickest and where salt movement has taken place along basement faults developed during Permo-Triassic rifting (Davison, 2004). Growth of salt diapir structures, both during

and after Palaeogene sediment deposition, has played an integral role in Palaeogene trap formation (Ahmadi *et al*., 2003). Salt-induced anticlinal traps such as those at the Andrew, Lomond, Maureen, Cod and several of the Gannet complex fields are located above deep-seated salt diapir structures. Where salt diapir structures have penetrated through the reservoir unit, salt-abutment or piercement traps may be formed, as at the Banff, Kyle, Machar, Monan, and Pierce fields.

The interaction between salt movement and Palaeogene sediment deposition is complex, with factors such as the timing of halokinesis and its impact on the sea level bathymetric relief potentially influencing flow pathways and the relative thickness of turbidites at the time of deposition (Hodgson *et al*., 1992; Davison, 2004). Movement of salt diapirs post-deposition may also have greatly influenced the Palaeogene strata by causing slumping, faulting, fracturing and soft-sediment deformation (Davison *et al*., 2000).

Several authors have suggested that salt diapir structures may facilitate migration of fluids vertically into the Palaeogene strata via the fault and fracture systems which develop around such features along the line of maximum flexure (Cayley, 1987, Evans *et al*., 2003; Kubala *et al*., 2003). Gas columns or 'chimneys,' which are commonly observed above salt diapirs on seismic data, provide further evidence of migration pathways above such features caused by the extensional fracturing they induce.

2.4.4. *Sandstone remobilisation*

Within the study region, remobilisation of the Cromarty, Tay and Grid sandstone members is considered to be relatively widespread and has been documented in the southern parts of UK quadrants 16 and 21, and the northern parts of UK quadrants 28 and 29 (Hurst *et al*., 2005; Huuse *et al*., 2005; Murphy and Wood, 2011). Remobilisation of the Caran and Brodie sandstone units belonging to the Grid Sandstone Member was previously discussed in *section 2.3.7*; the Caran sands are thought to be of a completely injected origin sourced from the underlying Palaeocene sandstone members (Huuse *et al*., 2005; Murphy and Wood, 2011), and the Brodie sandstone unit is thought to be of depositional origin with subsequent remobilisation

(Huuse *et al.*, 2005; Lonergan and Cartwright, 1999; Szarawarska *et al.*, 2010; Murphy and Wood, 2011).

Similar post-depositional remobilisation features to those observed within the Brodie Sandstone Unit are found within the Cromarty and Tay sandstones. Cromarty sandstone remobilisation is well documented from the Danica Intrusion Complex located in UK block 29/6, where discordant wing-like sand intrusions project from a deeper, bedding-parallel, Cromarty sand body cross-cutting through the Balder Formation into the Horda Formation above (Szarawarska *et al.*, 2010). Due to the shape of the intrusion complex and its similarity to the Brodie (Nauchlan) sands of the Alba Field, Szarawarska *et al.* (2010) suggest post-depositional remobilisation of a deposited sandstone channel. Injected Tay and Cromarty sands are also apparent around the Catcher and Varadero fields in UK block 28/9 and the Fyne and Dandy fields in UK block 21/28 (Jon Gluyas, pers. comm.). Here, once again, it is thought that the majority of sands are of depositional origin with post-depositional remobilisation producing thinner injected sands sourced from the larger parent body (Graham Bull, pers. comm.).

The presence of injected sands may act to greatly improve reservoir communication vertically (Hurst *et al.*, 2003), as well as to provide hydrocarbon migration routes into younger Eocene reservoirs (Huuse *et al.*, 2005; Murphy and Wood, 2011). The widespread occurrence of sand injectites along the western basin margin and around UK quadrant 16 suggests that vertical connectivity between sandstone members may be common in these areas.

2.5. Palaeogene petroleum system

According to Eriksen *et al.* (2003), the Palaeogene petroleum system accounts for approximately 14% of total discovered reserves within the Central and Northern North Sea, making it the third most economically successful petroleum play within the basin, after the Lower/Middle Jurassic and Upper Jurassic systems. The distribution of all presently known Palaeogene hydrocarbon discoveries across the Central North Sea coloured by hydrocarbon type is shown in **Figure 2.14** and tabulations of hydrocarbon
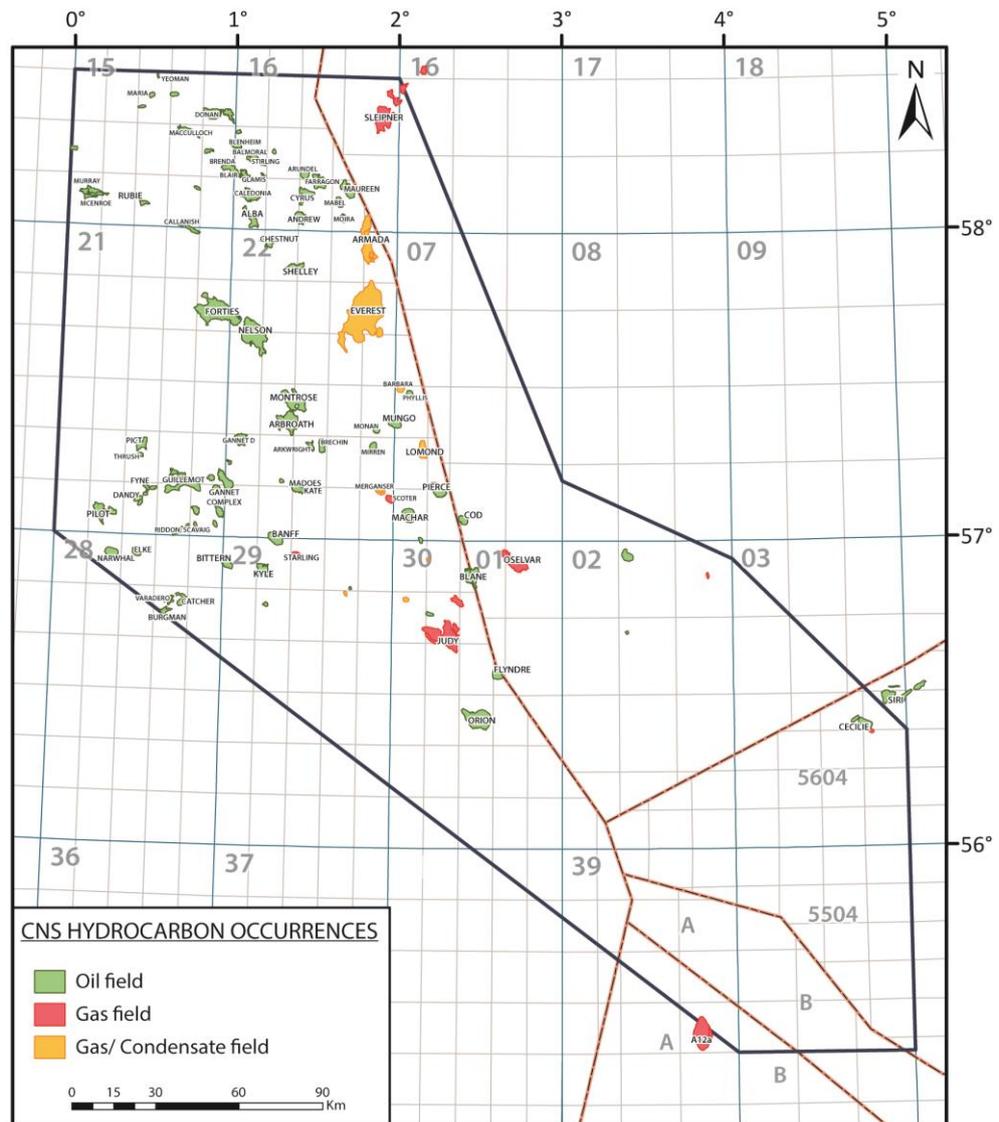
Figure 2.14 - Map of Central North Sea study region showing the location and names of all presently known Palaeogene hydrocarbon fields and discoveries (modified from Eriksen *et al.*, 2003).

accumulations for each Palaeogene reservoir interval are given in **Appendix A**. It can be seen that although oil, gas and condensate accumulations are geographically widespread across the Palaeogene system, the vast majority of Palaeogene hydrocarbons have been found within the UK sector, corresponding to the distribution of reservoir sandstones (Eriksen *et al.*, 2003). Details of each individual field and discovery are tabulated in **Appendix A** along with a brief description of the play fairways, trap types and play risks for each Palaeogene sandstone member**.**

The source rock for all Palaeogene hydrocarbon occurrences is the regionally extensive Upper Jurassic Kimmeridge Clay Formation, which is mature for both oil and gas generation across large parts of the basin (Ahmadi *et al*., 2003). Where the Kimmeridge Clay is most deeply buried, it is also most mature (Kubala *et al*., 2003). This relationship is reflected in the distribution and phase of Palaeogene hydrocarbons, with Palaeogene gas and condensate fields such as the Judy, Oselvar, Merganser, Everest, Armada and Sleipner being found solely along the Eastern Central Graben and the South Viking Graben, where the Kimmeridge Clay is most deeply buried (**Figure 2.14**).

Oil is by far the more common hydrocarbon phase found within the Palaeogene reservoirs. Oil gravities range from 20°-43° API and 14°-40° API within Palaeocene and Eocene reservoirs, respectively. Heavier oil, of lower API gravity, is found towards the margins of the basin, where reservoirs are buried at shallower depths and temperatures are lower. Biodegradation poses a high risk to hydrocarbons where temperatures are less than approximately 60-80 °C, corresponding typically to reservoir burial depths of around 1700 m in the Central North Sea region (Barnard and Bastow, 1991). At temperatures above 60-80 °C the bacteria responsible for oil degradation are destroyed (Kubala *et al*., 2003). In the study region, biodegradation poses a high risk to Palaeogene hydrocarbons along the western margin of the basin around UK quadrants 15 (west), 21 (west) and 28 (**Figure 2.11**). Eocene hydrocarbons appear to have been most extensively influenced by biodegradation, with heavy, partly biodegraded oils recorded within the Tay reservoir at the Elke (UK 28/03, 16° API), Narwhal (UK 28/02, 14° API) and Pilot (UK 21/27, 14-16° API) fields. Hydrocarbons are also at risk of biodegradation within Grid sands which are buried at depths less than 1700 m across most of their distribution, although relatively few hydrocarbon accumulations have yet been discovered in these areas. The recent discoveries of slightly biodegraded, moderate gravity Eocene oil (24-30° API) at the Catcher, Varadero and Burgman fields in UK block 28/09 have shown that areas at risk of biodegradation should not automatically be regarded as being non-prospective.

The principal reservoir members for the Palaeogene system have been described in detail within this chapter and comprise the Maureen, Mey/Heimdal, Forties, Cromarty, Tay and Grid sandstone members. The Maureen, Mey and Forties Palaeocene fan reservoirs are regionally continuous with good connectivity, facilitating

the long-distance lateral migration of hydrocarbons (Cayley, 1987). In contrast, the Cromarty, Tay and Grid reservoirs are laterally restricted, and have more local importance. Porosities for the sand-rich Palaeocene reservoirs are good, with average porosities and permeability in the ranges 17-33% and 10-16 mD, respectively (Ahmadi *et al.*, 2003). Quality of the Eocene reservoirs is higher, being more sand-rich and relatively unconsolidated. Average porosities for the Eocene reservoirs are in the range 20-35%, with permeabilities of 100-1000 mD (Jones *et al.*, 2003).

Migration of hydrocarbons into the Palaeocene strata from the Upper Jurassic source rocks must be facilitated vertically, since these two systems are nowhere in contact and are separated by up to ~ 2000 m of Cretaceous shales and carbonates. Migration is thought most likely to occur vertically along deep, basement-rooted graben-bounding faults (Cayley, 1987), or via the faults and fracture networks associated with salt diapirism (Ahmadi *et al.*, 2003). Several authors have noted the relationship between failed Palaeocene traps and the locations of Eocene hydrocarbon accumulations (e.g. Mason *et al.*, 1995; Jones *et al.*, 2003). Migration of hydrocarbons from Palaeocene to Eocene strata is thought to occur via injected Caran sandstones (Huuse *et al.*, 2005; Murphy and Wood, 2011). Other authors have suggested that hydrocarbon migration between these two systems may have been additionally facilitated via polygonal faults networks (Jones *et al.*, 2003; Murphy and Wood, 2011), although there is no evidence that such faults are permeable (Goulty, 2008; 2012).

Palaeogene hydrocarbon accumulations are sealed by the overlying or encapsulating lower permeability Tertiary muds and shales. For any well, it is normal for hydrocarbons to accumulate within the highest Palaeogene reservoir interval, as shown on the hydrocarbon occurrence maps in **Appendix A**, suggesting that 1) the intra-formational Palaeogene muds and shales act as poor seals; and 2) reservoir intervals which are overlain by younger Palaeogene sands have an increased topseal risk for any hydrocarbons accumulating within them. This observation explains why stratigraphic trapping is common along the eastern margin of each Palaeocene fan member and, similarly, why a larger number of discoveries have been made within the Forties fan sand than in the underlying Mey/Heimdal and Maureen fans: the Forties fan is, over most of its extent, covered solely by the thick sequence of overlying Tertiary shales. There are, however, a few exceptions, such as the Rubie Field (UK 15/28) and

Murray discovery (UK 15/26), where the Balmoral Tuffite Unit acts as a seal to hydrocarbons within the underlying Andrew Sandstone Unit.

3 | Pore pressure in the subsurface

"When we long for life without difficulties, remind us that oaks grow strong in contrary winds and diamonds are made under pressure" Peter Marshall (1926-present) [American TV entertainer]

3. Pore pressure in the subsurface

In this chapter, the theoretical background and basic principles of pressure evaluation are described, followed by a more detailed explanation of overpressure and basin hydrodynamics in the Central North Sea region.

3.1. Units of pressure

Pressure is a force per unit area. The SI unit of pressure is the newton per square metre (N m^{-2}), more commonly referred to as the pascal (Pa). In the hydrocarbon industry, imperial units of pounds per square inch (psi or lb in^{-2} are still used to express pressures, as are feet and inches to express units of distance. Consequently throughout this thesis psi and psi ft^{-1} shall be the preferred unit of pressure and vertical pressure gradient, unless otherwise stated. Additional values of either kPa or MPa and kPa m^{-1} or MPa m^{-1}, shall also be provided in brackets.

For a list of conversions between commonly used units of pressure and pressure gradient, see the front cover of this thesis as well as the file entitled 'Pressure conversion tables' in the enclosed CD.

3.2. Basic pressure terminology

In order to illustrate some basic pressure terms, a generalised pressure versus depth (P-D) plot is shown in **Figure 3.1**. P-D plots can be used to: calculate values of abnormal pressure; calculate values of effective stress; analyse pressure data taken from a single well and multiple wells; determine fluid type and fluid density; and predict depths of fluid contacts. Several of the basic terms vital to pressure and overpressure analysis are described below.

Hydrostatic pressure. Normal hydrostatic pressure at any depth is the pressure exerted by the weight of the overlying column of water, which is a function of fluid density. Hydrostatic pressure can be expressed by the equation:
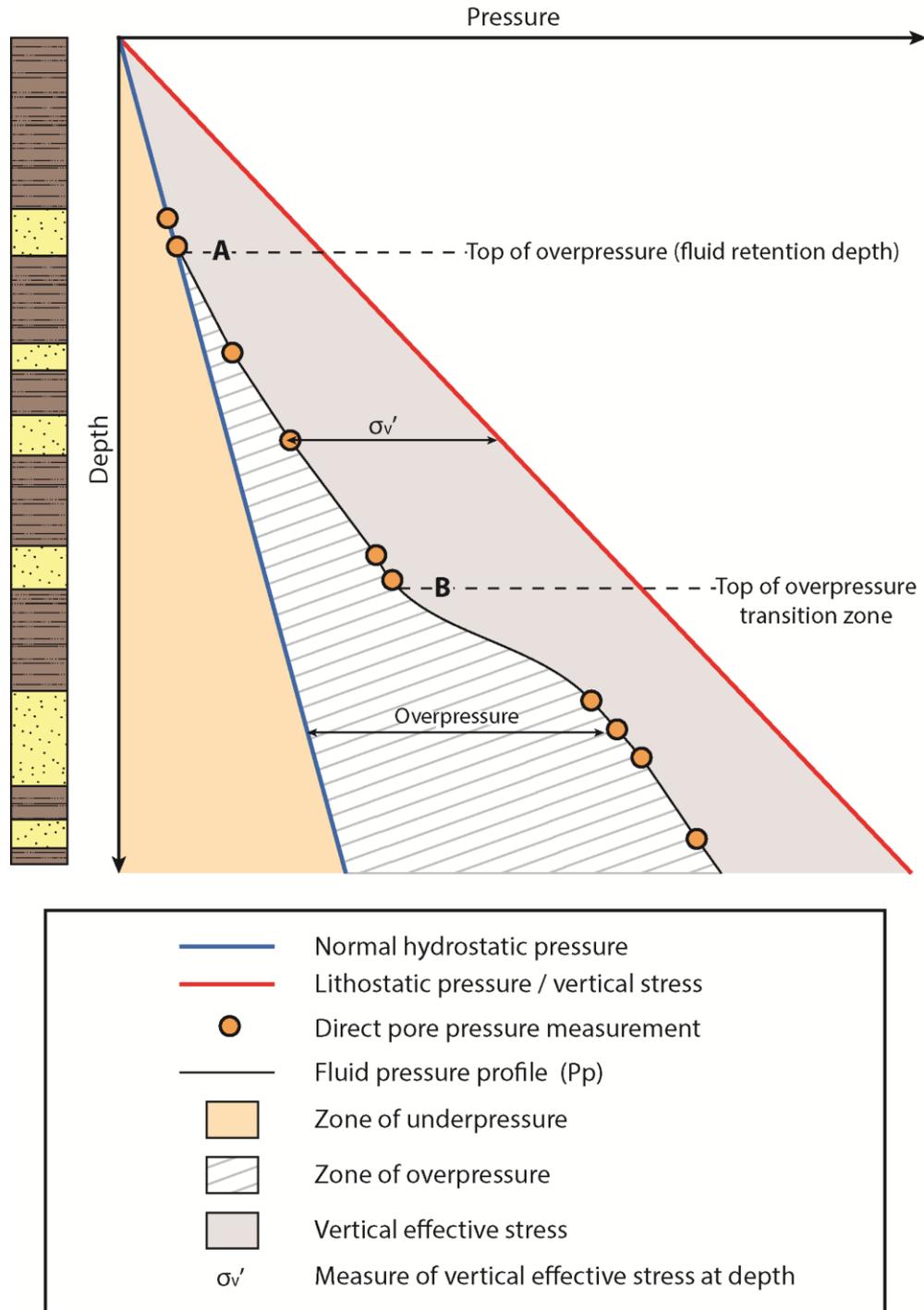
Figure 3.1 - Typical pressure-depth (P-D) plot encountered within a sedimentary basin illustrating some of the key concepts and terms used in pressure analysis and evaluation.

$$P_{hyd} = \rho_w \cdot g \cdot z \qquad \text{(3.1)}$$

where P_{hyd} is the hydrostatic pressure, ρ_w is the average density of water, g is the acceleration due to gravity at the Earth's surface (9.81 m s^{-2}), and z is the vertical depth below a surface datum, e.g. sea level or the water table (on land). The vertical gradient of hydrostatic pressure in water-saturated sedimentary rock is given by the equation:

$$\frac{dP_{hyd}}{dz} = \rho_w \cdot g \qquad \text{(3.2)}$$

where ρ_w is now the local density of pore water. In sedimentary basins such as the Central North Sea, the datum for calculating hydrostatic pressure is sea level. At sea level, atmospheric pressure of 14.7 psia (0.101 MPa) is continually exerted onto the sea surface; consequently, in order to give the *absolute pressure*, the magnitude of atmospheric pressure should be added to the value of hydrostatic pressure calculated from the height of the water column.

The rate of hydrostatic pressure increase with depth is dependent upon the density of the fluid, which in turn is largely dependent upon the salinity of the subsurface water. Fresh water with a fluid density of 1.00 g/cc gives a hydrostatic gradient of 0.433 psi ft^{-1} (9.8 kPa m^{-1}). In contrast, brine-saturated water may have a density of up to 1.20 g/cc, with a fluid gradient of up to 0.52 psi ft^{-1} (11.8 kPa m^{-1}). It is typical on P-D plots for the hydrostatic gradient to be depicted as a straight line. This implies that water salinity and density are constant with depth, there is continuity of the water column from depth to the sea surface, and that the water column is in static equilibrium. In reality, the hydrostatic gradient varies with depth and location according to the salinity of formation waters. However, it is rare to have detailed information on water salinity variations with depth and consequently, in the absence of known water composition, an average water gradient across the area of interest is used. In the Central North Sea, a regional average water gradient of 0.445 psi ft^{-1} (0.0101 MPa m^{-1}) can be used (Holm, 1998; O'Connor and Swarbrick, 2008), which is equivalent to an average water density of 1.03 g/cc. The hydrostatic gradient acts as a comparison and reference gradient to the measured/estimated formation water pressure profile, enabling the determination of abnormal pressure conditions.

Although increasing temperatures and pressures with depth also act to influence fluid density, their effects are considered minimal in relation to salinity (Mouchet and Mitchell, 1989). This is because the effects of increasing pressure and temperature on density are in opposite senses, and their combined effect is smaller than the effect of typical variations in salinity.

Lithostatic pressure. The lithostatic pressure is also known as overburden pressure, overburden stress or vertical stress, and refers to the normal stress acting in the vertical direction that is exerted by the weight of the overlying sediments (or overburden), taking into account both the sediment matrix and pore fluid. In **Figure 3.1**, the lithostatic pressure gradient is represented by the red line. Lithostatic pressure can be expressed by the equation:

$$S_V = \rho_b . g . z \tag{3.3}$$

where S_V is the lithostatic pressure (vertical stress) and ρ_b is the average bulk density of the sediment. The lithostatic pressure gradient is given by the equation:

$$\frac{dS_V}{dz} = \rho_b . g \tag{3.4}$$

where ρ_b is the local bulk density of the sediment.

Bulk density (ρ_b) is a function of both the rock matrix and fluid filled pores, according to the relative volumes they occupy within the rock:

$$\rho_b = \rho_m(1 - \phi) + \rho_f (\phi) \tag{3.5}$$

where ρ_m is the density of the rock matrix, ρ_f is the average density of the fluid occupying the pore space, and ϕ is porosity.

A default lithostatic gradient of 1 psi ft^{-1} (22.62 kPa m^{-1}) is commonly used and corresponds to a common bulk density value of 2.31 g/cc. In reality, sediment density does not remain constant with increasing depth below the seabed. Changes in lithology, porosity and rates of compaction affect sediment density, so a far more accurate method of generating the overburden (lithostatic) gradient is required for detailed pressure analysis.

Formation pore pressure. Pore pressure is the pressure of the fluid within the pore spaces of a rock. The value of formation pore fluid pressure can be obtained through both direct and indirect means depending upon the permeability of the formation being tested (see *section 3.5*). In the example of **Figure 3.1**, direct measurements of pore pressure have been obtained for the subsurface reservoir intervals, enabling interpolation of the formation fluid pressure profile (black line). Pore pressures may be lower or higher than the hydrostatic pressure, but they do not exceed lithostatic pressure. In cases where the pore pressure reaches lithostatic pressure, fractures open so that the pore fluid bears the full weight of the overburden.

Abnormal pressure. Where the formation pore fluid pressure recorded at depth is not equal to the normal hydrostatic pressure for that depth, it is described as being abnormal. Wherever pore pressure exceeds hydrostatic pressure, the rock is said to be overpressured, whereas rocks with pore pressures below hydrostatic pressure are said to be underpressured. **Figure 3.1** illustrates these 'zones' of abnormal pressure. In the example shown, all of the direct pore pressure measurements below depth A are classified as being overpressured. Depth A marks the top of overpressure or the fluid retention depth (discussed further in *section 3.3.1.1*). Underpressure is not discussed further here, except to say that within the Central North Sea where values of underpressure have been found, their likely causes are either reservoir depletion during hydrocarbon production or the use of too high a water density in calculating the hydrostatic gradient.

Vertical effective stress (σ_V'). The vertical effective stress is the difference between the lithostatic pressure (vertical stress) and the pore fluid pressure (Terzaghi, 1943):

$$\sigma_V' = S_V - P \qquad\qquad (3.6)$$

Remembering that lithostatic pressure takes into account the pressure exerted by both the combined overlying rock matrix and pore fluid, it can be seen that, in physical terms, the vertical effective stress is the pressure which is borne solely by the grain to grain contacts making up the rock matrix (**Figure 3.2**). Under conditions of normal burial, i.e. hydrostatic conditions, vertical effective stress can be seen to increase with depth (**Figure 3.3**).

$$S_v = P_p + \sigma_v'$$
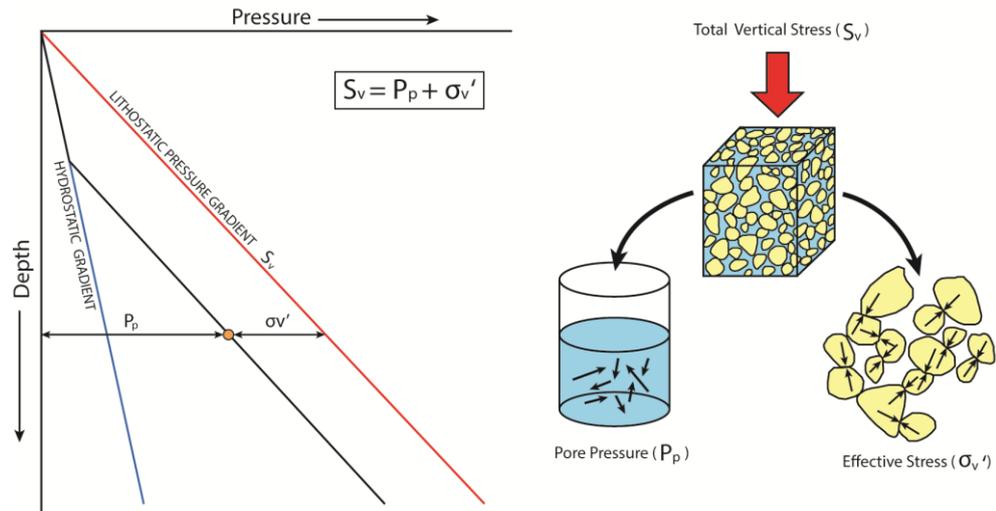
Figure 3.2 - P-D plot illustrating vertical effective stress and Terzaghi's (1943) equation.

Vertical effective stress cannot be measured directly. As *Equation 3.6* above indicates, its calculation is dependent upon the measured/estimated values of pore pressure and lithostatic pressure at a given depth.

3.3. Overpressure and the main mechanisms of generation

Overpressure can be described as the excess pressure above the predicted hydrostatic pressure at a particular depth (Mouchet and Mitchell, 1989; Swarbrick and Osborne, 1998), as shown in **Figure 3.1**. Overpressure is a common phenomenon in many of the world's basins (Hunt, 1990; Law and Spencer, 1998) and numerous mechanisms have been proposed for its generation within the subsurface. Swarbrick *et al.* (2002) provide the most recent critical review of the main overpressure generating mechanisms, along with estimations of the relative magnitudes of overpressure which may realistically be produced from such mechanisms.

Mechanisms capable of generating large magnitudes of overpressure can be classified as either stress-related, i.e. loading mechanisms, or due to fluid volume increase, i.e. fluid expansion or unloading mechanisms. Small magnitudes of overpressure may also be generated through other mechanisms, including hydrocarbon buoyancy and fluid movement (Swarbrick *et al.*, 2002). In many situations, more than one mechanism of overpressure generation may be responsible for the observed

52
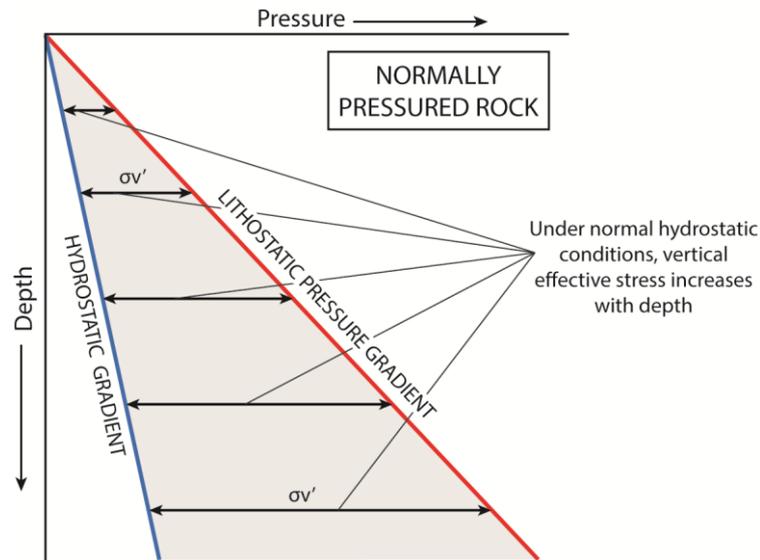
Figure 3.3 - Pressure-depth plot showing that under circumstances of normal burial, i.e. hydrostatic pressure conditions, vertical effective stress increases with depth.

magnitudes of overpressure present within a basin (Gaarenstroom *et al.,* 1993; Kooi, 1997). A brief summary of each mechanism is provided within the following sub-sections.

3.3.1. Stress-related mechanisms

The stress-related mechanisms for overpressure generation reviewed by Swarbrick and Osborne (1998) include disequilibrium compaction and tectonic stress. Both of these mechanisms involve compression of the rock volume, either vertically or horizontally. When fluids cannot escape fast enough from the reducing rock volume increased pore pressure results. Stress-related mechanisms of overpressure generation have commonly been described as 'loading mechanisms' within the literature, because the root cause of overpressure is increase in confining stress, albeit other criteria must be met for overpressure to develop.

3.3.1.1. Disequilibrium compaction

During sediment compaction, increases in vertical stress caused by progressive gravitational loading can result in incomplete dewatering of sediment and consequently

53

the generation of overpressure, since pore fluids begin to bear some of the overburden weight. This process termed 'disequilibrium compaction', is considered the most effective mechanism for generating overpressures in young sedimentary basins (Swarbrick *et al.*, 2002), where rapid burial of typically muddy sediments means that fluids cannot be expelled fast enough to maintain hydrostatic pressure conditions (Swarbrick and Osborne, 1998). Generation of overpressure through disequilibrium compaction is controlled principally by the rate of sediment loading and the rate of fluid escape from the compacting sediments, the latter being dependent upon rock properties such as rock compressibility, porosity and permeability (Luo and Vasseur, 1992; Swarbrick and Osborne, 1998).

The depth at which overpressure is developed by disequilibrium compaction is termed the 'fluid retention depth' (Swarbrick *et al.*, 2002) or 'top of overpressure' (**Figure 3.4**). Swarbrick *et al.* (2002) noted how depth to top overpressure relates directly to the magnitude of overpressure which can be generated via disequilibrium compaction, since overpressure will increase along a gradient that is no steeper than the lithostatic gradient. For example, where top overpressure develops at shallow depth, due to rapid sedimentation rates of lower permeability, highly compressible sediments such as mudrock, large magnitudes of overpressure are developed at depth (**Figure 3.4**). In contrast, smaller magnitudes of overpressure, if any, are likely to develop where higher permeability, less compressible sediment such as sandstone has been gradually compacted. In such cases, the fluid retention depth is likely to be much greater.

3.3.1.2. *Tectonic stress*

By the same principle that increased vertical stress associated with gravitational loading can cause overpressure generation, increased horizontal stresses may also generate overpressures within a sediment column. Lateral compressive stresses in excess of those generated by passive burial are the result of tectonic forces, and examples of overpressure generation derived by this mechanism have been documented by Byerlee (1993) in and around major fault zones; by Davis *et al.* (1983), Neuzil (1995) and Fisher and Zwart (1996) within accretionary sedimentary prisms related to tectonic subduction; and by Darby and Funnell (2001) within the East Coast Basin, New Zealand, i.e. a
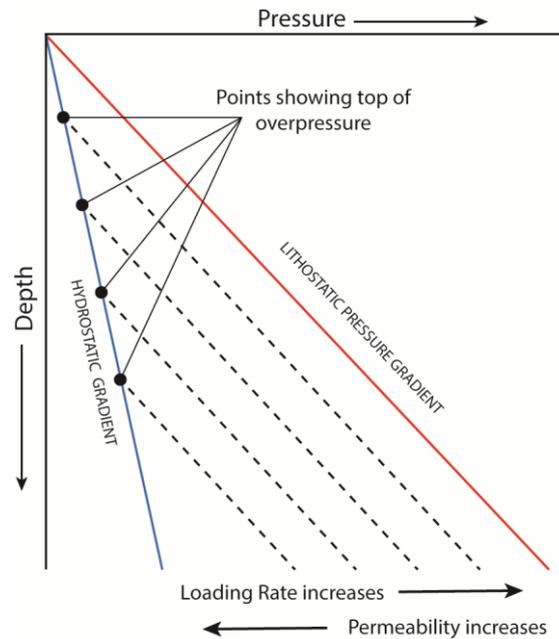
Figure 3.4 - P-D plot illustrating varying pressure profiles created through disequilibrium compaction of fine-grained sediments. In each case, the depth of top overpressure (or fluid retention) is controlled by the sedimentation rate, i.e. loading rate, and sediment permeability (modified from Swarbrick *et al.*, 2002).

convergent plate margin setting. Van Ruth *et al.* (2003) give an example of overpressure generation due to tectonic lateral stresses in the Cooper Basin, Australia.

3.3.2. *Fluid volume increase mechanisms*

Overpressures can be generated within sedimentary rocks where there is an increase in pore fluid volume in situ, which implies some inhibition of pore fluid escape from the system. They may result from expansion of pre-existing pore fluids or from the generation of new pore fluids associated with changes in the ratio of solid to liquid in the rock (Swarbrick and Osborne, 1998). In all fluid volume increase mechanisms, the magnitude of overpressure generated is controlled by the rate of volume change, as well as the rock properties within which the change occurs (Swarbrick *et al.*, 2002).

Fluid volume increase mechanisms are often referred to as 'unloading' mechanisms since the effective stress decreases when these mechanisms generate additional pore pressure (Lahann and Swarbrick, 2011). In cases where load-bearing

55

grains are fully or partially transformed into fluid, stresses which were previously carried by grain-to-grain contacts are transferred to the pore fluid (**Figure 3.5**). In this way, fluid volume increase mechanisms differ from the stress-related (loading) mechanisms of overpressure generation, since the latter do not cause effective stress to decrease, but rather fluid retention inhibits the effective stress from decreasing by preventing the sediment from compacting. The most commonly cited causes of fluid expansion mechanisms (i.e. volume increase) within the literature are hydrocarbon generation, clay diagenetic processes, and aquathermal expansion (Osborne and Swarbrick, 1997). These mechanisms are briefly discussed below.

3.3.2.1. Hydrocarbon generation

Hydrocarbons are generated via two principal routes: transformation of kerogen into oil and gas, and cracking of pre-existing oil into gas (Swarbrick *et al.*, 2002).

Generation of hydrocarbons from kerogen typically occurs at depths of around 2.0-4.0 km and at temperatures of around 70-120 °C (Tissot *et al.*, 1987). Overpressure generated during the transformation of kerogen can result from two coeval processes, expansion of pore fluids and transference of any load previously borne by the solid kerogen onto the pore fluid (i.e. load transfer as illustrated in **Figure 3.5**). Overpressure generation resulting from kerogen maturation occurs solely within the source rock of a basin. With regard to expansion of pore fluid, there is considerable uncertainty within the literature concerning the total volume change which accompanies kerogen maturation into hydrocarbons (Meissner, 1978; Ungerer *et al.,* 1983; Swarbrick and Osborne, 1998). Volumes may vary depending upon the type of kerogen being transformed, as well as the density and volume of the petroleum products generated (Swarbrick *et al.,* 2002). Meissner (1978) showed that for a type II kerogen within a sealed environment, volume increase could be as large as 25% during oil generation, and more than 100% during generation of dry gas. In contrast, however, Ungerer *et al.* (1983) show a small volume decrease of around 3-6 % during maturation of type II kerogen into oil, but a large volume increase of 57% during the generation of gas (**Figure 3.6**). Calculations by Swarbrick *et al.* (2002), have shown that volume increases may be as high as 75-140 % in the source rock during the later stages of oil maturation into gas generation, which they estimate to be an overpressure increase of
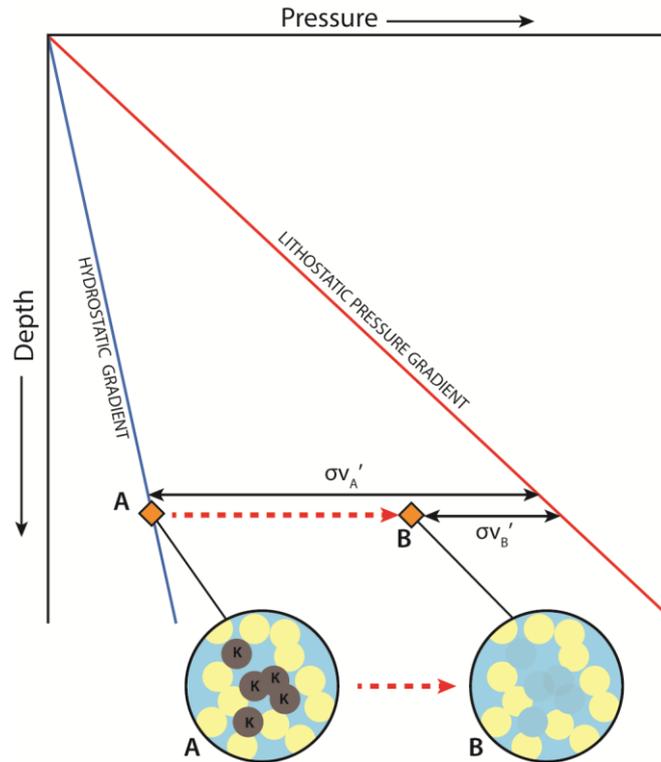
Figure 3.5 - Schematic P-D plot showing overpressure generation through load transfer whereby transformation of grains (in the above example, kerogen) into pore fluid (i.e. oil or gas) means that the overburden stress borne by grain-to-grain contacts is transferred to pore fluids and thus the effective stress is decreased (modified from Swarbrick and Osborne, 1998).

around 70-6000 psi (0.4-41 MPa) in most sedimentary basins. Hansom and Lee (2005) most recently estimated, through numerical modelling of the Delaware Basin USA, that oil and gas generation could increase overpressures by approximately 40% and 110%, respectively, above that generated through disequilibrium compaction, with oil generation producing overpressures as high as 1837 psi (~ 13 MPa) and gas generation, caused by both kerogen transformation and oil cracking, accounting for up to 4776 psi (~ 33 MPa) overpressure.

Cracking of oil into gas typically occurs at depths of around 3.0-5.5 km and temperatures of around 90-150°C (Barker, 1990). Overpressures are generated by oil cracking, through expansion of pore fluids only, with no influence of load transfer. Large volume increases have been calculated for gas generation in a sealed environment, where resulting pressures may approach the lithostatic gradient (Barker, 1990; Swarbrick and Osborne, 1998). Cracking is not likely to occur within sealed

After Meissner (1978):

After Ungerer _et al._ (1983):
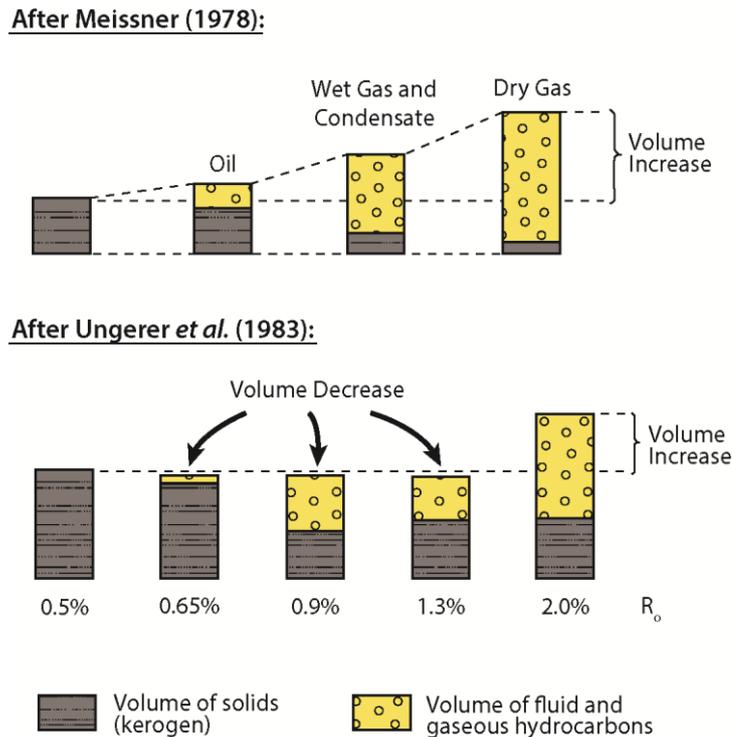
Figure 3.6 - Estimations of volume change generated when Type II kerogen matures, as made by Meissner (1978) for the Bakken shale, Williston Basin; and Ungerer _et al._ (1983) for the Toarcian Black shale, Paris Basin (after Swarbrick and Osborne, 1998).

source rocks, but rather within reservoir rocks where pre-existing oil accumulations exist. Consequently, Swarbrick _et al._ (2002) stated that magnitudes of overpressure produced from gas generation are likely to be proportionately reduced where pore volumes within the reservoir are connected.

It is clear that hydrocarbon generation and in particular gas generation can result in significant magnitudes of overpressure, although the exact magnitudes of overpressure are still subject to debate.

3.3.2.2. Clay diagenetic processes

There are several clay diagenetic processes which are thought to generate overpressures during sediment burial, including smectite dehydration, smectite-illite transformation, kaolinite-illite transformation and gypsum dehydration to anhydrite. Each process involves the release of mobile water and may result in overpressure generation because

58

the products of the reaction would occupy a greater volume than the reactants under conditions of constant stress and pore pressure. Additionally, during transformation processes, overpressure may be generated through compaction of the matrix such that the normal compaction curve shifts to lower porosity for the same value of effective stress (**Figure 3.5**). If escape of the excess fluid is inhibited, overpressure develops by load transfer because the pore fluid bears an increased proportion of the confining stress (Lahann and Swarbrick, 2011).

Smectite dehydration. Water bound within the mineral lattice of smectite is progressively removed during dehydration. Swarbrick and Osborne (1998) estimated that such removal of bound water accounts for a volume increase of 4.0%, which occurs over three equal stages of ~ 1.3 % volume. The first two stages of smectite dehydration occur at shallow depths of around 0.5-1.0 km, where sediments are relatively un-compacted and of high permeability, so overpressure generated at this depth is likely to be negligible (Swarbrick *et al.*, 2002). Swarbrick *et al.* (2002) estimated that the third stage of smectite dehydration, occurring at depths of 3.0-5.0 km, could generate overpressures up to 100 psi (0.7 MPa). This value is likely to be an overestimate, since it assumes all muds to be composed entirely of smectite.

Smectite-illite transformation: Around temperatures of 80°C, smectite is chemically altered to produce illite (Boles and Franks, 1979). This reaction can be summarized as:

$$smectite + K^+ \text{ ions} \longrightarrow illite + silica + H_20$$
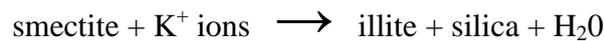
where K^+ ions are typically sourced from the dissolution of K-feldspar or mica during progressive burial (Hower *et al.*, 1976). The exact chemistry of this reaction is at present still fairly poorly understood (Swarbrick and Osborne, 1998) and several estimations of the volume change which accompanies the smectite to illite reaction have been made (Hower *et al.*, 1976; Boles and Franks, 1979; Swarbrick and Osborne, 1998). Most recently, Osborne and Swarbrick (1999) calculated a range of volume changes from a 4.1% increase to a 8.4% decrease, for 10 different reaction pathways, again assuming that the reacting initial mud is composed entirely of smectite. Swarbrick *et al.* (2002) concluded that pore fluid volume changes associated with the smectite to illite transformation are unlikely to contribute significantly to overpressure generation since

rates of volume increase is too low. Alteration of smectite to illite is also thought to generate overpressures through the process of load transfer (Lahann, 2002; Lahann and Swarbrick, 2011) whereby the dissolution of load-bearing smectite, along with the preferential orientation of neoformed illite during diagenesis and compaction, may act to weaken the sediment framework (Lahann and Swarbrick, 2011) decreasing sediment permeability, increasing sediment compressibility and potentially increasing pore fluid pressures. Much larger magnitudes of overpressure are thought to be generated through load transfer associated with smectite-illite transformation. Lahann and Swarbrick (2011) calculated up to 1500-3000 psi (10.3-20.7 MPa) overpressure for the Gulf of Mexico, albeit in Neogene sediments that are anomalously rich in smectite (Tingay *et al.*, 2013).

Kaolinite-illite transformation. Much like the smectite-illite transformation, kaolinite can be transformed into the less hydrous mineral illite during compaction, resulting in the release of bound water and load transfer. Transformation of kaolinite occurs at temperatures around 130°C (Bjørlykke, 2006), slightly higher than the smectite to illite reaction.

Gypsum-anhydrite dehydration. At temperatures of 40-60°C, gypsum is progressively transformed into anhydrite through dehydration (Swarbrick and Osborne, 1998). This release of bound water within evaporite sections can generate large magnitudes of overpressure at relatively shallow depths. Through modelling, Jowett *et al*. (1993) showed that overpressures in excess of the lithostatic stress can potentially exist at depths of only 1.0 km. Obviously; however, such mechanisms can only be active at shallow depths within basins where large thicknesses of gypsum are present.

3.3.2.3. Aquathermal expansion

When heated above 4°C water expands. Barker (1972) first suggested that thermal expansion of pore water during burial could be a contributory factor in the development of overpressure and coined the term, 'aquathermal expansion'. When heated in a perfectly sealed environment, water pressure rise is rapid, with the overall amount of pressure increase being dependent upon the density and thus compressibility of the water (Osborne and Swarbrick, 1997, Fig. 5). As an example, they calculated that heating a sealed body of water with a density of 0.99 g/cm^3 from 54.4°C to close to
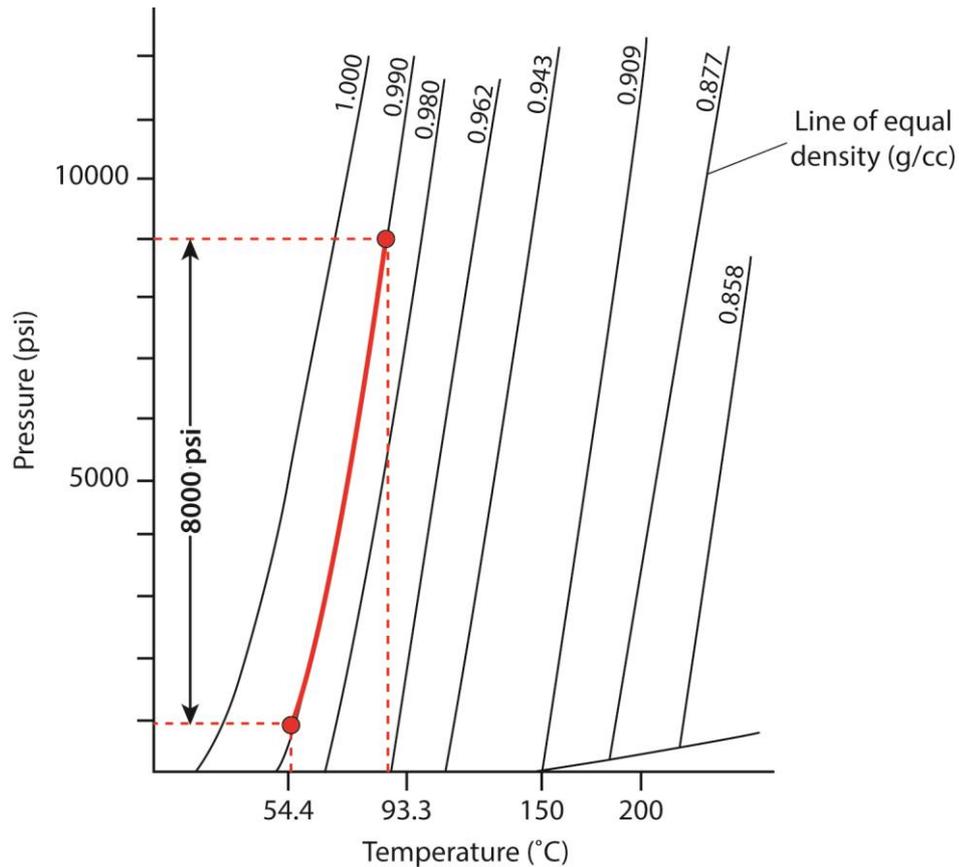
Figure 3.7 - Pressure-temperature plot showing how the magnitude of overpressure developed from aquathermal expansion is influenced by water density (after Osborne and Swarbrick, 1997).

93.3°C would cause a pressure increase of around 8000 psi (**Figure 3.7**). A completely isolated environment with zero permeability is therefore required for large magnitudes of overpressure to be generated through aquathermal expansion (Swarbrick and Osborne, 1998). In reality, environments such as these are unlikely to exist. Luo and Vasseur (1992) have shown using one-dimensional numerical modelling that negligible amounts of overpressure are generated in mudstones through aquathermal expansion, even when unrealistically low permeabilities of 10^{-12} mD were used in models, which are several orders of magnitude lower than the measured permeabilities of actual shales (Deming, 1994). A simple calculation carried out by Swarbrick *et al.* (2002) further supports the work of Luo and Vasseur (1992) by showing that under a range of typical basin conditions overpressures of only approximately 100 psi (0.7 MPa) are produced by aquathermal expansion. Several authors have argued that aquathermal expansion mechanisms may still be evoked for generating large magnitudes of overpressure. Hunt

61

(1990) argued that diagenetic seals with permeabilities close to zero are feasible in sedimentary basins. Alnes and Lilburn (1998) argued that perfectly sealed environments are not necessary to generate large volumes of overpressure through aquathermal expansion, but rather that water volume increases caused by expansion be maintained via some other process such as smectite-illite transformation.

3.3.3. Other processes

The following mechanisms are those which are have been found to generate relatively low magnitudes of overpressure, and thus are only important on a more local scale as opposed to regional, basin-wide scales (Swarbrick *et al.*, 2002). These processes, which relate more specifically to fluid movement and buoyancy, may act as contributory processes to the previously discussed mechanisms of overpressure generation.

3.3.3.1. Hydrocarbon buoyancy

All gases and most oils have densities which are lower than that of formation water, meaning that they have lower associated pressure gradients. Where hydrocarbons are present within a reservoir that is hydrostatically pressured in the water leg, small amounts of overpressure will always be developed locally within the hydrocarbon phase. The example provided in **Figure 3.8** illustrates this concept. The magnitude of overpressure generated through buoyancy is

$$\Delta P = (\rho_w - \rho_{hc})gh \qquad (3.7)$$

where ΔP is overpressure, ρ_{hc} is hydrocarbon density, and h is the hydrocarbon column height.

3.3.3.2. Hydraulic head

Elevation of the water table in highland areas results in a hydraulic head, and overpressure, within the sediments of adjacent low-lying areas. Where a continuous reservoir unit is in hydraulic connectivity with the charge area, overpressure of the same
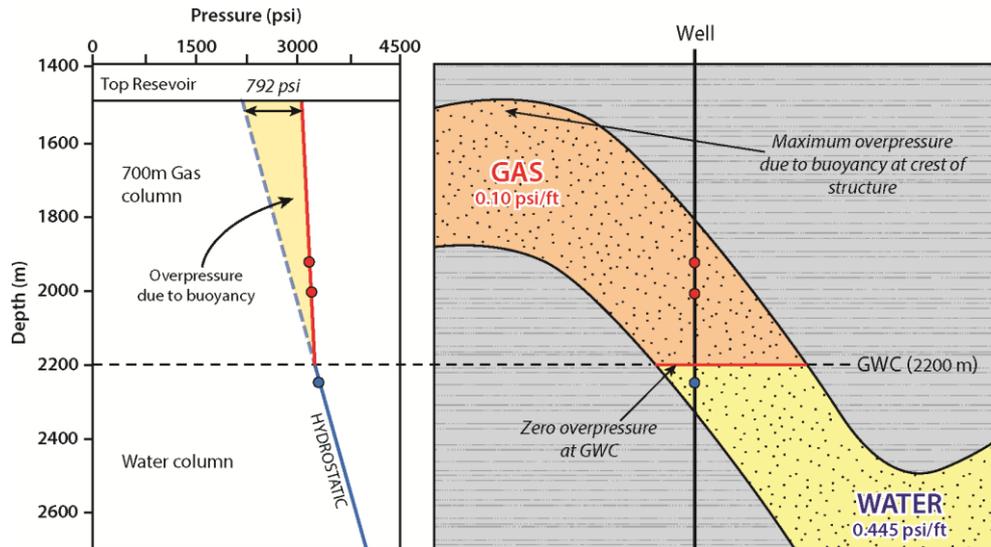
Figure 3.8 - Overpressure due to gas buoyancy, where the pore water in the saturated reservoir is at normal hydrostatic pressure with a pressure gradient of 0.445 psi ft^{-1}. In the above example there is a 700 m gas column with pressure gradient of 0.1 psi ft^{-1}; maximum overpressure of 792 psi due to buoyancy is located at the crest of the structure, falling to zero overpressure at the gas water contact (adapted from Swarbrick and Osborne, 1998).

magnitude as the additional pressure exerted by the hydraulic head may result (**Figure 3.9**). This principle is observed in artesian wells (Swarbrick and Osborne, 1998). Assuming that there is no pressure drop due to water flow in this area, the magnitude of overpressure, *OP*, experienced within the reservoir will be:

$$OP = \rho_w . g . H \qquad (3.8)$$

where *H* is the vertical height of hydraulic head measured above the reference datum, commonly taken to be sea level (Mouchet and Mitchell, 1989).

3.3.3.3. Osmosis

Large contrasts in the salinity of pore fluids across a semi-permeable membrane induce fluid flow by osmosis, from the region of dilute (lower salinity) water to the region of higher salinity water (Marine and Fritz, 1981). Using typical North Sea shales, with 5% porosity and 55% clay content, Swarbrick and Osborne (1998) calculated an upper limit to the magnitude of overpressure generated from osmosis of only 440 psi (3.0 MPa),
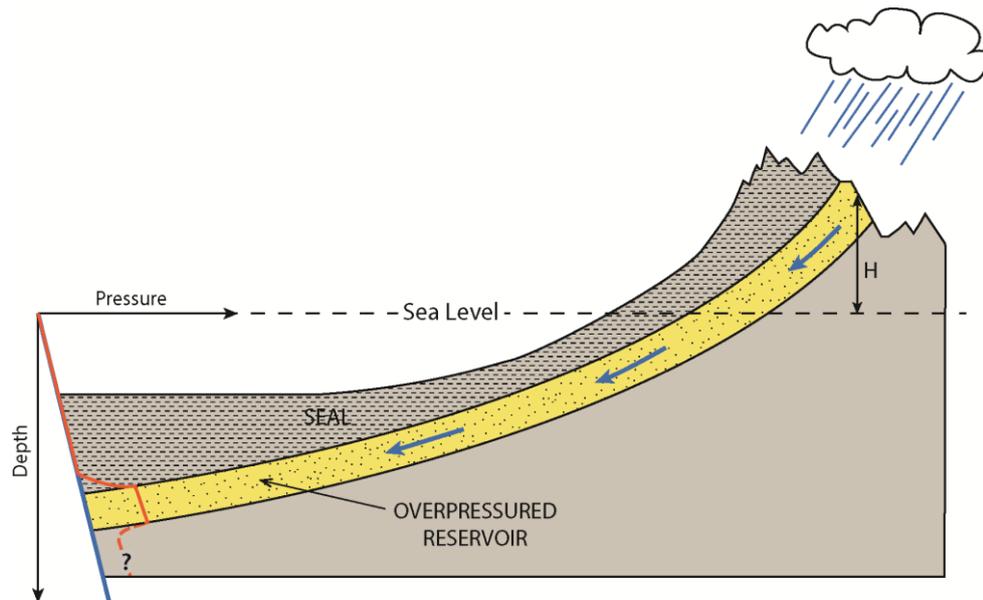
Figure 3.9 - Overpressure due to hydraulic head, H and hydraulic connectivity between a laterally continuous reservoir extending from the recharge area into the subsurface. P-D plot shown to the left of figure illustrates how this reservoir will be overpressured so long as it is capped by a sealing lithology (modified from Swarbrick and Osborne, 1998).

even where salinity contrasts were as large as 35 wt % NaCl equivalent, suggesting that this mechanism is only of local importance (Swarbrick and Osborne, 1998, Fig.9).

3.4. Fluid flow and overpressure as a transient process

Overpressure is a transient process and its distribution and magnitude within a basin will alter over time, depending upon the basin's evolution (Swarbrick and Osborne, 1998). If all overpressure-generating mechanisms within a basin were to cease, the overpressure present would dissipate through time in order to regain a state of hydrostatic equilibrium (**Figure 3.10**). This concept of overpressure as a dynamic process is important to hydrodynamics and fluid migration (Neuzil, 1995; Holm, 1998), and emphasises the importance of sediment permeability as a primary control on the presence and distribution of overpressure (Swarbrick and Osborne, 1998).

Fluid flow through subsurface sediment can be modelled using Darcy's flow equation, which relates the volumetric rate of fluid to the effective permeability of the
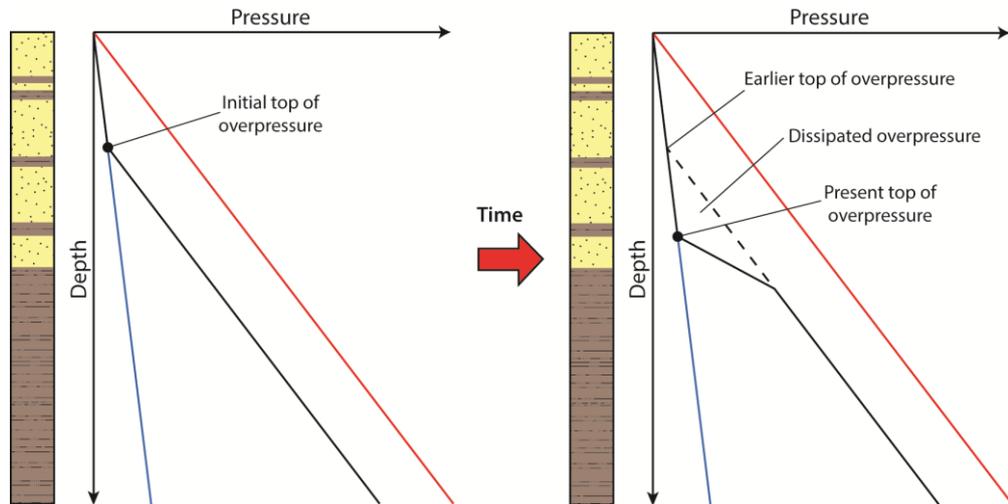
Figure 3.10 - Schematic P-D plots showing overpressure dissipation over time. Assuming that the mechanism for generating overpressure has ceased, the rate of pressure dissipation depends upon sediment permeability. In the above example it can be seen that, over time, the top of overpressure deepens, since fluids are able to dissipate through the higher permeability sandstones in order to equilibrate back to hydrostatic pressure conditions.

rock, flow path dimensions, and the overpressure difference experienced along the length of the flow path:

$$Q = \frac{-k\,A\,\Delta P}{\mu L} \qquad\qquad (3.9)$$

where Q is the flow rate, k is the permeability, A is the area across which flow takes place, ΔP is the overpressure drop along the flow path, μ is the fluid viscosity, and L is the flow path length.

3.4.1. *Pressure transference*

Redistribution of excess pore pressures within the subsurface can lead to areas of locally enhanced pore pressure, or equally areas of diminished pore pressure. Higher permeability sandstones are effective in redistributing excess pore pressure internally, whereas lower permeability lithologies such as shale take longer periods of geological time to equilibrate overpressure profiles (Bjørlykke, 1993).

65

Although not specifically a mechanism for generating overpressure, higher overpressures may be encountered at the structural crests of tilted sandstone bodies where the sandstone is encased within a lower permeability shale sequence, a phenomenon that Yardley and Swarbrick (2000) termed lateral transfer. **Figure 3.11** illustrates lateral transfer where the primary mechanism for generating overpressure is disequilibrium compaction. The pore pressure profile through the higher permeability sandstone body is hydrostat-parallel, at constant overpressure, since fluids can flow easily and equilibrate within the sand. At the top of the tilted sand body, pore pressure is greater than within the surrounding shale, and fluid flows out from the sand into the shale. In contrast, towards the base of the sand, where pressure in the sandstone is lower than those in the surrounding shale, fluids flow from the adjacent shale into the sand. The point where pressures within both the sand and surrounding shales are assumed to be in equilibrium with each other is termed the centroid (**Figure 3.11**). Transference of pressure can also take place vertically, most typically along active non-sealing faults, as documented by Tingay *et al.* (2007).

In all but exceptional circumstances, within for example a pressure seal or any other zone of zero effective permeability (Swarbrick and Osborne, 1998; Deming, 1994), fluids will flow from regions of higher to lower overpressure for as long as there is a source of overpressure available to maintain the pressure gradient. O'Connor and Swarbrick (2008) coined the term 'lateral drainage' for pressure transference on a regional scale, where the direction of fluid flow (along an overpressure gradient) is out of the basin (i.e. fluid escape). Lateral drainage occurs within overpressured basins where higher permeability pathways to the surface/near-surface are available to facilitate fluid flow (**Figure 3.12**). Such pathways may comprise faults, fractures and laterally connected reservoir packages (O'Connor and Swarbrick, 2008). The presence of drainage within a basin can be recognised on pressure-depth plots where deeper buried sediments are at lower overpressure than the sediments directly above them, i.e. 'pressure reversals' (**Figure 3.12**) (O'Connor and Swarbrick, 2008). Such reversals are characteristic signatures of dewatering, along with 'shoulder effects' (O'Connor and Swarbrick, 2008), where lower overpressure draining units are surrounded vertically above and below by more highly overpressured sediments. Recognising such pressure regressions on actual pressure data is complicated by the fact that direct pore pressure
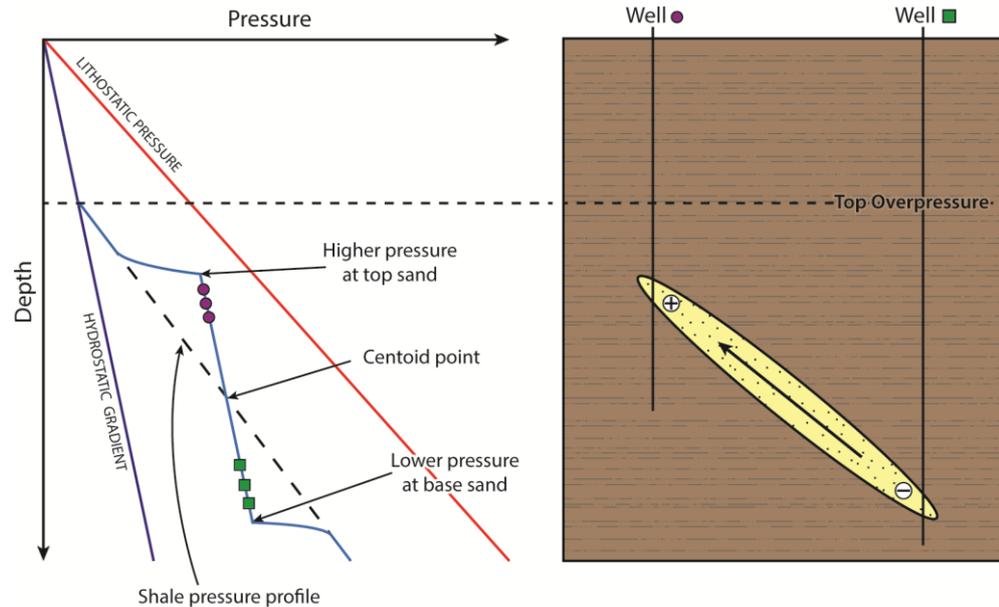
Figure 3.11 - Schematic illustration and P-D plot showing how lateral transfer may enhance and lessen overpressures at the structural crest and base of a tilted sandstone body respectively, when compared to pore pressures within the surrounding mudrock. The depth at which overpressure within the sand and surrounding mud is equal is termed the 'centroid'.

measurements are usually restricted to high permeability reservoir units (see following *section 3.5*).

3.5. Detecting pressures in the subsurface

Understanding sub-surface pressures is complicated by the fact that direct pressure measurements can only be recorded within sediments of sufficient permeability to enable fluids to permeate between the pressure testing tool and the formation over a reasonable period of time. Such lithologies typically comprise reservoir rocks. In lower permeability sediments such as mudrocks and shales, direct pore pressure measurements cannot be obtained due to the length of time that is required for the pressure testing tool to stabilize with the formation. If the tool is left for too long a length of time, there is a risk that it may stick in the borehole, proving costly to the drilling programme. Indirect methods must therefore be used to estimate pressures within lower permeability sediments (Mouchet and Mitchell, 1989; Bowers, 2002; O'Connor *et al.,* 2008).
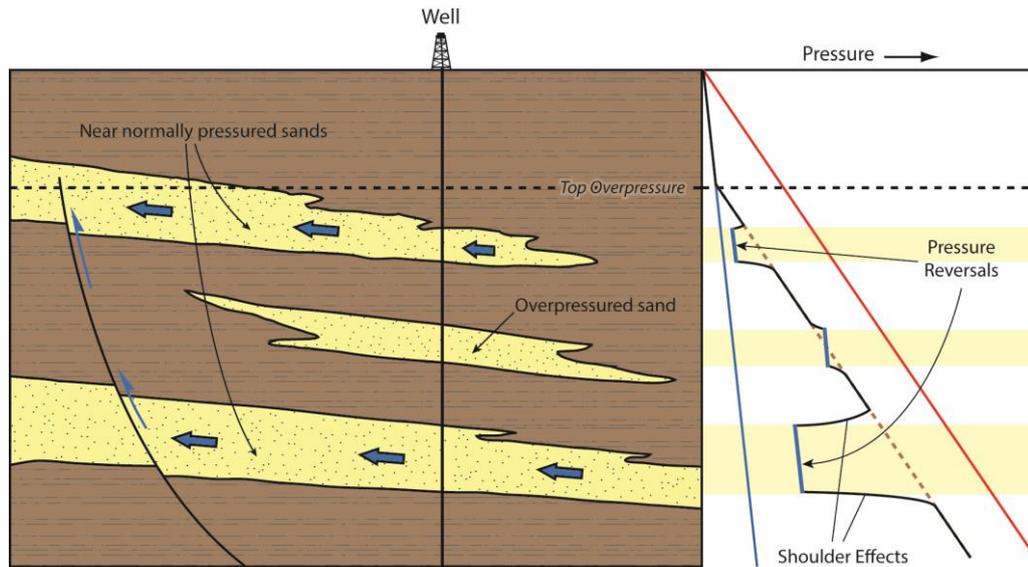
Figure 3.12 - Schematic block diagram and P-D plot illustrating lateral drainage. Fluids flow preferentially along higher permeability pathways from regions of higher to lower overpressure. Pathways for fluid flow may include higher permeability sandstones or non-sealing faults (as above). On P-D plots lateral drainage is identified by pressure reversals, where sandstone overpressure is lower than in the surrounding mudrock. Shoulder effects may occur where fluids drain out from the surrounding mud. In the example above, the smaller middle sands further illustrates lateral transfer as was shown in **Figure 3.11**.

3.5.1. *Direct pressure measurements*

There are several types of test which can be used to directly measure formation pressures, where permeability of the sediments is sufficiently high. These include wireline formation testing tools such as the commonly used Repeat Formation Tester (RFT), the Formation Multi-Tester (FMT), the older Formation Interval Tester (FIT) and the most recently developed Modular Formation Dynamics Tester (MDT). Ireland *et al.* (1992) discussed the evolution of each of these tools through time. For each of the wireline formation tester tools, pressure measurements are obtained during wireline logging in an open hole. The selected tool is lowered down the uncased hole on a drill string, and is then jacked and sealed against the borehole wall. A small probe, extending from the tool, is inserted into the formation wall and the rate at which pressure builds up within the tool is recorded using a pressure gauge (**Figure 3.13**).

Other methods of obtaining direct pore pressure measurements include the Drill Stem Test (DST), which is typically carried out during drilling when zones containing
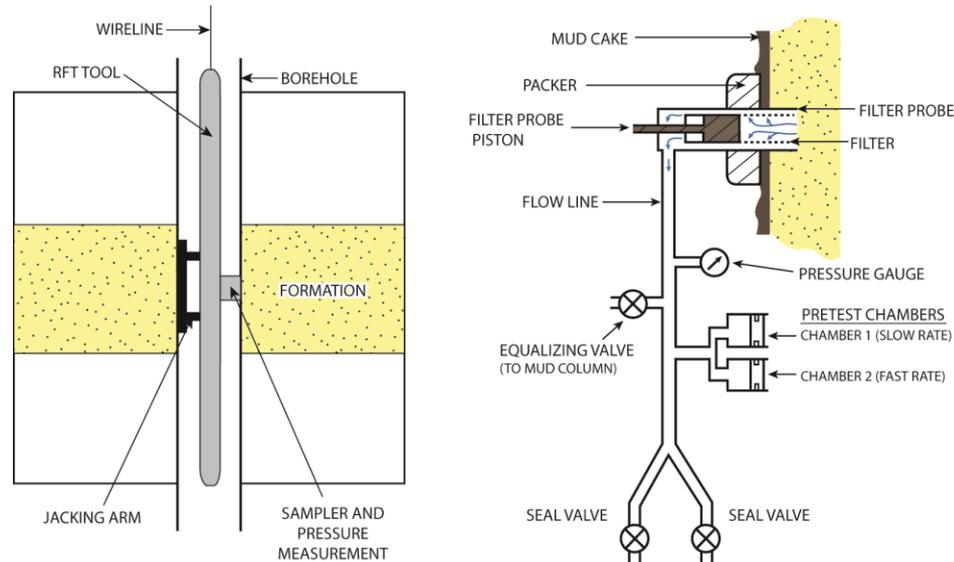
Figure 3.13 - Schematic illustration of the RFT wireline tool (courtesy of Schlumberger).

hydrocarbon have been found using perforated drill pipe and packers; and production tests, which are typically used to sample hydrocarbons during the final stages of well completion. Well 'kicks' may also provide a direct indication of formation pressures. Kicks occur where formation pressures exceed the weight of mud being used whilst drilling. In such cases, the borehole will gain fluid, causing mud volumes to increase within the mud pit on the drilling rig floor. Since the density of drilling mud is known, the formation pressure can be calculated, provided that the depth at which fluid influx occurred is known.

3.5.2. *Indirect pressure measurements*

Detection or estimation of subsurface fluid pressures through indirect means can be obtained from a variety of methods including mud weight history, gas detection, drilling parameter analysis, interpretation of wireline or LWD/MWD log data, seismic interval velocities, and basin modelling (Mouchet and Mitchell, 1989). Depending upon which method is employed; pore pressures may be inferred before, during, or after the drilling programme. Only those methods of indirectly inferring pore pressures which are of most relevance to this research are briefly discussed here:

Mud weight history. In order to maintain optimum conditions during drilling, the mud weight used should be 'balanced' or slightly higher than formation pressures encountered within the uncased borehole. If such conditions are not met in formations of sufficient permeability, mud losses may occur when the drilling mud weight is too heavy, or formation fluids will invade the borehole when the drilling mud weight is too light. The latter is of great importance to drilling safety, and can lead to mud gains and potentially blow-outs. Where drilling occurs through low permeability units, such as claystones, shales and some chalks, drilling may be carried out 'underbalanced' using mud weights which are less than formation pressure, since the low permeability of the formation means that fluids are not able to escape the formation. Apart from not providing an accurate estimation of formation pressure, underbalanced drilling is risky if there is any possibility of encountering sandstone bodies that are encased in mudrocks. The record of mud weight used whilst drilling can provide a useful, albeit imprecise, indicator of formation pore pressures and, except in cases of underbalanced drilling, pressures derived from the mud weight are upper limits to the formation pressure (Darby *et al.,* 1996; Holm, 1998).

Interpretation of wireline or LWD/MWD log data. Pore pressure in fine-grained sediments can be estimated using log data acquired whilst drilling, or after drilling using wireline tools. When data are acquired during drilling, sensors are placed behind the drill head in a process known as Logging While Drilling (LWD) or Measurement While Drilling (MWD). Typical logs obtained and used for pressure analysis of fine-grained sediments include the density, sonic, neutron and resistivity/conductivity logs, since each of these logs can be used to indirectly calculate porosity. Comparisons of the log-derived porosity against a 'normal compaction curve' can then be made to derive formation pore pressures.

Basin modelling. 1D, 2D and 3D basin modelling techniques offer an alternative and complementary approach to predicting pore pressures within subsurface sediments, other than the log-based prediction methods mentioned. Basin modelling is a technique used to numerically model the physical processes operating within a sedimentary basin (Hermanrud, 1993) and requires creating a physical description of the evolution of a sedimentary basin and its component parts in time and space (Giles *et al*., 1999). As with all prediction methods, there are limitations and assumptions implicit in the techniques applied, the main uncertainties in basin modelling being associated with the

porosity and permeability evolution of mudrocks during compaction (Swarbrick *et al.*, 2005).

3.6. Central North Sea overpressure

A multi-well P-D plot for the Central North Sea region is shown in **Figure 3.14.** This plot was composed using direct pressure measurements supplied to the study for several wells within UK blocks 23/26 and 23/27 and represents one of the deeper areas of the Central Graben, where the top Chalk is at depths around 10830 ft (3300 m) TVDSS. Direct pore pressure measurements are recorded within higher permeability reservoir intervals, most notably belonging to the Late Jurassic Fulmar sandstone, the Eocene/ Palaeocene submarine fan sands, and occasional sands within the upper Tertiary sediments. Pore pressure measurements are rarely recorded within the intervening lower permeability Tertiary shale and Chalk sequences and consequently formation pressures must be obtained via indirect methods such as the mud weights used during drilling (**Figure 3.14**), although as previously noted in *section 3.5.2* such methods do not always provide an accurate assessment of formation pressures (Darby *et al.,* 1996). The pressure profile can be divided into separate vertical sections (Leonard, 1993) that appear to be based largely on lithology, corresponding to the Tertiary mudstones, the Eocene/Palaeocene sandstones (situated towards the base of the Tertiary sequence), the Chalk group, and the pre-Cretaceous sediments. Although overpressures vary laterally across the Central North Sea, there are several significant features which should be noted in the P-D plot that do apply across the basin: 1) overpressure develops within the Tertiary shale sequence; 2) the Eocene and Palaeocene sandstone members act as a pressure sink (Holm, 1998) with direct pressure measurements indicating that these sands have generally lower pressures than are to be expected within the overlying and underlying lower permeability sequences; 3) most notably, that pressures measured within the pre-Cretaceous sediments are much larger (> 7500 psi or 50 MPa) than those measured within the post-Cretaceous sediments, so much so that they approach the assumed lithostatic pressure gradient of 1 psi ft^{-1} (0.023 MPa m^{-1}); and 4) a zone of pressure transition must occur between the Palaeocene and Jurassic intervals, which is likely to incorporate the low permeability Chalk sequence. The P-D plot highlights the complexity of the Central North Sea pressure system, in addition to several of the uncertainties associated with pressure evaluation of the region. For example, the shape
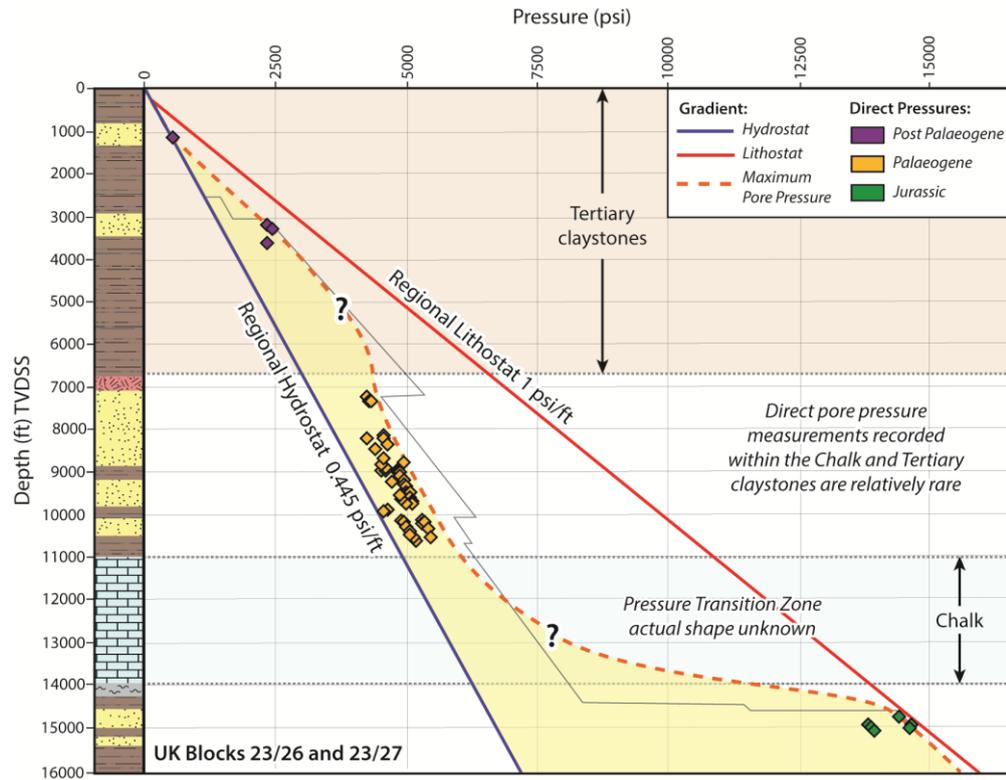
Figure 3.14 - Typical pressure profile for the deeper part of the Central North Sea region generated using data collected from multiple wells in UK blocks 23/26 and 23/27.

and positioning of the pressure transition zone between the Chalk and pre-Cretaceous sediments is uncertain, as is the extent of the shoulder effect which is created around the Palaeogene sandstone members.

3.6.1. *Main mechanisms for generating overpressure in the CNS*

The general consensus is that the primary mechanism for overpressure generation in the Central North Sea is disequilibrium compaction, with secondary mechanisms such as gas generation and lateral transfer contributing to overpressure in deeper areas of the basin (Darby *et al.*, 1998; Swarbrick *et al.*, 2000; Daniel 2001; Swarbrick *et al.*, 2005). Continued debate still surrounds the actual magnitudes of overpressure which may be generated through each of these mechanisms (Holm, 1998; Swarbrick *et al.*, 2000; Daniel 2001; Yardley and Swarbrick, 2000; Swarbrick *et al.*, 2005). In the Palaeogene

strata of the Central North Sea, disequilibrium compaction is thought to be the sole mechanism of generating overpressure, owing to the rapid rates of burial which have persisted since the early Palaeocene (see *section 2.4.1*). Approximately 9840 ft (3000 m) of sediment has been deposited since the Oligocene, i.e. over the past 34 Ma alone (Fyfe *et al.,* 2003) with the upper 4920 ft (1500 m) of this sediment thought to have been exclusively deposited during the Pleistocene and Quaternary (Swarbrick *et al.*, 2000). Rates of compaction greatly exceeded rates of fluid escape within the accumulating low-permeability sequences and large magnitudes of overpressure have resultantly developed over time. The top of overpressure across the basin (marked by the fluid retention depth) is thought to occur at around depths of 1.0 km (3280 ft) (O'Connor and Swarbrick, 2008; Leonard, 1993); however, the actual variability of top overpressure across the basin remains largely unknown and, consequently, so too does the overall magnitude of overpressure which may be generated through disequilibrium compaction. Modelling techniques carried out by several authors (Cavanagh *et al*., 1996; Swarbrick *et al.*, 2000, 2005) have shown that disequilibrium compaction alone cannot account for the large magnitudes of overpressure recorded within the pre-Cretaceous strata of the Central North Sea, where pore pressures approach the fracture pressure (**Figure 3.14**). Cavanagh *et al*. (1996) found that simulated overpressure based on disequilibrium compaction alone was nearly 25% lower than the measured pressures recorded within Late Jurassic reservoirs, whereas Swarbrick *et al.* (2005) found it was closer to 30% lower. Consequently, other mechanisms of overpressure generation must be in operation (Swarbrick *et al.*, 2002). Gas generation is thought to be the most likely candidate (Holm, 1998; Swarbrick *et al.*, 2005), owing mainly to the presence of the high TOC, Kimmeridge Claystone which is currently gas generative below depths of 12700 ft (4000 m) (Cornford, 1994). Lateral transfer may also contribute to overpressure in deeper areas of the basin; however, Yardley and Swarbrick (2000) have found through 1D and 2D modelling of the Central Graben that the overall effectiveness of this mechanism is minor, contributing only 7% of the total overpressures measured. Other mechanisms such as clay diagenesis are thought to have minimal contributions to overpressures in the Central North Sea, particularly since smectite is generally not abundant in the North Sea sediments (Osborne and Swarbrick, 1999).

3.6.2. Distribution of overpressure

Overpressure is a dynamic process which varies both laterally and vertically within the Central North Sea Basin. Many authors have examined the lateral pressure variations which occur across the basin at different stratigraphic intervals (Cayley, 1987; Gaarenstroom *et al.*, 1993; Leonard, 1993; Holm, 1998; Moss *et al.*, 2003; O'Connor and Swarbrick, 2008; Robertson *et al.*, 2013), with Moss *et al.*, (2003) providing a concise account for each interval.

In the pre-Cretaceous strata, overpressure can be seen to increase towards central areas of the basin, reaching magnitudes in excess of 7250 psi (50 MPa) around UK quadrants 22 south and 29 north (Moss *et al.*, 2003, Fig. 18.12a) where the sediments are most deeply buried (Gaarenstroom *et al*., 1993). Additionally, this area corresponds to the area of greatest rates of post-rift sedimentation, the highest graben temperatures, in excess of 200°C, and areas where the Kimmeridge Clay source rocks are most mature (even overmature). As Moss *et al*. (2003) states, each of these factors are likely to contribute towards the observed overpressure distribution. Several pressure compartments exist across the basin, which are largely controlled by the underlying basement fault pattern (Burhig, 1989; Gaarenstroom *et al.,* 1993). Each fault-bounded pressure compartment is seen to contain pre-Cretaceous overpressures of similar magnitude and there are commonly considerable changes in overpressure between adjacent compartments (Holm, 1998). The presence of such 'fault-bounded' pressure compartments implies that there is limited or slow lateral flow of fluids within the pre-Cretaceous strata, caused perhaps by sealing boundary faults or discontinuity of sandstone members (Holm, 1998).

Direct pressure measurements recorded within the Chalk are usually rare, being restricted to reservoir intervals and occasional highly fractured zones. Reservoir chalk comprises approximately 10% of the entire Chalk succession (Mallon and Swarbrick, 2008) and its distribution is largely limited to the Upper Cretaceous section, most commonly around the Ekofisk hydrocarbon fields in Norwegian quadrant 2. Overpressures within the Upper Cretaceous section have been mapped most recently by Moss *et al*. (2003, Fig. 18.12b) and Dennis *et al.* (2005, Fig. 3). Such maps indicate that Chalk overpressures are above hydrostatic almost everywhere, with the highest overpressures occurring towards the southeast of the basin (UK quad 30 and Norwegian quad 2); where the overlying Tertiary sandstone reservoirs are thin or absent (Dennis *et*

al., 2000, 2005). Chalk overpressures decrease gradually towards the NW, suggesting lateral drainage of fluids within the Chalk or simply that overpressures may be bleeding-off into the overlying Tertiary sands (Dennis *et al.,* 2005). Little is known regarding pressures within the remainder of the Lower Cretaceous non-reservoir chalk sequence, other than it is likely that the pressure transition to high Jurassic overpressure is developed within this unit.

Within the laterally extensive, largely unfaulted Palaeocene fan sandstones, pore pressure is close to hydrostatic pressure over a wide area, increasing gradually towards the distal margins of the fans in the SE of the basin (**Figure 3.15**). The Palaeocene fan sandstones, which progressively thicken and sub-crop beneath the Moray Firth seabed in the NW of the basin (Dennis *et al.,* 1998), provide a pathway for fluids to drain laterally from the surrounding more highly overpressured areas of the graben. There are several published regional scale examinations of Palaeogene overpressure distribution within the Central North Sea (Lindberg *et al.,* 1980; Cayley, 1987; Holm, 1998; O'Connor *et al.,* 2008), although in most of these previous works, the Palaeocene strata have been classified as a single draining unit, with little detail regarding individual fan units.

The early attempt by Lindberg *et al.* (1980) to understand regional pressure distributions in the North Sea concentrated solely on the Norwegian sector, where pressure data were collected from 60 wells across two distinct regions of the Northern and Central North Sea. Due to the comparatively small number of wells available, the sole conclusion was that Tertiary overpressures decrease northwards across the basin.

Cayley (1987) inferred that deep graben-bounding faults and diapiric salt structures provide pathways for hydrocarbon migration into the Palaeogene strata, since fracture networks within the Chalk are likely to have formed around such features, facilitating vertical migration of fluids up from the highly overpressured Jurassic strata. He observed local lows in Jurassic overpressure around diapiric salt domes in the northern part of UK quadrant 29, which he associated with vertical 'bleed-off'. Cayley (1987) also found that Palaeogene overpressures increase to 3000 psi (20 MPa) in the south-east of the study region, where the Palaeogene sandstones thin and die out (Cayley, 1987, Fig. 8); and he noted that once hydrocarbons had entered the extensive Palaeogene system, they could migrate laterally for long distances.
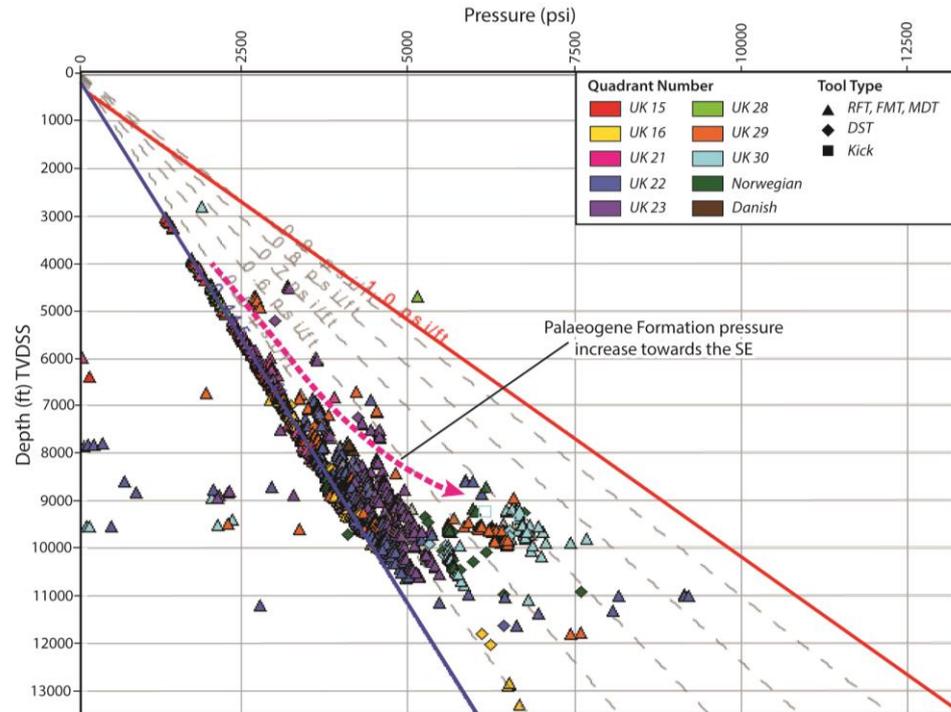
Figure 3.15 - Multi-well P-D plot for the Palaeogene pressure data, organised by quadrant number. The plot shows that overpressures within the Palaeogene increase gradually from hydrostatic pressures in the NW of the basin to higher overpressures of around ~3000 psi in SE areas.

Holm (1988) suggested that locally high overpressure anomalies in the Palaeocene strata of the Central North Sea were the result of isolated and uplifted rafts of Palaeocene sands situated above salt diapirs. O'Connor *et al*. (2008) presented an overpressure distribution map for the Mey Sandstone Member, Central North Sea, which they referred to as the Andrew Formation. They located two high overpressure anomalies in the southern part of UK quadrant 15, where fluid may be draining upwards from the Upper Cretaceous Kopervik (also known as Britannia) Sandstone Member into the Mey Sandstone Member.

3.7. Implications of overpressure and fluid flow within the subsurface

An accurate understanding of subsurface pressure is required in order to ensure safe and successful drilling. Drilling set-backs relating to misinterpretation of subsurface pressures can result in costly and time consuming problems such as loss of muds, well

76

kicks and even blow-outs. From an exploration viewpoint, lateral variations in overpressure resulting in subsurface fluid flow can influence the migration pathways of hydrocarbon through a reservoir (Law and Spencer, 1998) and also cause hydrodynamic trapping and tilted oil-water contacts (Hubbert, 1953).

The migration of hydrocarbons in the subsurface is governed by buoyancy and spatial variations in capillary pressure, in addition to spatial variations in overpressure. For migration of hydrocarbons within a reservoir formation, variations in capillary pressure may generally be neglected. It follows therefore, that the force per unit mass, $\mathbf{E_o}$, driving hydrocarbon migration in a reservoir comprises a buoyancy term and a term proportional to the gradient of the overpressure, OP, in the ambient groundwater (Hubbert, 1953):

$$\mathbf{E_o} = -\left(\frac{\rho_w - \rho_o}{\rho_o}\right)\mathbf{g} - \frac{1}{\rho_o}\mathrm{grad}\,OP \qquad (3.10)$$

where ρ_o and ρ_w are densities of hydrocarbon and pore water, respectively, and $\mathbf{g}$ is the gravitational acceleration. Buoyancy drives hydrocarbons vertically, so for dip α there is an up-dip component of magnitude $\left[(\rho_w - \rho_o)/\rho_o\right]g\sin\alpha$.

Thus it can be seen that oil and gas will migrate differently, depending upon the reservoir dip and water overpressure gradient as illustrated in **Figure 3.16**. In order to determine the direction of hydrocarbon flow at any point in a reservoir, detailed depth maps of the reservoir top are required, in addition to maps of overpressure distribution.

Since the production of accurate depth maps for individual Palaeogene reservoir formations was outside the scope of this study, a simple numerical example is instead provided to illustrate the relative importance of the two effects. The forces per unit mass due to buoyancy and overpressure gradient that drive lateral migration of oil of 30°API in a reservoir, will have the same magnitude where reservoir dip is 2° and the overpressure gradient is 7 psi km^{-1} (48 kPa km^{-1}).

Where hydrocarbon has accumulated under conditions of lateral reservoir drainage, the hydrocarbon-water contact is tilted towards the direction of diminishing water pressure. This phenomenon was first noted by Hubbert (1953) and numerous examples have since been studied by Dennis *et al.* (2000; 2005). **Figure 3.17** illustrates the different behaviour between oil and gas accumulations within a hydrostatic and

77
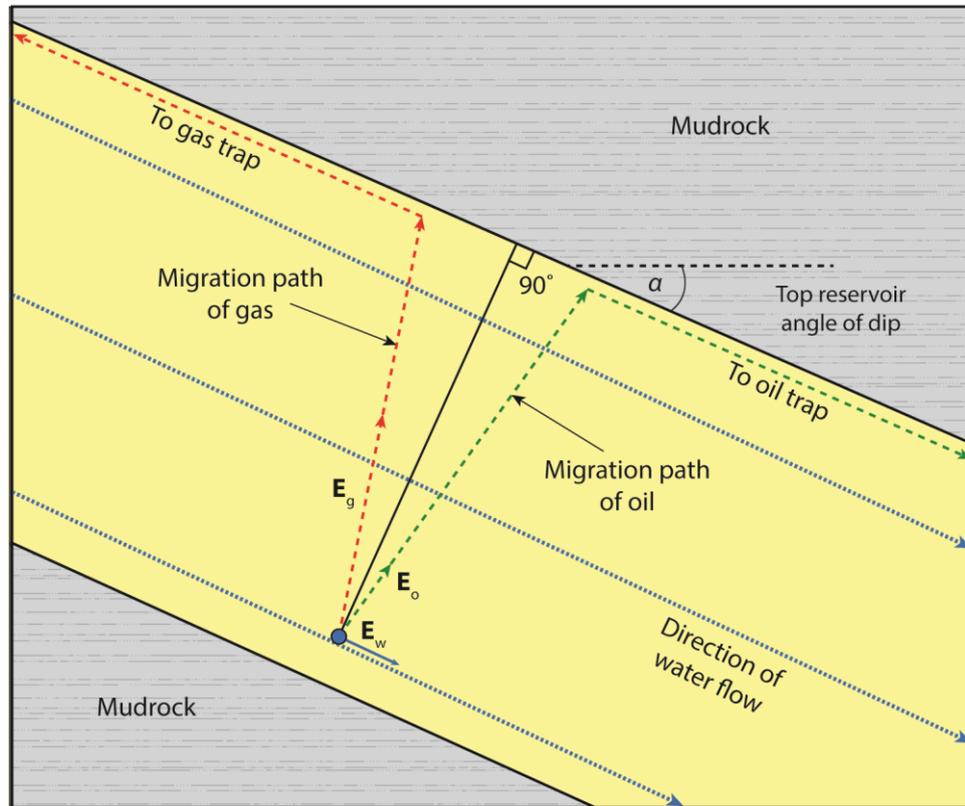
Figure 3.16 - Divergent migration of oil and gas in a hydrodynamic environment (from Hubbert, 1953).

hydrodynamic pressure environment. Dennis *et al.* (2000) noted how the principle of hydrodynamic tilting strictly applies solely to the 'free-water level' (FWL) and only by extension to the oil-water or gas-water contact (OWC or GWC). The free-water level can be defined as the point of zero capillary pressure, where both the hydrocarbon and water pressures are equal. In contrast the hydrocarbon-water contact technically occurs at the base of hydrocarbon saturation, above the FWL. In most reservoir intervals the vertical difference between the FWL and hydrocarbon-water contact is negligible and thus the two are synonymous with one another. The amount of tilt at the hydrocarbon-water contact is a function of the fluid density contrast and the lateral aquifer pressure gradient and can be calculated using the equation of Dennis *et al.* (1998):

$$dz/dx = \frac{dp/dx}{dp/dh_{(w-h)}}$$

(3.11)
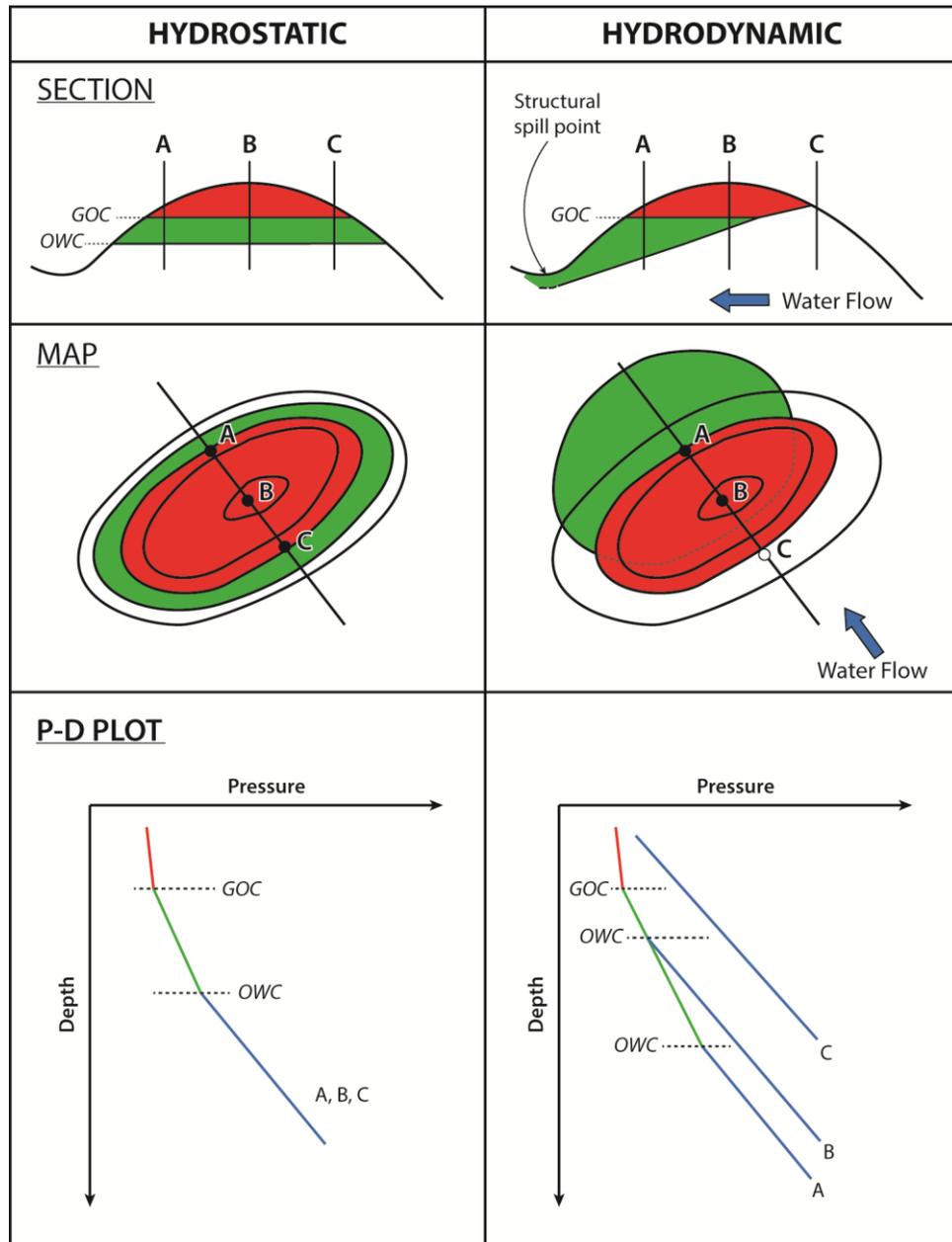
Figure 3.17 - The effect of hydrodynamic behaviour on oil and gas accumulations and how this may be recognised on pressure-depth plots. In the hydrodynamic situation, aquifer pressure decreases across field towards the NW, causing the oil-water and gas-water contacts to become tilted as a result. The gas-water contact is less tilted than the oil-water contact, due to the greater buoyancy of the gas and consequently the larger difference in density between gas and underlying water. Hydrodynamic tilting may act to increase or decrease the level of reserves depending upon the structure. In the above example, tilt of the OWC is large enough to reach the structural spill point (from Dennis *et al.*, 2000).

where dz/dx is the dip in radians of the OWC; dp/dx is the horizontal component of pressure gradient in the aquifer; and $dp/dh_{(w-h)}$ is the difference in vertical pressure gradients between the aquifer water and the hydrocarbon phases.

For a constant lateral aquifer pressure gradient, the degree of tilt will be greater for an oil-water contact (OWC) than for a gas-water contact (GWC), since the densities of oil and water are more similar and, consequently, the denominator of $dp/dh_{(w-h)}$ is of a smaller value than would be the case for gas and water phases (Dennis *et al.,* 2000).

In the Central North Sea, tilted hydrocarbon contacts are likely to occur where lateral reservoir drainage is taking place within the Palaeogene submarine fan sandstones. Dennis *et al.* (2000; 2005) have modelled tilted contacts for the several Chalk and Palaeogene fields of the Central North Sea, including Arbroath, Blane, Everest, Pierce, Valhall/Hod, Joanne and Dan. Where values of measured pressure and hydrocarbon-water contact depth vary across structure, confusion may arise as to whether such variations are caused through hydrodynamic variations or structural compartmentalization. For example, at the Pierce Field, variations of fluid contacts have in the past been explained as resulting from sealing faults or stratigraphic compartments, although hydrodynamic tilting of the oil-water contact is now the preferred explanation (Scott *et al.*, 2010). Where sufficient pressure data are available, tilted hydrocarbon contacts are easily recognised on multi-well P-D plots, where several different water pressure gradients can be fitted to a single hydrocarbon gradient, as illustrated in **Figure 3.17**.

4 Research methodology

"If we knew what it was we were doing, it would not be called research, would it?" Albert Einstein (1879-1955) [German physicist]

4. Research methodology

The principal aim of the study was to utilize pressure data from a number of Central North Sea wells to calculate values of overpressure and map them for each of the major Palaeogene reservoir members and units, as defined by Knox and Holloway (1992) (**Chapter 2**). Pressure data for a total of 336 Central North Sea wells were analysed using Ikon Science's RokDoc software. Data for each well typically comprised direct pore pressure measurements, as well as mud weight profiles which provided an indirect indication of the pore pressures experienced whilst drilling. The vast majority of pressure data, 331 wells in total, was supplied by IHS Energy with data for the remaining five wells, covering UK block 28/9, being supplied by EnCore Oil.

Single well pressure-depth (P-D) plots were analysed for each well. For those wells containing direct pore pressure measurements, values of overpressure were calculated for each representative reservoir interval. By this means, a database was created containing values of overpressure for each Palaeogene sandstone interval. The initial overpressure database comprised a total of 523 overpressure values taken from 336 wells. Nine wells contained mud weights only, with no direct pore pressure measurements, and so values of overpressure could not be established for these wells. Quality control and rejection of pressure values that might have been affected by production in nearby fields further reduced the database down to 427 overpressure values taken from 286 wells. The final overpressure distribution maps for each Palaeogene reservoir interval were created using the ArcGIS ArcMap software.

4.1. Deriving values of overpressure from single well P-D plots

In order to calculate values of overpressure from direct measurements of pore pressure, a constant hydrostatic gradient of 0.445 psi ft^{-1} (10.1 kPa m^{-1}) was assumed for the entire Central North Sea study region. Fluid gradients were identified from the pressure measurements recorded within each well using best-fit straight lines. The resultant gradients revealed the types of pore fluid present within the reservoir (i.e., gas, condensate, oil or water), and these were cross-checked where possible against known hydrocarbon accumulations. Interpreted water gradients ranged from a fresh water

gradient of 0.43 psi ft^{-1} (9.7 kPa m^{-1}) to a saturated brine gradient of 0.59 psi ft^{-1} (13.3 kPa m^{-1}) across the region. Hydrocarbon gradients varied over the range 0.29–0.41 psi ft^{-1} (6.6–9.3 kPa m^{-1}) for oil, and 0.01–0.3 psi ft^{-1} (0.2–6.8 kPa m^{-1}) for gas. This analysis led to accurate definition of water, oil and gas columns within individual reservoir units, along with calculated depths to the associated oil−water, gas−water and gas−oil contacts.

For all water-bearing reservoir units in each well, a value of overpressure representative of the entire reservoir unit was calculated using the shallowest pore pressure measurement interpreted to lie directly on the water gradient for that reservoir interval (**Figure 4.1**). The shallowest measurement to lie directly on the water gradient was always used for consistency, because the pressure-depth profile within each sandstone interval is not always hydrostat-parallel. Thin mudrock layers within sandstone intervals can cause overpressure values to increase with depth within the interval. Where a reservoir unit contained only hydrocarbons, the deepest direct pore pressure measurement interpreted to lie on the hydrocarbon gradient was used. Such values provided overestimates of the overpressure in the water column because of the added effects of hydrocarbon buoyancy (*section 3.3.3.1*). These values are referred to as 'hydrocarbon down to points' and are labelled in the database with a < sign before the value of calculated overpressure. Where possible, depth to the free water level (FWL), i.e., synonymous with the gas-water contact (GWC) or oil-water contact (OWC) for North Sea Palaeogene reservoirs (Dennis *et al*., 1998), was recorded for such values to assess whether the additional effect of hydrocarbon buoyancy on the measured pressures was negligible, or whether these data points were to be excluded from the maps of overpressure distributions, as described in *section 4.6*.

4.2. Accurately assessing well stratigraphy

Accurate assignment of overpressure values to the corresponding reservoir unit was carried out using a variety of data sources including: (1) available composite logs, (2) biostratigraphic data, (3) the IHS database, (4) nearby wells, and (5) a range of published literature sources (Knox and Holloway, 1992; Ahmadi *et al*., 2003; Jones *et*

83
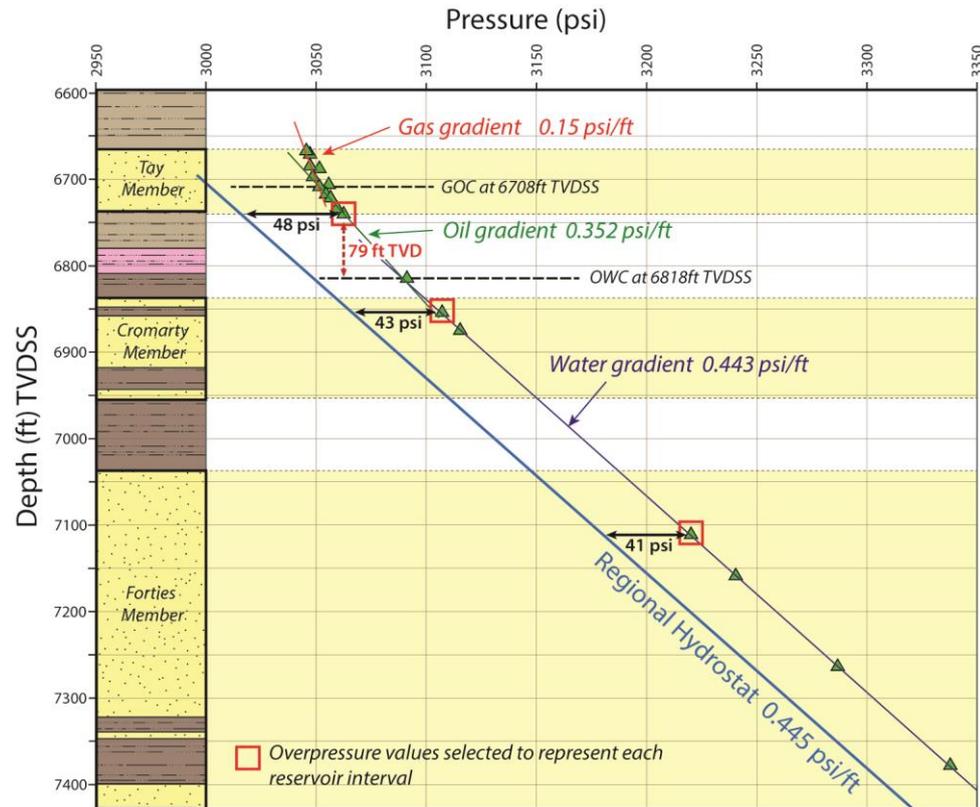
Figure 4.1 - Pressure-depth plot from UK well 21/25-6 showing how overpressure values were estimated for each reservoir interval. Fluid gradients were fitted to the pressure measurement distributions using Ikon's RokDoc software. The shallowest pressure measurement in the water-filled Forties and Cromarty sandstone members were used to calculate overpressure. Both are classified as category 3 data points because they come from a common water gradient with little scatter (s*ection 4.3.1*). For the hydrocarbon-filled Tay Sandstone Member, the deepest pressure measurement on the oil gradient has been used to calculate a maximum estimate of overpressure. The data point is classified as category 1 and is not used in the contouring process because it is more than 35ft (11m) above the oil-water contact.

al., 2003) including UK, Norwegian and Danish government websites – the UK Department of Energy and Climate Change (DECC); the Norwegian Petroleum Directorate (NPD); and the Geological Survey of Denmark and Greenland (GEUS). Where multiple sources were available for a single well, each data source was cross-checked against each other. Where conflicts occurred between sources, the lithology recorded on the composite log, wireline log characteristics, and biostratigraphic data were used to assign overpressure values to the correct reservoir units.

4.2.1. Composite logs

Composite logs were available for 231 out of the 287 wells containing acceptable Palaeogene pressure data (**Figure 4.2a**). Logs were supplied to the study by IHS Energy, Maersk Oil and Encore Oil. The lithological and wireline log characteristics enabled reservoir sands present within each well to be correctly identified, ensuring that the values of overpressure calculated were assigned to the correct reservoir interval according to the stratigraphic scheme of Knox and Holloway (1992). The lithological characteristics of Central North Sea formations were described in **Chapter 2**.

4.2.2. Biostratigraphic data

Biostratigraphic data were available for 55 wells, mostly located in the Outer Moray Firth and along the western margin of the basin (**Figure 4.2b**). The locations of these wells were fortuitous because individual sand units were considered most difficult to distinguish in this region, as they thicken and coalesce onto the shallowing shelf. The presence of biostratigraphic data ensured that reservoir units were more easily correctly identified. The typical biostratigraphic schemes present for the Central North Sea area were briefly discussed in *section 2.2.2*.

4.2.3. IHS database, nearby wells and published sources

Where wells with Palaeogene pressure data lacked a corresponding composite log, as was the case for 56 wells, various other sources were used to accurately identify each reservoir interval. Pressure data for wells supplied to the study by IHS commonly contained information about the formation or reservoir member within which the data were recorded, although some of this information was found to be inconsistent with the nomenclature scheme of Knox and Holloway (1992) when cross-checked against wells with biostratigraphic data. Nearby wells often provided a good indication as to what reservoir intervals might be expected to occur and at what depths; however, these indications were never relied upon without other evidence. Detailed information regarding stratigraphy was found in published sources, including Knox and Holloway (1992), Evans *et al*. (2003) and Gluyas and Hichens, (2003). Published sources proved
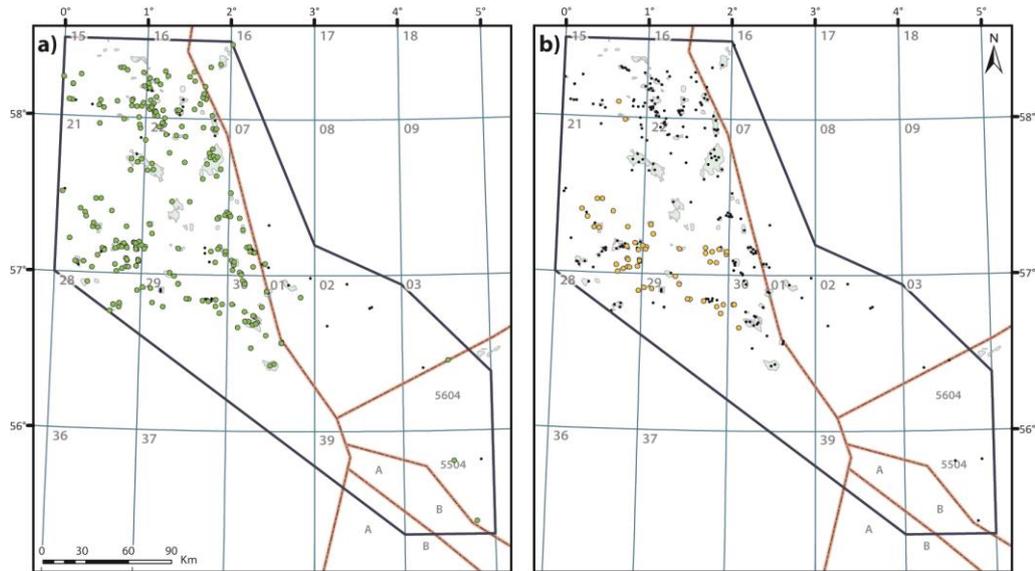
Figure 4.2 - Maps showing location of wells with **a)** composite logs available, 231 wells, and **b)** biostratigraphic data available, 55 wells.

particularly useful for wells which had been drilled into named hydrocarbon accumulations. The UK, Norwegian and Danish government websites, DECC, NPD and GEUS, were also extremely useful sources for determining well stratigraphy. Such websites provided information taken from composite logs and, in the cases of the NPD and GEUS websites, the actual composite logs and well reports themselves.

4.3. Quality control and selection of data

The distribution and quality of direct pore pressure measurements varied for each well, with some wells containing numerous pressure measurements from which fluid gradients were easily established to others containing solitary pressure measurements or highly scattered data where fluid gradients proved difficult to establish. In order to assess the reliability of each calculated overpressure value, a system was used to categorise each pressure dataset from which fluid gradients were drawn and overpressure values calculated.

Quality control checks were made on each accepted overpressure value to ensure that each value was of sound quality. A total of 19 overpressure values were deleted from the database for reasons related to the measurement quality, including operational

errors such as 'supercharging' or 'misrun tests' which had been observed when recording the measurement, and errors thought likely to be related to the IHS data conditioning process, e.g., where direct pore pressure measurements recorded within a well consistently exceeded the mud weights used whilst drilling. Composite logs were used, where possible, to check whether any error related to quality was known to exist for individual measurements. Other details relating to the overall quality of pressure measurement, from which overpressure values were calculated, that were also entered into the database included: tool type, gauge type, number of measurements used to define the fluid gradient, fluid type, and IHS's classification of data quality.

4.3.1. Overpressure category system

A modified version of the Ikon GeoPressure category system (Swarbrick *et al*., 2004) was adopted to classify the pressure data from which values of overpressure were calculated. Such a classification system was necessary since the quality of each representative overpressure value calculated depends upon the quality of data from which it is derived. The workflow used to check the quality of each overpressure value and assign it to a category is shown in **Figure 4.3**. The classification system comprises four categories. The category type was determined through examination of the individual pressure-depth plots for each well. Category 1 data represent overpressures which were calculated from a hydrocarbon gradient made up of more than two pressure measurements (**Figure 4.4**). All category 1 values are labelled as maximum estimates of overpressure because of hydrocarbon buoyancy. Category 2 values are overpressures that have been calculated from only one or two measurements in water- or hydrocarbon-saturated reservoirs, or from a measured water gradient containing a large amount of scatter (**Figure 4.5**). Such values of overpressure have the greatest uncertainty, although the errors are unlikely to exceed 100 psi (700 kPa). Category 3 overpressure values are those calculated from water gradients with only small levels of scatter and errors that are unlikely to exceed 20 psi (140 kPa) (**Figure 4.6**). Category 4 values are derived from water gradients containing little or no scatter, with associated errors of less than 5 psi (34 kPa) (**Figure 4.7**).
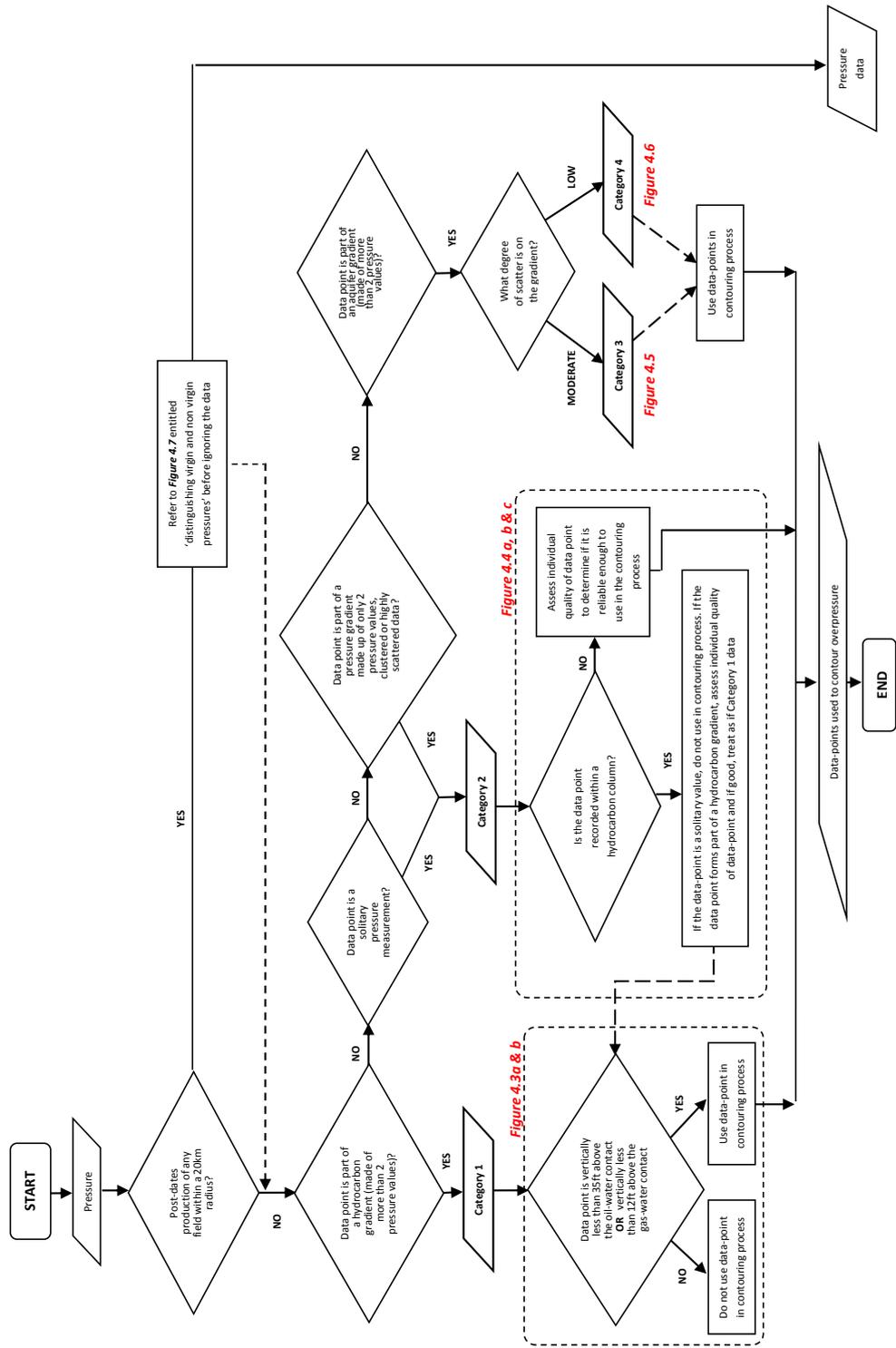
Figure 4.3 - Workflow for classifying the category and contouring suitability of overpressure data. See accompanying **Figures 4.4** to **4.7** for actual examples.
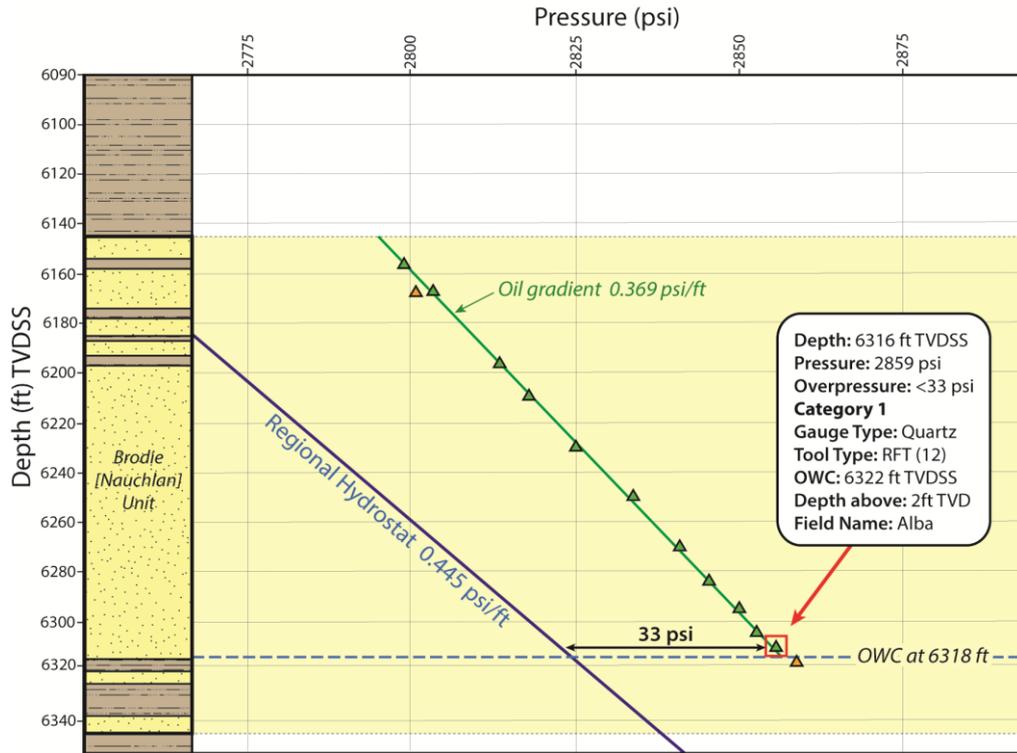
Figure 4.4a - Example of a Category 1 overpressure value calculated to represent the Brodie [Nauchlan] Sandstone Unit in UK well 16/26 -15. Oil gradient of 0.369 psi ft[-1] is created from twelve RFT pressure measurements. The deepest pressure measurement to lye directly on the oil gradient (2859 psi at a depth of 6316ft TVDSS) is used to calculate a maximum representative overpressure of 33 psi. According to the composite log and paper by Mattingly and Bretthauer (1992), the OWC is situated at a depth of 6318ft TVDSS. Since the pressure measurement is recorded only 2ft TVD above the OWC, the value can be used to contour the overpressure distribution, as the additional effects of hydrocarbon buoyancy to the overpressure calculated will be less than 5 psi.
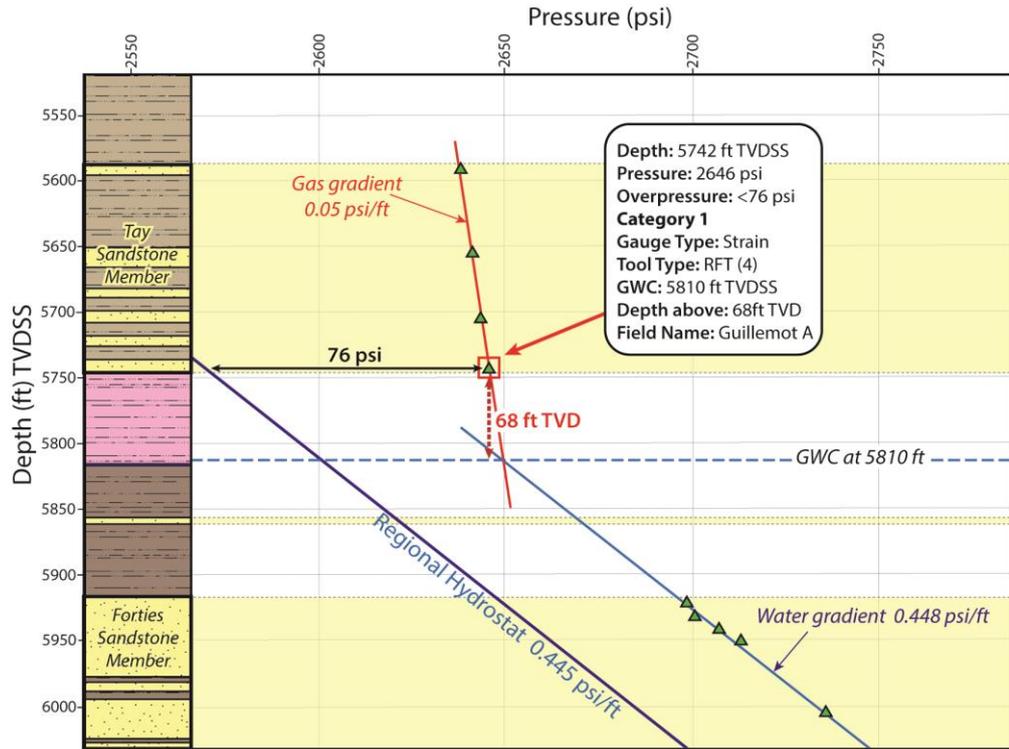
Figure 4.4b - Example of a Category 1 overpressure value calculated to represent the Tay Sandstone Member in UK well 21/25 -2. Gas gradient of 0.05 psi ft[-1] is created from four RFT pressure measurements. The deepest pressure measurement to lye directly on the gas gradient (2646 psi at a depth of 5742ft TVDSS) is used to calculate a maximum representative overpressure of 76 psi. Pressure data indicates that the GWC is situated at a depth of 5810ft TVDSS. Since the pressure measurement is recorded at a distance of approximately 68ft TVD above the GWC, the value has not been used to contour the overpressure distribution map for the Tay reservoir, since the additional effects of hydrocarbon buoyancy to the overpressure calculated will be greater than 5 psi.
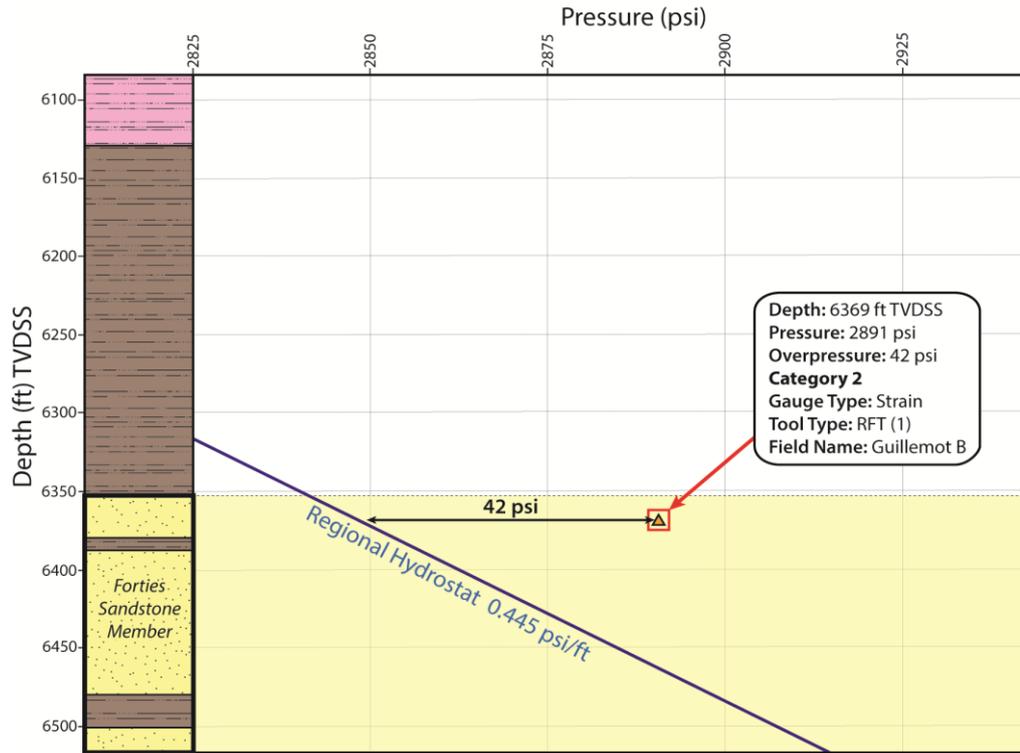
Figure 4.5a - Example of a Category 2 overpressure value calculated from a solitary pressure measurement to represent the Forties Sandstone Member in UK well 21/29a -6. The solitary RFT pressure measurement (2891 psi at a depth of 6369ft TVDSS) is used to calculate a representative overpressure of 42 psi. Composite log confirms that the solitary measurement was recorded in a water column. IHS quality of the data point is 'fair' and composite log does not indicate there is anything wrong with the test. Since the overpressure value calculated appears to fit well with surrounding (higher category) values for the Forties reservoir, this solitary value was deemed suitable to contour the overpressure distribution for the Forties Sandstone Member.
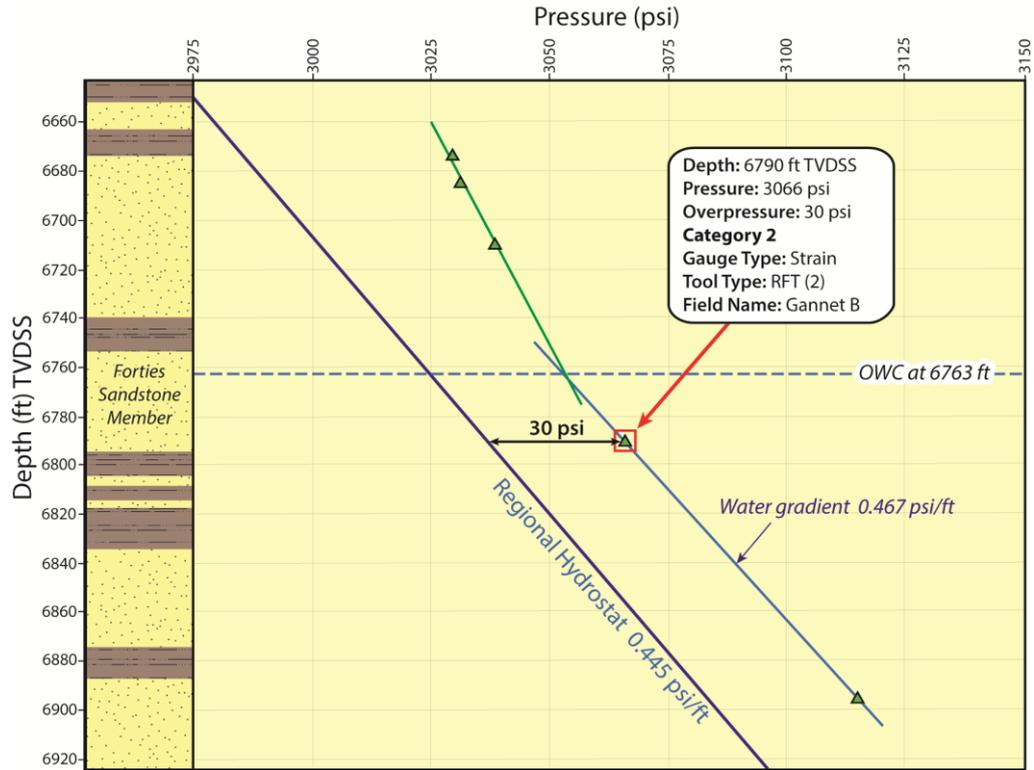
Figure 4.5b - Example of a Category 2 overpressure value calculated from only two pressure measurements, representing the Forties Sandstone Member in UK well 21/25 -1. Water gradient of 0.467 psi ft^{-1} is created from two RFT pressure measurements. The shallowest measurement to lye directly on the water gradient (3066 psi at a depth of 6790ft TVDSS) is used to calculate a representative overpressure of 30 psi. Composite log confirms that the measurement was recorded in a water column. Although IHS quality of the data point is 'unknown' the composite log does not indicate there is anything wrong with the test. Since the overpressure value calculated appears to fit well with surrounding (higher category) values for the Forties reservoir, this overpressure value was deemed suitable to contour the overpressure distribution for the Forties Sandstone Member.
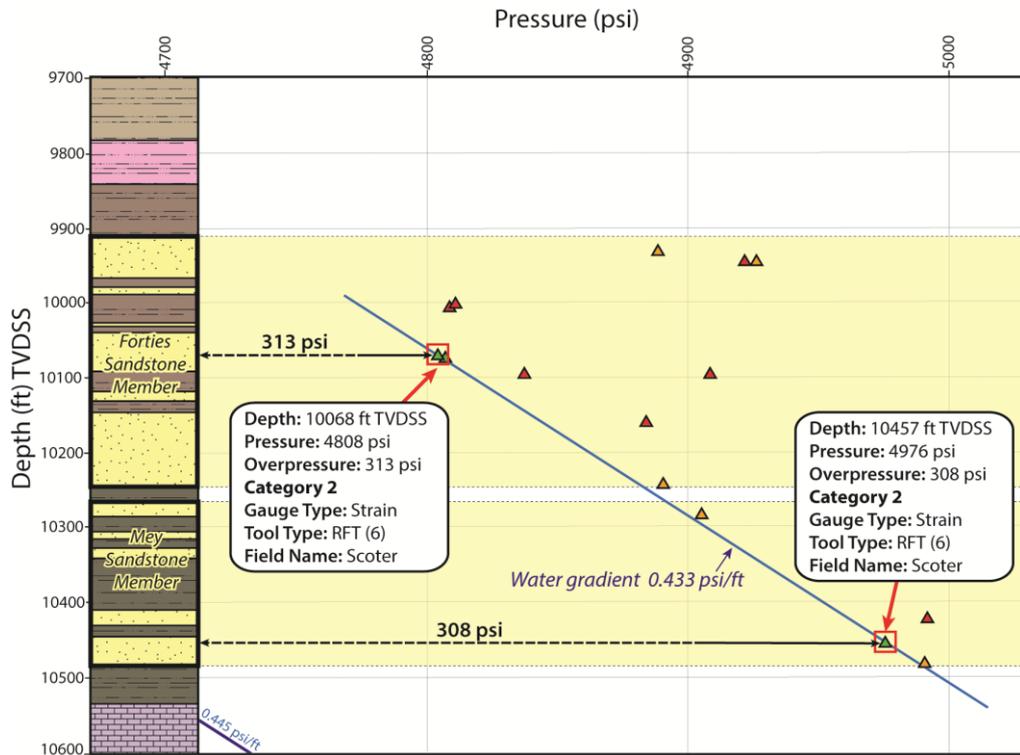
Figure 4.5c - Example of Category 2 overpressure values calculated from a highly scattered pressure dataset in well UK 22/30a -9. Water gradient of 0.433 psi ft[-1] is made up of effectively six RFT pressure measurements, with numerous 'poor to fair quality' measurements scattered around the gradient. The interpreted water gradient spans two reservoir intervals namely the 'Forties Sandstone Member' and the 'Mey Sandstone Member'. The shallowest measurements to lie directly on the water gradient (4808 psi at a depth of 10068ft TVDSS for the Forties and 4976 psi at a depth of 10457ft TVDSS for the Mey) are used to calculate overpressure values of 313 psi and 308 psi for each respective reservoir interval. Composite log confirms that the measurements were recorded in a water column, with some weak oil shows at the top of the Forties reservoir interval, possibly explaining the slightly greater value of overpressure and the larger scatter of data around this depth. Since both values are classified as 'good' quality by IHS and the composite log does not indicate there is anything wrong with the tests, thus both values were deemed suitable to contour the overpressure distributions for their corresponding reservoir intervals.
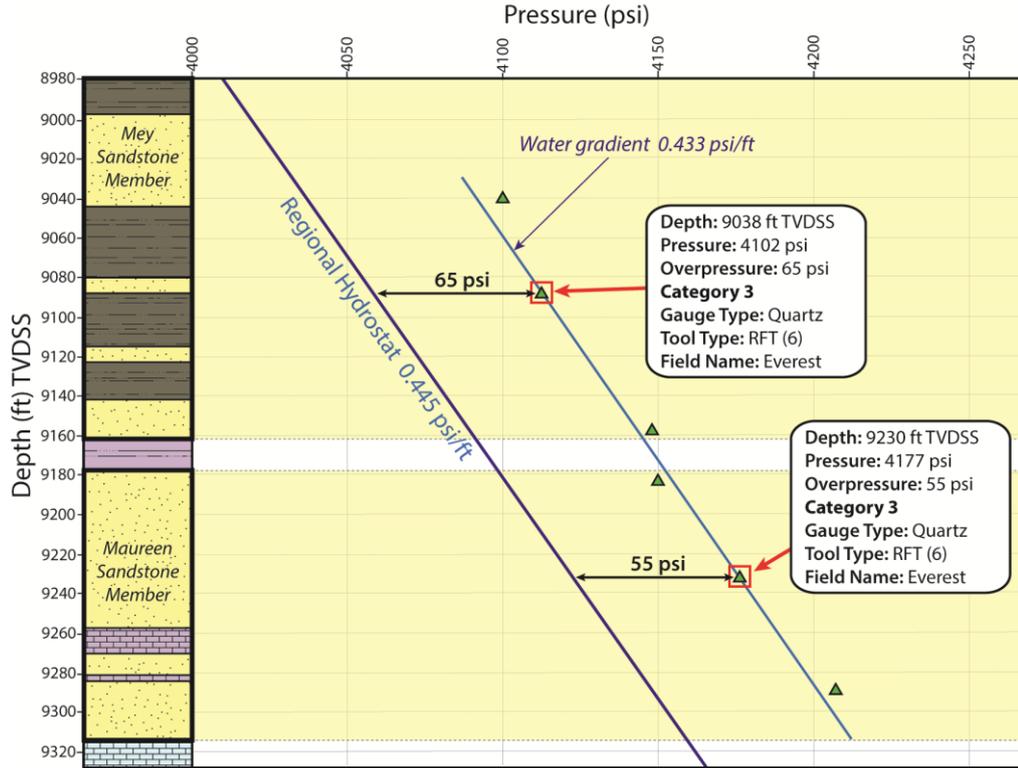
Figure 4.6 - Example of Category 3 overpressure values calculated to represent the Mey and Maureen sandstone members in UK well 22/09 -3. Water gradient of 0.433 psi ft^{-1} created from six RFT pressure measurements, with some slight scattering of data around the interpreted gradient (values lying up to a maximum of 7 psi from the interpreted water gradient). The interpreted water gradient is shared for both the Mey and Maureen reservoir intervals. The shallowest pressure measurements to lye directly on the water gradient (4102 psi at a depth of 9038 ft TVDSS for the Mey and 4177 psi at a depth of 9230ft TVDSS for the Maureen) are used to calculate overpressure values of 65 psi and 55 psi for each respective reservoir interval. Composite log confirms that the pressure measurements were recorded in a water column and that the pressure tests were of good quality. Both values are classified as 'good' quality by IHS. All category 3 overpressure values are used to contour the overpressure distribution maps for each respective reservoir interval. Levels of errors for all category 3 data-points are unlikely to exceed 20 psi (140 kPa).
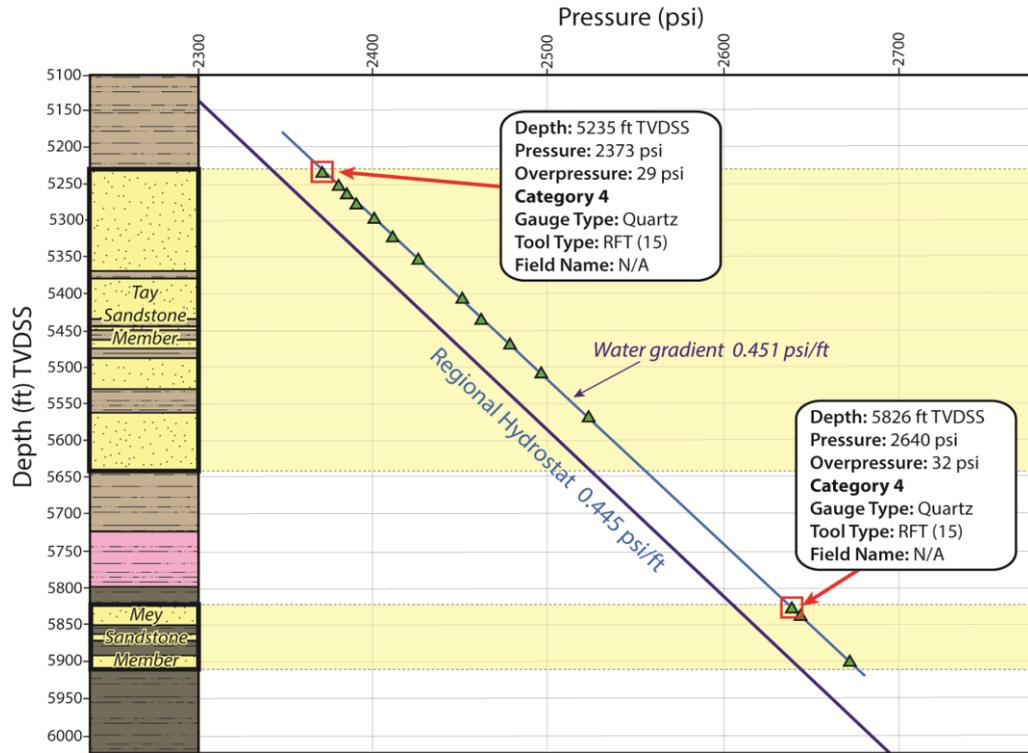
Figure 4.7 - Example of Category 4 overpressure values calculated to represent the Tay and Mey sandstone members in UK well 21/23c -5. Water gradient of 0.451 psi ft^{-1} created from fifteen RFT pressure measurements, with no scatter of data from the interpreted water gradient. The water gradient is shared for both the Tay and Mey reservoir intervals. The shallowest pressure measurements to lye directly on the water gradient (2373 psi at a depth of 5235 ft TVDSS for the Tay and 2640 psi at a depth of 5826ft TVDSS for the Mey) are used to calculate overpressure values of 29 psi and 32 psi for each respective reservoir interval. Composite log confirms that the pressure measurements were recorded in a water column and that the pressure tests were of good quality. Both values are classified as 'good' quality by IHS. All category 4 overpressure values are used to contour the overpressure distribution maps for each respective reservoir interval. Levels of errors for all category 4 data-points are less than 5 psi (34 kPa).

95

4.3.2. Tool type

Pressure data were recorded using a variety of pressure tools. The vast majority of measurements were recorded using the Repeat Formation Tester (RFT) tool. Other measurements were made using RFT-type tools such as the Selective Formation Tester (SFT) tool, Formation Multi-Tester (FMT) tool and the most modern tool, the Modular Formation Dynamic Tester (MDT) tool. The RFT and similar tool types provide higher quality pressure data than measurements made during drill stem tests (DSTs) or formation interval tests (FITs). Kick values are thought to be the least accurate measurements.

4.3.3. Gauge type

The type and age of pressure tool used to collect measurements has a direct influence over the type of pressure gauge which was used to take a recording. Pressure gauge types have advanced over time, with improvements being made to the resolution and accuracy of measurements (Vella *et al*., 1992). Out of the 427 pressure values used in this study, 262 were recorded using the conventional strain gauge, having a resolution of 0.2 psi (1.4 kPa) and an accuracy of ±15 psi (±100 kPa). Fewer measurements (147 overpressure values in total) were recorded using the more accurate standard quartz gauge, with a resolution of 0.001 psi (0.007 kPa) and an accuracy of ±[0.025% of reading + 0.5 psi (3.4 kPa)]. Quartz pressure gauges became common usage in pressure tools from around the late 1980s (Vella *et al*., 1992). Only 14 overpressure values were recorded using the new generation of quartz gauge, the combinable quartz gauge (CQG), with a resolution of 0.003 psi (0.02 kPa) and an accuracy of ±[0.01% of reading + 1 psi (6.9 kPa)]. The CQG is found in pressure tools from the mid-1990s onwards in tools such as the MDT tool (Ireland *et al*., 1992). The type of gauge used to record measurements is shown on the overpressure distribution maps by changes in symbol size. Differences in performance between the conventional strain gauge, the standard quartz gauge, and the CQG are summarized in **Table 4.1**.

	GAUGE TYPE		
	Conventional Strain Gauge	**Standard Quartz Gauge**	**Combinable Quartz Gauge**
Advantages	Better resolution, fast response, rugged and small	Higher resolution, higher stability, higher accuracy	Best dynamics, best stability, higher pressures than standard quartz gauge
Disadvantages	Medium stability, resolution and accuracy	Very sensitive to temperature change, limited pressure range	More electronics
Maximum Range	20,000 psi	11,000 psi	15,000 psi
	175°C	175°C	175°C
Resolution	0.2 psi (at 15,000 psi; 1-sec sampling)	0.001 psi (at 12,000 psi; 1-se sampling)	0.003 psi (at 15,000 psi; 1-sec sampling)
Accuracy	15 psi	± [0.025% of reading + 0.5 psi]	± [0.01 % of reading + 1 psi]
Drift	<3 psi 1st day, then < 1.5 psi/week (10,000 psi; 150°C	± 0.2 psi in 18 days then < 0.1 psi/week (5,000 psi; 120°C)	± 0.2 psi in 7 days then <0.1 psi/week (10,000 psi; 150°C)
Stabilisation Time			
5000 psi step	30 sec	6 min	Always within 1 psi
10°C step	10 min	25 min	2 sec

Table 4.1 - Comparison of pressure gauge performance for the conventional strain gauge, standard quartz gauge, and conventional quartz gauge (modified from Vella *et al*., 1992).

4.3.4. *Virgin versus non-virgin pressures*

Further checking of the data was performed to ensure that all overpressure values were calculated from pressure measurements that had not been affected by hydrocarbon production at nearby fields. Depletion during production can lead to pore-pressure drawdown, and fluid injection can increase pore pressure. The workflow used to assess the virgin non-virgin status of each overpressure value is shown in **Figure 4.8**. The lateral distance from a field, up to which pore pressures can be affected by production is
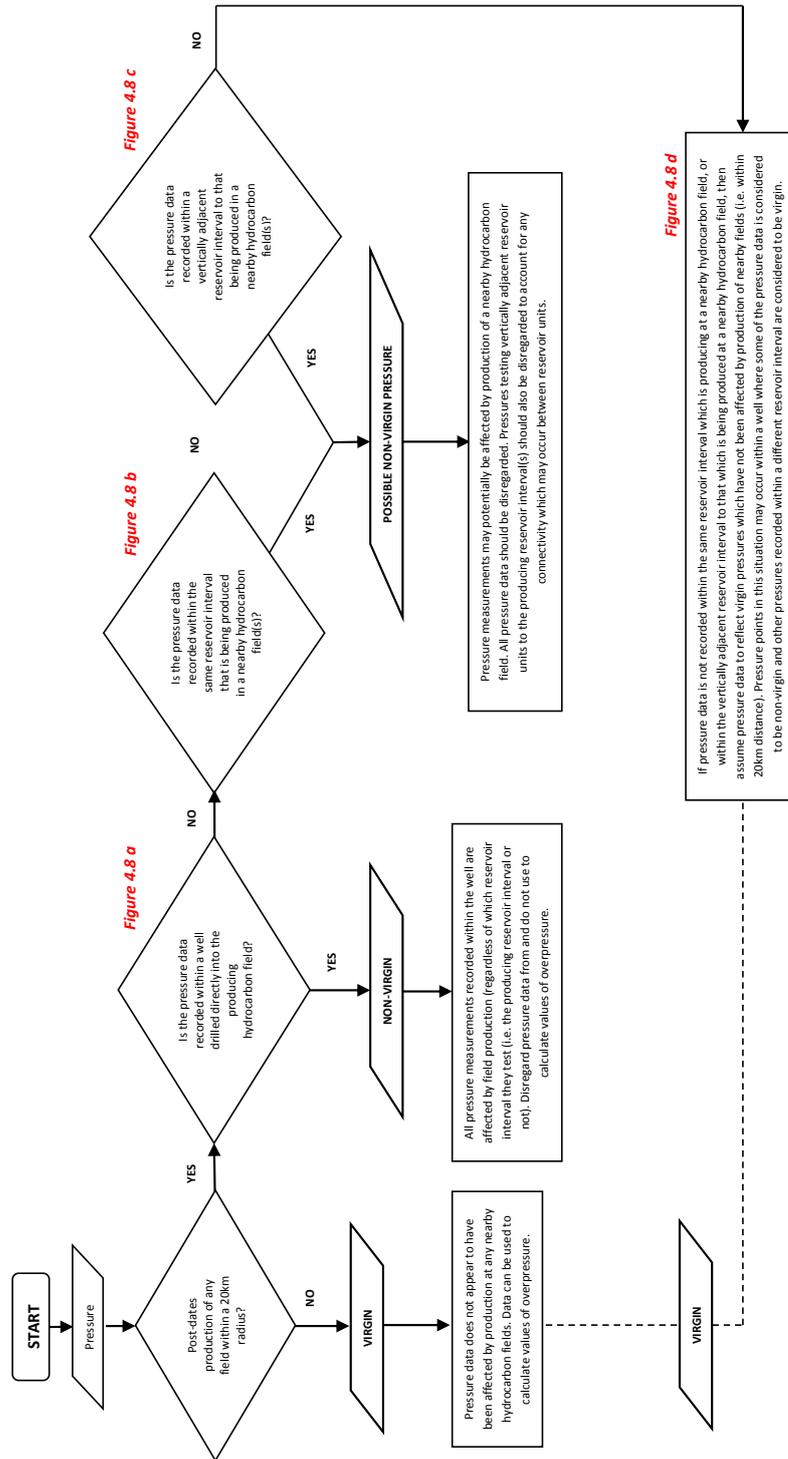
Figure 4.8 - Workflow for classifying the virgin or non-virgin status of pressure data. See accompanying **Figure 4.9** for simplified examples.

variable and difficult to estimate. In this study, it was assumed that pore pressure could be affected up to a radial distance 20 km from producing fields. Unless there were good reasons for thinking that pore-pressure drawdown had not occurred, any pressure value within this 20 km radius, which was recorded within the producing reservoir after production has started in the field in question, was deleted from the study. The same principle was applied to pressure values recorded within vertically adjacent reservoirs to the producing reservoir. **Figure 4.9** illustrates the situations in which pressure data was deemed to represent non-virgin pressures.

A total of 96 overpressure values (taken from over 50 wells) were deleted from the study due to the possibility of them being affected by production of nearby fields (i.e. potentially 'non-virgin' values). The final overpressure dataset comprised 427 overpressure values taken from over 286 wells.

4.4. Errors associated with using a constant hydrostatic gradient

The use of a constant hydrostatic gradient of 0.445 psi ft^{-1} (10.1 kPa m^{-1}) for the entire Central North Sea region implies that there are no variations in salinity, and hence negligible variations in pore water density, across the region. This assumption is unrealistic and must introduce some error into the values of overpressure calculated. Regional salinity distribution data for the Palaeogene strata of the Central North Sea are presented in Warren and Smalley (1993, 1994) and Moss *et al*. (2003). **Figure 4.10** shows the water-salinity distribution map for the Cenozoic strata as presented in Moss *et al*. (2003). Despite the map lacking significant detail on a regional scale, due to the sparse intervals across which water is sampled, it can be seen that Palaeogene formation water salinity generally increases with depth, reflecting increasing solubility with temperature Superimposed on this overall trend, anomalous regions of higher salinity are found in the Central Graben above positive structural features such as the Forties–Montrose High and Josephine Ridge. Various authors have suggested that such anomalies imply the upward migration of salt-saturated pore waters, from the Zechstein successions below, along the graben-bounding faults responsible for the structural highs (Gaarenstroom *et al*., 1993; Moss *et al*., 2003). In interpreting the mapped overpressure
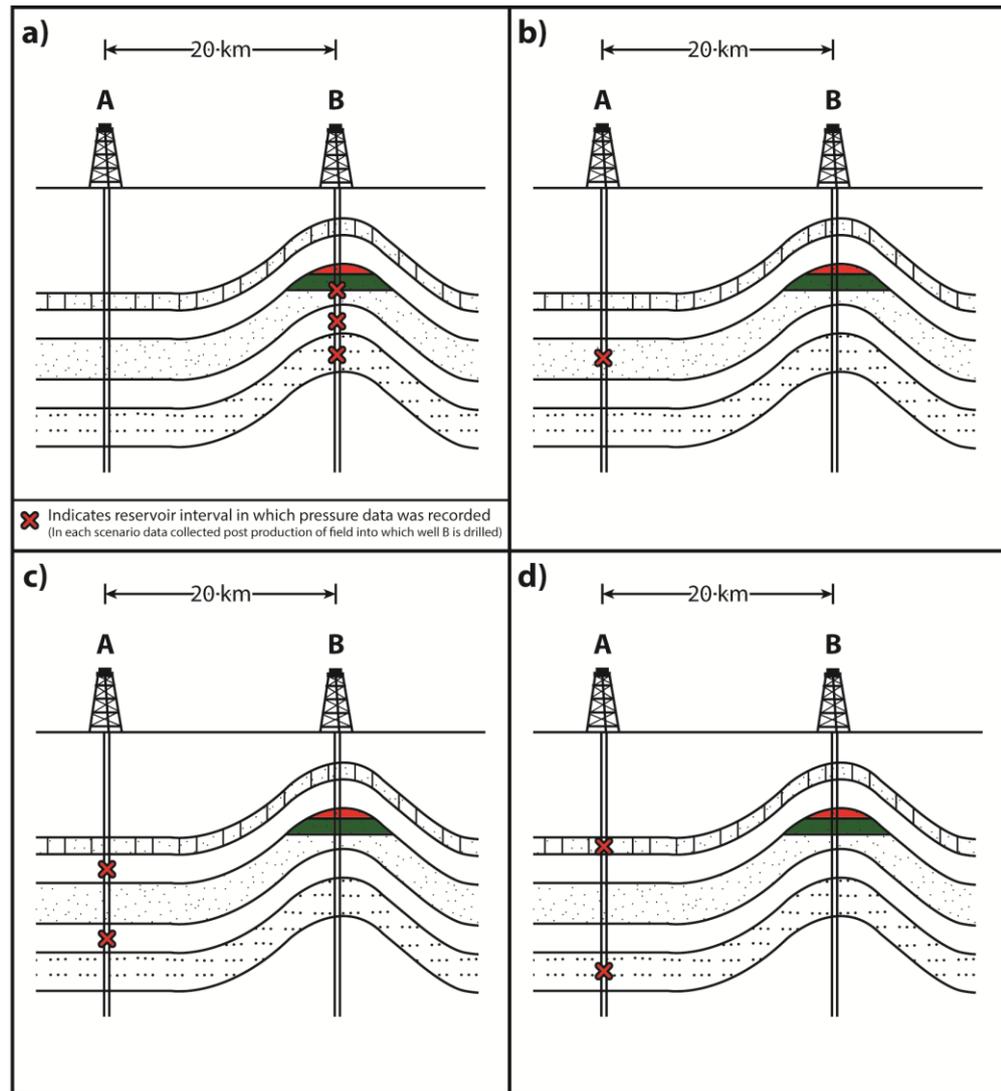
Figure 4.9 - Simplified block diagrams helping to illustrate the workflow used for classifying virgin and non-virgin status of the pressure data (see **Figure 4.8**). In each scenario, the pressure data collected from wells A and B are recorded post-production of the hydrocarbon field into which well B is drilled. **a)** Pressure data is collected from within a producing reservoir interval and will consequently be affected by production. Pressure measurements collected from within any reservoir interval in well B are classified as non-virgin pressures and are discarded from the study. **b)** Pressure data in well A have been collected from within the same reservoir interval that is being produced in well B. Since both wells are situated within 20km distance of one another, the pressure data are considered to be potentially non-virgin and are disregarded in the study. **c)** Pressure data in well A have been collected from within vertically adjacent reservoir intervals to that interval which is being produced in well B. Since both wells are situated within 20km distance of one another, the pressure data are considered to be potentially non-virgin and are disregarded in the study. **d)** Pressure data in well A are collected from reservoir intervals which differ from the producing reservoir in well B and are also not vertically adjacent. Despite both wells being situated within 20km distance of one another, the pressures are considered to be virgin and are incorporated into the overpressure database.

100
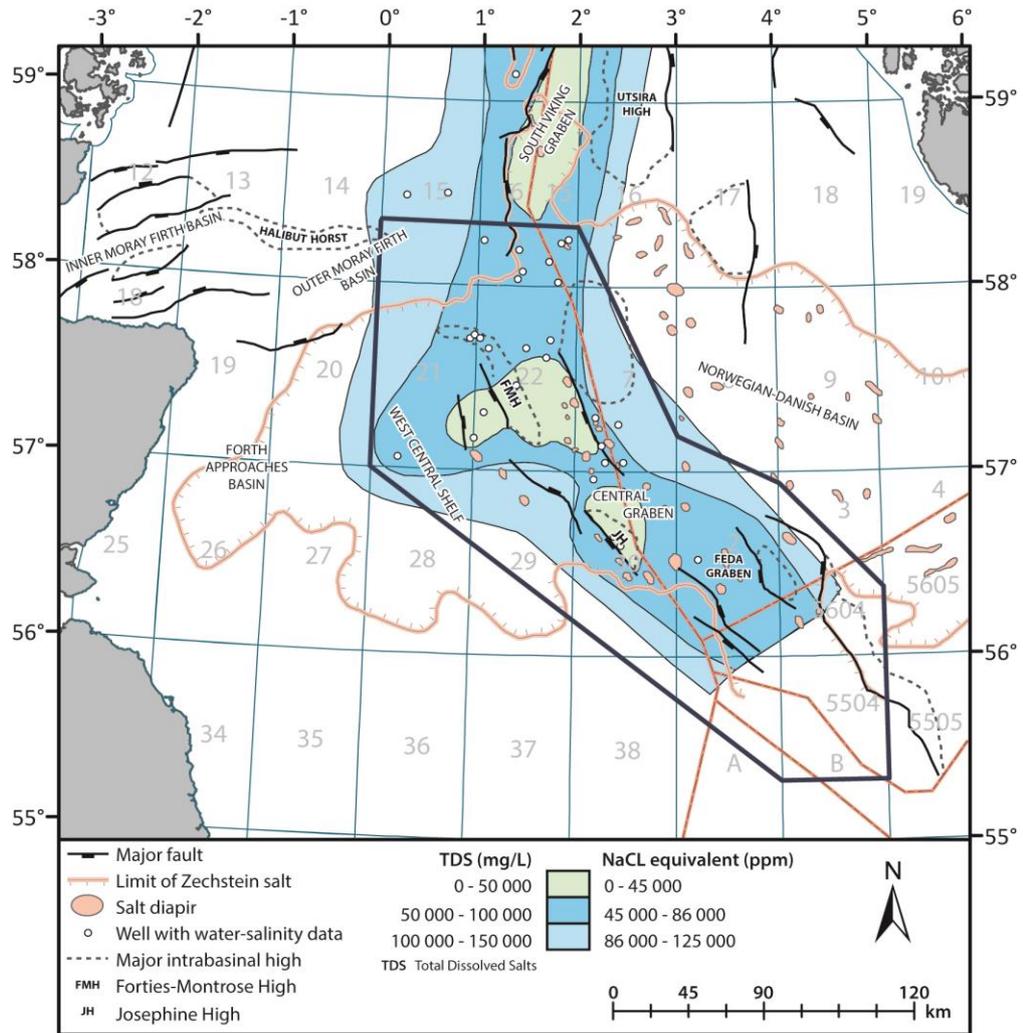
Figure 4.10 - Water-salinity distribution map for the Cenozoic strata (adapted from Moss *et al.*, 2003 to show study region). Brine bodies are located in the South Viking Graben and over the Forties-Montrose and Josephine highs with a general trend of landward dilation. Reasons for the salinity variation may reflect past or present meteoric recharge, increasing depth of burial towards the basin axis or most favourably upward leakage from the underlying Zechstein salt.

distributions, we have assumed that salinity variations are of sufficiently long wavelength that they are not the cause of significant errors in local lateral or vertical overpressure gradients.

The level of error that can be induced from assuming a constant regional hydrostatic gradient of 0.445 psi ft^{-1} (10.1 kPa m^{-1}) to calculate overpressure has been quantified in this study by using several pressure values recorded in the Forties Sandstone Member in Block 21/10. This region was selected because of its location

101

above the Forties-Montrose High, where formation water densities are amongst the highest, and because of the availability of detailed fluid density and salinity data in the Forties Field. Macleod and Casey (1994) recorded salinity values within the Forties reservoir of the Forties Field (Block 21/10) in the range 86,000-87,000 mg l^{-1} with an average brine density of 1.075 g cm^{-3}. Such a density is equivalent to a fluid gradient of 0.466 psi ft^{-1} (10.5 kPa m^{-1}), which is greater than the regional hydrostatic gradient of 0.445 psi ft^{-1} (10.1 kPa m^{-1}) used in the study. When values of overpressure were recalculated for this region using a regional hydrostatic gradient of 0.445 psi ft^{-1} (10.1 kPa m^{-1}) from mean sea level to the Top Forties horizon and 0.466 psi ft^{-1} (10.5 kPa m^{-1}) from Top Forties downwards, the greatest difference in estimated overpressure was only 4 psi. Although this analysis still assumes a constant hydrostatic gradient of 0.445 psi ft^{-1} (10.1 kPa m^{-1}) down to the Top Forties member, in the absence of any accurately known formation water salinities above this unit it was thought to be more realistic than extending the gradient of 0.466 psi ft^{-1} (10.5 kPa m^{-1}) from the seabed. If the study were to have calculated overpressure values below the Palaeogene strata, errors caused as a result of salinity variations may have been more significant with fluid densities increasing with depth as a result of the increasing temperature and proximity to the Zechstein salt (Moss *et al*., 2003).

4.5. Sandstone member distributions

Regional play distribution maps supplied to the study by Ternan Ltd provided accurate outlines for most of the Palaeogene reservoir members. In addition to these maps, evaluation of wireline log data was carried out for each well containing pressure data, and also for wells which were situated in regions where reservoir distributions remained largely unknown (e.g., upper parts of UK quadrant 28 and 29 where the distribution of the smaller Tay and upper Sele sandstone members remain unmapped). Such work was calibrated against seismic and biostratigraphic data, where available, and used in combination with previously interpreted work from a large number of published sources (Armstrong *et al*., 1987; Jennette *et al*., 2000; Ahmadi *et al*., 2003; McCormick and Leisham, 2004; Hempton *et al*., 2005; Davis *et al*., 2009).

4.6. Contouring the data

When contouring the overpressure distribution for each reservoir interval, priority was given to category 4 data, followed by category 3 data. Category 1 (hydrocarbon) values were only used in the contouring process if they were known to be recorded vertically within 35 ft (11 m) TVD of the oil−water contact or 12 ft (4 m) TVD of the gas−water contact. Such distances ensured that overpressure estimates calculated from hydrocarbon gradients would lie within 5 psi (34 kPa) of the overpressure in the water column (Figure 4.11). Each category 2 value was individually assessed for reliability before being used in the contouring process. Where solitary measurements had been recorded within a hydrocarbon column, they were not used to contour the data.
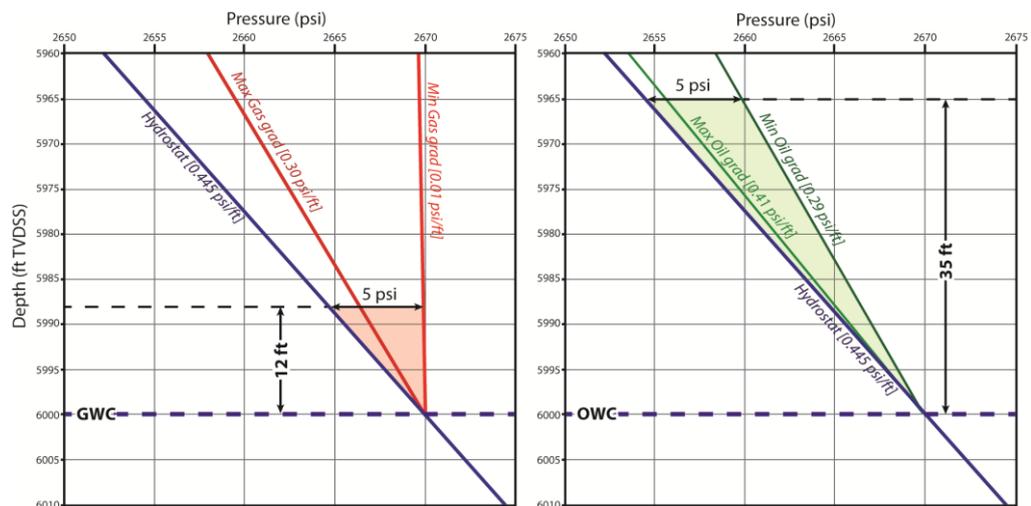
Figure 4.11 - Pressure-depth plots illustrating the acceptable distances of overpressure values from gas-water and oil-water contacts for contouring. Interpreted gas gradients in the study area were in the range 0.01–0.3 psi ft^{-1} (0.2–6.8 kPa m^{-1}). Overpressure values derived from gas gradients (i.e. category 1) were only used to contour the overpressure distributions if they had been recorded vertically within 12 ft (4 m) TVD of the gas-water contact. Interpreted oil gradients ranged from 0.29–0.41 psi ft^{-1} (6.6–9.3 kPa m^{-1}). Overpressure values derived from oil gradients (category 1) were only used to contour the overpressure distribution, so long as they had been recorded vertically within 35 ft (11 m) TVD of the oil-water contact. Such vertical distances ensured that the overpressure estimates were within 5 psi (34 kPa) of the overpressure in the water column.

103

5 Palaeogene overpressure maps and fluid migration pathways

"Turn him to any cause of policy, The Gordian Knot of it he will unloose, Familiar as his garter" Shakespeare (Henry V, Act 1 Scene 1, 45-47)

5. Palaeogene overpressure maps and fluid migration pathways

Overpressure is a transient phenomenon, and tends to dissipate over time unless renewed by active generation mechanisms. Where areas of overpressure occur within a basin, fluids will naturally attempt to re-equilibrate to hydrostatic pressure, provided that a flow route is available for fluids to escape, whether laterally or vertically. The direction of pore water flow is in the direction of overpressure decrease, with flow from areas of high to low overpressure. The rate at which this flow occurs is governed by Darcy's law and depends upon the permeability of the sediments within which the fluids are contained, as well as the magnitude of the overpressure gradient. For hydrocarbons in reservoir formations, assuming variations in capillary pressure are negligible, the driving force for fluid flow is the vector sum of the forces due to buoyancy and the negative gradient of overpressure (Hubbert, 1953).

In this chapter, overpressure distribution maps for each Palaeogene sandstone member in the Central North Sea are presented and discussed in detail. Drainage pathways are identified for each sandstone, as well as likely areas of hydrodynamic trapping. Potential areas of vertical drainage between sandstone members are identified using anomalous overpressure values, and differences in overpressure between sandstone members and hydrocarbon accumulations. These areas are examined and evaluated at the end of this chapter, with additional discussion regarding areas of the basin that may provide the best potential for future exploration. Regional distributions of Palaeogene overpressures in the Central North Sea have previously been investigated by Lindberg *et al.* (1980), Cayley (1987), Holm (1998), and O'Connor *et al.* (2008); however, in most cases the Palaeocene strata was classified as a single unit.

The content of this chapter regarding the Forties, Cromarty and Tay sandstone members has been published in Petroleum Geoscience (Robertson *et al.*, 2013). **Appendix A** contains maps and tables concerning all known hydrocarbon accumulations in the Palaeogene strata of the Central North Sea.

5.1. Lateral drainage pathways

In this section, the overpressure distribution maps are presented. Where overpressure magnitudes in the sands are less than 50 psi (0.35 MPa), the sands are described as being 'near-hydrostatically pressured'. Overpressure contouring for each of the Maureen, Mey/Heimdal and Forties Palaeocene fan units was carried out at 100 psi (0.69 MPa) intervals, in addition to the 50 psi (0.35 MPa) contour to delimit 'near-hydrostatic' pressures. For the younger Cromarty and Tay sandstone members, data were contoured at intervals of 10 psi (0.07 MPa). Contour lines are interpolated between overpressure data points, so the maps should not be over-interpreted in areas where measurements are sparse.

5.1.1. Maureen Sandstone Member

The uncontoured and contoured overpressure distribution maps for the Maureen sandstone are shown in **Figure 5.1**. A total of 51 overpressure values were calculated within the Maureen Sandstone Member and 42 of them were deemed suitable for contouring the overpressure distribution. The majority of overpressure data points are restricted to the eastern margin of the sandstone member within UK quadrant 23 and around the Everest Field in UK blocks 22/9 and 22/10. Several other overpressure values were calculated for wells drilled further to the south-west, along the western axial fairway of the Maureen fan in UK quadrants 29 and 30. The remaining overpressure values are sparsely scattered across the remainder of the fan, although the distribution remains adequate for contouring. Two values of overpressure were also recorded within the Maureen-equivalent, Vale Sandstone Member located in the Danish and Norwegian sectors of the Central North Sea; however, these values, recorded in Norwegian well 3/7-4 and Danish well Elna-1, are not shown on the overpressure map since coverage does not extend far enough to the east.

The majority of Maureen overpressure values are classified as category 2 data points, meaning that they have been derived from solitary pressure measurements or fluid gradients determined from only two pressure measurements. It can be seen in **Figure 5.1a** that such category 2 data points are concentrated in the southern regions of the fan, where reservoir quality diminishes.

106
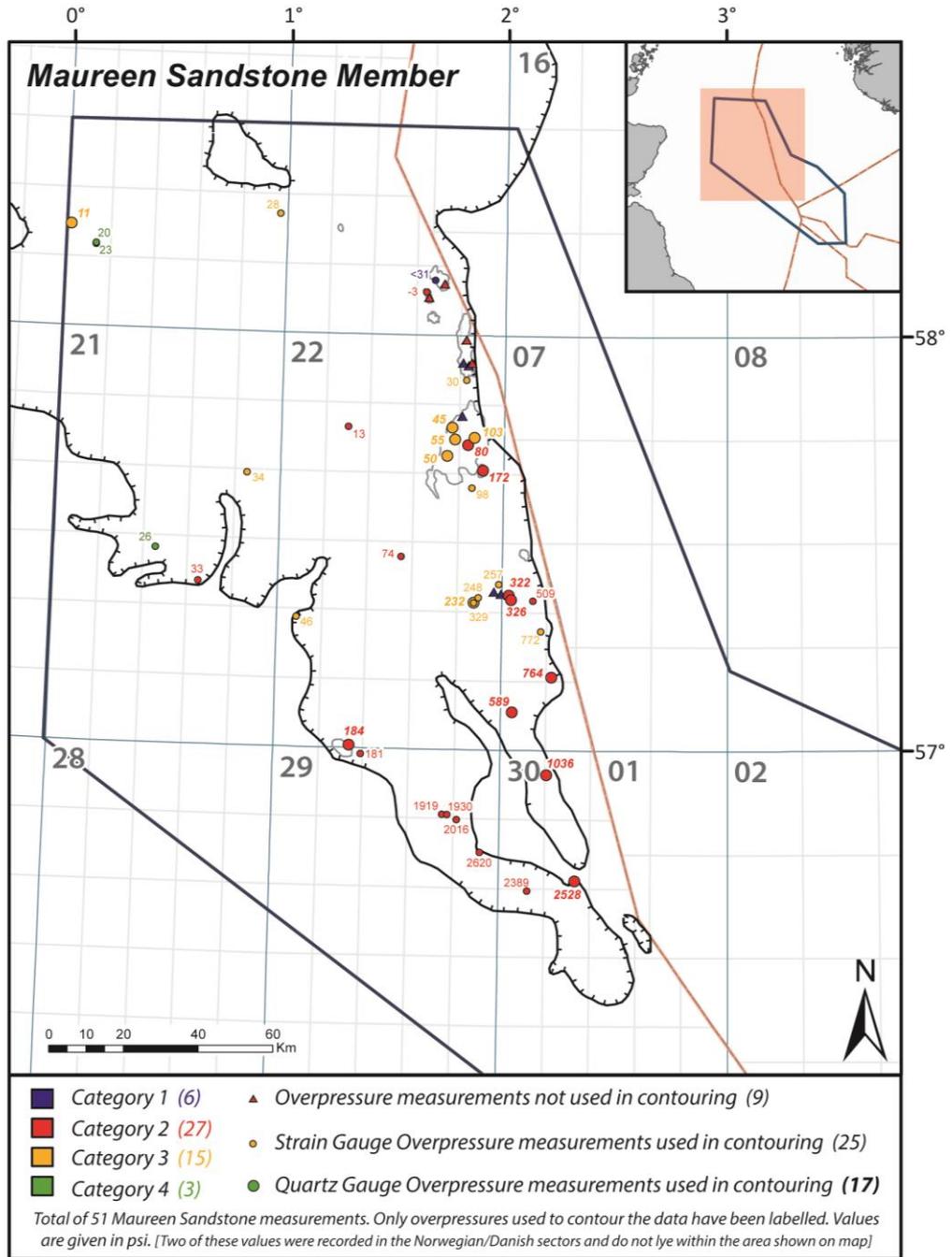
Figure 5.1a - Uncontoured overpressure distribution for the Maureen Sandstone Member. In total, 51 overpressure values were calculated for the Maureen Sandstone Member, but only 42 of these values were used to contour the distribution shown in **Figure 5.1b**. Values that were not used during contouring are not shown. Hydrocarbon fields whose reservoir is the Maureen Sandstone Member are shown in outline.
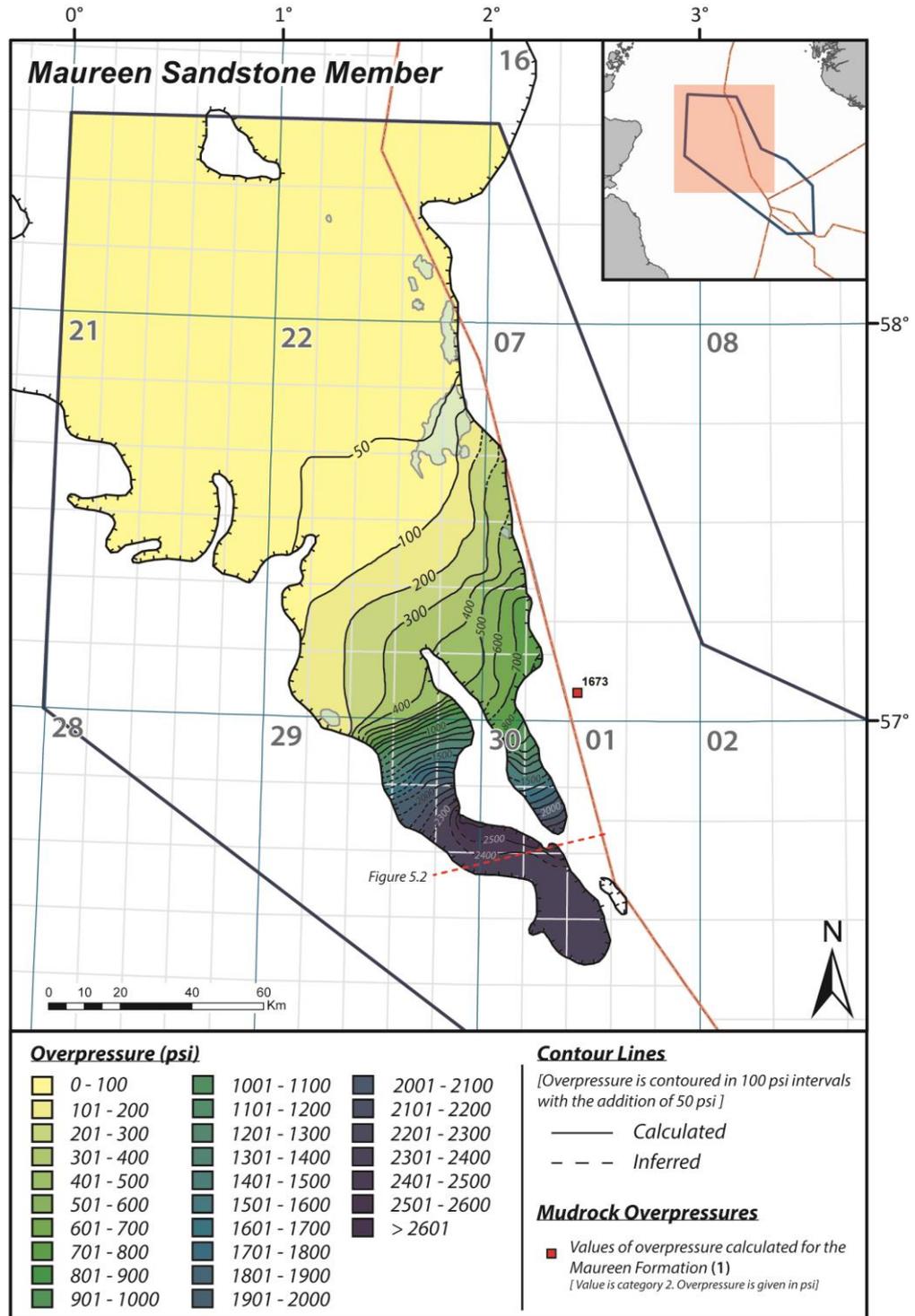
Figure 5.1b - Contoured overpressure distribution map for the Maureen Sandstone Member. Hydrocarbon fields for which the Maureen Sandstone Member is a reservoir are shown in pale blue. The red dashed line is the line of section for **Figure 5.2**.

There is a regional trend of overpressure increase towards the south-east, with overpressures reaching magnitudes in excess of 2500 psi (17.2 MPa) within UK quadrants 29 and 30. Hydrostatic conditions are observed in the north-western parts of the fan, covering UK quadrants 15, 16 and 21, and a large proportion of UK quadrant 22. In these areas, the Maureen Sandstone Member has effectively dewatered into shelf sediments further to the north-west and vertically into the overlying Palaeogene sandstone members.

For the most part, the rate of overpressure increase is fairly gradual up towards the 500 psi (3.45 MPa) contour line (**Figure 5.1b**). To the south-east of this contour, however, overpressure increases more rapidly, as indicated by the tightly spaced contours. This increase in overpressure is observed within both the western and eastern axial fairways of the Maureen Sandstone Member, although within the eastern fairway, development of this ramp starts slightly further to the south, beyond the 800 psi (5.52 MPa) contour line. Within the western axial fairway, overpressure increases dramatically from 500 psi (3.45 MPa) at the northern limit of UK quad 29, to 2400 psi (16.6 MPa) across UK blocks 29/9 and 29/10, corresponding to a hydrodynamic gradient of ~ 67.5 psi km^{-1} (0.47 MPa km^{-1}) for this area of the fan. In contrast, the hydrodynamic gradient is ~ 44.5 psi km^{-1} (0.31 MPa km^{-1}) for the overpressure ramp in the eastern Maureen fairway.

The highest magnitude of overpressure recorded within the whole of the Maureen Sandstone Member is 2620 psi (18 MPa) in well UK 29/10-1, situated on the eastern margin of the western axial fairway. Net sand thickness of the Maureen Sandstone Member within this well is 55 ft (17 m) TVD. A similar high magnitude value of 2528 psi (17.4 MPa) is recorded in UK 30/07a-8, once again on the margin of the fan, where net Maureen sand thickness is ~ 40 ft (12 m) TVD. Contouring in this area of the fan suggests that the direction of fluid flow is NE-SW, perpendicular to the regional flow direction. The contours here are based on a very limited number of overpressure values and the reality is presumably that fluid flow at the fan margins is locally inwards into the thicker, more channelized central areas of the fan, where the permeability is lower. This interpretation is supported by thickening of the Maureen sands to more than 150 ft (46 m) in the northern parts of UK blocks 30/11 and 30/12, where overpressure of 2389 psi (16.5 MPa) has been calculated in well UK 30/11a-2 (**Figure 5.2**). Alternatively, these high overpressures may be related to structural

109
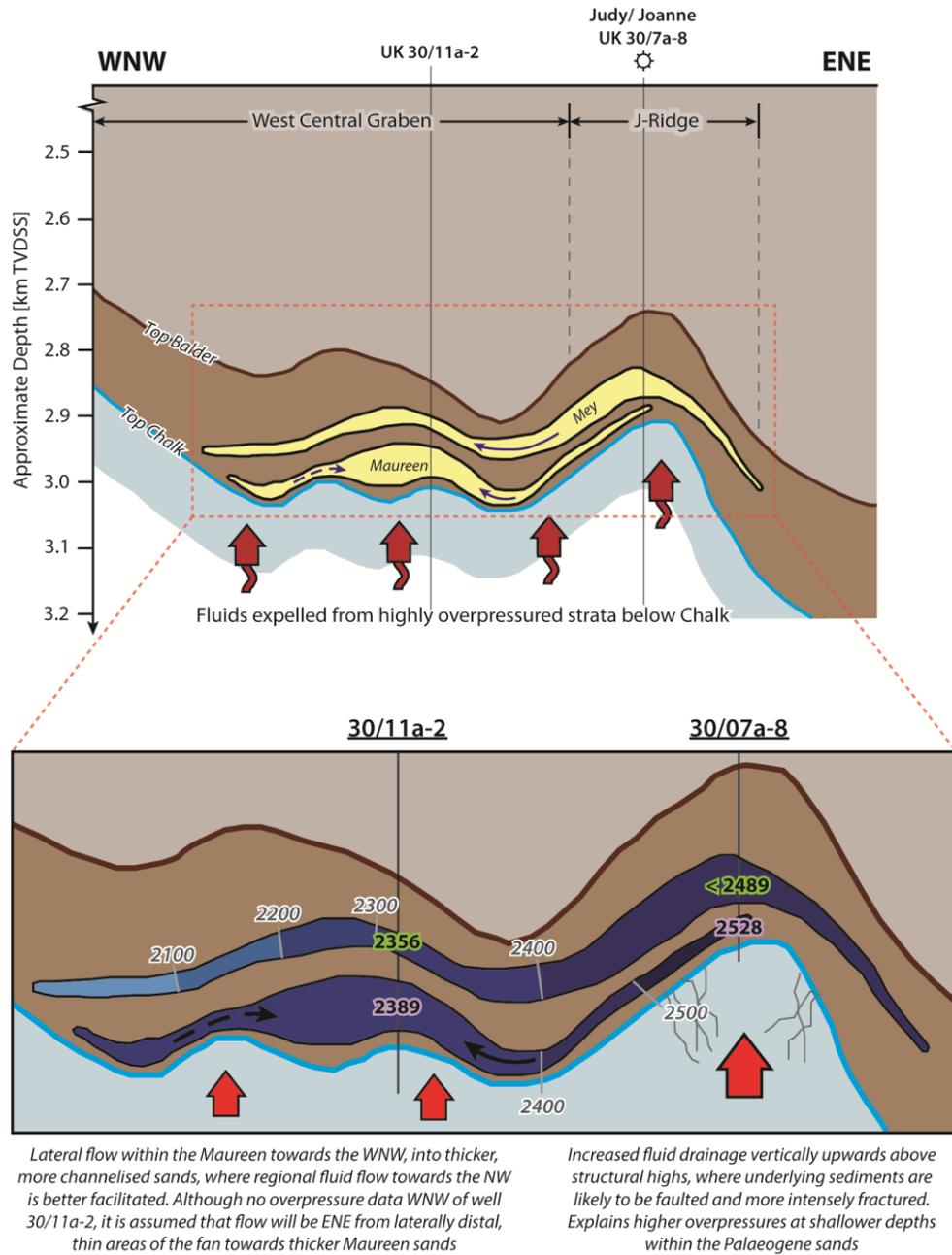
Figure 5.2 - Schematic cross-section showing the variations in thickness, depth and overpressure between the Maureen and Mey sandstone members towards the south of the study region. Line of section is shown in **Figures 5.1b** and **5.3b**.

features within the basin. For example, the highest overpressure magnitude of 2620 psi (18 MPa) in the Maureen Sandstone Member was recorded at the relatively shallow depth of 8945 ft (2726 m) TVDSS, in comparison with other overpressures of similar magnitude. Well UK 29/10-1, where this overpressure was recorded, is located above a structural high, as seen in the Top Balder contoured depth map (**Figure 2.11**), which

110

may be associated with an underlying salt diapir (Davison, 2004). Similarly, the second highest overpressure value of 2528 psi (17.4 MPa) in the Maureen Sandstone Member was recorded in well UK 30/07a-8, located above the Josephine Ridge (J-Ridge) at a depth of 9693 ft (2954 m) TVDSS, whereas immediately to the WSW, Maureen overpressures are lower at greater depths. Perhaps these higher magnitudes of overpressure may indicate that structurally high areas are favourable areas of vertical fluid entry from deeper underlying formations, as was suggested by Cayley (1987).

Other deviations from the regional SE-NW direction of fluid flow are observed towards the eastern margin of the Maureen fan in UK quadrant 23, where contours appear orientated almost parallel to the margin of the sandstone body, indicating fluid flow from east to west. Again, this is likely to be caused by the thinning of the Maureen Sandstone Member at the margins of the sand body, where overpressures are likely to be closer to those in the surrounding mudstones.

5.1.2. Mey and Heimdal sandstone members

A combined total of 98 overpressure values were calculated in the Mey and Heimdal sandstone members, of which 67 were accepted for contouring. Most of the overpressure data points are situated in the northern and southern parts of the fan sandstone, within UK quadrants 15, 16, 29 and 30. Several overpressure values have also been calculated along the eastern margin of the fan, in UK quadrant 23 and around the Everest Field in UK blocks 22/9 and 22/10. A large void in data distribution exists within UK quadrants 21 and 22, but coverage across the entire fan is still sufficient for contouring (**Figure 5.3**). A value of overpressure representative of the Siri Sandstone Member was calculated within Danish well Elna-1. The Siri Sandstone Member is time equivalent with the Mey and Heimdal sands. This overpressure value is not shown in **Figure 5.3**, as the map coverage does not extend far enough to the east. As is the case with the Maureen Sandstone Member, category 2 values are largely confined to the southern distal areas of the fan, where sandstone quality diminishes and pressure measurements are more difficult to record.

Overpressure decreases towards the north-west, following the regional trend of shallowing and gradual thickening of the Palaeocene sands. Pressures are hydrostatic
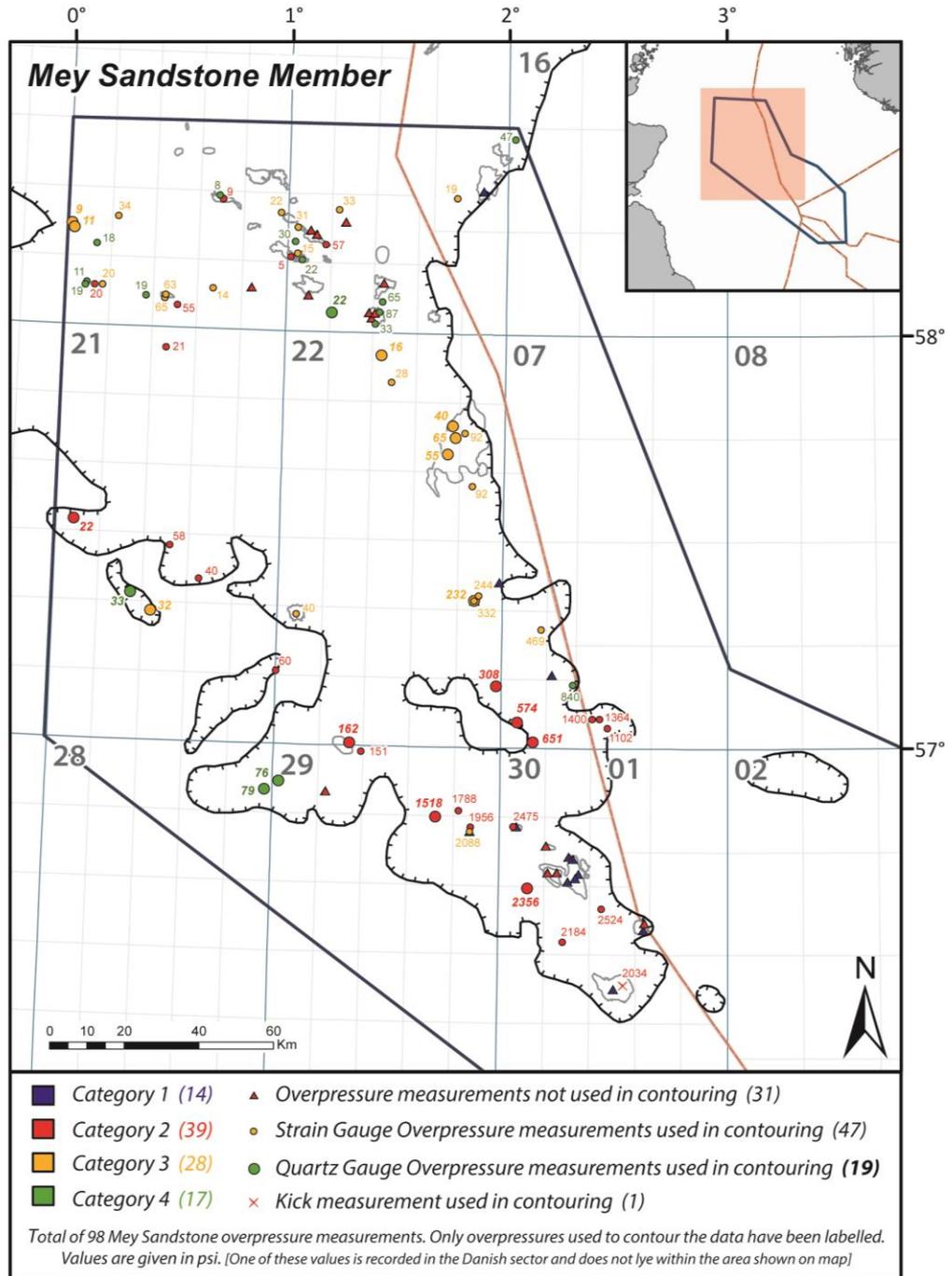
Figure 5.3a - Uncontoured overpressure distribution for the Mey and Heimdal sandstone members A total of 98 Mey/Heimdal overpressure values were calculated, but only 67 of these values were used to contour the distribution shown in **Figure 5.3b.** Overpressure values that were not used during contouring are not shown. Hydrocarbon fields reservoired in the Mey and Heimdal sandstone members are shown in outline.
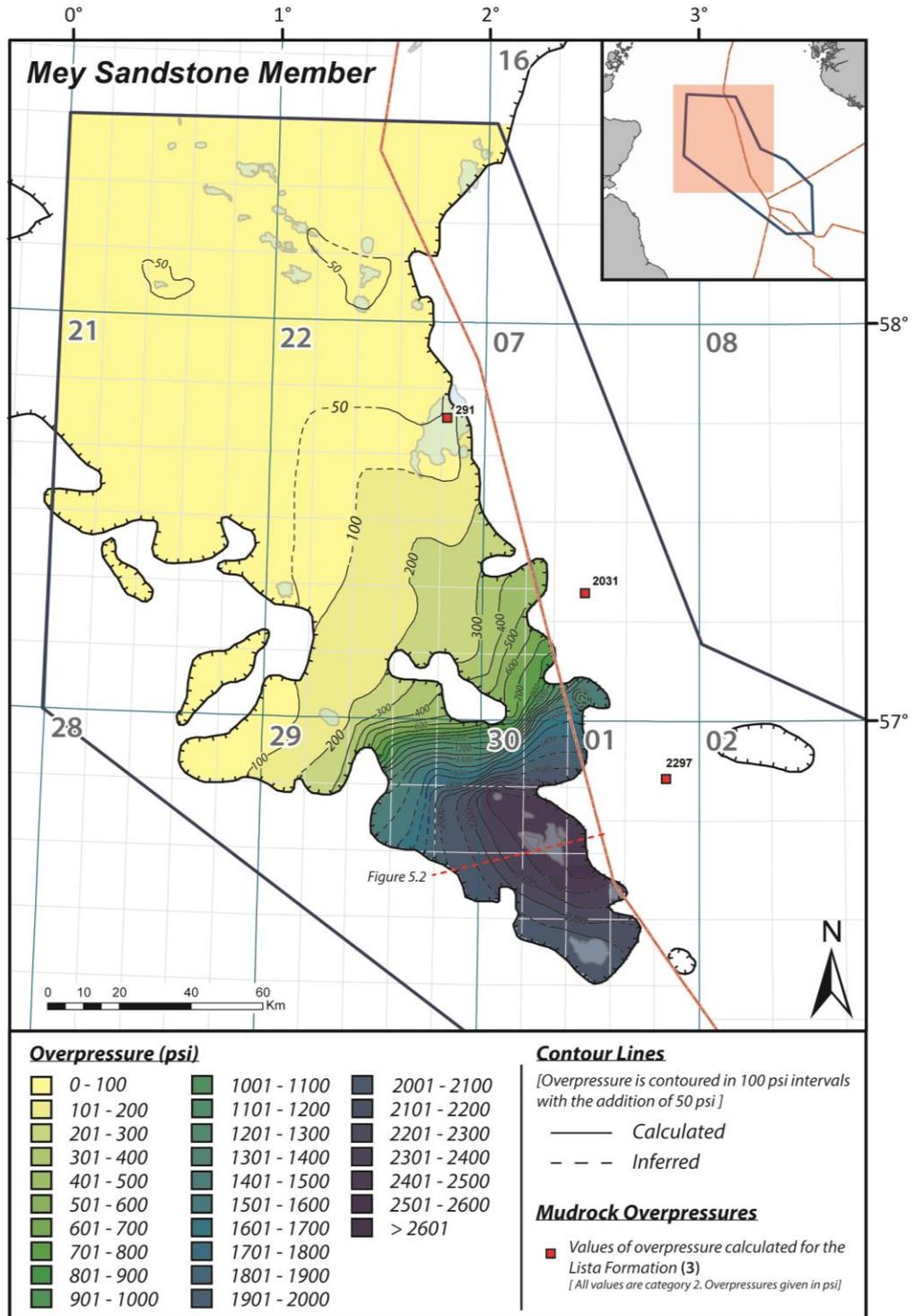
Figure 5.3b - Contoured overpressure distribution map for the Mey/Heimdal Sandstone Member. Hydrocarbon fields for which the Mey/Heimdal Sandstone Member is reservoir are shown in light blue. The red dashed line is the line of section for **Figure 5.2**.

and near hydrostatic within the Mey fan across the majority of UK quadrants 15, 16, 21 and 22, with small local overpressure highs in UK block 15/28 around the Rubie Field, and across UK blocks 16/21, 16/26 and 16/28 above the Balmoral, Cyrus and Andrew fields, where overpressures exceed 50 psi (0.35 MPa). Discussion of these local overpressure highs is deferred to *section 5.2.1*.

Overpressure increases gradually south-eastwards towards the 200 psi (1.38 MPa) contour line located in UK quadrant 22 (**Figure 5.3b**), where the average hydrodynamic gradient is only 4.0 psi km^{-1} (0.03 MPa km^{-1}). Further to the south-east, the Mey Sandstone Member is divided into two distinct sandstone fairways, separated by an area where there is no logged Mey sand in UK block 22/30. Within the eastern fairway, largely contained within UK quadrant 23, the overpressure ramp progressively steepens to over 1000 psi (7 MPa). Hydrodynamic gradients of 20.5 psi km^{-1} (0.14 MPa km^{-1}) are recorded in this area of the fan, across the Merganser, Scoter (UK 22/30) and Machar (UK 23/26) fields, with fluid flow to the north-west. In UK block 23/27, overpressure increases very steeply from 800 psi (5.5 MPa) to 1400 psi (9.65 MPa) over a distance of approximately 5 km, corresponding to a hydrodynamic gradient of 120 psi km^{-1} (0.83 MPa km^{-1}).Within the western Mey fairway, there is a similar ramp in overpressure although it starts slightly further to the north, with overpressure increasing south-eastwards from 400 psi (2.76 MPa) to 2000 psi (13.8 MPa) over a distance of 27 km.

To the south-east of the overpressure ramp in UK quadrant 30, overpressure reaches magnitudes in excess of 2400 psi (16.5 MPa), with the largest calculated value of overpressure being 2524 psi (17.4 MPa) in well UK 30/13-2X. Overpressure appears to decrease south-westwards in the distal parts of the fan, with lower overpressures of 2034 psi (14.0 MPa) and 2184 psi (15.1 MPa) calculated in wells UK 30/12b-2 and UK 30/11a-2, respectively. This local variation in fluid flow direction may be associated with the distribution of the underlying Maureen Sandstone Member. The Mey overpressure is greatest, as seen in wells UK 30/6-2 and UK 30/13-2X, where the Maureen sand is absent, so dewatering of the highly overpressured underlying Mesozoic strata is taking place directly into the Mey Sandstone Member.

In Norwegian block 7/11, there is an overpressure low based on overpressure calculated from within a single well. In Norwegian well 7/11-3, a value of 1102 psi (7.6

MPa) overpressure is calculated for the Mey Sandstone Member at a depth of 10287 ft (3136 m) TVDSS (**Figure 5.3a**). Although based only on data collected from a single well, the overpressure measurement is considered to be reliable. This low is situated at the margin of the Mey Sandstone, where overpressures would ordinarily be expected to increase as the sandstone thins. Consequently, this decrease in overpressure could potentially represent an area of vertical drainage where fluids are draining out of the Mey Sandstone into the underlying or overlying sediments, and is further examined in *section 5.2.1*.

Although there is only limited data coverage for UK quadrants 21 and 22, contouring indicates that fluid flows north-westwards along the eastern margin of the fan across UK blocks 22/9, 22/15 and 22/20, in the vicinity of the Everest Field. In the western part of the fan, the predominant fluid flow direction is west-north-westwards, towards the Moray Firth and Western Platform, as indicated by the orientation of the contouring around the Gannet D Field in UK blocks 22/21 and 22/22 (**Figure 5.3b**). Fluid flow towards the Western Platform is also indicated further south within the study region, around UK blocks 22/26, 29/01 and 29/02. In these areas, low overpressures indicate fluid drainage through some of the minor westerly fed fan systems which fed the larger axial Mey fan from the west (Kilhams *et al*., 2012).

5.1.3. Forties Sandstone Member

A total of 105 overpressure values were collected from within the Forties Sandstone Member, although only 75 of these values were deemed suitable for contouring the overpressure distribution. The uncontoured and contoured overpressure distribution maps for the Forties Sandstone Member are shown in **Figure 5.4**. There is a relatively good distribution of overpressure data across the Forties fan, facilitating accurate contouring. Areas where data distribution is relatively sparse include the northern part of UK quadrant 21 and the central part of UK quadrant 22. In the latter area, several data points were deleted due to the effects of production at the nearby Forties and Nelson fields. Similar numbers of category 2 and 3 overpressure data points were used to contour the Forties overpressure distribution, with fewer category 4 values. It can be seen on **Figure 5.4a** that the majority of category 2 data points lie in the southern, distal
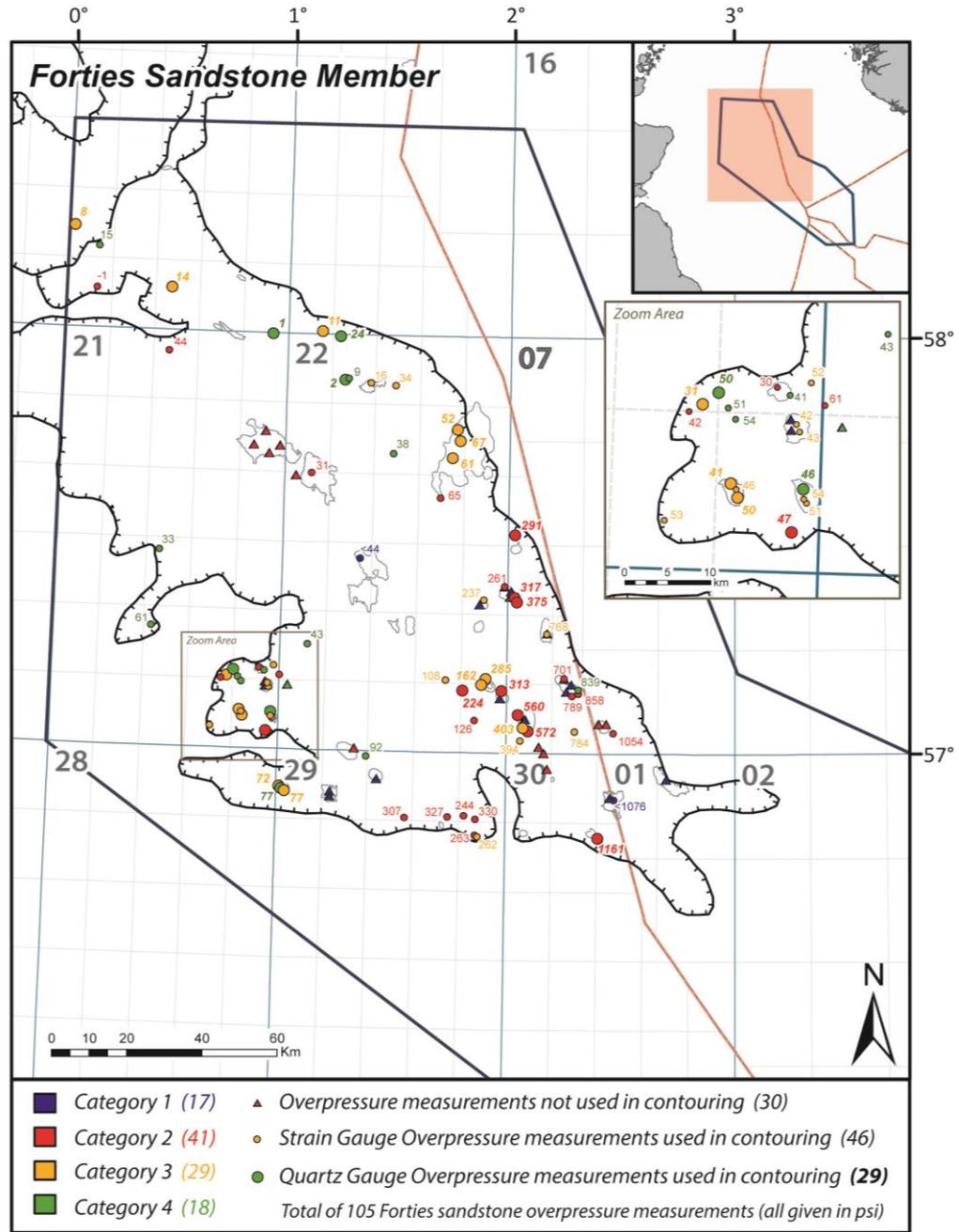
Figure 5.4a - Uncontoured overpressure distribution for the Forties Sandstone Member. A total of 105 overpressure values were calculated, but only 75 of these values were used to contour the distribution shown in **Figure 5.4b**. Overpressure values that were not used during contouring are not shown. Hydrocarbon fields for which the Forties Sandstone Member is a reservoir are shown in outline.
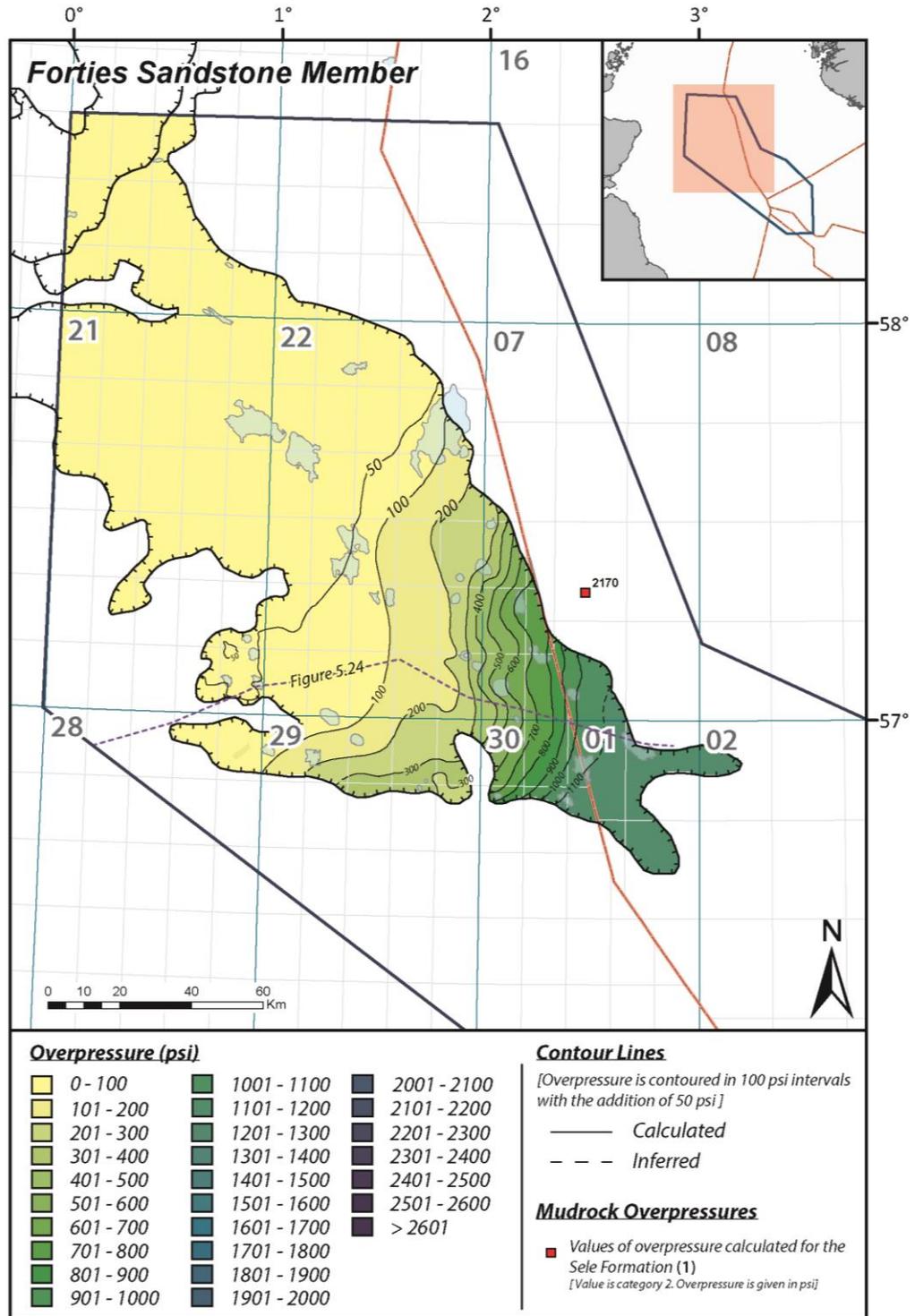
Figure 5.4b - Contoured overpressure distribution map for the Forties Sandstone Member. Hydrocarbon fields for which the Forties Sandstone Member is a reservoir are shown in light blue. The purple dashed line is the line of section for **Figure 5.24**.

117

areas of the fan, whilst category 3 and 4 values are more common in northern areas where the sands thicken and reservoir quality improves.

As observed within the other sandstone members, overpressure increases south-eastwards, in the direction of increasing distance from the sediment source and decreasing gross reservoir thickness. In the north-western part of the study area, where the sands are shallowest, pressures are close to hydrostatic and it is inferred that fluids drain laterally into the shelf sandstones belonging to the Dornoch Formation. Indeed, values of overpressure obtained from within the Dornoch Formation sands appear to confirm this, with calculated values of overpressure lying between hydrostatic pressure and the near-hydrostatic overpressures measured within the adjacent Forties Sandstone Member.

Overpressure rises gradually south-eastwards towards the 50 psi (0.34 MPa) contour, which cuts across UK quadrant 22, and then more steeply to exceed 1100 psi (7.6 MPa) in UK block 30/08 (**Figure 5.4b**). In these distal parts of the Forties fan system the overpressure is less than in the underlying Mey Sandstone Member. In Norwegian quadrant 1, where the underlying Mey Sandstone is not present, Forties overpressure may increase substantially towards the far south-eastern limits of the fan. However, since there are no overpressure data from the Forties Sandstone Member in this area of the basin, the overpressure appears to reach a plateau, not exceeding 1200 psi (8.3 MPa).

Within UK quadrants 23 and 30, closely spaced contours indicate a more rapid increase in overpressure across the Machar (UK block 23/26), Lomond (UK block 23/21) and Pierce (UK block 23/27) fields, with a hydrodynamic gradient of ~ 25 psi km^{-1} (0.17 MPa km^{-1}). Hydrocarbons within the Forties Sandstone Member in this area are typically trapped above or around salt diapir structures and hydrocarbon–water contacts are likely to be hydrodynamically tilted, as documented for the Pierce Field (Dennis *et al.*, 2005). Maximum overpressures in the range 1100–1200 psi (7.6–8.3 MPa) are attained around the Blane Field (UK 30/3) and along the far south-eastern limits of the Forties Sandstone Member in UK block 30/8 and in Norwegian quadrant 1.

Although the predominant direction of overpressure drainage is north-westwards, additional drainage towards the west also occurs as is evident from the N–S orientated contours in the south of UK blocks 22 and 23. In this part of the basin, fluids

probably drain laterally along the smaller, westerly derived basin fans of the Forties Sandstone Member. These E–W orientated fans, hosting hydrocarbon fields such as Gannet, Bittern and Scoter, exhibit updip and downdip variations that are similar to those in the larger NW–SE oriented axial fan system, with reservoir net-to-gross, porosity and permeability decreasing eastwards towards the distal reaches of the smaller fans (Hempton *et al.*, 2005).

There is a negative overpressure anomaly consisting of three values in the range 200–300 psi (1.4–2.1 MPa) around the common boundary of UK blocks 29/5 and 29/10, where the Forties Sandstone Member thins and terminates (**Figure 5.4a**). This reduction in overpressure could indicate vertical drainage of fluids out of the Forties sands upwards into the Cromarty Sandstone Member above, and is discussed further in *section 5.2.1*.

A small positive anomaly, comprising two values of overpressure slightly greater than 50 psi (0.34 MPa), is situated in UK 21/30, around the Guillemot West Field. It is possible that this positive anomaly is due to pressure gauge error, because both measurements were recorded using a strain gauge with an accuracy of ±15 psi (±0.1 MPa). This explanation appears most likely since values recorded within the Tay and Cromarty reservoir members of the same wells also appear to be slightly higher than surrounding overpressures, assuming that all measurements in each well were recorded using the same pressure gauge.

5.1.4. Cromarty Sandstone Member

A total of 42 overpressure values were calculated within the Cromarty Sandstone Member, of which 33 values were deemed suitable to contour the overpressure distribution. The majority of values were category 3 with some category 4 values and yet fewer category 2 values. As with all of the other sandstones examined, category 2 values tend to be located towards the distal margins of the fan sands, where diminishing reservoir quality makes it more difficult to perform pressure tests. In contrast, good quality category 3 and 4 data values are obtained where sands are shallower and closer to the sediment source on the Western Platform. The uncontoured and contoured overpressure distribution maps for the Cromarty sands are shown in **Figure 5.5**.

119
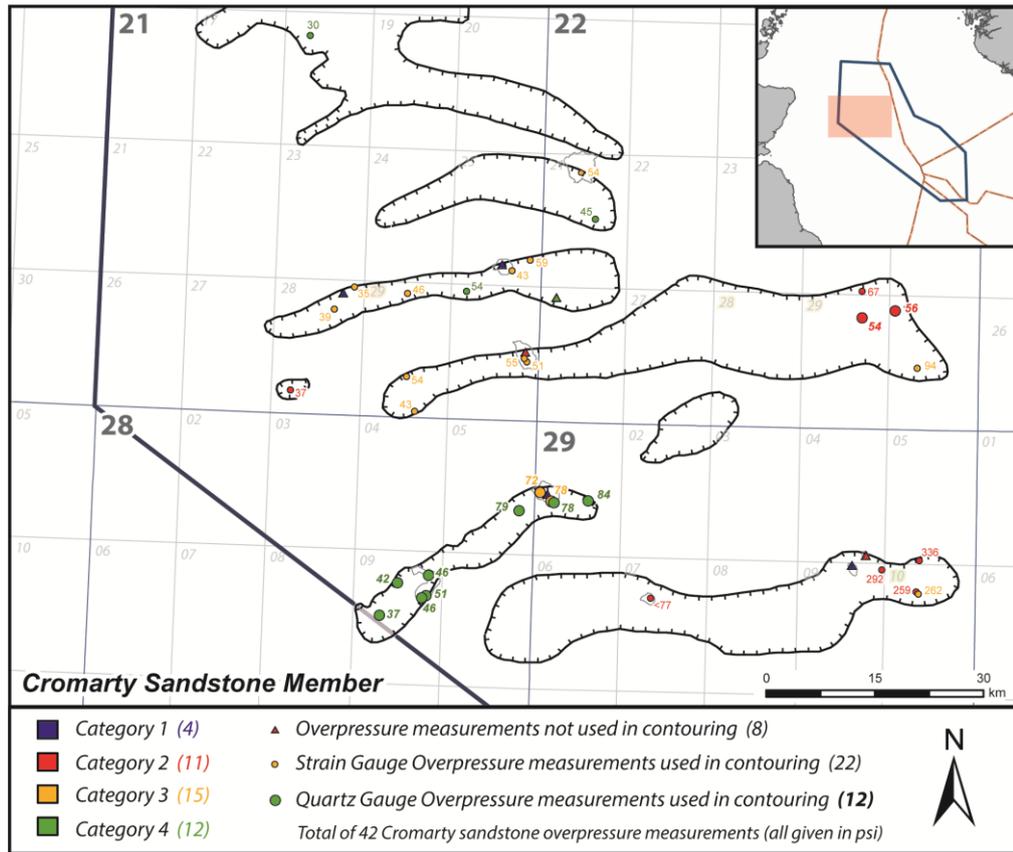
Figure 5.5a - Uncontoured overpressure distribution for the Cromarty Sandstone Member. A total of 42 overpressure values were calculated, but only 33 of these values were used to contour the distribution shown in **Figure 5.5b**. Overpressure measurements which were not used during contouring are not shown.

Overall, there appears to be a general trend of decreasing overpressure north-westwards, similar to the underlying Forties Sandstone Member but with lower overpressure magnitudes. Within each of the individual channelized sandstone units, lateral flow is constrained by the geometry of the units and is generally westwards.

The greatest magnitudes of overpressure occur within the southernmost Cromarty sand unit, orientated almost W-E extending from UK blocks 28/10 to 29/5 and 29/10 (**Figure 5.5a**). Overpressures within this unit reach magnitudes in excess of 300 psi (2 MPa) in block 29/5, very similar to the overpressure in the Forties Sandstone Member below. Although the contouring in **Figure 5.5b** shows that overpressure decreases westwards within this sand body, interpretation of this gradient is heavily dependent on the pressure data from well UK 29/07-1, the discovery well for the Curlew A Field. Ordinarily, this overpressure value (< 77 psi) would not have been used

120
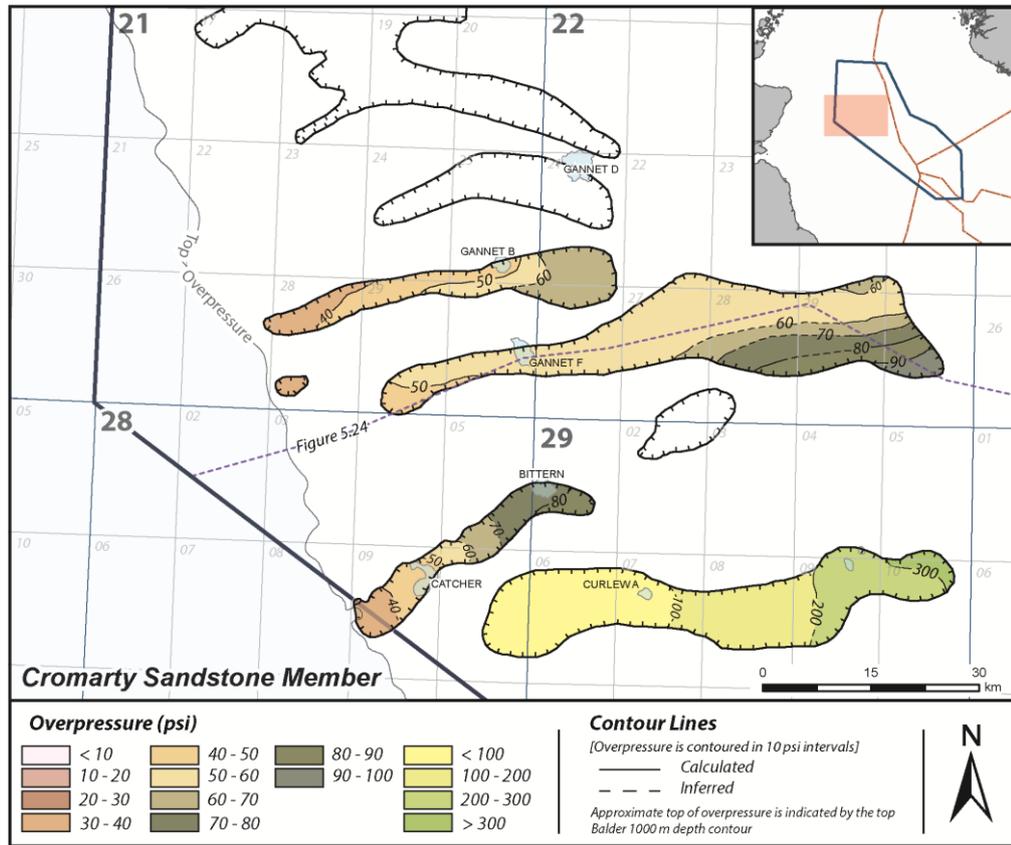
Figure 5.5b - Contoured overpressure distribution map for the Cromarty Sandstone Member. Hydrocarbon fields for which the Cromarty Sandstone Member is a reservoir are shown and labelled. An approximation of top overpressure is shown on the map as being the 1000 m (3300 ft) top Balder formation contour line. The Cromarty sands are situated ~370 ft (112 m) below the top Balder, although areas of direct contact exist locally. The purple dashed line is the line of section for **Figure 5.24**.

to contour, because it is a solitary measurement recorded in oil-filled sandstone at an unknown vertical distance above the oil–water contact; however, considering the scarcity of data within the sand body, and that overpressure within the water leg would be even lower because of hydrocarbon buoyancy, an exception was made for this data point.

Within the other Cromarty sand bodies, calculated overpressure values are everywhere lower than 100 psi (0.7 MPa). In the SW-NE oriented sand body extending from UK block 28/09 to UK block 29/1, overpressure decreases south-westwards, from the Bittern Field to beyond the Catcher discovery with a hydrodynamic gradient of ~ 1.6 psi km^{-1} (11 kPa km^{-1}). Small lateral overpressure gradients such as these indicate that

121

the sand units are dewatering laterally, and that there is an oil migration pathway through the sequence. The characteristic westwards dewatering of the individual Cromarty sand units is not evident north of UK blocks 21/22 to 22/21, where data are too sparse to be accurately contoured.

5.1.5. Tay Sandstone Member

A total of 52 overpressure values were collected from within the Tay Sandstone Member, with 37 of these values being deemed suitable for contouring the overpressure distribution. The uncontoured and contoured overpressure distribution maps for the Tay Sandstone Member are shown in **Figure 5.6**. The vast majority of overpressure data values used for contouring were classified as category 3 or 4. Data distribution across the sand is predominantly confined to the western, channelized areas, with relatively few values being calculated in distal areas of the fan (**Figure 5.6a**). Distribution is particularly sparse within UK quadrant 22, although it is adequate for contouring. The greatest magnitudes of overpressure recorded within the Tay Sandstone Member are 73 psi (0.503 MPa) in UK well 21/17-1 at the north-western margin of the fan, and 72 psi (0.496 MPa) in UK well 22/30a-1 towards the south-eastern margin of the fan. Higher magnitudes of overpressure are found towards the distal margins of the sandstone member with overpressure generally decreasing towards the west-south-west.

Overpressures reach a minimum of 10 psi (0.07 MPa) around the Pilot (UK 21/27) and Narwhal (UK 28/2) fields, indicating drainage of fluids along Tay feeder channels. Such channels can be identified by the numerous hydrocarbon accumulations trapped within them, e.g., Pilot (21/27), Fyne and Dandy (21/28) and Guillemot (21/19) define one such feeder channel and Narwhal (28/02), Elke (28/03), Riddon and Scavaig (21/29) define a second channel system further south. A similar pattern of drainage towards the south-west is observed in UK blocks 28/09 and 29/06, around the newly discovered Catcher and Varadero fields, although the data in this region have not been contoured, partly due to quality, with the majority of measurements being taken from within oil columns at vertical depths greater than 35 ft (11 m) above the oil–water contact, and partly due to the lack of knowledge concerning Tay sandstone distribution.
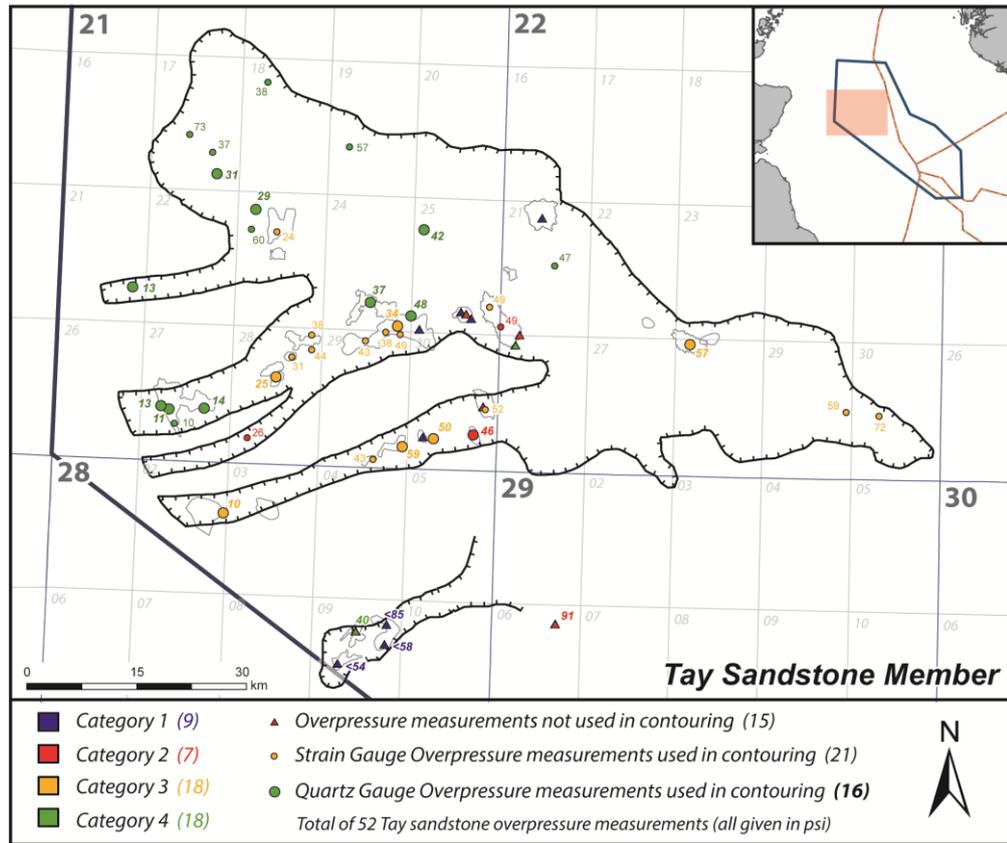
Figure 5.6a - Uncontoured overpressure distribution for the Tay Sandstone Member. A total of 52 overpressure values were calculated, but only 37 of these values were used to contour the distribution shown in **Figure 5.6b**. Overpressure values that were not used during contouring are not shown.

Along the western slope of the basin, within UK blocks 21/21, 21/26, 21/27, 28/02 and 28/03, the Tay Sandstone Member is buried at depths less than 3300 ft (1000 m) TVDSS, corresponding to the approximate top of overpressure for the Central North Sea according to Leonard (1993) and O'Connor and Swarbrick (2008). This depth contour is shown in **Figure 5.6b**. Consequently, it is to be expected that overpressure is exceptionally low in this area of the Tay fan. Hydrodynamic gradients established within the Tay Sandstone Member range from ~ 1.3 psi km^{-1} (9 kPa km^{-1}) along the Narwhal–Gannet F channel system, up to 2 psi km^{-1} (13.8 kPa km^{-1}) along the Pilot–Fyne/Dandy channel system. As with the underlying Cromarty sands, these small lateral changes in overpressure can have only a minor effect in hydrodynamic trapping
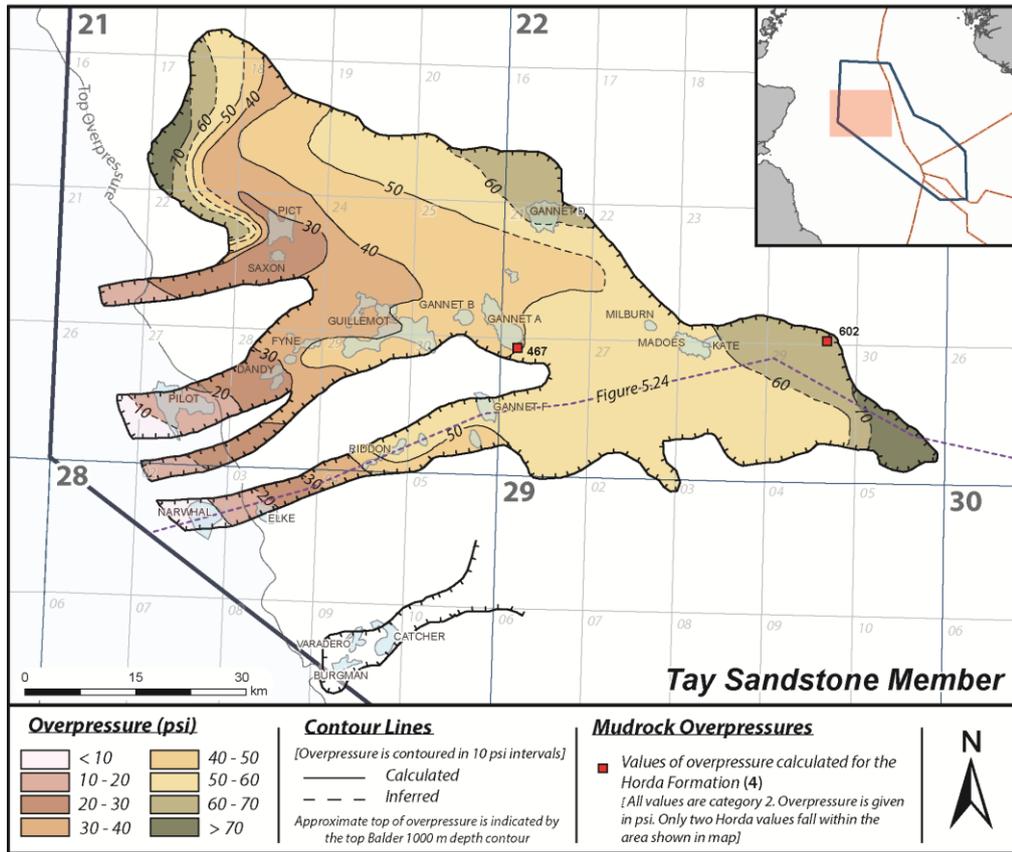
Figure 5.6b - Contoured overpressure distribution map for the Tay Sandstone Member. Hydrocarbon fields for which the Tay Sandstone Member is a reservoir are shown and labelled. An approximation of top overpressure is shown on the map as being the 1000 m (3300 ft) top Balder formation contour line. The Tay sands are situated on average ~260 ft (80 m) above the top Balder, although areas of direct contact exist locally. The purple dashed line is the line of section for **Figure 5.24**.

of hydrocarbons, albeit the amount of tilt depends upon the density of hydrocarbons present. The occurrence of such hydrodynamic gradients, however small, does indicate that the sands provide a potential migration pathway for fluids, including hydrocarbons.

5.1.6. Grid Sandstone Member

Two separate overpressure distribution maps are presented for the Grid Sandstone Member in **Figure 5.7**. The first map shows overpressures calculated within the lower and older Caran Sandstone Unit, whilst the second shows overpressures within the younger Brodie Sandstone Unit. The Brodie Sandstone Unit comprises the Brioc and
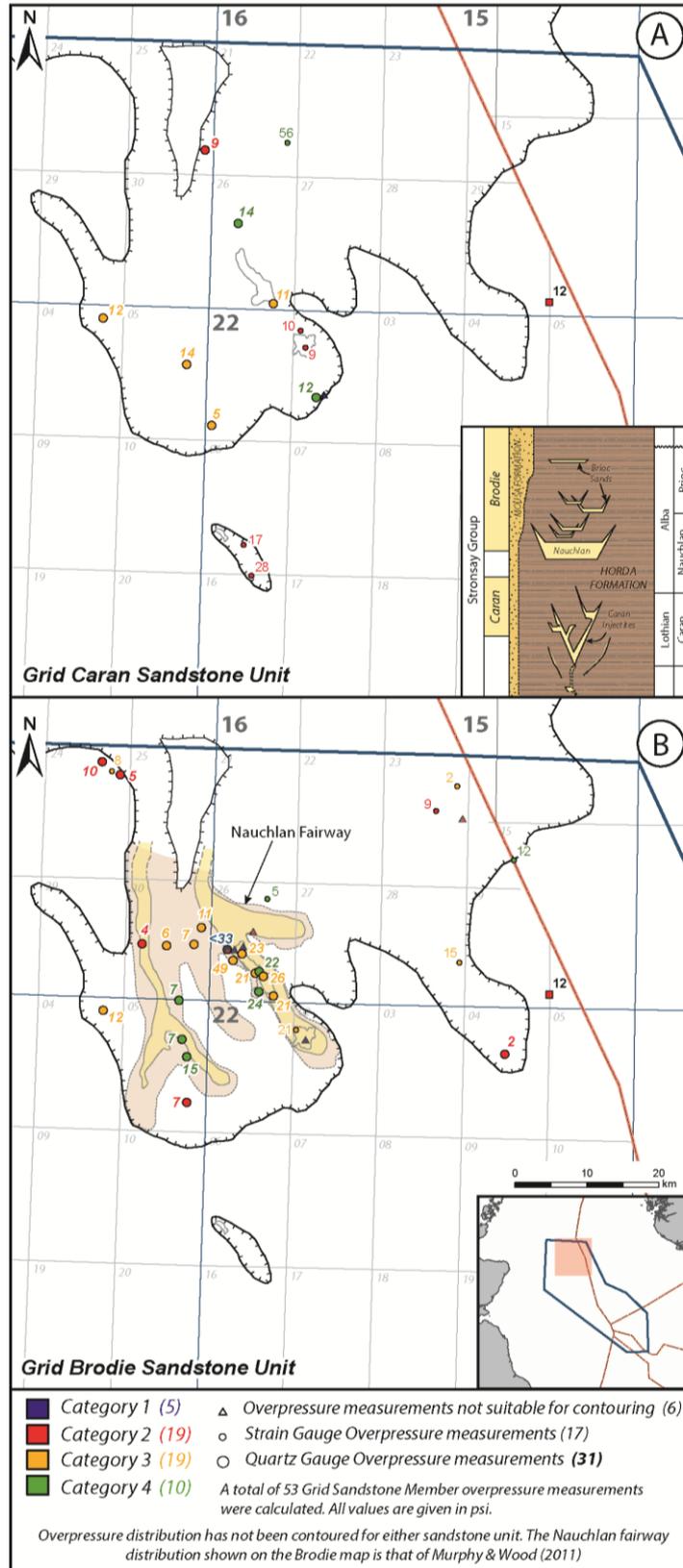
Figure 5.7 - Uncontoured overpressure distribution for the Grid Sandstone Member. (A) Overpressures within the older (deeper) Caran Sandstone Unit (B) Overpressures within the younger and shallower Brodie Sandstone Unit

Nauchlan sandstone members of Newton and Flannagan (1993). The lowermost Brodie (i.e. the Nauchlan Sandstone) serves as reservoir for both the Alba (UK 16/26) and Chestnut (UK 22/02) fields, and is thought to be of a depositional origin, with subsequent remobilisation post-deposition (Huuse *et al*., 2005; Lonergan and Cartwright, 1999; Szarawarska *et al*., 2010; Murphy and Wood, 2011). In contrast, there is much uncertainty regarding the mode of deposition for the older Caran Sandstone Unit, since it is not known whether these sands were fully injected or remobilized post-deposition (Knox and Holloway, 1992; Mattingly and Bretthauer, 1992; Jones *et al*., 2003; Huuse *et al*., 2005; Murphy and Wood, 2011). Several of the more recent publications favour a completely injected origin (Huuse *et al*., 2003; Murphy and Wood, 2011), with continuing debate about whether the source of sediment is pre- or post-Balder.

For both units, the overpressure distributions remain uncontoured, partly due to the irregular distribution of overpressure data points, and partly due to the uncertainties surrounding the Caran and Brodie sandstone distribution. In both the Caran and Brodie sandstone units, overpressures are mostly below 50 psi (0.35 MPa), the only exception being in well UK 16/21-4a where an overpressure of 56 psi (0.39 MPa) is calculated within the Caran Sandstone Unit. This well location lies within the local overpressure high that was observed in the underlying Mey Sandstone Member around the Balmoral, Cyrus and Andrew fields, suggesting that these reservoirs intervals may be in vertical hydraulic communication around this area.

A total of 13 overpressure values could be calculated within the Caran Sandstone Unit. All of these values are of very low magnitude, between 5 psi (0.04 MPa) and 14 psi (0.1 MPa) in the main Grid sand body, with the exception of the value in well 16/21-4a mentioned above. In wells UK 22/06a-10 and UK 22/11-1, where the Caran Sandstone Unit appears to be isolated from the main Grid sand, magnitudes of overpressure are slightly higher, at 17 psi (0.12 MPa) and 28 psi (0.19 MPa), respectively.

A greater number of 35 overpressure values were calculated for the Brodie Sandstone Unit, with magnitudes ranging from 2 psi (0.01 MPa) up to 49 psi (0.34 MPa). All but seven Brodie overpressure values are derived from pressures measured using a standard quartz gauge, with an accuracy of ± [0.025% of reading + 0.5 psi (3.4

126

kPa)]. Consequently, although the overpressures being discussed are of low magnitude, the vast majority of individual values are of high accuracy. Most overpressure values calculated are <15 psi (<0.10 MPa). However, around the Alba and Chestnut fields in UK blocks 16/26 and 22/02, overpressures are of slightly greater magnitude than the rest of the sandstone unit, ranging from 21 psi (0.15 MPa) to 49 psi (0.34 MPa). Interestingly, overpressures in this area also appear to be higher than in the underlying Caran Sandstone Unit, and underlying Forties Sandstone Member, by approximately 10 psi (0.07 MPa). This pressure reversal between the adjacent Brodie and Caran sandstone units implies that these two units are not hydraulically connected in this area of the basin.

The Nauchlan sand fairway as mapped by Murphy and Wood (2011, Fig. 6) is shown on the Brodie Sandstone Unit overpressure map in **Figure 5.7.** It can be seen that the Nauchlan sands are sourced from the NNW (Murphy and Wood, 2011) and extend across the Alba Field to terminate south-west of the Chestnut Field. Overpressures within the main Nauchlan fairway do not decrease towards the direction of sediment source as was observed in the larger underlying Palaeocene fan sandstones. Owing to the complexity of the sands around this area and the presence of hydrocarbons within the Brodie Sandstone Unit, further examination of overpressures within this area is provided in *section 5.2.2* and *section 5.2.2.3*.

5.2. Vertical drainage pathways

Where overpressure changes with depth, there is the potential for vertical movement of fluids. Just like lateral flow, water will flow vertically in the direction of decreasing overpressure. Since within the Central North Sea, overpressure generally increases with depth, the vertical component of pore water flow is commonly upwards, although there are areas where water flows vertically downwards as may be indicated by pressure reversals on pressure–depth plots.

The rate of vertical fluid flow depends not only on the vertical overpressure gradient, but also on the vertical permeability of the strata through which water is flowing. In areas, where thick, lower permeability shale intervals are present between reservoir sandstone members, vertical fluid flow will not be easily facilitated and

pressure dissipation is likely to be very slow, occurring over geological timescales. Where intraformational seals between Palaeogene sands are present, fluid flow within the Palaeogene will be predominantly lateral. Deming (1994) noted that the rate of pressure leakage through a seal is directly proportional to its vertical permeability and inversely proportional to its thickness. In areas where higher permeability sandstone members are in direct contact with each other, or where higher permeability pathways exist between sandstone members, the rate of vertical fluid flow will be enhanced. Higher permeability pathways which will facilitate such flow might comprise injected sandstones, sandy-silty regions, faults and/or fractures.

Pressure data available for the Palaeogene of the Central North Sea were analysed in order to determine areas of pressure connectivity between sandstone members, and areas where vertical fluid flow is likely to be occurring. Using pressure data recorded in water, areas of pressure connectivity can be recognized where 1) pressure data available across multiple sandstone members plot on the same water gradient, and 2) differences in overpressure between vertically adjacent sandstone members equate to zero, or very nearly so. In these areas, sandstone members are in hydraulic communication with each other, suggesting that the intraformational sediments separating sandstone members (if present) are non-sealing.

Potential areas of enhanced vertical fluid flow may be recognized where 1) there are anomalous values of overpressure or irregularities found within the regional lateral trends, and 2) pressure data available across multiple sandstone members plot on different water gradients, meaning that differences in overpressure between vertically adjacent sandstone members exist. Areas of enhanced vertical drainage are difficult to identify using pressure data alone since alternative interpretations can also be made for each of the criteria mentioned above, e.g. the existence of a pressure seal between sandstone members.

Where large overpressure differences exist vertically, fluid flow is a feasible explanation; however, where low permeability mudrocks are present between sandstone members it is dependent upon the presence of higher permeability pathways to facilitate fluid flow. Detailed structural maps were not available to this study, and so interpretation of vertical drainage is largely based on pressure data alone. Where possible, attempts have been made to assess the likelihood of such flow pathways in

128

certain areas, using the regional depth maps for key horizons, composite well data, and various published sources.

The locations of known hydrocarbon accumulations can also be used to assist with identification of vertical flow pathways between the Palaeogene sandstone members as discussed in *section 5.2.3*.

5.2.1. *Areas of hydraulic connectivity*

Maps of overpressure difference have been generated for each pair of adjacent sandstone members to show hydraulic connectivity between them. Where a single water gradient can be fitted to pressure data extending across sandstone members in a single well, good hydraulic connectivity is indicated and such wells are represented by a circular symbol on the maps. Wells within which two separate water gradients must be fitted to the two sandstone members denote a pressure transition or reversal, and are represented by a triangular symbol on the corresponding map (**Figure 5.8**). For each map, wells are labelled with the difference in vertical overpressure between the overlying sandstone member and the underlying sandstone member.

Differences were calculated by subtracting the value of overpressure within the shallower sand, from the value of overpressure within the deeper sand (**Figure 5.8**). Where the calculated overpressure difference is zero, it is likely that the two vertically adjacent sands are in good pressure connection with each other, so that hydrocarbons can migrate vertically between sands. Positive differences represent pressure transition zones on P-D plots, and are likely to signify that the two adjacent reservoir sands are separated by a seal; however, the potential for fluid flow does exist, in the vertically upward direction. Negative differences represent pressure reversals on P-D plots, again signifying the presence of a seal, but with the potential for downward fluid flow if pathways are available. Interpretation of vertical overpressure differences in terms of fluid flow requires consideration of the overpressure distribution and seal transmissivity in three dimensions, so the overpressure differences can only be used as a guide to potential areas of enhanced vertical flow.

Where sandstone members are well connected to each other hydraulically, differences in calculated overpressures are not always zero. Many small variations

129
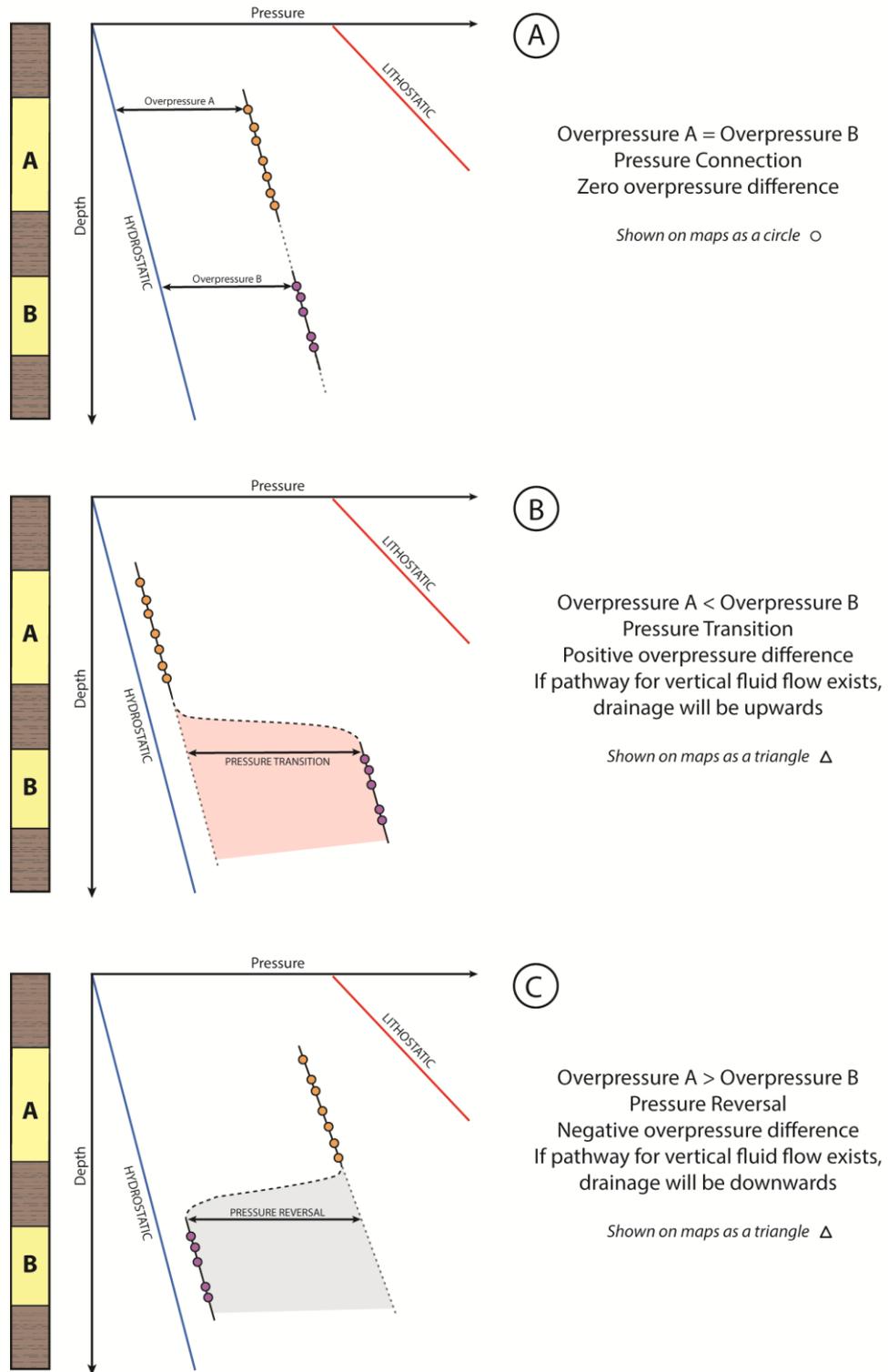
Figure 5.8 - Schematic P-D plots showing three idealised outcomes of determining where sandstones are in pressure connection. (A) Pressure connectivity, where a single water gradient can be fit to pressure data across different reservoir intervals and overpressure differences equate to zero. For (B) and (C) separate water gradients must be fit to pressure data in different reservoir intervals. (B) Pressure transition, where overpressure differences are positive; (C) Pressure reversal, where overpressure differences are negative.

around zero exist, which are thought to be related to data quality. However, larger magnitude differences, of both polarities, ranging from -12 psi (-83 kPa) to 33 psi (268 kPa) have also been calculated for some areas of the basin. Such large magnitude differences where sands are in pressure connection are largely due to variations in water density and salinity when using a constant hydrostatic gradient of 0.445 psi ft^{-1} (0.01 MPa m^{-1}) to calculate overpressures (**Figure 5.9**). Positive differences of high magnitude are observed around salt diapir structures, where water gradients are often greater than 0.445 psi ft^{-1} (0.01 MPa m^{-1}); whereas negative differences are found where fresher water gradients less than 0.445 psi ft^{-1} (0.01 MPa m^{-1}) have been recorded using the pressure data (**Figure 5.9**).

Only a relatively small number of wells sampled pressures within both the Maureen and Mey sandstone members. The majority of these wells indicate good hydraulic connectivity between the two sands (**Figure 5.10**). Three instances of good connectivity are located towards more southerly areas of the fans, focused around salt diapir structures, the Banff diapir around UK blocks 22/27 and 29/02, and an unnamed salt diapir in UK 30/11. Differences in overpressure between the Mey and Maureen sands in these wells are greater than 20 psi (138 kPa), reflecting more saline pore waters with gradients ranging from 0.5 psi ft^{-1} (11.3 kPa m^{-1}) to 0.53 psi ft^{-1} (12 kPa m^{-1}) according to the pressure measurements recorded. Only two wells indicate small magnitude pressure reversals between the Mey and Maureen sandstone members, but in both wells, UK 21/19-2 and UK 22/18-3, it is thought that such reversals are actually related to the poor quality of pressure data. Overall the similarities seen between the overpressure contouring of these two sandstone members (**Figures 5.1b** and **5.3b**), along with the majority of shared water gradients, appear to suggest that the Mey and Maureen sandstone members are largely well hydraulically connected to each other, in areas where their distributions overlap.

A total of 27 wells sample pressures within both the Forties Sandstone Member and one of the underlying sandstone members, i.e. either the Mey or the Maureen (**Figure 5.11**). The majority of these wells indicate that the Forties and Mey/Maureen sandstone members are in good connection across a large area of the Forties fan, particularly within UK quads 22 and 23. Hydraulic connectivity between these two sands within UK quad 23 may be through salt-related structures, since numerous diapirs

For all wells a hydrostatic water gradient of 0.445 psi/ft was used to calculate overpressures
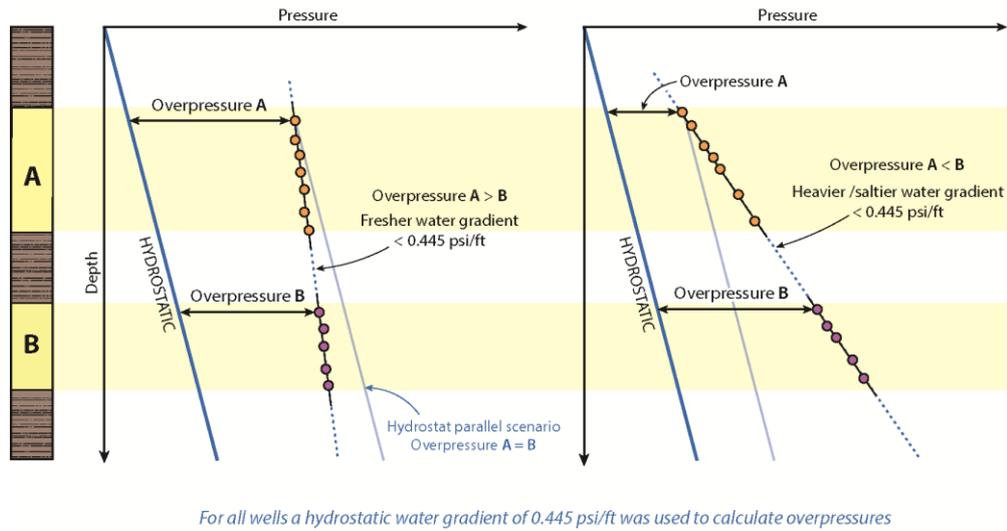
Figure 5.9 - Schematic P-D plots showing how variations in water salinity may influence calculations of overpressure, when made assuming a constant regional hydrostatic gradient. Such discrepancies will ultimately be carried forward when calculating differences in overpressures between vertically adjacent reservoir intervals, to be used for the purpose of assessing vertical fluid flow.

piercing the Palaeogene succession are present in this area of the basin, e.g. Pierce, Machar and Scoter.

Around southern areas of the Forties fan, towards the eastern part of UK quad 29, several wells record a pressure transition between the Forties and Mey/Maureen sandstone members, with magnitudes of overpressure difference ranging from 1534 psi (10.6 MPa) to 1826 psi (12.6 MPa) (**Figure 5.11**). The multi-well P-D plot for UK quadrant 29 (**Figure 5.12**) shows the large pressure transition between the Forties and Mey sands in this area. Additionally, it can be seen that the Forties and Cromarty sandstone members, as well as the Mey and Maureen sandstone members, appear to be in good hydraulic connection with each other. Pressure data collected from the underlying Tor Formation in UK well 29/10-3 suggest that the Tor Formation may also be in hydraulic connection with the overlying Mey and Maureen sands, although this cannot be concluded definitively because of the limited amount of Tor pressure data available. A pressure transition zone of similar magnitude, ~1500 psi (10.3 MPa), exists between the Forties and Mey sandstone members within UK quadrant 30, as calculated using the available pressure data for this quadrant.

132
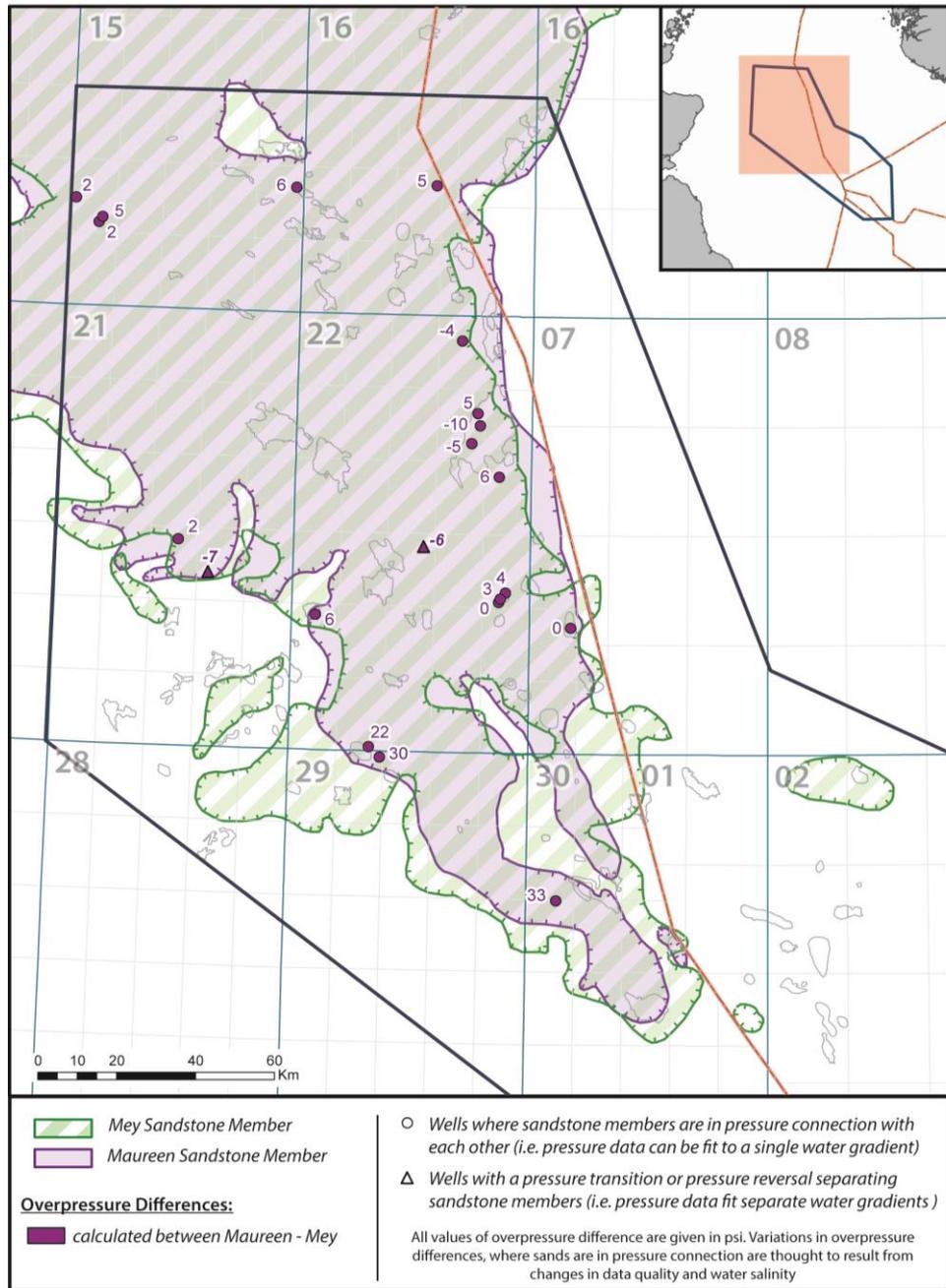
Figure 5.10 - Map showing locations of pressure connectivity and pressure separation between the Mey and underlying Maureen sandstone members. Values of overpressure differences (in psi) are also shown.

Overpressure contouring indicates that where there is a rapid increase in Mey overpressures towards the southeast (**Figure 5.3b**), overpressure increase within the overlying Forties is more gradual (**Figure 5.4b**). Analysis of well data across UK quads 29 and 30 indicates that the Forties Sandstone Member has an average net sand

133
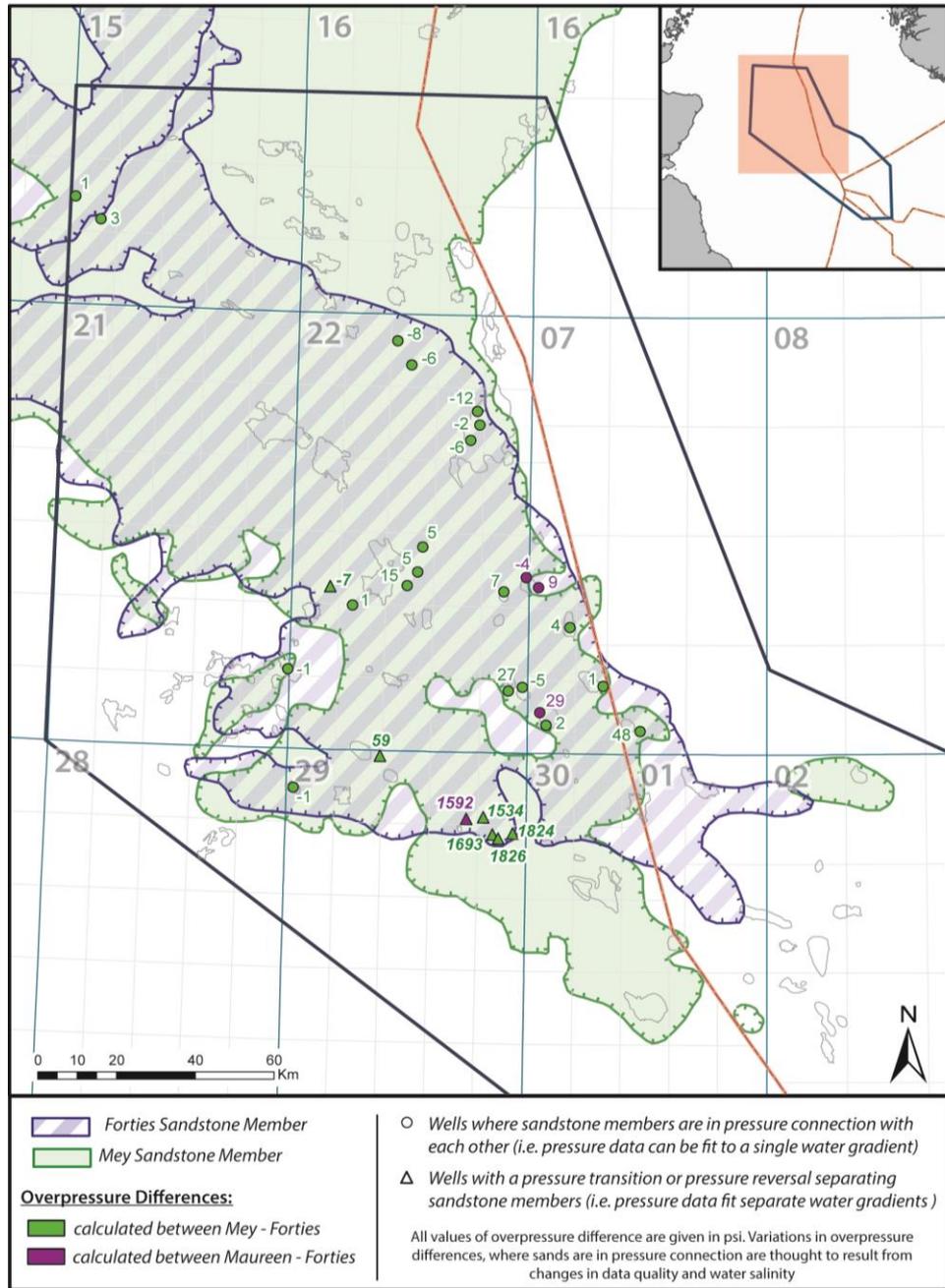
Figure 5.11 - Map showing locations of pressure connectivity and pressure separation between the Forties and underlying Mey or Maureen sandstone members. Values of overpressure differences (in psi) are also shown.

thickness of 108 ft (33 m) TVD for this area of the basin, whereas both the underlying Mey and Maureen sandstone members are thinner on average, having net sand thickness of 55 ft (16.8 m) and 75 ft (23 m), respectively. Assuming that thicker sands have greater permeability, this might explain why there is a rapid increase of overpressures within the thinner Mey and Maureen sands, which is not observed within the thicker,

134
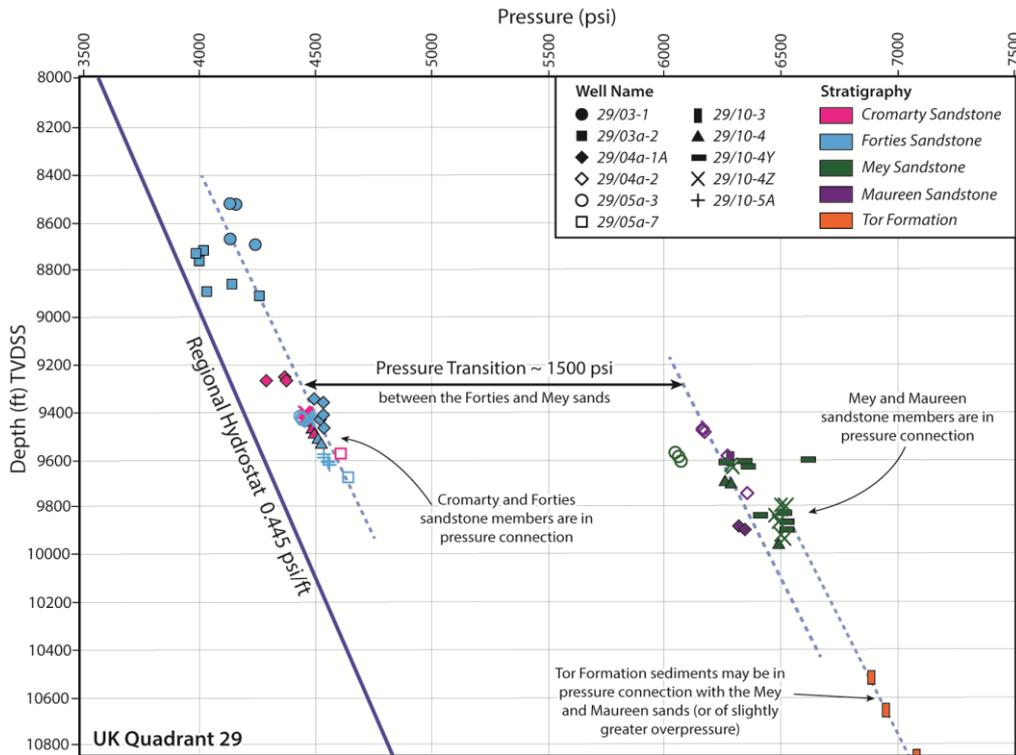
Figure 5.12 - P-D plot showing the pressure transition between the Forties and underlying Mey/Maureen sandstone members developed in UK quadrant 29, with an approximate magnitude of 1500 psi. The Forties and overlying Cromarty sands in this area appear to be in pressure communication, suggesting fluid drainage between these two sandstone members is likely. Additionally, the Mey, Maureen and underlying Tor (Chalk) sediments may potentially be in pressure communication, although there are insufficient data to confidently ascertain this.

overlying Forties. Thickness of the intraformational Sele and Lista muds, which separate the Forties and Mey sandstone members, ranges from 50 ft (15 m) TVD to 220 ft (67 m) TVD across this area, with no known areas of direct contact between the sands. Consequently, as the pressure data indicate, it is highly likely that the Forties and Mey sands are acting as two separate drainage systems in this southern area of the basin, with better drainage in the Forties sandstone member than in the underlying Mey and Maureen sands.

The overpressure difference map generated between the Cromarty Sandstone Member and underlying Palaeogene sandstone members is shown in **Figure 5.13**. The majority of wells showing good hydraulic connectivity between the Cromarty and Forties sandstone members are situated along the western basin margin, with calculated differences in overpressure mostly being negligible (**Figure 5.13**). In this area, the

135
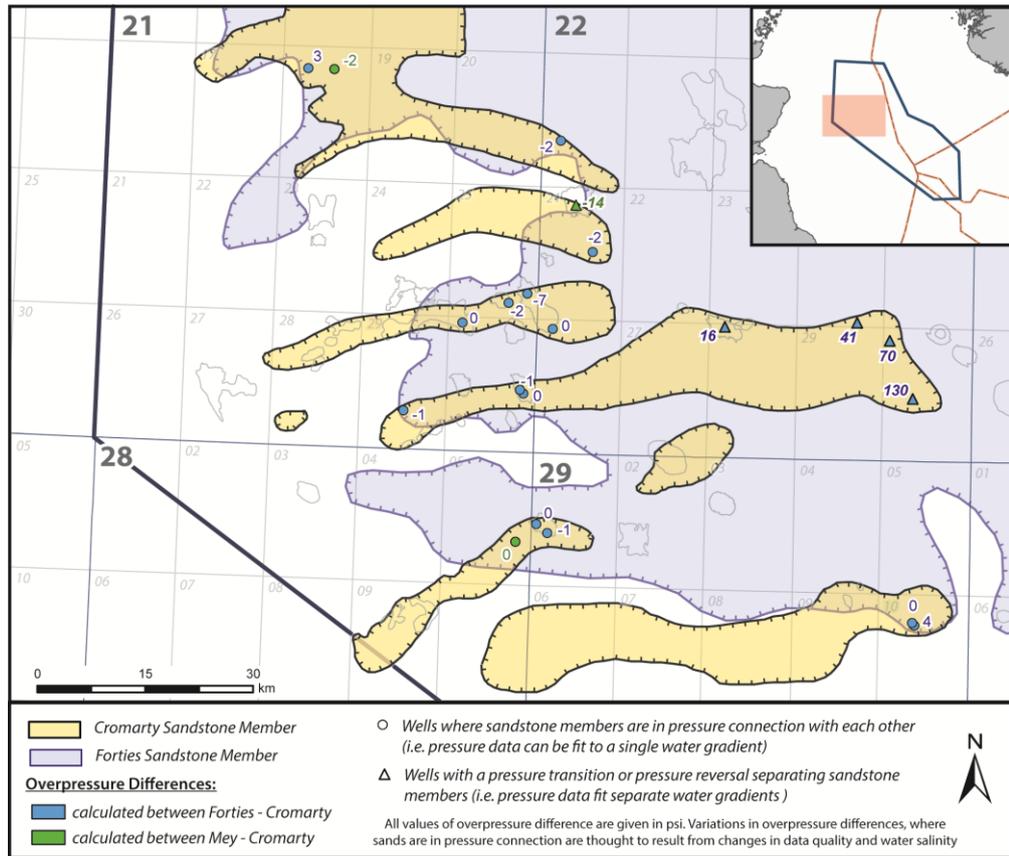
Figure 5.13 - Map showing locations of pressure connectivity and pressure separation between the Cromarty and underlying Forties or Mey sandstone members. Values of overpressure differences (in psi) are also shown.

thickness of intraformational Sele mudrock separating the Cromarty and Forties sandstone members is variable, ranging up to ~ 200 ft (60 m) TVD with an average thickness of 50 ft (24 m) TVD across the area. Direct contact between the sands occurs locally, particularly above and around salt-related structures such as at the Gannet B and Banff fields.

Four wells located in the south-eastern corner of UK quadrant 22 show that there is a pressure transition zone between the Cromarty Sandstone Member and the underlying Forties Sandstone Member, with variable differences in overpressure: a maximum of 130 psi (0.9 MPa) in UK well 22/30a-1; approximately 70 psi (0.48 MPa) in UK well 22/30a-2; 40 psi (0.28 MPa) in UK well 22/24b-4Z; and only 16 psi (0.11 MPa) further westwards in UK well 22/28a-3. Pressure measurements recorded within several of these wells capture the pressure transition zone and show that it is situated

136

partly within the upper part of the Forties Sandstone Member (**Figure 5.14**). Its development must result from vertical variations in reservoir quality of the Forties Sandstone Member across this area, with some mudrock interbeds that impede vertical flow. The transition also shows that there is potential for dewatering of the Upper Forties upwards, with vertical drainage of fluids escaping into the overlying Cromarty Sandstone Member.

The general distribution of overpressure in the Forties Sandstone Member suggests that there is some drainage vertically upwards, into the Cromarty Sandstone Member, because the 200 psi (1.4 MPa) contour curves around the south-eastern part of UK quadrant 22 (**Figure 5.4b**) where the Cromarty sand body extends westwards from UK block 22/30 towards the Gannet F Field in UK block 21/30. Available well data indicate that the sandstone members are separated by up to 50 ft (15 m) TVD of intraformational Sele muds in the area of UK blocks 22/29 and 22/30, with an average separation of less than 20 ft (6 m) TVD. Decreasing overpressure differences westwards across the area imply increasing hydraulic connectivity between the two sandstone members in this direction. Fluids within the Forties Sandstone Member are interpreted as draining vertically upwards into the overlying Cromarty Sandstone Member across this area, in addition to the lateral drainage within both sandstones members.

The Tay and Cromarty sandstone members appear to be well connected hydraulically across the entire distribution of the Tay Sandstone Member, with only one well, UK 21/28b-7, showing a pressure transition of 11 psi (0.076 MPa) between the Cromarty and Tay sandstone members (**Figure 5.15**). In the area around this particular well, the underlying Cromarty sands are isolated on the slope margin and separated from the overlying Tay sands by approximately 325 ft (99 m) TVD of intraformational Sele and Balder sediments. In UK well 21/19-2, the Mey and Maureen overpressures are lower than those recorded within the overlying Tay Sandstone Member, resulting in a pressure reversal of -17 psi (-0.12 MPa). This value may represent an area where the Mey and Maureen sands are better drained than the overlying Tay, particularly since the well is drilled into a proximal area of the Tay fan.

Lastly, overpressure differences calculated between the Grid Sandstone Member and underlying Palaeocene sandstone members are shown in **Figure 5.16**. Although differences could only be calculated for a total of fourteen wells, the majority of these
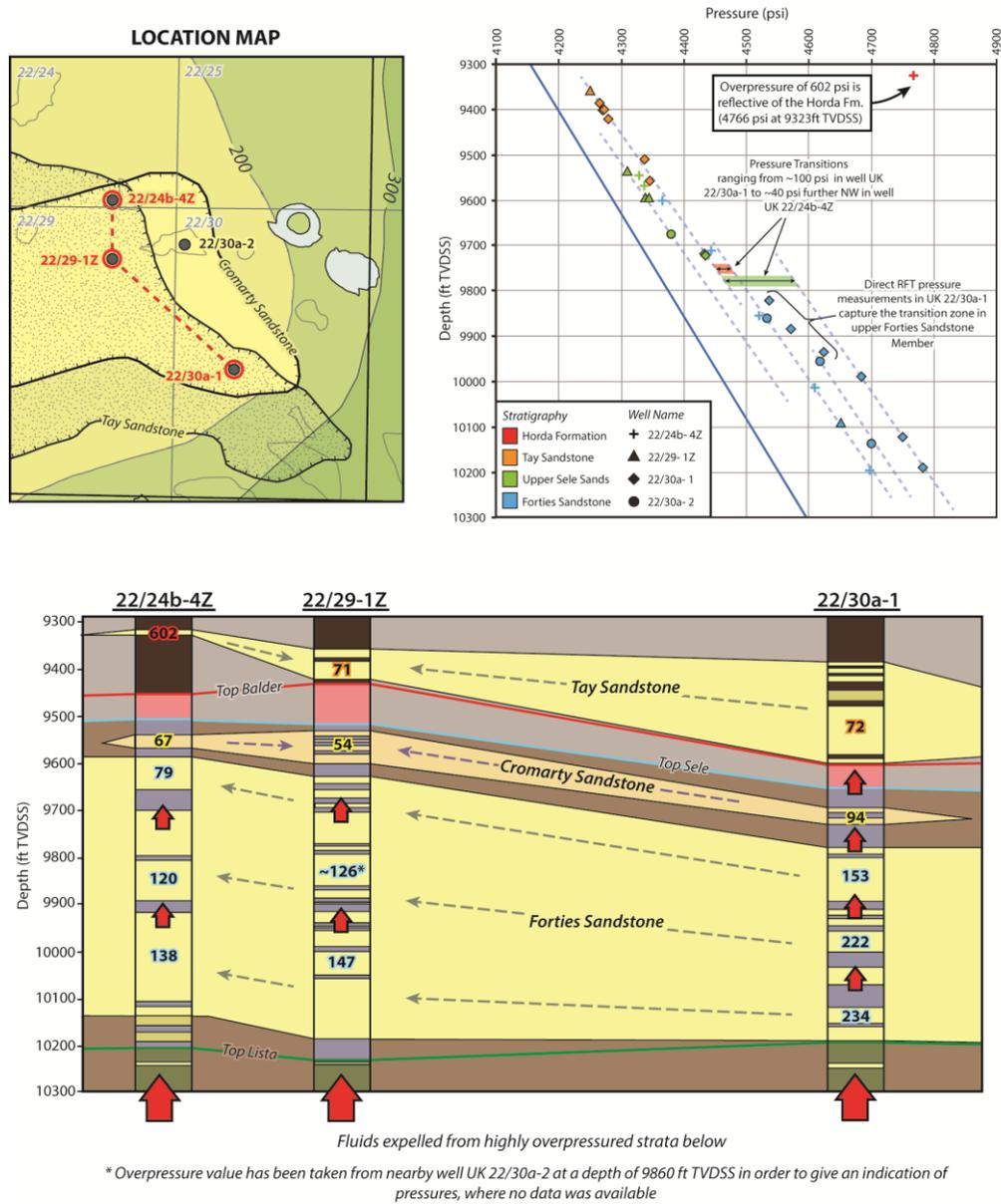
Figure 5.14 - Area of interpreted vertical drainage within the Forties Sandstone Member. *Top Left*: map showing well locations around south-western corner of UK quadrant 29 along with distributions of the Tay and Cromarty sandstone members. Overpressure contours for the underlying Forties Sandstone Member are also shown. Curvature of Forties overpressures appears coincident with the occurrence of overlying sands. *Top Right:* Multi-well P-D plot for the area. *Bottom:* Cross-sectional diagram illustrating the lateral and vertical changes in overpressure within the Forties Sandstone Member. Arrows indicate directions of fluid flow if no barriers permit flow. The Forties sandstone appears to be draining both laterally towards the NW, in the direction of well UK 22/24b-4Z, and vertically everywhere upwards. Vertical drainage between the Tay and Cromarty is thought unlikely to occur, due to the thick intervening Balder and Horda muds. Line of section is shown in map *top left.*
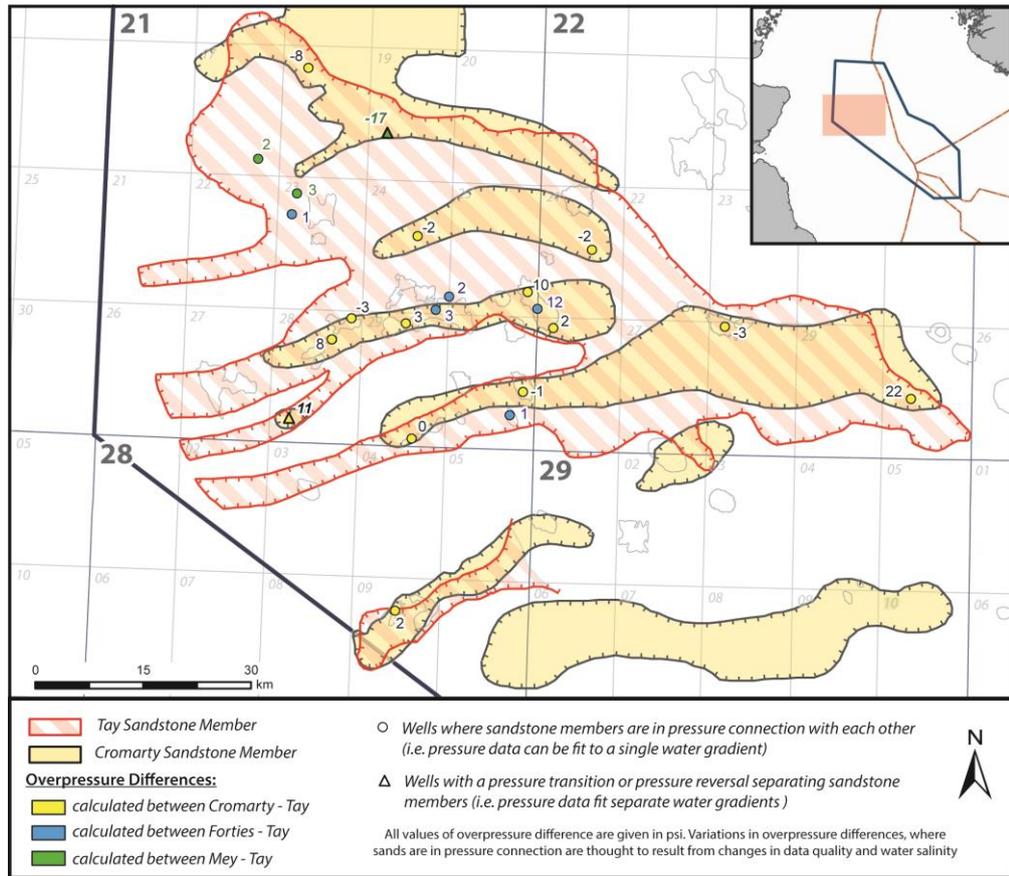
Figure 5.15 - Map showing locations of pressure connectivity and pressure separation between the Tay and underlying Cromarty, Forties or Mey sandstone members. Values of overpressure differences (in psi) are also shown.

wells indicate hydraulic connectivity between the Grid and underlying Palaeocene sands. Several wells around UK blocks 15/30, 21/04 and 21/05 show that a single water gradient can be fitted to pressure data recorded within the Brodie and Caran sandstone units, collectively forming the Grid Sandstone Member, and to the more deeply buried Palaeocene Forties Sandstone Member. Where the Forties Sandstone Member is not present, towards the north-east area of the basin, wells UK 15/25b-3 and UK 16/21-4a show similar good hydraulic connectivity between the Caran Sandstone Unit and deeper Mey Sandstone Member: the calculated differences in overpressure in these two wells are less than 2 psi (14 kPa).

Well data indicate that, across the basin, the Grid Sandstone Member is separated from the underlying Palaeocene sandstones by more than 850 ft (260 m) TVD of Horda and Balder formation sediments, which largely comprise muds and claystones

139

(Knox and Holloway, 1992). The proposed hydraulic connectivity between the Eocene and Palaeocene sandstone members in this area is, therefore, most likely to be facilitated via injected Caran sands, which are not easily identified using well data alone. Huuse *et al*. (2005) originally proposed this hypothesis, suggesting that Caran injectites provide the most likely migration pathway for hydrocarbons into the Alba/Chestnut Eocene fairway, reasoning that (1) the injectites appear to be sourced from the pre-Balder Palaeocene sands, (2) seismic data show that the injected sands cross-cut the lower Eocene Horda mudstones, (3) several injected sands are known to be present below the Alba and Chestnut fields, and (4) it is likely that the injected sands are of good porosity and permeability, based solely on comparisons of their acoustic character in seismic data with other sands of known porosity and permeability. Work carried out by Murphy and Wood (2011) further supports this hypothesis, showing that a mutually exclusive relationship exists between accumulations of hydrocarbons within the Palaeocene and the presence of overlying Caran sandstones.

In contrast to the findings of Huuse *et al*. (2005) and Murphy and Wood (2011), overpressure data collected from several wells around the Alba and Chestnut fields in UK blocks 16/26 and 22/02 indicate that there is a small magnitude pressure reversal between the Brodie and underlying Caran/Forties sandstone unit/member (**Figure 5.16**), suggesting that the sands in this area may not be hydraulically connected. Differences in overpressure are ~ 10 psi (0.07 MPa) calculated within UK wells 16/26-7Y and 16/26-8. The multi-well P-D plot shown in **Figure 5.17**, confirms that separate water gradients exist for the Grid Brodie and Caran sandstone units, and that the relatively small differences in overpressure cannot be explained by variations in water column salinity.

The large pressure reversal of ~ 141 psi (0.97 MPa) recorded within UK 22/01b-10 does not reflect virgin pressures since drilling completion of this well post-dates production start-up of the nearby Alba Field (~ 3 km away) by over a year. The effects of water injection at nearby Alba are clearly seen in the highly elevated overpressures recorded within the Brodie Sandstone Unit, although the same elevation is not shown in the underlying Caran overpressures, which remain similar to those recorded in surrounding wells. Although the overpressures within UK 22/01b-10 were not used to generate the Grid Sandstone Member overpressure distribution map, they can be used here to show the lack of hydraulic connectivity between the Grid Brodie and Caran
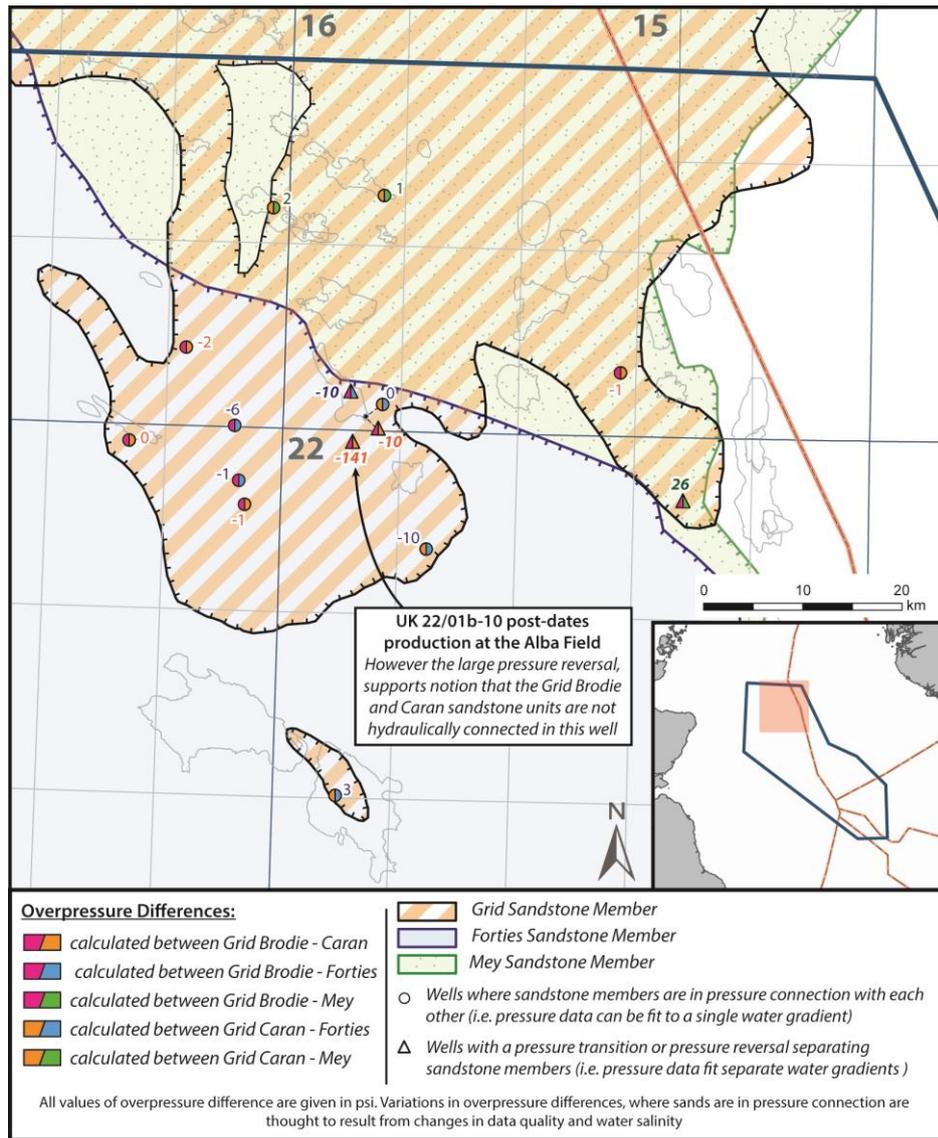
Figure 5.16 - Map showing locations of pressure connectivity and pressure separation between the Grid sandstone member and underlying Forties or Mey sandstone members, in addition to the Grid Brodie and Grid Caran sandstone units. Values of overpressure differences (in psi) are also shown.

sandstone units. Good hydraulic connectivity in the area of the Alba and Chestnut fields is still evident between the Grid Caran and underlying Forties sandstones (**Figure 5.16**).

The pressure reversal between the Brodie Sandstone Unit and the underlying sands implies a downward direction of water flow, opposite to the direction of hydrocarbon migration into the Alba/Chestnut fairway (Huuse *et al*., 2005; Murphy and Wood, 2011). Unlike the pore water, hydrocarbon migration is governed not only by

141
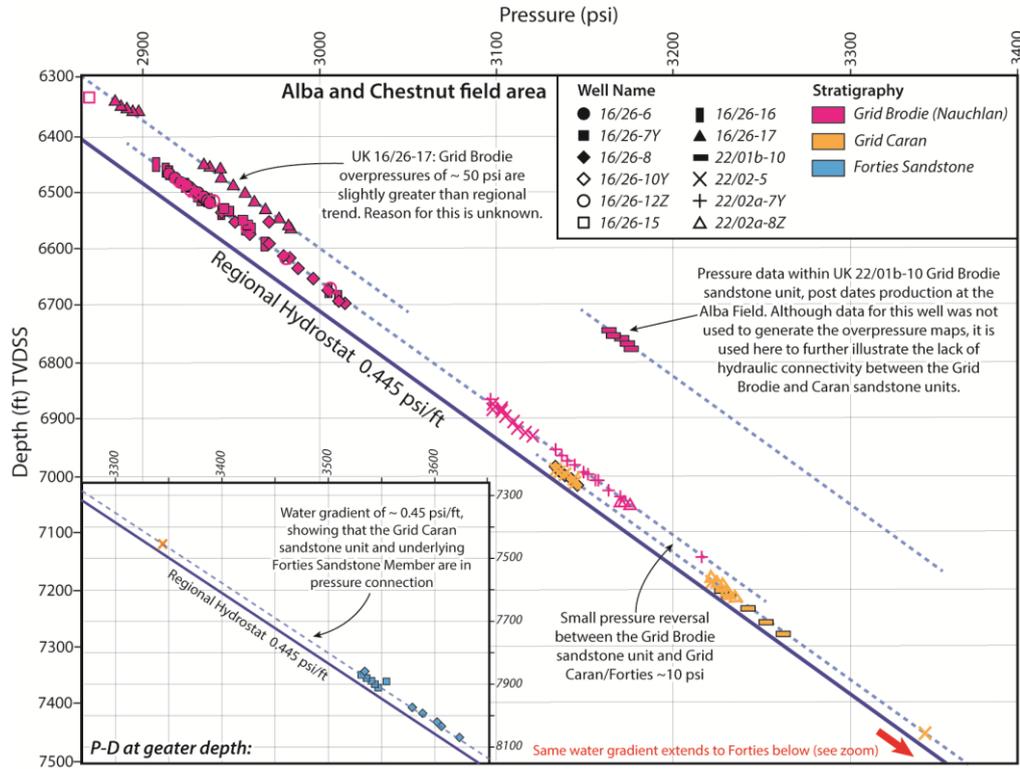
Figure 5.17 - P-D plot showing low magnitude pressure reversal between the Grid Brodie Sandstone Unit and underlying Grid Caran Sandstone Unit in the area of the Alba and Chestnut fields. Data show that the Caran Sandstone Unit and underlying Forties Sandstone Member are in apparent pressure connection, sharing the same water gradient. Assuming that fluid flow is facilitated between the two Grid Sandstone units due to hydrocarbon charging of the Alba and Chestnut fields, then water will flow vertically downwards from the Brodie Sandstone Unit along the overpressure gradient.

spatial variations in overpressure, but also by spatial variations in capillary pressure and buoyancy forces (Hubbert, 1953). Their buoyancy means that hydrocarbons can migrate upwards into the Grid Brodie Sandstone Unit in spite of the pressure reversal (**Figure 5.18**).

5.2.2. *Anomalous values of overpressure*

Within each of the individual overpressure distribution maps, values of overpressure which are anomalous relative to the regional trend may be indicative of vertical fluid flow. Areas of anomalously low overpressure within a sandstone member indicate that fluids are draining out from that sandstone into one of the vertically adjacent sandstones
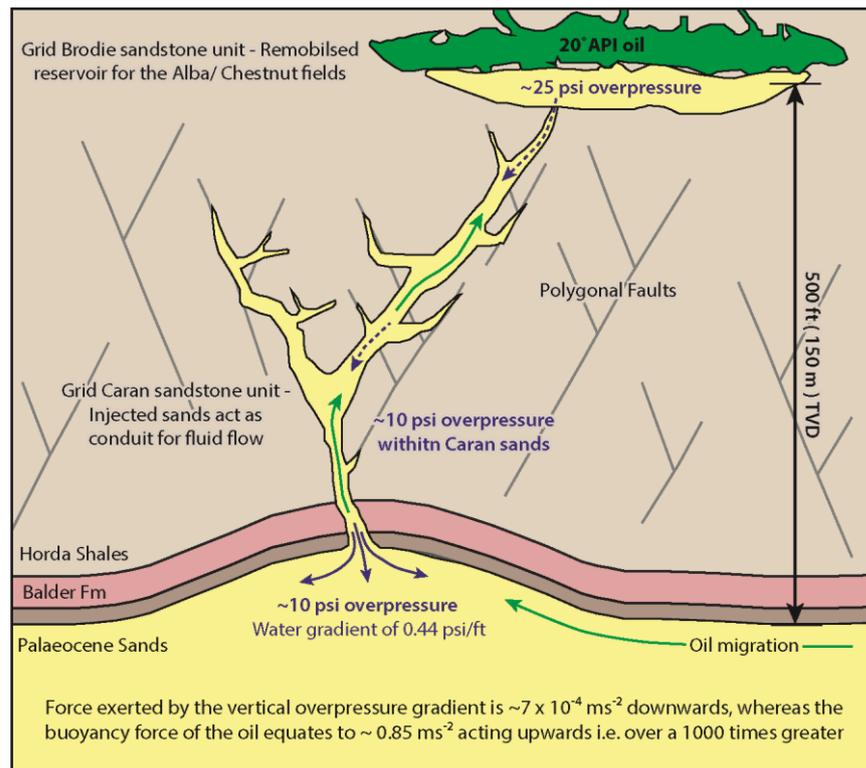
Figure 5.518- Schematic cross section W-E across the Alba Field area of UK block 16/26, used to illustrate how the upwards force of hydrocarbon buoyancy will greatly exceed the downward force generated by vertical overpressure gradient. Hydrocarbons will easily migrate from the underlying Forties Sandstone Member into the Brodie Sandstone Unit, along Caran injected sands, as proposed by Huuse *et al.* (2005). Modified from Murphy and Wood (2011).

or surrounding sediment. In contrast, areas of anomalously high overpressure within a sandstone member indicate that fluids are entering the sandstone. Such anomalies were not found within every sandstone member, but those which were encountered are examined here in detail.

5.2.2.1. *Mey Sandstone anomalies*

Several anomalous values of higher overpressure were calculated in the north-western area of the Mey fan, around UK block 15/28, close to the Rubie Field, and UK blocks 16/21, 16/26 and 16/28, above the Balmoral, Cyrus and Andrew fields (**Figure 5.3**). These anomalies are of small magnitude, reaching up to 65 psi (0.45 MPa) in the UK 15/28 area, and up to 87 psi (0.6 MPa) in UK block 16/28. Previous work carried out by

143

O' Connor and Swarbrick (2008) attributed such anomalies in this area of the Mey fan to vertically upward leakage of fluids from the underlying Albian/Aptian Lower Cretaceous strata. They suggested that vertical drainage in these areas is most likely via faults and/or fractures. Indeed, the overpressure high recorded in UK block 15/28 appears to be situated near to the Renee Ridge. The highs recorded in UK quadrant 16 may similarly be associated with faulting around the Fisher Bank area, observed at Cretaceous level. It seems unlikely that such anomalies could be explained by changes in reservoir permeability or thickness in this area of the basin, where the Mey Sandstone Member generally thickens and shallows towards the north-west. Unfortunately, no overpressure values have been calculated in the underlying Maureen Sandstone Member or Cretaceous strata in this area to confirm whether vertical drainage is the explanation.

Good hydraulic connectivity between the Mey and Caran intervals is suggested in UK well 16/21b-4a, where locally high overpressures are recorded within both the Mey Sandstone Member and overlying Caran Sandstone Unit, overpressure magnitudes being greater than 50 psi (0.35 MPa). It appears likely in this area that more highly pressured fluids drain upwards from the Chalk into the Mey Sandstone Member, and upwards from the Mey into the overlying Grid Caran Sandstone Unit.

Another area of anomalous overpressure within the Mey Sandstone is found around the Cod Field in Norwegian block 7/11 (**Figure 5.3**). The value of overpressure in well NO 7/11-3 is lower than might be expected for this area of the basin, where the Mey sands thin distally towards the SE margin of the fan. Overpressures decrease southwards across three wells, which is opposite to the regional trend. In well NO 7/11-1, the discovery well for the Cod Field, the water-filled Mey appears to be overpressured by 1364 psi (9.4 MPa). Approximately 2 km to the north-west of this well, in well NO 7/11-2, a slightly higher Mey overpressure of 1400 psi (9.65 MPa) was calculated. Finally, a much lower overpressure of 1102 psi (7.6 MPa) is calculated within the Mey Sandstone Member of well NO 7/11-3, lying approximately 3.7 km to the SE of well NO 7/11-1 (**Figure 5.3a**). For each well, values of Mey overpressure were classified as category 2 data points, being calculated from solitary DST values, or in the case of well NO 7/11-3 from a water gradient made up of only two DST values. Although category 2 data points carry the greatest levels of uncertainty, with potential errors reaching up to 100 psi (700 kPa), that is insufficient reason to ascribe the reversal in the regional trend to measurement errors.

144

When examining the Cod Field, Kessler *et al.* (1980) suggested that the Mey sands in well NO 7/11-3 had been fed by an earlier and subsequently abandoned lobe system of the Mey fan, other than the main lobe system which fed the Mey sands encountered in wells NO 7/11-1 and 2. Different depositional systems for the Mey sands in this area may have led to the overpressure discrepancies observed between wells. However, as D' Heur (1992) noted, sandstone facies observed within well NO 7/11-3 suggest that the south-eastern Mey lobe had a more distal depositional setting (i.e. poorer quality reservoir) than the north-western Mey lobe, which would not explain why overpressures within north-western lobe wells are of much higher magnitude.

Contrary to the impression given by the Mey overpressure contouring presented in **Figure 5.3b,** it may be that the overpressure values recorded within Norwegian wells NO 7/11-1 and NO 7/11-2 are anomalously high for this area, with the value of overpressure recorded within NO 7/11-3 better representing the regional trend of overpressure for the Mey Sandstone Member in this area. An overpressure high in this area would fit better with the structural setting of the Cod Field, and may represent an entry point for fluids draining into the Mey sands from below. The local overpressure high observed in wells NO 7/11-1 and NO 7/11-2 corresponds to the salt-induced anticlinal crest of the Cod Field, which is underlain by a seismically visible, NNE orientated fault system from above the top Palaeocene to below the base Chalk (D' Heur, 1992). This fault system may provide a conduit for fluid flow of both hydrocarbons and water vertically upwards, from deeper, higher overpressured areas of the basin into the Mey Sandstone.

5.2.2.2. *Forties Sandstone anomalies*

The overpressure low of 200–300 psi (1.4–2.1 MPa) observed at the margins of the Forties Sandstone Member in UK blocks 29/5 and 29/10 (**Figure 5.4**) is most likely associated with vertical drainage of fluids upwards into the overlying Cromarty Sandstone Member. Lower overpressure magnitudes of 263 psi (1.81 MPa), 262 (1.81 MPa) and 244 psi (1.68 MPa) are calculated for UK wells 29/10-4, 29/10-4Z and 29/05a-3, respectively, contrasting to the overpressures of around 330 psi (2.3 MPa) within surrounding wells UK 29/04a-1 and UK 29/05a-7 (**Figure 5.4a**). This overpressure decrease at the distal margin of the Forties fan is anomalous, since

reservoir quality is known to diminish with increasing distance from the sediment source, the Forties sands becoming thinner, muddier and of lower porosity and permeability (Hempton *et al.*, 2005). In this area, the Cromarty and Forties sandstone members are vertically separated by only 10 ft (3 m) of mudstone in some wells, so vertical drainage between them is plausible. As was shown in **Figure 5.12**, pressure data within the Cromarty and Forties sandstone members plot on a single water gradient, and differences in overpressure are calculated at zero and 4 psi (28 kPa) according to the data collected in UK wells 29/10-4Z and 29/10-4, respectively (**Figure 5.13**), confirming that there is good hydraulic connectivity where the Cromarty sands are thickest.

5.2.2.3. *Grid Sandstone anomaly*

An area of higher overpressure is calculated within the Grid Brodie Sandstone Unit, around the Alba and Chestnut fields in UK blocks 16/26 and 22/02 (**Figure 5.7**). As was previously discussed, this overpressure high cannot be due to vertical input of fluids from the Caran and Forties sandstones below, since the overpressures recorded within these underlying sands are of lower magnitude (**Figures 5.16** and **5.17**). Depositional character of the Brodie Sandstone Unit around the Alba/Chestnut field area (Jones *et al.*, 2003; Huuse *et al.*, 2005) is complicated by the presence of post-depositional remobilized and injected sands, in addition to the simple channel-fill sands. Consequently, it is suggested that the slightly higher overpressures recorded within the Brodie sands of this area are more representative of the overpressures in the surrounding Horda muds.

5.2.3. *Vertical connectivity and hydrocarbon accumulations*

The occurrence and distribution of Palaeogene hydrocarbons across the basin can assist with identification of areas where vertical fluid flow may be occurring between sandstone members, and areas where sealing units separate sandstone members. Within each major Palaeocene fan, i.e. the Maureen, Mey and Forties sandstone members, known hydrocarbon accumulations are mostly restricted to areas where no overlying sandstone members are present, and consequently top seal risk is low (see **Appendix**

A). In the deepest Maureen Sandstone Member, only a relatively few hydrocarbon discoveries have been made, with the majority being located along the eastern margin of the Maureen fan where both the overlying Mey and Forties reservoirs are absent or of poor quality. Within the overlying Mey/Heimdal Sandstone Member, a similar pattern is observed, where known accumulations are mostly restricted to the north-east and south-eastern areas of the fan where the overlying Forties Sandstone Member is absent. For the youngest of the Palaeocene fans, the Forties Sandstone Member, hydrocarbon accumulations are abundant and generally well distributed across the fan, reflecting coverage of the fan across most of its area, by the overlying, sealing Tertiary mudrocks. As with the underlying sands, relatively few oil and gas accumulations are found where the Cromarty, Tay and Grid sandstone members overlie the Forties (Murphy and Wood, 2011). This general observation of regional hydrocarbon distributions, reinforced by the increasing number of hydrocarbon discoveries within younger fans, implies that the intraformational sediments which separate Palaeogene fan members are largely non-sealing, enabling the migration of fluids and hydrocarbons between sands over geological time.

In some areas of the basin, hydrocarbons are present across multiple reservoir intervals within the same field/discovery. In such cases, there is the possibility of interconnectivity between reservoir intervals, with implications for fluid flow and migration pathways. Examples of fields which share common hydrocarbon gradients are found at the Gannet F, Gannet D, Banff, Bittern and Catcher fields (see **Appendix A**). Common oil–water contacts are shared by the Tay, Cromarty and Forties sandstone members at the Gannet F Field (Banner *et al*., 1992); by the Tay and Cromarty sands at the Gannet D (Kloosterman *et al*., 2003) and Catcher fields; by the Forties, Mey, Maureen and Ekofisk Chalk reservoirs at the Banff Field; and by the Cromarty and Forties sandstone members at the Bittern Field (McCormick and Leisham, 2004).

The Gannet F, Gannet D and Banff structures are all salt-related, suggesting the potential presence of salt-related faults and fractures which may act as conduits for vertical fluid flow. P-D plots for each of these fields are shown in **Figures 5.19** to **5.21**. Both the Gannet F and Gannet B fields are salt-induced anticlinal traps, whilst Banff forms a salt piercement structure.

147
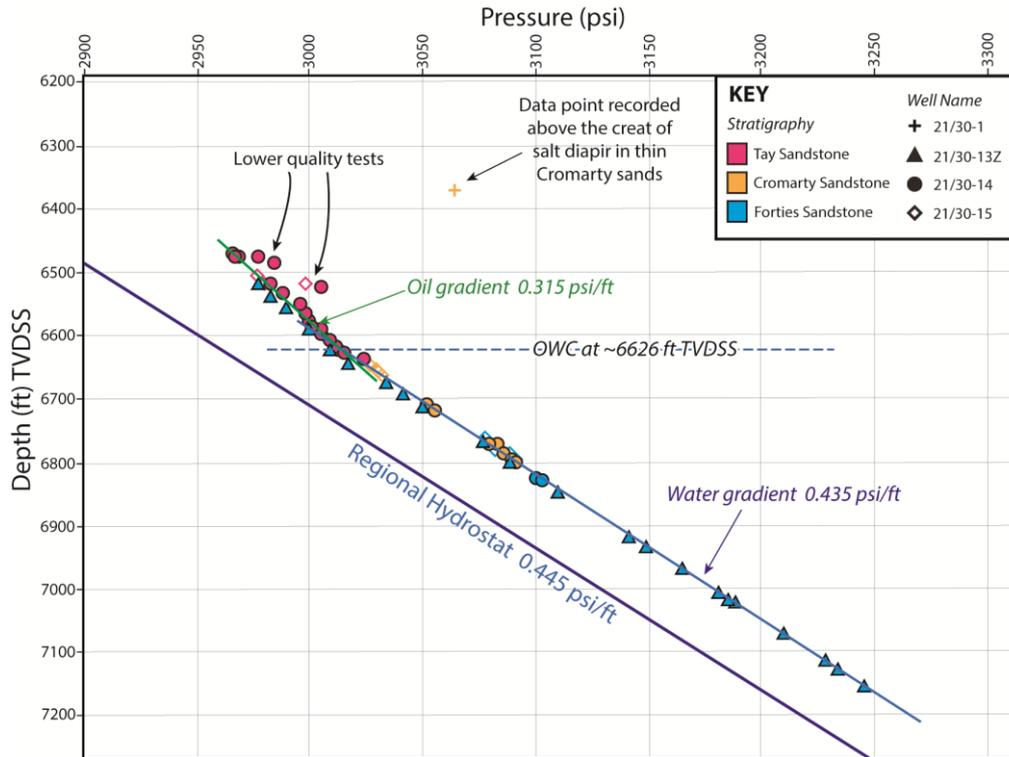
Figure 5.196 - Multi-well P-D plot for the Gannet F Field, located in UK block 21/30. A single oil gradient and water gradient can be fit to Tay, Cromarty and Forties pressures, indicating pressure connectivity between sandstone members.

Pressure data collected from the Gannet F Field, situated in UK block 21/30, show that a single oil gradient and a single water gradient can be fitted across the Tay, Cromarty and Forties sandstone members, with a common OWC at a depth of ~ 6625 ft (2020 m) TVDSS (**Figure 5.19**). The common OWC across the field is controlled by a structural spill point at Tay level, and emphasizes the hydraulic connectivity between Gannet F reservoirs, since the underlying Forties accumulation appears under-filled (Banner *et al*., 1992). Hydrocarbon migration into the structure is thought to have occurred along fault–fracture systems associated with the underlying diapir. Geochemical analysis carried out by Banner *et al*. (1992) shows that Gannet F oil underwent relatively short migration routes, favouring vertical migration, in contrast to the neighbouring Gannet E field where the hydrocarbons are likely to have experienced longer, lateral migration pathways from the Kimmeridge Clay source. Well analysis carried out within this study shows that the Cromarty and Forties sandstone members are separated by up to 65 ft (20 m) TVD of informational Sele muds in northern areas of

148
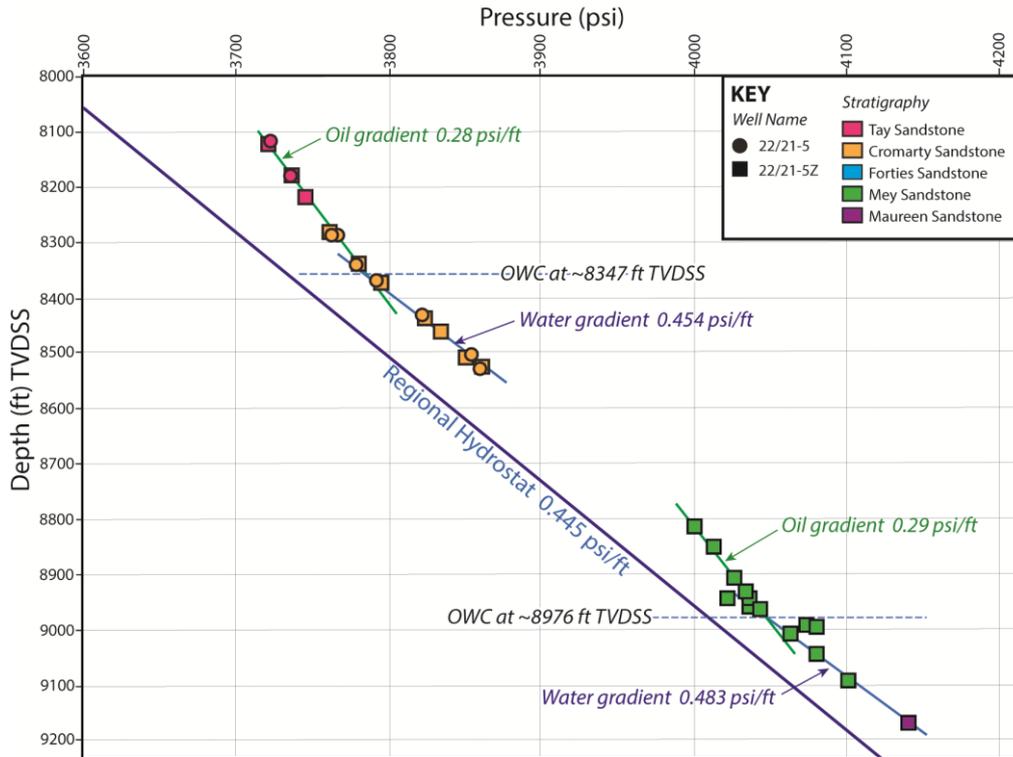
Figure 5.20 - Multi-well P-D plot for the Gannet D Field, located in UK block 22/21. The shallowest oil accumulation within the Tay and Cromarty sandstone members indicates that the sands in this area are in hydraulic communication, due to the close proximity of the sands, resulting from erosion. A second, deeper oil accumulation is found within the Mey Sandstone Member.

the field, decreasing down to thickness of only 10 ft (4 m) TVD in southern areas, where it is likely that the sands may be direct contact with each other. In contrast, where both the Tay and Cromarty sands are present across the field, they are separated by intraformational sediments ~115 ft (35 m) TVD thick and areas of direct contact are much less likely. Hydraulic connectivity between these two sands is most likely to be facilitated via faults and fractures, or perhaps even injected/remobilized Cromarty sands.

At the Gannet D Field, located in UK block 22/21, hydraulic connectivity is established between the Cromarty and Tay sandstone members, which are in extremely close proximity with each other, being separated by less than 3 ft (1 m) TVD mud in well UK 22/21-5. The absence of Balder Formation between reservoir intervals within this well suggests that the direct contact between the Tay and Cromarty sands in this

149

area is associated with erosion. The P-D plot presented in **Figure 5.20** shows that a separate oil accumulation is present within the underlying Mey Sandstone Member, with lower overpressure than the accumulation in the Tay and Cromarty sands.

At the Banff Field, located within UK blocks 22/27 and 29/02, hydraulic connectivity exists between the Forties, Mey and Maureen sandstones members, in addition to the underlying Ekofisk Chalk. Pressure data were only available from wells UK 22/27a-3Z and UK 29/02a-6 across the structure, and the resultant multi-well P-D plot for the field is shown in **Figure 5.21**. Well UK 29/02a-6, drilled into the southern flank of the field, is completely oil-filled from the Forties to the Ekofisk. In UK 22/27a-3Z, situated on the northern flank of the field, an OWC is encountered at ~ 7650 ft (2332 m) TVDSS within the Mey Sandstone Member, corresponding well to the FWL depth of ~ 7610 ft TVDSS that was recorded on the southern flank of the structure, within the Tor Formation of UK well 29/02a-7 (Evans *et al.*, 1999). Thus, the pressure data suggest the possibility that there is a regional OWC around the Banff structure, with hydraulic connectivity between the rafted Chalk and Palaeogene reservoirs. Such connectivity may be facilitated by areas of direct contact between the reservoirs or through fault and fracture systems associated with the Banff diapir. Although hydraulic connectivity has not been established between the Palaeogene sands and underlying Ekofisk in any of the other wells examined in this study, the Banff Field is a rather unique situation where part of the Chalk reservoir appears to have been rafted and isolated as a result of salt piercement.

The Catcher Field, located in UK block 28/09, is distinct from other Central North Sea discoveries in that hydrocarbons are shared between reservoir sands across a non-sealing fault. The multi-well P-D plot for the Catcher Field (**Figure 5.22**) indicates that a common OWC at 4690 ft (1430 m) TVDSS is present across the field, with a shared oil gradient of 0.33 psi ft^{-1} (7.47 kPa m^{-1}) within the Tay and Cromarty reservoir sands. The two separate gas columns seen on the P-D plot indicate separate gas pockets located within the thin remobilized Tay sands, which branch off irregularly from the top of the main Tay sandstone body.

The shared hydrocarbon accumulation at Bittern is consistent with vertical drainage between the Forties and Cromarty sands in UK block 29/01, as previously identified from pressure measurements in the water legs. Connectivity between sands in
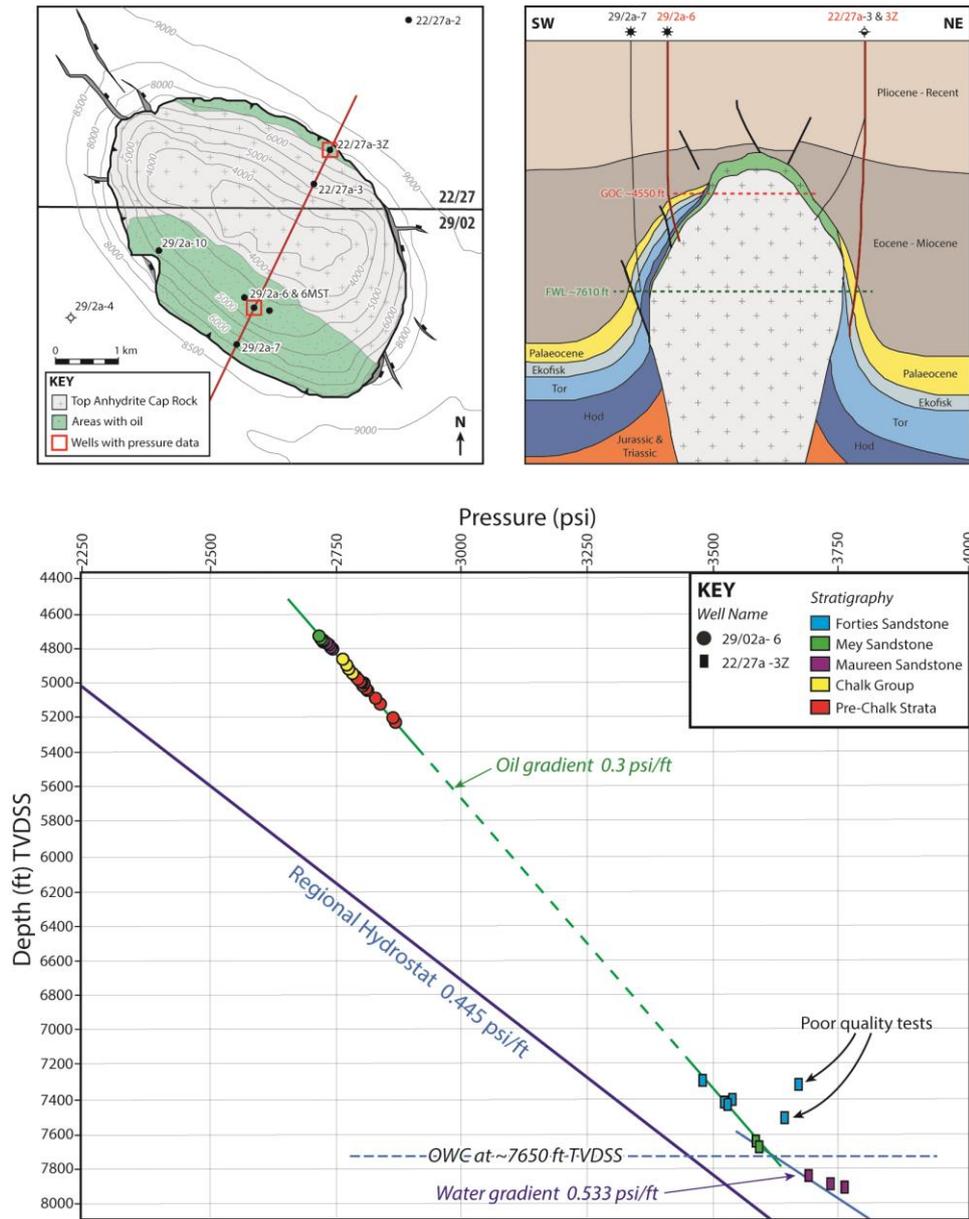
Figure 5.21 - Multi-well P-D plot for the Banff Field, located across UK blocks 22/27 and 29/02. Location map and schematic cross-section across the field are also provided for reference.

this area is likely to be associated with the compensational stacking around the Bittern area, as noted by McCormick and Leisham (2004). Fluids entering this unit of the Cromarty Sandstone Member drain laterally south-westwards towards the Catcher discovery in UK block 28/09.

The general inference that the intraformational sediments which separate Palaeogene sandstones are largely non-sealing is not always correct. There are several

151
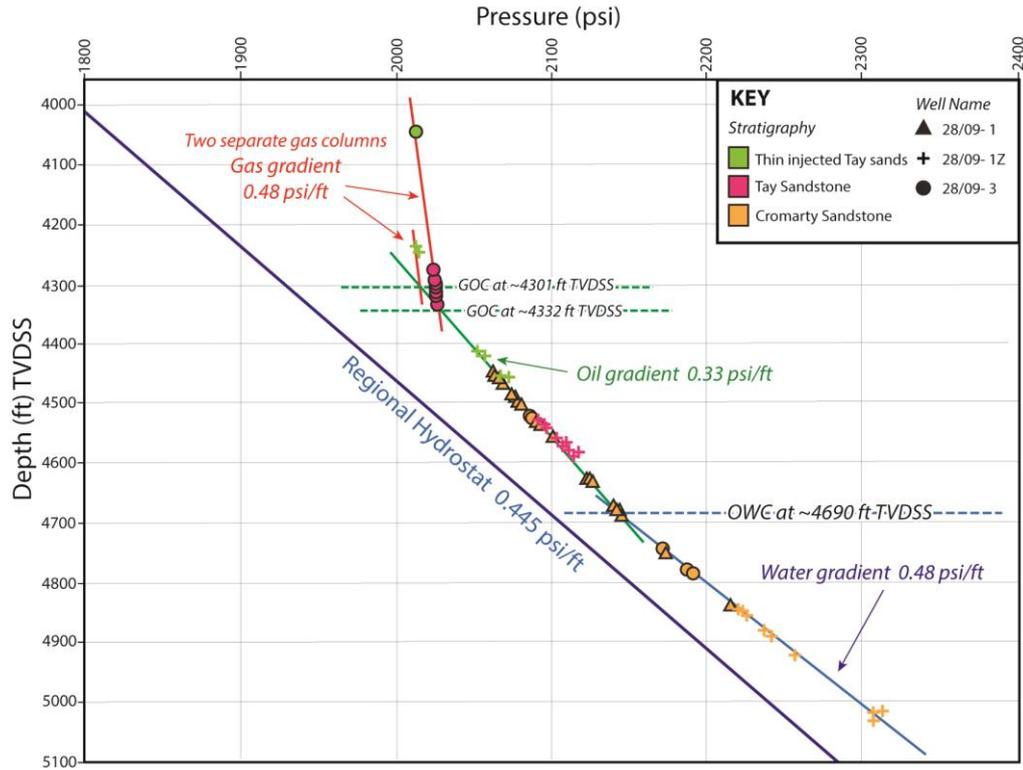
Figure 5.722 - Multi-well P-D plot for the Catcher Field situated in UK block 28/09. There is a shared oil gradient of 0.33 psi ft^{-1} within the Tay and Cromarty reservoir sands. Connectivity is established across a non-sealing basin margin fault. Two separate gas columns (of the same gradient, but different overpressures) may exist, due to separation of gas accumulations in individual Tay injectite features.

areas across the basin where hydrocarbon accumulations indicate that this is not the case. Specific field examples where the intraformational sediments separating sandstone members have proven to be sealing include the Rubie Field (UK block 15/28) and the Gannet D Field (UK block 22/21). At the Rubie and the Gannet D field's similar situations exist, whereby two separate oil accumulations occur within the Cromarty and underlying Mey sandstone members (shown in **Figure 5.20** for the Gannet D Field). In the case of Gannet D, thick intraformational Lista and Sele muds provide top seal for the Mey reservoir, reaching up to ~ 180 ft (55 m) TVD thickness in UK well 22/21-5. At Rubie, the intraformational Balmoral Tuffite Unit acts as top seal to the lower oil column, although the approximate thickness remains unknown. Recent discoveries,

152

such as McEnroe and Murray, further highlight the sealing potential of the Balmoral Tuffite Unit in the southern part of UK quadrant 15.

5.3. Discussion

From the overpressure maps presented, it can be seen that each of the Palaeogene sandstone members, with the exception of the Grid Sandstone, is laterally draining towards the sediment source. Each of the Maureen, Mey, Forties, Cromarty and Tay sandstone members exhibit a pattern of increasing overpressure distally, reflecting increasing distance from sediment source, increasing depth of burial, and decreasing thickness, net-to-gross, degree of channelization, grain size and permeability (Hempton *et al*., 2005). Over a large area of the basin around UK quadrants 15, 16 and 21 and the northwest part of quadrant 22, overpressures within each of the major Palaeocene fan members are near-hydrostatic, being less than 50 psi (0.35 MPa). These areas of lower overpressure are thought to represent areas where fluids are draining to the north-west, where sandier sediments are more abundant in the Dornoch shelf formation around UK quadrant 14 and the western parts of quadrant 15. Vertical overpressure differences between sands in this area, although relatively few, suggest that sands are in direct hydraulic connection vertically with each other.

The greatest magnitudes of overpressure, in excess of 2600 psi (17.9 MPa), were recorded within the deepest Palaeocene fan sand, i.e. the Maureen Sandstone Member, with similar high overpressure magnitudes in excess of 2500 psi (17.2 MPa) recorded within the overlying Mey Sandstone Member. Regional overpressure maps generated for the Maureen and Mey sandstone members indicate that the overpressure distribution across these two sands is remarkably similar, particularly across UK blocks 29 and 30 where the overpressure increases steeply to the south-east in both sands, producing hydrodynamic gradients in excess of 60 psi km^{-1} (0.41 MPa km^{-1}). Vertical overpressure differences indicate that the Mey and Maureen sandstone members are in hydraulic connection across most of their distributions, suggesting that these two sandstone members may act largely as a single unit with regards to fluid flow within the basin.

The regional overpressure distribution map for the Forties Sandstone Member shows that overpressures calculated in the distal areas are of much lower magnitude

than those within the Mey and Maureen sands. The greatest magnitudes of Forties overpressure encountered within UK quadrant 30 and Norwegian quadrant 1 are less than 1200 psi (8.3 MPa). Differences in overpressure between the Forties and underlying Palaeogene sands may imply that fluid drainage is better within the Forties Sandstone Member, or that a lesser amount of overpressured fluid is entering into the Forties Sandstone Member from the surrounding sediments.

Within all three Palaeocene sandstone members, the predominant direction of fluid flow is north-westwards, towards shelfal sands in the area of the Moray Firth. Additional lateral drainage towards the west of the basin is observed in distal areas of the Mey and Forties sandstone members, in and around UK quadrants 21, 28 and 29. Such westerly drainage appears to be better established within the Forties sandstone than within the underlying Mey sandstone, since Forties overpressure contours are more strongly oriented in a N–S direction across south-eastern parts of the fan. Distortion of Forties contours around southern parts of UK quadrant 22 suggests increased vertical drainage into overlying Cromarty sands, and perhaps Tay sands.

Overpressures mapped within the smaller Cromarty and Tay sandstone members are of low magnitude, being mostly less than 100 psi (0.69 MPa). Despite these low magnitudes, the distributions of overpressure within each sand body indicate that flow is laterally westwards and south-westwards, where fluids are likely to drain into the adjacent shelfal sands belonging to the Dornoch and Mousa formations.

Potential areas of vertical drainage between the Maureen, Mey and Forties sands have been identified above and around salt piercement structures such as Banff (UK blocks 22/27 and 29/02), Machar (UK 23/26), Merganser (UK 22/30) and Moira (UK 16/29), where shared hydrocarbon columns are observed across multiple reservoir intervals. Calculated differences of vertical overpressure have shown that the sands around such structures are typically in pressure connection, with shared hydrocarbon and water gradients usually being fit to pressure data across multiple reservoir intervals. The anomalously high values of overpressure identified within the Mey Sandstone around the Norwegian Cod Field in NO block 7/11 may represent additional entry of fluids into the Mey Sandstone, from vertically below. It is likely that such upwards fluid flow is facilitated via the radial NE-SW orientated fault network present at Cod (D' Heur, 1992), which is likely to be associated with salt diapirism at the Cod Field. Lack

of pressure data available for this area means that the overpressure contouring may not represent what is really occurring in this area.

Vertical drainage is thought to be most common between the Forties and overlying Cromarty members, since these sands remain in fairly close proximity to one another across their distribution. A relatively thin interval of intraformational Sele mudrock, with a mean average thickness of 50 ft (15 m) TVD (measured in 68 wells), separates the two sandstone members and direct contact between the sands occurs locally, in particular above and around salt-related structures. Differences in overpressure between the Forties and Cromarty decreases westwards from around 100 psi (0.7 MPa) at the margins of the Cromarty sands to negligible values in the west, implying connectivity increases westwards towards the sediment source.

Specific areas of vertical drainage were identified between the Forties and Cromarty sands in and around UK blocks 29/05 and 29/10, where the sands were found to be either in direct contact with each other or separated by a thin interval of intraformational Sele mud up to 30 ft (9 m) thick. Pressure data from several wells in this area indicate that the Forties and Cromarty sands are in pressure connection. In combination with the anomalously low Forties overpressure observed in this area, it indicates that fluid flow is vertically upwards, from the Forties into the overlying Cromarty sands.

Around the Bittern Field, in UK block 29/01, differences in overpressure calculated between the Forties and Cromarty are zero, implying that there is good vertical connectivity between sands. In this area, the two sandstone members are separated by a mudrock interval that is only 15–30 ft (5–9 m) thick, and compensational stacking is known to occur between the sands at Bittern (McCormick and Leisham 2004). The shared hydrocarbon accumulation at Bittern between the Forties and Cromarty sands is consistent with such vertical drainage. Around UK blocks 22/29 and 22/30, pressure data collected from several wells indicate that Forties overpressure decreases vertically upwards, in addition to laterally westwards across the block, supporting the notion of vertical drainage between the Forties and Cromarty sands in this area.

Vertical drainage between the Tay and underlying Cromarty or Forties sandstone member is not as effective as between the underlying Cromarty and Forties

155

sands, which are commonly in direct contact with each other. Nevertheless, almost all of the wells for which vertical differences in overpressure were calculated indicate that the Tay and Cromarty sands are well connected hydraulically. Differences in overpressure magnitude are mostly less than 3 psi (0.02 MPa) with the greatest differences being found towards the distal margins of the sandstone members, where permeability is lower and the sand bodies thin as they become increasingly surrounded by mudrocks. The thickness of mudrock separating the Tay from the next underlying sandstone member is greater than 100 ft (30 m) across much of the Tay, but thins to less than 30 ft (9 m) above many of the salt-related structures which affect the Tay Sandstone Member in and around UK blocks 21/24, 21/25 and 21/28. Hydraulic connectivity could be greatest around such features, perhaps enhanced by the fracture–fault systems which are commonly associated with such structures (Banner *et al*., 1992), but may also be enhanced locally elsewhere by injectites or other faults below seismic resolution. Common oil–water contacts shared by the Tay, Cromarty and Forties sandstone members at the Gannet F Field (Banner *et al*., 1992) and by the Tay and Cromarty sands at Gannet D (Kloosterman *et al*., 2003) are further evidence of good hydraulic connectivity of these sands around salt diapir features. At the newly discovered Catcher Field in UK block 28/09, where an oil gradient is shared between the Tay and Cromarty sands, hydraulic connectivity is established across a non-sealing basin margin fault, suggesting that similar faults along the western margin may provide migration routes for fluids and hydrocarbons alike.

The Grid Sandstone Member is near-hydrostatically pressured with overpressure magnitudes not exceeding 50 psi (0.35 MPa) except at UK well 16/21-4A, where an overpressure of 56 psi (0.39 MPa) is calculated. Distribution of overpressure within the Grid Sandstone Member does not indicate any lateral drainage towards the north-west. Hydraulic connectivity between the Grid Brodie and Grid Caran sandstone units, as well as the underlying Palaeogene sandstone members, is known to occur in some areas of the basin, although around the Alba and Chestnut area a small pressure reversal indicates that subsurface waters could only be flowing downwards between the two units. Nevertheless, hydrocarbons could still migrate vertically upwards into the Alba and Chestnut fields along Caran injected sands, since the hydrocarbon buoyancy would overcome the difference in overpressure (**Figure 5.18**).

5.3.1. Where is the continual supply of overpressure coming from?

In order to maintain the hydrodynamic flow observed within the Palaeogene sand system, a continual supply of fluid is required to maintain the observed overpressure gradients. The main mechanisms thought to be responsible for the generation of overpressure in the Central North Sea were discussed in **Chapter 3**. Fluid input into the Palaeogene system is expected to occur from all directions, with primary input coming from the highly overpressured Chalk and the Jurassic strata below, and a lesser amount from the overlying Tertiary shales where overpressure has been generated through disequilibrium compaction.

Using Darcy's law (see *Equation 3.9*), the overpressure maps generated can be used to quantify the fluid flow out of the Palaeogene fan sands. For the Forties Sandstone Member, the regional overpressure gradient from the West Central Graben at 57°N to the Inner Moray Firth Basin at 2°W is 2.65 MPa (385 psi) over a distance of 170 km. Assuming a constant viscosity of 0.5 centipoise (cP), and using the average permeability of the Forties Sandstone Member at the Montrose Field of 80 mD (Crawford *et al.*, 1991), the average bulk water flow rate at the present day is 8 cm yr^{-1}. For the underlying Mey Sandstone Member, the regional overpressure gradient is 5.45 MPa (790 psi) over a distance of 190 km. Assuming again a constant viscosity of 0.5 cP, and using the average permeability of the Mey Sandstone Member at the Montrose Field of 200 mD (Jolley, 2003), the average bulk water flow rate at the present day is 36 cm yr^{-1}. The cross-sectional area of the Mey Sandstone Member is about half the cross-sectional area of the Forties Sandstone Member, so it can be concluded that the volumetric rate of water flow being laterally drained out of the Mey Sandstone Member is about twice that being laterally drained out of the Forties Sandstone Member.

Insights into the magnitudes of overpressure attained within the surrounding lower permeability strata are rare. Work carried out by Dennis *et al.* (2000, 2005) shows that overpressures within the Chalk are greatest where the Tertiary sandstone members are thin or absent. Chalk overpressures reach maximum magnitudes of around 3000 psi (21 MPa) in Norwegian block 02/07, where the Chalk is at its deepest, buried at approximate depths of 9800 ft (3000 m) TVD. Overpressures within the Chalk gradually diminish outwards from the Central Graben towards shallower areas of the basin, signifying hydrodynamic fluid flow, similar to the overlying Palaeocene sands

157

(Dennis *et al*., 2000). The overpressure distribution map generated by Dennis *et al*. (2005) for the Chalk reservoir interval is shown in **Figure 5.23**.

In this study, several direct pore pressure measurements recorded within thin, isolated sand units are thought to represent pressures in the encasing muds. Overpressure magnitudes calculated within such isolated sands reach in excess of 2000 psi (13.8 MPa) at depths around 8000 ft (2440 m) TVD (see **Chapter 6** for further discussion of such values).

The greatest magnitudes of overpressure are encountered within the deepest of the three major fan sandstones, the Maureen Sandstone Member. Within the Mey Sandstone Member, the greatest magnitudes of overpressure are experienced within UK quadrant 30, where the underlying Maureen Sandstone Member is largely absent. Similarly, within the Forties Sandstone Member, the greatest magnitudes of overpressure are encountered within Norwegian quadrants 1 and 2, where the underlying Maureen and Mey sandstone members are both absent. This pattern is consistent with decreasing reservoir quality with increasing distance from sediment source within each fan, and with the vertical input of highly overpressured fluids through the Chalk in the distal parts of each fan.

Where the Forties Sandstone Member is underlain by the Mey or Maureen sandstone member, and where the Mey Sandstone Member is underlain by the Maureen, the overlying sand is effectively 'buffered' from vertical fluid input from the underlying Chalk. This may partly explain why magnitudes of overpressure within the Forties Sandstone Member are generally smaller those in the Maureen and Mey sands, and why overpressures in the Mey sand are slightly lower than those in the Maureen sand. However, the Maureen and Mey sands appear to act largely as a single lateral drainage unit which may result from the close proximity of these sands in deeper parts of the basin.

The schematic cross-section shown in **Figure 5.24** has been generated in order to summarize the main routes of fluid flow within the basin, as well as potential sources of fluid input into the Palaeogene system.

Figure 5.23 - Overpressure distribution map for the Chalk Group of the Central North Sea, modified from Dennis *et al*. (2005). The Chalk overpressure is contoured at intervals of 10 bar (145 psi).

5.3.2. *Implications for hydrodynamic trapping*

As was explained in **Chapter 3**, lateral differences in reservoir overpressure can result in tilted hydrocarbon-water contacts. Fluid density contrast and the lateral aquifer pressure gradient control the amount of tilt at the hydrocarbon-water contact. Hydrodynamic gradients have been used to estimate the angle of tilt that may be expected on hydrocarbon-water contacts for several areas within the major Palaeocene

159

Figure 5.24 - Schematic west–east cross-section showing Palaeogene overpressure relationships and inferred areas of fluid flow. Line of section is shown in **Figures 5.4b, 5.5b** and **5.6b**. Fluids enter the Palaeogene sands from the Chalk below and the Tertiary muds above. Lateral fluid flow in the Maureen, Mey and Forties sandstone members is predominantly to the NW, so the main exit areas are out of the plane of this section. Lateral flow is towards the west in the Cromarty and Tay sands, with fluids exiting into the Dornoch and Mousa shelf sands, respectively, on the Western Platform. Vertical drainage between the Forties, Cromarty and Tay occurs where sands are in close proximity, and through fault–fracture systems associated with salt diapirs. Although not shown, additional drainage between the Cromarty and Tay is also likely to be associated with injected Cromarty sands.

sandstone members. Tilt was calculated using *Equation 3.11* (Dennis *et al.*, 1998). For all calculations of tilt an average water pressure gradient of 0.445 psi ft^{-1} (0.01 MPa m^{-1}) was assumed. Similarly an average oil density of 39°API was used for Palaeocene sands, which is equivalent to an oil gradient of 0.358 psi ft^{-1} (8×10^{-3} MPa m^{-1}).

In the Maureen and Mey sandstone members, the largest tilts of the oil–water contact would be where hydrodynamic gradients are greatest within the steep lateral ramp in overpressures along the upper parts of UK quadrants 29 and 30. In this area of the basin, maximum hydrodynamic gradients within the Maureen range from 44.5 psi km^{-1} (0.31 MPa km^{-1}) and 67.5 psi km^{-1} (0.47 MPa km^{-1}) along the eastern and western limbs of the sandstone distribution, respectively, resulting in tilted contacts of approximately 9° and 14° for the respective limbs. In the Mey Sandstone Member, similar steep hydrodynamic gradients of 59.3 psi km^{-1} (0.41MPa km^{-1}) are observed across the northern parts of UK quadrant 29, where hydrocarbon–water tilts of ~ 12° are predicted. Within UK block 23/27, the Mey hydrodynamic gradient is exceptionally high at ~ 120 psi km^{-1} (0.83 MPa km^{-1}), with contact tilt of ~ 23° calculated for this part of the fan. In this area of the basin, high angles of predicted hydrocarbon tilt increase exploration risk, rather than increase the likelihood of hydrodynamic trapping, because the structural dip is not high enough to create hydrodynamic traps. However, detailed mapping of reservoir structure would be necessary to assess trapping potential accurately.

In the Forties Sandstone Member, hydrodynamic gradients are much lower than those observed within the underlying sandstone members, with the greatest hydrodynamic gradient of 25 psi km^{-1} (0.17 MPa km^{-1}) recorded in UK quadrant 23. Predicted tilts of 5° are calculated for this area of the fan. Across the remainder of the Forties fan, hydrodynamic gradients are smaller and so the impact of tilted OWC becomes less significant.

Although much lower hydrodynamic gradients, ranging between ~ 1.3 psi km^{-1} (9 kPa km^{-1}) and 2 psi km^{-1} (14 kPa km^{-1}), are observed within the Cromarty and Tay sandstone members, tilted oil-water contacts could still occur where heavy oils are present. Heavy, partially biodegraded hydrocarbon accumulations are commonly found around UK quadrants 21 and 28, where the Cromarty and Tay sands are shallowest, such as seen at Narwhal (14° API oil), Pilot (14°-16° API), Elke (16° API), and

Fyne/Dandy (25° API). Oils ranging between 15° API and 25° API could generate hydrocarbon-water tilts of around 0.5° and 1.5°, which may increase levels of estimated oil significantly within subtle traps.

6 | Mudstone overpressures

"Mud is the most poetical thing in the world" Reginald H. Blyth (1898-1964) [English author]

6. Mudstone overpressures

In **Chapter 5** the pressure distributions within each major Palaeogene sandstone member were examined. Although it is assumed that pressures within the surrounding lower permeability shales and mudrocks are of greater magnitude, the actual magnitudes of overpressure remain largely unknown. Direct pore pressure measurements are rarely recorded within lower permeability muds and shales, due to the length of time required for the pressure testing tool to stabilize with the formation. Occasionally, however, direct pore pressure measurements may be recorded within thin isolated bodies of higher permeability that are encased by the surrounding muds. Such recorded pressures are likely to be representative of the surrounding lower permeability sediment. Within this chapter, several such pressure measurements are discussed.

6.1. Mudrock overpressures derived from direct measurements

Fifteen solitary pressure measurements were successfully recorded within thin isolated sand/silt bodies encased by lower permeability mudrocks belonging to the Nordland Group and the Lark, Horda, Sele, Lista and Maureen formations. Such measurements are generally of high magnitude, reflecting the pore pressure within the surrounding mudrocks. **Table 6.1** shows these fifteen data values and **Figure 6.1** shows their distribution across the study region. With the exception of two data points (UK 22/02a-8Z and UK 22/10a-3), all of the values discussed are known to be of sufficient quality with no known tool errors and no supercharging.

6.1.1. Nordland Group

Two data points are thought to reflect the magnitude of overpressure within the Nordland Group mudrocks. In Norwegian well 2/4-16, overpressure of 10 psi (0.07 MPa) was recorded by a solitary RFT measurement at a depth of 2376 ft (724 m) TVDSS. In UK well 29/10-5A, overpressure of 1342 psi (9.25 MPa) was calculated from a kick value encountered at a depth of 5337 ft (1627 m) TVDSS. The contrast between the near-hydrostatic pressure measured in well NO 2/4-16 and the large

164
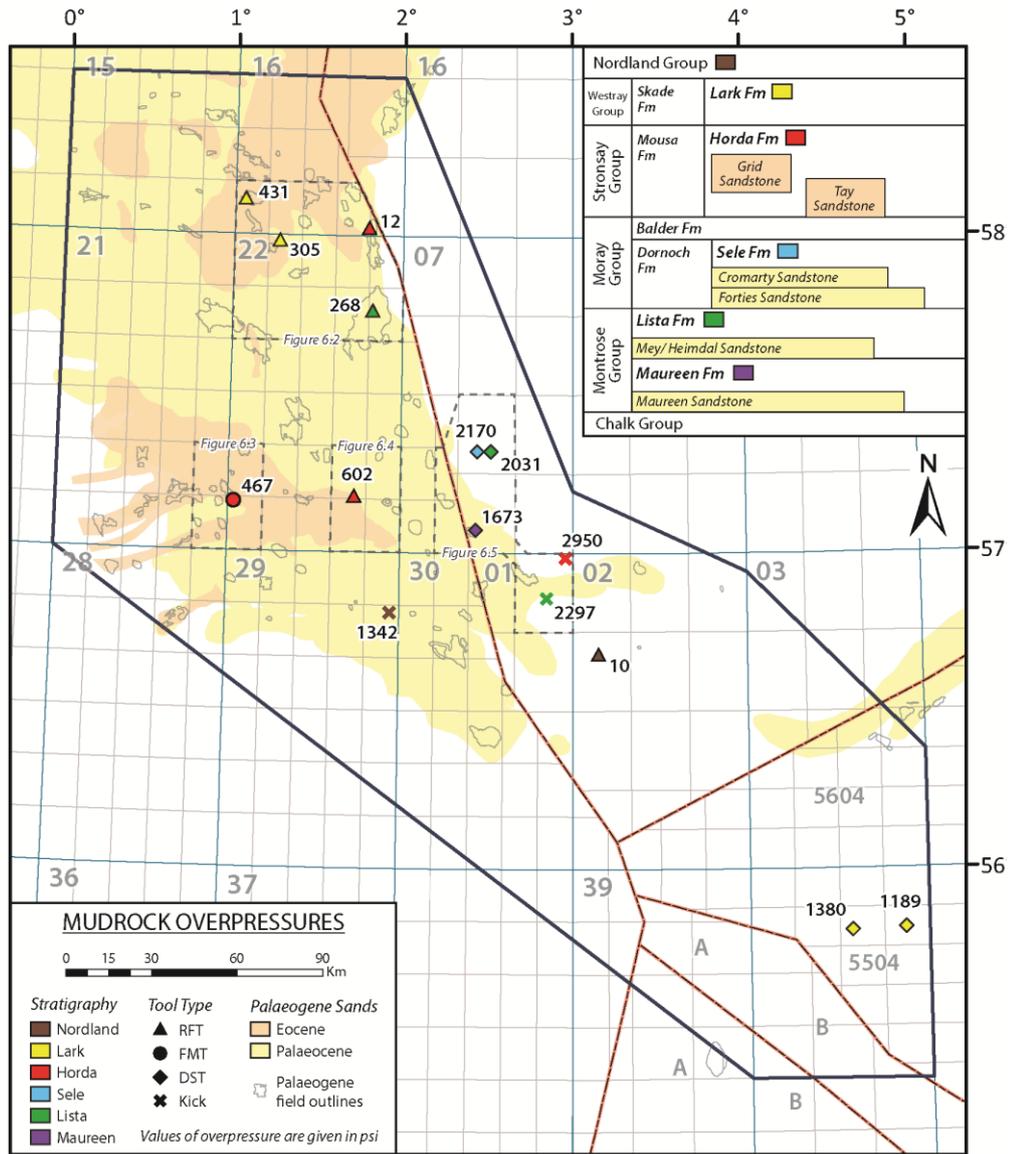
Figure 6.1 - Map showing the location of the fifteen direct pore pressure measurements within the surrounding lower permeability Palaeogene mudrocks. Locations of the P-D plots shown in **Figures 6.2** to **6.5** are outlined.

magnitude of overpressure calculated at greater depth in UK well 29/10-5A support the idea that top overpressure across the Central North Sea region lies at depths around 1000 m (3280 ft) (Leonard, 1993; O' Connor and Swarbrick, 2008).

Longitude	Latitude	Well Name	Depth (ft)	Pressure (psi)	Overpressure (psi)	Category	Quality	Group	Formation	Fluid Type	Measurement Type	Gauge Type	Comments
1.951	56.809	29/10- 5A	5337	3732	1342	2	U	Nordland		Water	KICK	N/A	KICK value recorded within the Hordaland/ Nordland shales, according to the composite log
3.151	56.677	NO 2/4- 16	2376	1082	10	2	Poor	Nordland		Water	RFT (solitary)	Strain	Composite log and NPD web pages indicate that the value was collected from within the Hordaland claystones
1.065	58.108	16/26- 13	5627	2950	431	2	Good	Westray	Lark	Water	RFT (solitary)	Quartz	Thin sandstone unit (~30ft thick) surrounded by Lark Formation shales
1.219	57.975	22/02a- 8Z	6541	3230	305	2	U	Westray	Lark	Water	RFT (solitary)	Strain	Solitary RFT value of unknown quality. No composite log for well so interpretation may be incorrect or value may be supercharged. Mud weight is however greater than pressure measured
4.869	55.810	Adda-1	6643	4160	1189	2	U	Westray	Lark	Water	DST (solitary)	Strain	Recorded within the Lower Eocene shales above Balder Formation
4.572	55.802	Bo- 1	6499	4287	1380	2	U	Westray	Lark	Water	DST (solitary)	Strain	Recorded within the Lower Eocene shales above Balder Formation. Lower Eocene is composed of shales with a lesser amount of claystones, limestone and dolomite
1.800	58.018	16/29a- 9	7977	3577	12	2	Good	Stronsay	Horda	Water	RFT (solitary)	Quartz	Thin clay/limestone bed within the Horda Formation < 10 ft thick
1.734	57.172	22/24b- 4Z	9323	4766	602	2	Fair	Stronsay	Horda	Water	RFT (solitary)	Strain	Thin sandstone unit in the Horda (likely to be the margin of the Tay sandstone member, but pressures are more reflective of Horda muds)
1.038	57.155	22/26a- 2	7118	3649	467	2	Good	Stronsay	Horda	Water	FMT (solitary)	Strain	Composite log the FMT value is recorded within a dolomitic region of the Horda Formation ~200 ft TVD above the Tay Sandstone
2.959	56.983	NO 1/3- 9 ST2	7910	6485	2950	2	N/A	Stronsay	Horda	Water	KICK	N/A	KICK in the Nordland/ Hordaland Group
2.475	57.322	NO 7/8- 1	8075	5778	2170	2	U	Moray	Sele	Water	DST (solitary)	Strain	Composite log and NPD data pages indicate that the value was recorded within the Sele Formation shales. Pressure regression exists between the Sele and Lista Formation shales

1.825	57.760	**22/10a- 3**	8419	4029	268	2	U	Montrose	Lista	Water	RFT (solitary)	Strain	No composite log for the well so interpretation may be incorrect or value may be supercharged.
2.852	56.856	**NO 1/3- 1**	10343	6914	2297	2	U	Montrose	Lista	Water	KICK	N/A	KICK in the Lista Formation sediments
2.475	57.322	**NO 7/8- 1**	8206	5697	2031	2	U	Montrose	Lista	Water	DST (solitary)	Strain	Composite log and NPD data pages indicate that the value was recorded within the Lista Formation shales. Pressure regression exists between the Sele and Lista Formation Shales.
2.440	57.071	**NO 7/11- 1**	10088	6177	1673	2	U	Montrose	Maureen	Water	DST (solitary)	Strain	Measurement was recorded within the Maureen Formation Limestone.

Table 6.1 - Showing the fifteen solitary pressure measurements recorded within thin isolated sand/silt bodies encased by lower permeability mudrocks.

6.1.2. Lark Formation

Four overpressure values were calculated from solitary pressure measurements that had been recorded within sandy, silty or dolomitic intervals of the low-permeability Lark Formation (**Figure 6.1**). The P-D plot in **Figure 6.2** shows an overpressure of 431 psi (2.97 MPa) calculated at approximately 5630 ft (1716 m) TVDSS in UK well 16/26-13 and an overpressure of 304 psi (2.1 MPa) at approximately 6540 ft (1994 m) TVDSS in UK well 22/02a-8Z. Overpressures in the Lark Formation are much greater than those recorded within the nearby Brodie and Caran sandstone units (**Figure 6.2**), which for the most part have near-hydrostatic pressures at similar depths. Overpressures of 1189 psi (8.2 MPa) and 1380 psi (9.52 MPa) were recorded within Danish wells Adda-1 and Bo-1 at depths of 6643 ft (2025 m) and 6499 ft (1981 m) TVDSS, respectively (**Figure 6.1**). Much larger magnitudes of overpressure were recorded in this area of the basin because there are no sandstone members present to facilitate lateral drainage of overpressured pore fluids.

6.1.3. Horda Formation

Four overpressure values were measured in Horda Formation mudrocks. The lowest magnitude of 12 psi (0.08 MPa) was recorded in UK well 16/29a-9 within a thin limestone unit less than 10 ft (3 m) thick at a depth of around 7980 ft (2432 m) TVDSS, which is deeper than the typical top of overpressure expected for the Central North Sea region (Leonard, 1993; O' Connor and Swarbrick, 2008). Such a low overpressure magnitude at this depth implies that the Horda mudrocks in this area have dewatered, with fluids most likely draining into the nearby sands of the Eocene Brodie and Caran sandstone units.

Much higher magnitudes of overpressure were calculated from the other three Horda Formation pressure values (**Figure 6.1**). In UK well 22/26a-2, an overpressure of 467 psi (3.22 MPa) was calculated at a depth of 7118 ft (2170 m) TVDSS within a thin, approximately 20 ft (6 m) thick, dolomite interval, situated around 200 ft (61 m) vertically above the Tay Sandstone Member (**Figure 6.3**). A second solitary overpressure value of 602 psi (4.15 MPa) was calculated at the very margin of the Tay Sandstone Member in UK well 22/24b-4Z at a depth of approximately 9320 ft (2841 m)

168
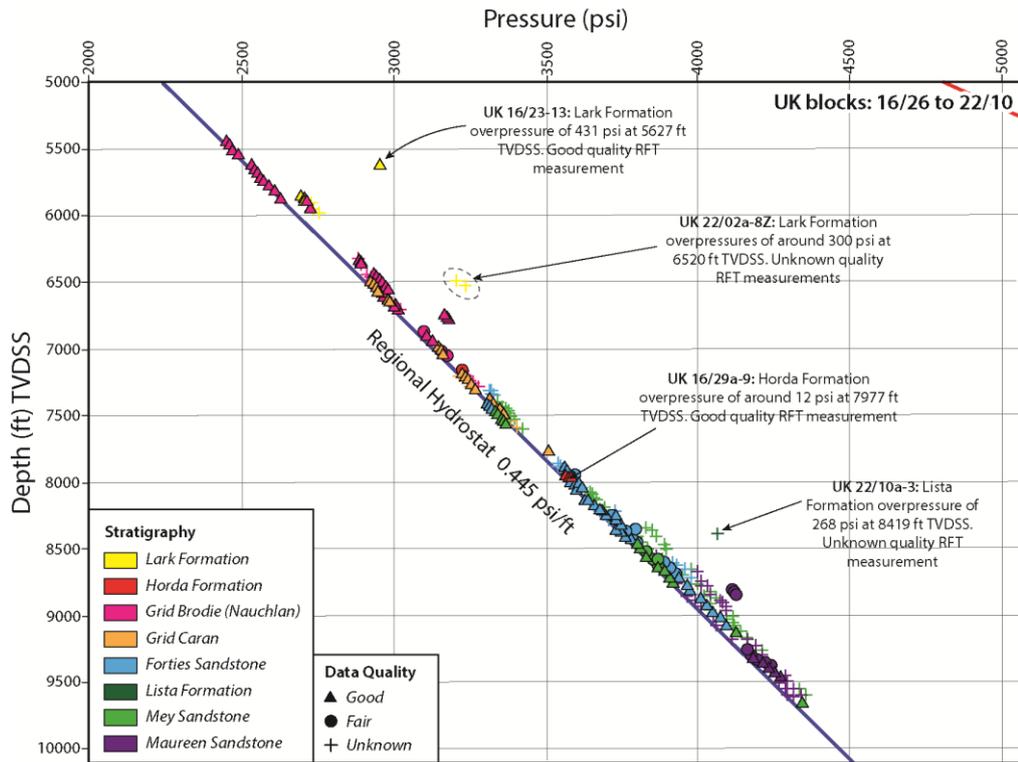
Figure 6.2 - Pressure-depth plot for all data points recorded within the area encapsulating UK blocks 16/26 to 22/10, as shown in **Figure 6.1**. Lark Formation pressures recorded within UK wells 16/23-13 and 22/02a-8Z are much greater than those recorded within the nearby hydrostatically pressured Grid Sandstone Member. In contrast, the Horda Formation value recorded within UK 16/29a-9 is hydrostatically pressured, being effectively dewatered due to the close proximity with the underlying Mey and nearby Grid sandstone members. A pressure value that may be representative of the Lista Formation shale was recorded in UK well 22/10a-3.

TVDSS, within a thin sandstone unit less than 10 ft (3 m) thick (**Figure 6.4**). Although the latter value may arguably be classified as belonging to the Tay Sandstone Member, its magnitude indicates that it represents overpressure in the surrounding Horda Formation mudrocks. Pressure measurements such as those in UK wells 22/26a-2 and 22/24b-4Z provide good examples of intraformational mudrocks dewatering into the vertically adjacent, higher permeability sands, continuously feeding the lateral drainage pathways described in **Chapter 5**.

A much higher Horda Formation overpressure of 2950 psi (20.3 MPa) was calculated in Norwegian well 1/3-9ST from a kick value at a depth of 7910 ft (2411 m) TVDSS. In this area of the basin, no Eocene or Palaeocene sandstone members are

169
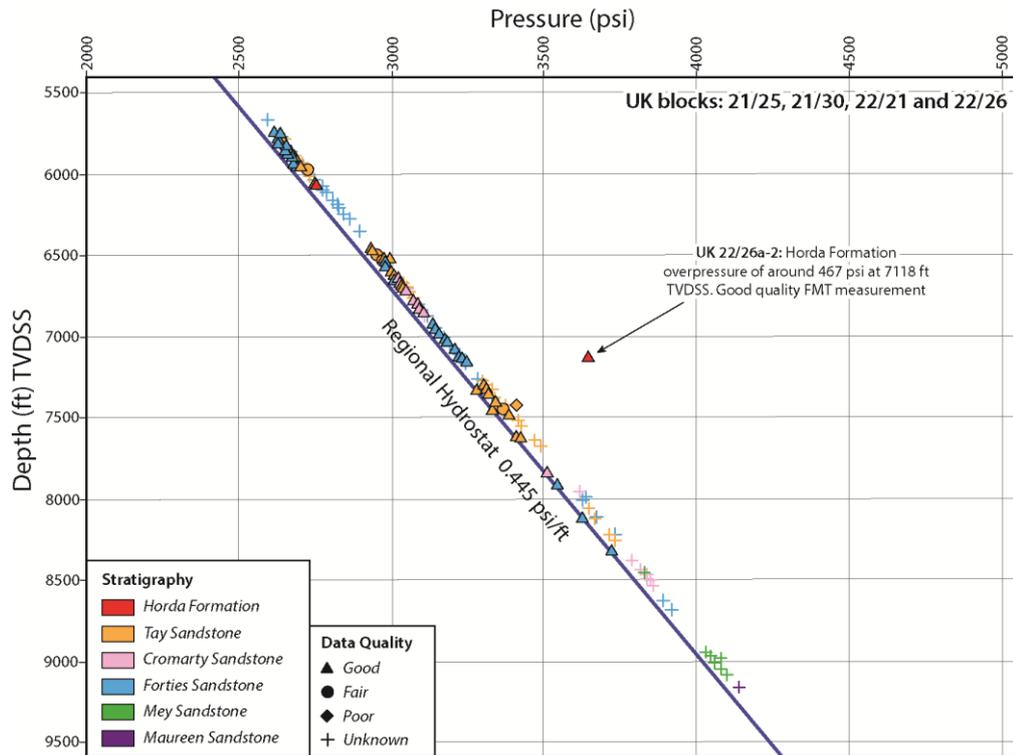
Figure 6.3 - Pressure-depth plot showing all data points recorded within UK blocks 21/25, 21/30, 22/21 and 22/26, the area shown in **Figure 6.1**. The pressure measurement recorded in UK 22/26a-2 is representative of the lower permeability Horda Formation and corresponds to much greater overpressure than in the near-hydrostatically pressured underlying and laterally adjacent Tay Sandstone.

present, which may explain why the magnitudes of Horda overpressure are much greater at shallower depth than those calculated within UK wells 22/26a-2 and 22/24b-4Z, furthering emphasizing that the high overpressures in the surrounding mudrock sequences must, to some extent, source the laterally draining Palaeogene sands.

6.1.4. Sele Formation

Only one pressure measurement was made in the Sele Formation, within a thin siltstone unit in Norwegian well 7/8-1, beyond the limit of the Palaeogene fan sandstones (**Figure 6.1**). The overpressure value of 2170 psi (15.0 MPa) calculated at a depth of 8075 ft (2461 m) TVDSS far exceeds overpressures recorded within the nearby Forties Sandstones at greater depths (**Figure 6.5**).
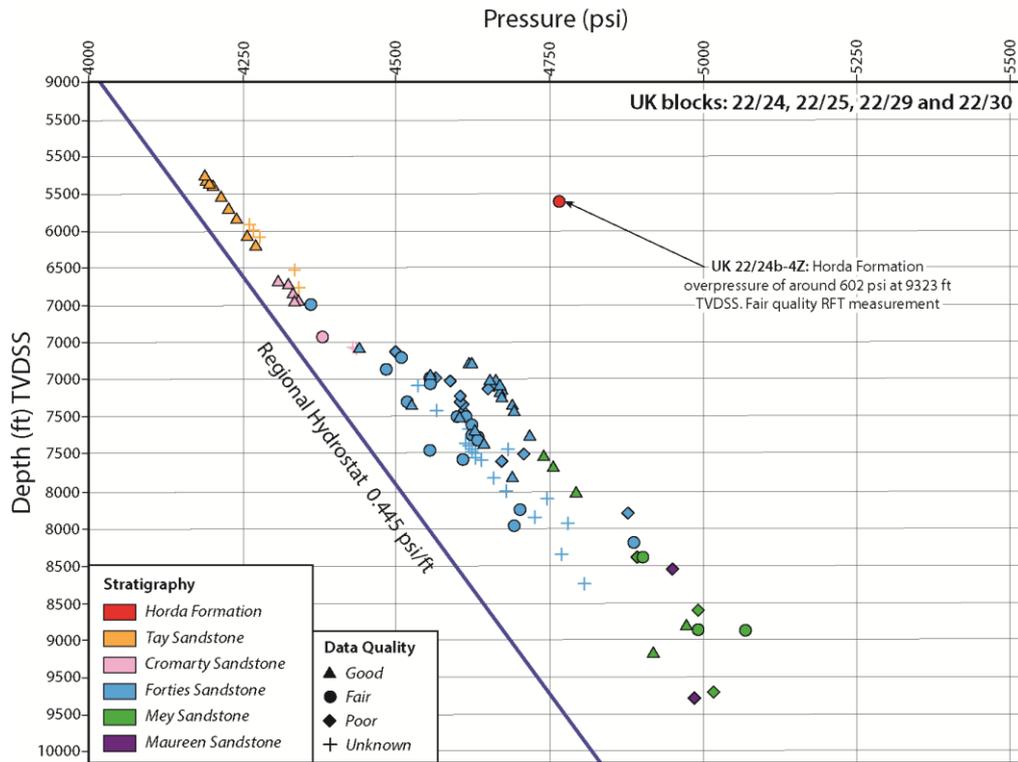
Figure 6.4 - Pressure-depth plot for the area of UK blocks 22/24, 22/25, 22/29 and 22/30, as shown in **Figure 6.1**. The Horda Formation pressure recorded in UK 22/24b-4Z corresponds to a much higher overpressure than those in the surrounding Eocene and Palaeocene sandstone members.

6.1.5. Lista Formation

Three values of overpressure were calculated within the Lista Formation (**Figure 6.1**), and are all higher than those measured within the nearby Mey Sandstone Member. In UK well 22/10a-3, an overpressure of 268 psi (1.85 MPa) was calculated at a depth of 8419 ft (2566 m) TVDSS (**Figure 6.2**), with the surrounding Mey Sandstone Member being near-hydrostatically pressured. In the adjacent Norwegian quadrant, Lista Formation overpressures are of greater magnitude because fluids cannot easily escape into the nearby Palaeogene sandstone members. In Norwegian wells 1/3-1 and 7/8-1, Lista Formation overpressures of 2297 psi (15.84 MPa) and 2031 psi (14.0 MPa) were calculated at depths of 10343 ft (3153 m) TVDSS and 8206 ft (2501 m) TVDSS, respectively.

171
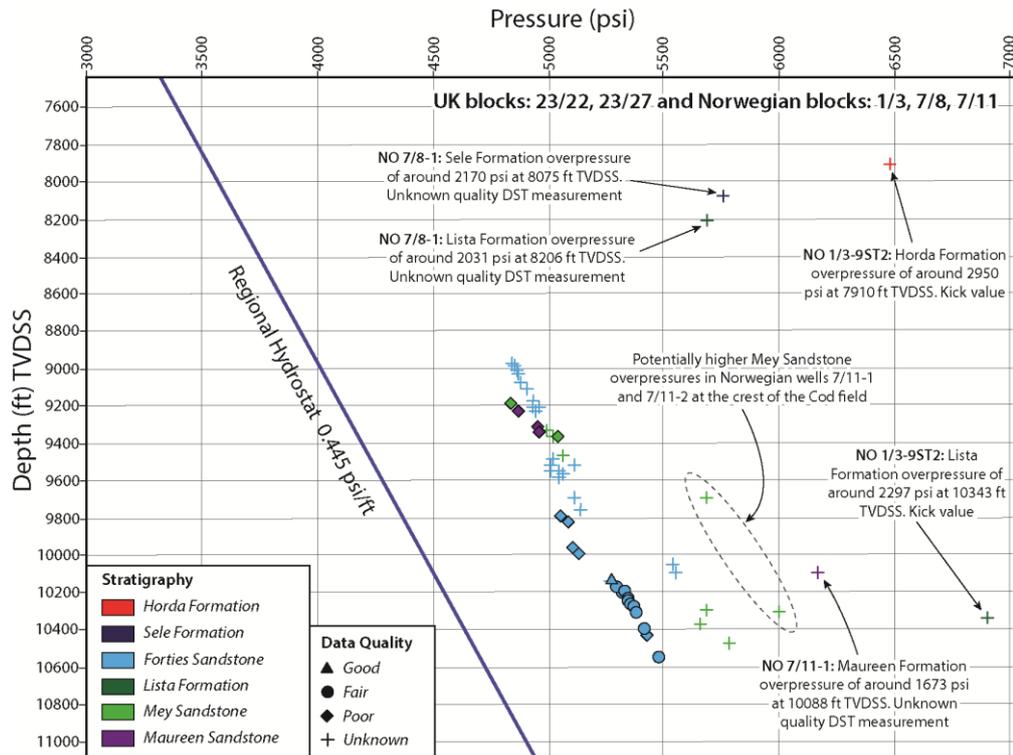
Figure 6.5 - Pressure-depth plot showing all pressure data recorded within UK blocks 23/22, 23/27 and Norwegian blocks 1/3, 7/8 and 7/11. This area, shown in **Figure 6.1** is situated towards the distal region of the Palaeogene fans and so distribution is limited. Data points which are representative of the surrounding lower permeability muds are at much higher overpressures.

6.1.6. *Maureen Formation*

An overpressure of 1673 psi (11.54 MPa) was calculated within a thin limestone interval of the Maureen Formation, at a depth of approximately 10088 ft (3075 m) TVDSS in Norwegian well 7/11-1, beyond the limit of the Maureen and Mey fan sandstone members (**Figure 6.5**).

6.2. Summary

The direct pore pressure measurements discussed above provide rare insights into the magnitudes of overpressure within the surrounding lower permeability mudstones. Overpressure appears to develop at relatively shallow depths, as indicated by measurements recorded within the Nordland and Lark formations, which is in

172

agreement with the depth of top overpressure inferred at around 1000 m by Leonard (1993) and O' Connor and Swarbrick (2008). The greatest overpressure magnitudes are recorded in areas beyond the distribution of Palaeogene sandstones, or at least where the submarine sands have become thin. Dewatering of the overpressured shales into nearby higher permeability sands is less likely to occur in these areas. Where overpressure measurements representative of mudstones are present towards the NW of the study region, it is apparent that the calculated overpressures are of lower magnitude, owing to the likelihood of fluid drainage into the surrounding higher permeability sandstones which are more abundant in this area.

7 | Basin modelling

"I have not failed. I've just found 10,000 ways that won't work" Thomas Edison (1847-1931) [American inventor and businessman]

7. Basin modelling

Attempts were made at 1D and 3D basin modelling, with the original intention of estimating the relative contributions from Tertiary and Mesozoic strata to the present-day lateral fluid flow through the Palaeogene sands. In general, such estimates may improve understanding of the hydrodynamics of the Central North Sea basin with particular reference to compaction processes in the Mesozoic strata, the nature of the pressure transition zone in the Cretaceous Chalk and the underlying Upper Jurassic mudrocks, the locations of fluid flow pathways, and the migration of hydrocarbons. Because of the difficulties in modelling gas generation and chemical compaction due to clay diagenesis, the results here are limited, but do contribute to a general understanding of flow pathways in the basin, the sources of overpressured fluids, and present-day operating processes. There are three main stages involved in the production of any basin model: 1) building the model, 2) populating the model with realistic parameters, and 3) calibrating the model so that the modelled results match the actual measured data as closely as possible. The following chapter details the production of a 1D model for UK well 30/11b-3 and documents the attempt made at producing a 3D model for the post-Jurassic strata of the Central North Sea. Results derived from each of these models are discussed in relation to the relative fluid contributions into the Palaeogene sands from Tertiary and Mesozoic strata.

7.1. 1D basin modelling

During the early stages of this research, 1D basin modelling was performed on UK well 30/11b-3 using the Temis Suite software. UK well 30/11b-3 was selected for modelling owing to the abundance of data available for this well and because of its location within the highly overpressured region of the Central Graben (**Figure 7.1**). The well is situated within the Appleton Field which contains oil, gas and condensate in the Jurassic aged Fulmar Sandstone Formation. The total drilled depth is 15955 ft (4860 m) TVDSS in Triassic sediments belonging to the Smithbank Formation. A generalised stratigraphy of UK well 30/11b-3 is shown in **Figure 7.2**.
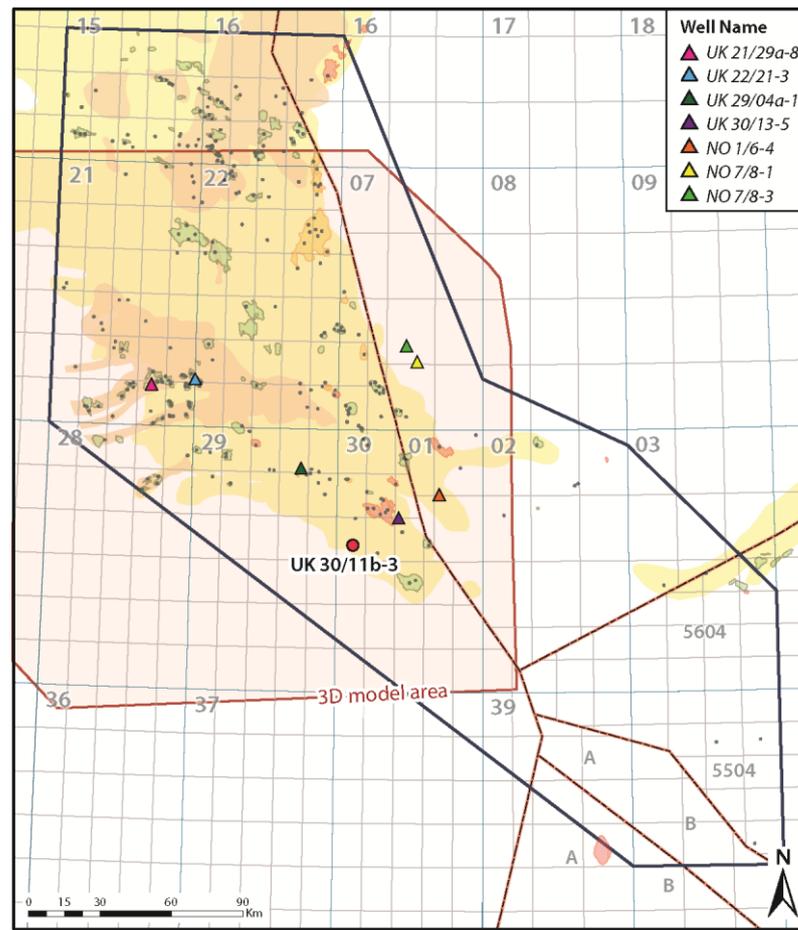
Figure 7.1 - Map showing the location of UK well 30/11b-3 which was selected for 1D basin modelling, the region of 3D basin modelling, and several wells selected for comparison in the 3D modelling work.

7.1.1. Present-day pressure distribution

The known present-day pressure distribution for well 30/11b-3 is shown in **Figure 7.3**. It is important to have a clear understanding of the present-day levels of overpressure within the well, since output basin models generated must match, or be comparable to, these observed values. All RFT pressure measurements were recorded within the Fulmar Sandstone Formation situated towards the base of the well from 14946 ft (4560 m) to 15077 ft (4600 m) TVDSS. Overpressures of approximately 5915 psi (40.8 MPa) are calculated in the Fulmar sandstone, assuming a constant hydrostatic gradient 0.445 psi ft^{-1} for the Central North Sea. No direct pressure data are available for any other part of the well. The overpressure distribution maps generated in **Chapter 5** indicate that overpressures of approximately 2200 psi (15.2 MPa) should be encountered within the

176
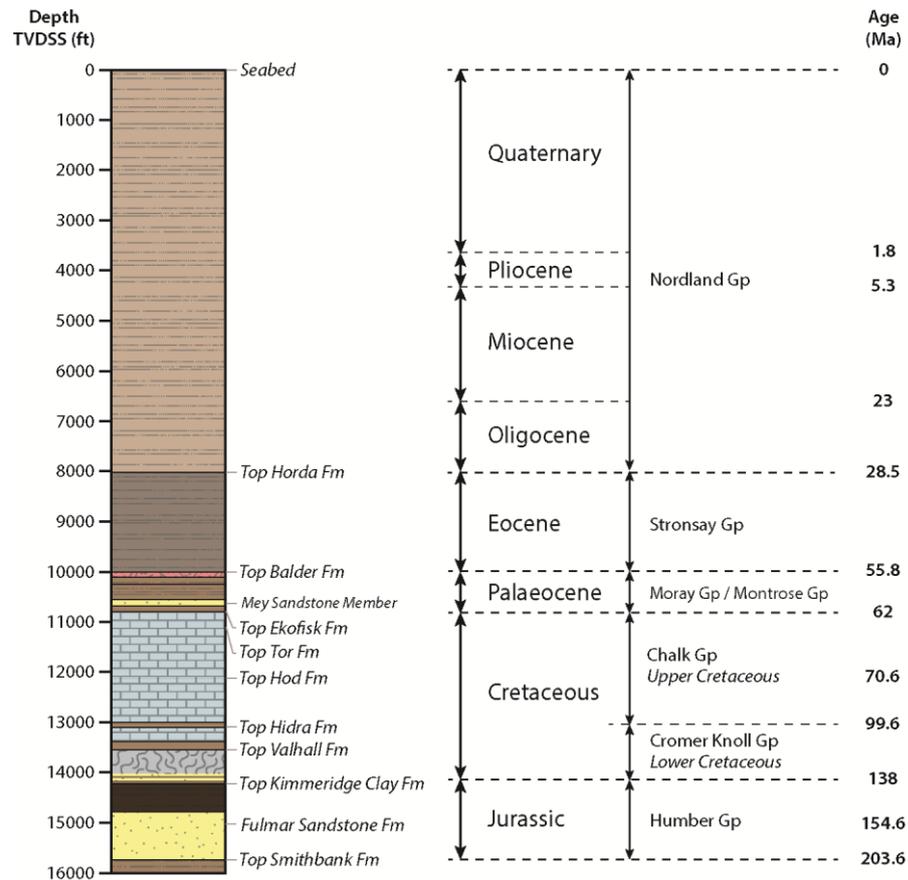
Figure 7.2 - UK 30/11b-3 generalized well stratigraphy showing depth in feet TVDSS to formation tops, as well as absolute ages in millions of years to significant horizons. Total depth of well is within the Triassic Smithbank Formation at a depth of 15955 ft (4860 m) TVDSS.

Mey Sandstone Member, in accordance with measurements in the nearest neighbouring wells. In the closest neighbouring well UK 30/12b-2, situated approximately 10.6 km to the SE, a Mey overpressure of 2184 psi (15.1 MPa) was calculated.

For the remainder of the well, mud weights used during drilling (**Figure 7.3**) can be used as an estimate of pore pressure (see *section 3.5.2*). Drilling mud weight was increased to 12 ppg below the 20-inch casing point at a depth of 2600 ft (793 m) TVDSS, suggesting an increase in formation pore pressures around this depth within the post-Oligocene, Nordland claystone, which may correspond to the top of overpressure within the well. A constant mud weight of around 12 ppg was used to drill through the Palaeogene and Cretaceous sediments. From depths of around 14000 ft (4270 m) TVDSS down to14816 ft (4516 m) drilling mud weights increase gradually from 12 ppg
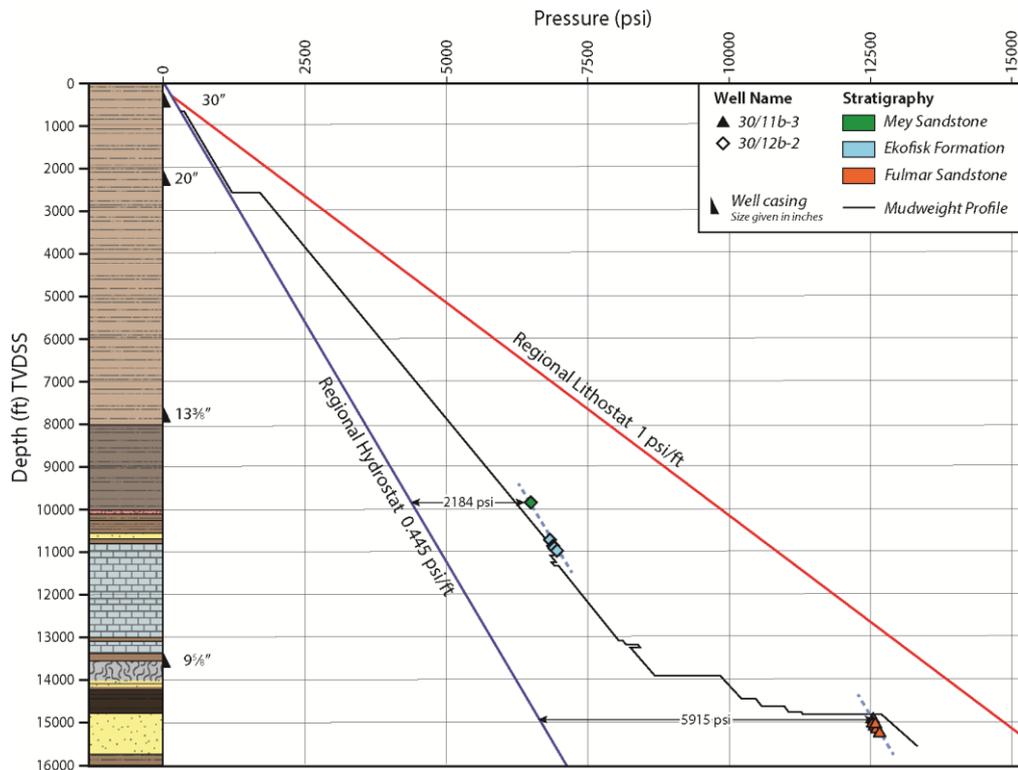
Figure 7.3 - Pressure-depth plot for UK 30/11b-3, showing direct pore pressure measurements recorded within the Jurassic Fulmar Sandstone Formation, where overpressures of 5915 psi (20.1 MPa) were recorded. Direct pore pressure measurements recorded within the Mey Sandstone Member and Ekofisk Formation of nearby well UK 30/12b-2 are also shown, where overpressures of ~ 2184 psi (15.1 MPa) were calculated.

to 16 ppg, suggesting a sharp pressure transition zone initiating near the base of the Valhall Formation and extending down to the Fulmar Sandstone Formation. The true location of the pressure transition zone is subject to debate. Earlier authors (Holm, 1998; Daniel 2001) agreed that pore pressures increase dramatically below the base of the Chalk Group into the highly overpressured Jurassic and Triassic reservoirs. Swarbrick *et al*. (2010) disagreed, noting that rare direct pore pressure measurements recorded within reservoir intervals of the Chalk almost always record pressures which exceed the drilling mud weight used and suggested that the low permeability Chalk Group has frequently been drilled underbalanced. Consequently, they consider a more realistic pressure transition zone to be one of gradual, steady-state overpressure increase, initiating within the upper regions of the low permeability Chalk Group extending down into the Jurassic and Triassic reservoirs.

7.1.2. *Present-day porosity distribution*

Figure 7.4 shows a series of porosity curves generated for UK well 30/11b-3 using wireline measurements of sonic velocity, resistivity, density and neutron porosity. The density and neutron wireline data are confined to the pre-Cretaceous strata, so only sonic and resistivity data could be used to estimate porosities through the Tertiary and Cretaceous sections.

7.1.2.1. *Density-derived porosity*

Density log-derived porosity was calculated from the bulk density log using the following equation:

$$\emptyset = \frac{\rho_{ma} - \rho}{\rho_{ma} - \rho_{fl}}$$

(7.1)

where ρ_{ma} is matrix density, ρ_{fl} is pore fluid density, and ρ is bulk density as measured by the density tool. The density log was only available for the Pre-Cretaceous strata in UK 30/11b-3. Average matrix densities of 2.75 g cc^{-1} and 2.65 g cc^{-1} were used for mudstone and sandstone sections of the well, respectively, discriminated by the gamma ray log with a threshold value of 65 API. An average pore fluid density was assumed to be 1.05 g cc^{-1}, as used by Hansen (1996). The log-derived density porosity indicates approximately 30 to 10 % over the Pre-Cretaceous depth interval of 13600 ft (4150 m) to 16000 ft (4880 m) TVDSS.

7.1.2.2. *Resistivity-derived porosity*

Values of porosity were derived from the deep resistivity log response, using the Archie (1942) equation:

$$R_t = a.\emptyset^{-m}.S_w^{-n}.R_w$$

(7.2)

where a is the tortuosity, $\emptyset$ is the porosity, m is the cementation factor, S_w is water saturation, n is the saturation exponent, R_w is the resistivity of the formation water and
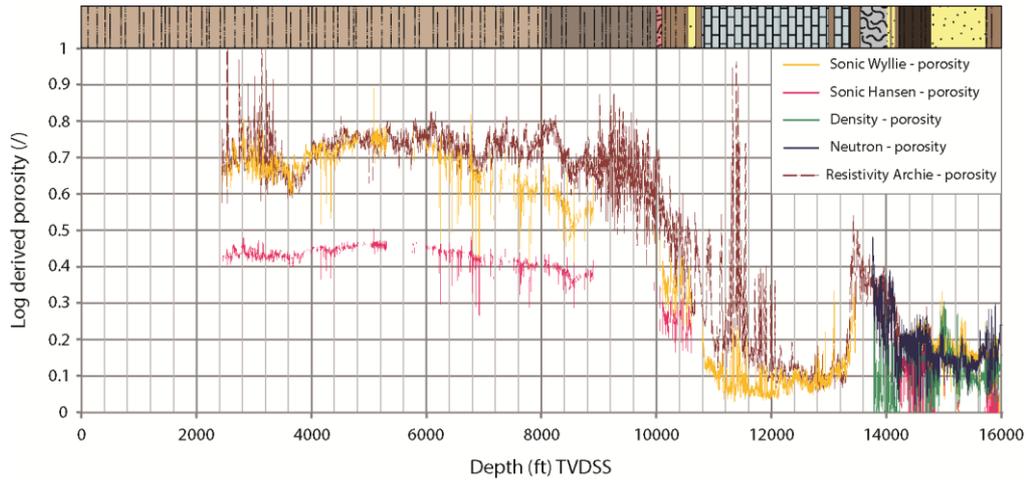
Figure 7.4 - Log-derived porosities in UK well 30/11b-3. The sonic-derived Hansen porosity was selected as being most representative for the Tertiary and Quaternary section, down to depths of 10795 ft (3290 m) TVDSS, with the sonic-derived Wyllie porosity being thought most representative for the remainder of the well.

R_t is measured log resistivity. The resistivity-derived porosity was only calculated for intervals of the borehole where water saturation was equal to one, i.e. no hydrocarbons were present. Values of 1 and 0.81 were used for the tortuosity constant a, for carbonate and consolidated sandstone lithologies, respectively. A constant value of 2 was used for both the cementation factor m and saturation exponent n. Resistivity of the formation water R_w at temperature T °F, was calculated using Arp's equation, transformed relative to a resistivity value of 0.649 Ω m^{-1} at 54 °F. A constant temperature gradient of 0.018144 °F ft^{-1} was assumed downhole:

$$R_w = 0.649 \times \frac{61}{T + 6.77} \tag{7.3}$$

Archie's formula was re-arranged to calculate values of porosity:

$$\varnothing = \sqrt{\frac{a.R_w}{R_t}} \tag{7.4}$$

The resistivity-derived porosity shown in **Figure 7.4** closely resembles the Wyllie sonic porosity. Average values of resistivity-porosity range between 80 and 35 % for the Tertiary mudstone section between depths of 2400 ft (730 m) to 10800 ft (3290 m)

180

TVDSS and 40 to 6 % for the Cretaceous section between depths of 10795 ft (3290 m) and 13385 ft (4080 m) TVDSS.

7.1.2.3. Sonic-derived porosity

The first method of evaluating porosity using sonic log data was that of Wyllie *et al.* (1958), whereby porosity is calculated from linear interpolation between zero porosity when the measured sonic transit time is equal to that of the rock matrix and 100% porosity when the measured transit time is equal to that of the pore fluid:

$$\emptyset = \left(\frac{t_{log} - t_{ma}}{t_f - t_{ma}} \right) \tag{7.5}$$

where t_{ma} is the rock matrix transit time (using values of 67 μsec ft^{-1} in mudstone, 46 μsec ft^{-1} in limestone, 47.5 μsec ft^{-1} in chalk and 55.5 μsec ft^{-1} in sandstone), t_f is the pore fluid transit time, equal to 187 μsec ft^{-1} in seawater, and t_{log} is the measured sonic transit time.

A second method of establishing porosity from sonic log data was that of Hansen (1996) who adapted the equation of Raiga-Clemenceau *et al.* (1988):

$$\emptyset = 1 - \left(\frac{\Delta t_{ma}}{\Delta t} \right)^{1/x} \tag{7.6}$$

where t_{ma} is the rock matrix velocity and x is the acoustic formation factor exponent. Both values are constants that depend upon the sedimentary basin. The Hansen (1996) equation is developed specifically for North Sea mudstones, where shale matrix transit time is equal to 76.5 μsec ft^{-1} and 1.17 is the constant value selected for the acoustic formation factor exponent:

$$\emptyset = 1 - \left(\frac{76.5}{\Delta t} \right)^{1/1.17} \tag{7.7}$$

The Hansen sonic porosity is used solely to calculate mudstone porosities within the well. Discrimination of mud-rich intervals from sandy, silty or chalk intervals within

UK 30/11b-3 was performed using the gamma ray log and an assumed mudstone threshold value of 65 API.

It can be seen in **Figure 7.4** that values of Wyllie sonic porosity calculated using *Equation 7.5* are greater than the values of Hansen sonic porosity calculated using *Equation 7.7*. Wyllie sonic porosities range predominantly from 70 to 30 % within the Tertiary and Quaternary mudstones, between depths of approximately 2400 ft (730 m) to 10800 ft (3290 m) TVDSS, whereas Hansen sonic porosities mostly lie in the range between 45 and 20 % across the same depth interval. Although it can be seen that the Wyllie sonic and resistivity methods produce similar estimates of porosity for the Tertiary section, the Hansen sonic curve is thought to produce more realistic estimates of porosity for this interval since it is calibrated using actual North Sea mudstone measurements (Hansen, 1996).

Wyllie sonic porosity values are used to represent the Cretaceous section of the well, which consists of limestone and chalk. Porosities for this section of the well range between approximately 3 and 24 % between depths of 10890 ft (3320 m) and 12130 ft (3700 m) TVDSS, with mean and modal average porosities of 8.5 % and 4.8 %. Wyllie sonic porosities are also used to represent the pre-Cretaceous sediments which comprise largely mixed claystones, siltstones and sandstones. The Wyllie sonic porosities calculated for the pre-Cretaceous strata largely resemble the density-derived porosities for this portion of the well.

7.1.3. Building the geometric framework

The present-day geometric framework of the well, comprising formation top depths and ages (**Figure 7.2**) was entered into the basin modelling software so that a burial history could be generated and the geometry of the basin calculated back through time, i.e. back-stripping. Depths of formation tops were obtained from the final well report of well UK 30/11b-3. In order to improve the resolution of the model, formations with significant thickness (> 100 m) were broken down into smaller more manageable units of 100 m thickness. For example, the Kimmeridge Clay Formation which has an approximate thickness of 170 m was broken down and entered into the model as two units of claystone, one of 100 m thickness and another of ~ 70 m thickness. By breaking

down large layers into smaller layers the sampling size of the model is increased, resulting in greater accuracy. The final geometric framework for the model comprised a total of 63 layers.

Absolute ages for a large majority of the well could be effectively constrained using palynological data provided to the study by Ikon Geopressure. Coverage of this data ranged from the top Horda Formation at 8020 ft (2445 m) TVDSS down to the top Fulmar Sandstone Formation at 14788 ft (4507 m) TVDSS, with absolute ages for this part of the well being confined between 28.5 Ma and 154.6 Ma, respectively. For the remainder of the well, accurate absolute ages were derived from interpreted seismic data and predicted sedimentation rates (Swarbrick *et al*., 2000; Gatliff *et al*., 1994).

Four unconformable contacts representative of erosive events in the basin history are found within UK 30/11b-3. Three such erosive events (the Early Cretaceous unconformity of 128–125 Ma, the Middle Palaeocene unconformity of 61.7–58.7 Ma, and the Late Eocene unconformity of 37–33.9 Ma) were thought to be too insignificant to include within the model. The longest erosive event, spanning the period 203.6 – 161 Ma from the Middle to Early Jurassic, was modelled as a major hiatus in sedimentation, since actual levels of erosion that occurred over this time interval were unknown and could not be reasonably estimated. This erosive event explains the lack of Middle and Lower Jurassic sediment within the well, and is thought to be associated with the doming of the Central North Sea basin which occurred around this time (Underhill and Partington, 1993). The final burial history of UK well 30/11b-3 generated during 1D modelling is shown as **Figure 2.13**.

7.1.4. *Populating the model with realistic lithological parameters*

Within the model each lithology is defined by a series of parameters e.g. thermal parameters, permeability relationships, compaction parameters such as porosity-depth, sediment density and chemical compaction. The relationships selected for these lithological parameters will ultimately influence the output results of the 1D model. When the model was run solely using the default parameters contained within the basin modelling software, the simulated results proved to be extremely unrealistic (**Figure 7.5**) A maximum overpressure magnitude of only 510 psi (3.52 MPa) was generated
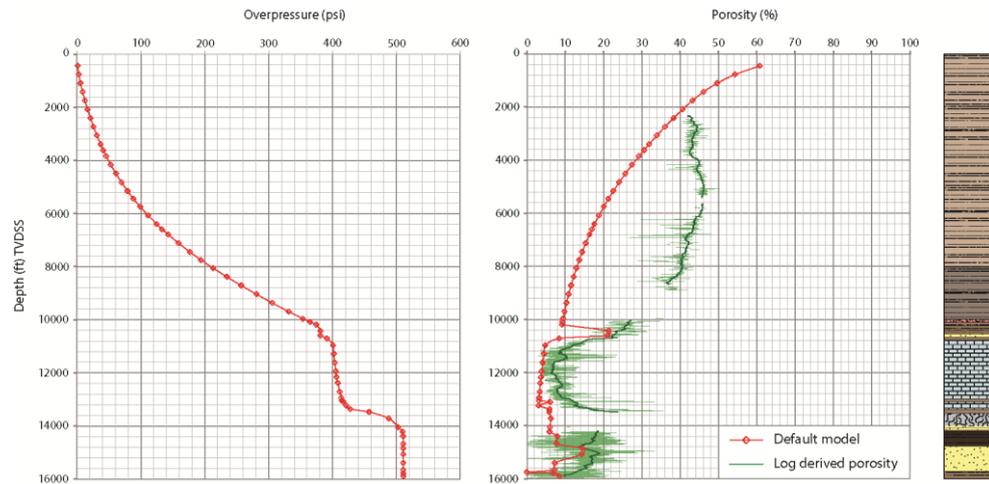
Figure 7.5 - Overpressure and porosity results generated when the 1D model was run using the Temis-Suite default lithological parameters. A maximum magnitude of only 510 psi (3.52 MPa) overpressure was generated within the Fulmar Sandstone Formation. Porosities for all lithologies appear to be underestimated, but most noticeably within the Tertiary and Quaternary section of the well, where differences exceed 20 %. The log-derived porosity is shown in green for comparison, with the curve averaged over a 250 ft (76 m) interval.

within the Fulmar Sandstone Formation, which is approximately 5400 psi (37.2 MPa) lower than the observed levels of overpressure at 5900 psi (40.7 MPa). Additionally only 380 psi (2.62 MPa) overpressure is generated within the Mey Sandstone Member, which greatly contrasts to the observed overpressure magnitudes of 2200 psi (15.2 MPa). Porosities generated by the default model do not match well with the log derived porosities, being generally much lower than those observed (**Figure 7.5**). The need to populate the model with more realistic lithological parameters, other than the default software parameters is consequently highlighted.

Swarbrick *et al*. (2005) emphasized the uncertainties which arise when modelling fine-grained sediments such as siliciclastic and carbonate mudstone, with particular regards to the poorly understood compaction and permeability behaviours of such sediments. Since UK well 30/11b-3 is composed predominantly of fine-grained claystones and chalks, the compaction and permeability relationships of these lithologies were the main focus of alteration. Parameters defining physical constants such as density, heat capacity and conductivity were not changed from the default starting point. Coarser grained lithologies such as sandstones and limestones making up a limited proportion of the well remained unaltered from the 'default' starting point

184

since the relationships which define such lithologies have been extensively researched (Ramm, 1992; Schneider and Hay, 2001, Marcussen *et al.*, 2010) and are more clearly understood. The default parameters for such lithologies were thought to be realistically representative for the Central North Sea.

7.1.4.1. *Tertiary and Quaternary muds and claystones*

The porosity-effective stress relationships of Yang and Aplin (2004) were used to model the Tertiary and Quaternary claystone sequence. The Yang and Aplin (2004) relationships are based on soil mechanics principles, relating void ratio to the vertical effective stress:

$$e = e_{100} - \beta ln \left(\frac{\sigma v'}{0.1} \right)$$
(7.8)

where e is the void ratio; e_{100} and β are compression coefficients and $\sigma v'$ is the vertical effective stress in MPa. The void ratio is defined as the ratio between the volume of voids and the volume of solid in a rock:

$$e = \frac{\varphi}{1 - \varphi}$$
(7.9)

The compression coefficients (e_{100} and β) are strongly dependent upon grain size, i.e. the clay fraction (weight fraction of particles < 2μm in diameter) of the mudstone:

$$e_{100} = 0.3024 + 1.6867 clay + 1.9505 clay^2$$
(7.10)

$$\beta = 0.0407 + 0.2479 clay + 0.3684 clay^2$$
(7.11)

where $clay$ is equal to the clay fraction. Consequently, a series of porosity-effective stress relationships were derived, according to the clay fraction of the mudstone being modelled.

The Yang and Aplin (2004) porosity-effective stress relationship provides a simple but practical way of describing the one-dimensional, mechanical compaction of fine-grained clastic mudstones. Swarbrick *et al.* (2005) used these relationships during

185

their 2D modelling of the Central North Sea, noting how they were particularly well suited to modelling the Tertiary mudstone sequence where overpressure is thought solely to be a result of disequilibrium compaction. The Yang and Aplin (2004) formula does not take into account the effect of chemical compaction, which is thought to occur within mudstones when temperatures exceed 80-100 °C (Peltonen *et al.*, 2009). Assuming a geothermal gradient of 35-41 °C km^{-1} (Kubala *et al.*, 2003), temperatures towards the base of the Tertiary sequence situated at a depth of 10830 ft (3300 m) TVDSS are in the range 116-136 °C. Consequently, chemical compaction processes may be operating within the lower regions of the Tertiary claystones, below depths of around 2.3 km TVDSS, corresponding to the top Eocene. Such processes are not taken into account within the 1D model.

The porosity-permeability relationship of Yang and Aplin, (2000) was also applied to the Tertiary and Quaternary claystone sequence. This relationship relates vertical absolute permeability (K_Z) to the void ratio (*e*), and thus porosity:

$$\ln(K_Z) = a_k + b_k.e + c_k.e^2 \tag{7.12}$$

where, constants a_k, b_k and c_k are dependent upon clay fraction:

$$a_k = -51.12 + 7.485.clay - 5.469.clay^2 \tag{7.13}$$

$$b_k = 47.45 - 94.85.clay + 49.36.clay^2 \tag{7.14}$$

$$c_k = -26.85 + 67.02.clay - 40.77.clay^2 \tag{7.15}$$

As with the porosity-effective stress relationships, a series of porosity-permeability relationships were derived according to the clay fraction of the mudstone being modelled.

The clay fraction distribution through the Tertiary and Quaternary claystone sequence of UK well 30/11b-3 is shown in **Figure 7.6.** This distribution was determined by Yang *et al.* (2004) who used direct measurements and artificial neural networks (ANNs) to accurately quantify it. At depths of around 2000 ft (610 m) TVDSS, the shallowest clay fraction recorded is around 60% to 65%, increasing gradually up to 80% between present-day burial depths of 3800 ft (1160 m) and 7000 ft (2135 m) TVDSS.
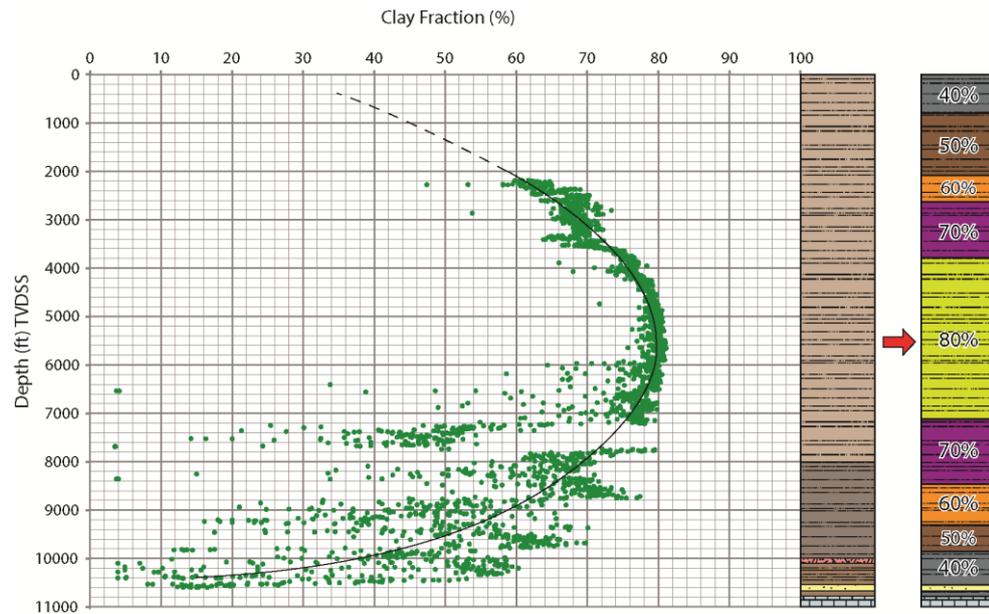
Figure 7.6 - Clay fraction distribution through the Tertiary and Quaternary claystone sequence of UK 30/11b-3. Data were collected by Yang *et al.* (2004). Stratigraphic columns indicate the assigned % clay content within the 1D model over 10 % intervals ranging from 40 to 80 %.

Below 7000 ft (2135 m) TVDSS, the clay fraction distribution becomes highly scattered, although the overall trend is a decrease in the clay fraction to below 40% towards the base of the Palaeocene strata at depths of around 9900 ft (3020 m) TVDSS. For the purposes of basin modelling, the clay fraction distribution observed within UK 30/11b-3 was classified in intervals of 10% to values of 40%, 50%, 60%, 70% and 80% clay fraction (**Figure 7.6**).

All fine grained muds and clays within the pre-Cretaceous sequence of the well were modelled as being 40 % clay fraction, as was assumed by Swarbrick *et al*. (2005).

7.1.4.2. Upper Cretaceous Chalk Group

The Upper Cretaceous sequence within UK well 30/11b-3 comprises predominantly non-reservoir, sealing chalk having porosities lower than 20%. Consequently, the chalk has been modelled entirely as a non-reservoir lithology and minor layers of reservoir chalk have been ignored.

187

The porosity-depth relationship of Mallon and Swarbrick (2002) was used to model the chalk interval. This compaction trend was constructed using sonic interval transit times, density logs and core samples collected from 59 selected wells within the Central North Sea region. With mechanical processes having the greatest impact on porosity reduction during the first 50 m of burial, and chemical compaction processes such as pressure dissolution taking precedence over mechanical processes between burial depths of approximately 50-200 m. At around 1500 m, a slower rate of porosity reduction is observed within the chalk, as indicated by a distinct change in gradient. Although several processes may be responsible for this declining rate of chemical compaction, i.e. changes in temperature, salinity or lithostatic pressure, Mallon and Swarbrick (2002) suggested that onset of overpressure generation is the most likely cause, and acts to impede the rate of chemical compaction. Consequently, use of the Mallon and Swarbrick (2002) porosity-depth relationship to model the chalk may have some impact on the validity of modelled results since it is not representative of hydrostatic burial conditions. However, no better porosity-depth curve for the Central North Sea chalk is available.

The porosity-permeability relationship of Mallon (2000) was used to model the chalk, based on actual measurements made within samples of sealing, non-reservoir and reservoir chalks. Samples analysed by Mallon *et al*. (2005) indicate that permeabilities of the non-reservoir chalks within the Central North Sea are everywhere lower than 40.5 nD, irrespective of burial depth. Typical values of permeability for chalks of approximately 2% porosity are thought to be in the range of 0.1-1 nD (Mallon, 2000).

The effects of chemical compaction were modelled within the chalk lithology since they have significant implications on the porosity and permeability of the chalk during burial and consequently the levels of overpressure that may be generated. The effects of chemical compaction are simulated within the basin modelling software using a pressure dissolution (viscoelastoplastic) algorithm, which replicates the physical phenomena of mineral dissolution, transport of the solute, and mineral precipitation. Values of three chemical compaction coefficients, minimum porosity, macroscopic solid viscosity (μs) and activation energy ($E\mu$) must be stipulated in order for the algorithm to run correctly, as shown in **Table 7.1**. Except for those given by Schneider *et al*. (1996), the values are specific to the Central North Sea chalk. A value of 2% was selected for the minimum porosity. Sensitivity analyses were carried out to find

Source	Activation Energy (KJ/Mole)	Macroscopic Viscosity (Pa.s)
Schneider *et al.* (1996)	40	8×10^{22}
Swarbrick *et al.* (2005)	70	4.7×10^{23}
Temis-Suite User Manual (2007)	15	2.4×10^{23}
Seldon and Swarbrick (2001)	40-60	$3.2 \times 10^{23} - 9.6 \times 10^{23}$

Table 7.1 - Values of activation energy and macroscopic viscosity suggested by various authors. These parameters are needed for modelling chemical compaction, more specifically pressure dissolution of the chalk lithology. All values, except for those of Schneider *et al.* (1996) are specific to the Central North Sea.

appropriate values for the chemical compaction parameters. Several models were run using activation energies ranging from 15 to70 kJ mole^{-1} and macroscopic viscosities ranging from 8.0×10^{22} to 1.1×10^{24} Pa s, covering all of those values suggested in **Table 7.1**. The modelled and observed present day porosities and permeabilities of chalk were best matched when an activation energy of 15 kJ mole^{-1} and macroscopic viscosity of 4.7×10^{23} Pa s were used to simulate chemical compaction. These parameters were therefore selected to populate the final 1D model whose results are discussed below in section 7.1.5.

7.1.5. 1D modelling result

Within the Tertiary and Quaternary mudstone section, porosities are generally seen to decrease from 60 % at the top of the well down to 40 % at depths of around 1000 ft (305 m) TVDSS (**Figure 7.7**). Porosities then gradually increase again up to almost 55 % at 4500 ft (1372 m) TVDSS, followed by a prolonged decreasing trend to values of around 25 % at depths of 10400 ft (3170 m) TVDSS, near to the base of the Tertiary mudstone sequence and Palaeogene section. Modelled overpressures across this section are initiated around a depth of 1250 ft (381 m) TVDSS (**Figure 7.8**), where there is a small porosity increase of just 4 %. This modelled depth to top overpressure is much shallower than the generally accepted regional depth of 3280 ft (1000 m) proposed by
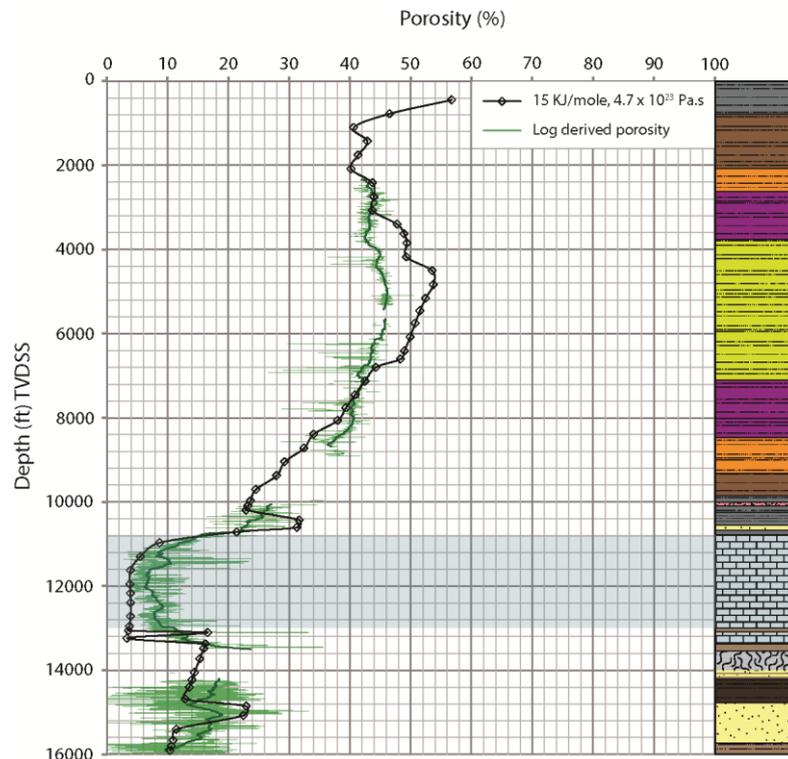
Figure 7.7 - Porosity versus depth plot showing log-derived porosity profile and the porosity profile generated through 1D modelling. It can be seen that higher modelled porosities exist over the interval extending between 3000 ft (915 m) and 6800 ft (2073 m) TVDSS, corresponding approximately to Tertiary mudstones of 80 % clay fraction. Similarly lower modelled porosities exist within the chalk. Differences are largest within the Lower Cretaceous, over the interval extending between ~ 12000 ft (3658 m) and 13200 ft (4023 m). Modelled and log-derived porosities appear to be suitably matched for the remainder of the well.

Leonard (1993) and O'Connor and Swarbrick (2008), but there is no lateral reservoir drainage simulated within the 1D model. Overpressure increases most rapidly over the interval from 2000 ft (610 m) TVDSS to 6400 ft (1950 m) TVDSS, as the clay fraction increases from 60 % to 80 %. Further down hole, as the clay fraction of the Tertiary mudstones gradually decreases to 40 %, modelled overpressure magnitudes increase at a much slower rate. Maximum overpressure magnitudes of 2742 psi (18.9 MPa) are generated towards the base of the Tertiary mudstone sequence, at depths approaching 11000 ft (3353 m) TVDSS. Such magnitudes are approximately 600 psi (4.1 MPa) greater than those which are measured and estimated for this interval of the Central North Sea basin. Overpressures calculated from several RFT measurements within the Upper Cretaceous Ekofisk Formation of UK 30/12b-3 are approximately 650 psi (4.5
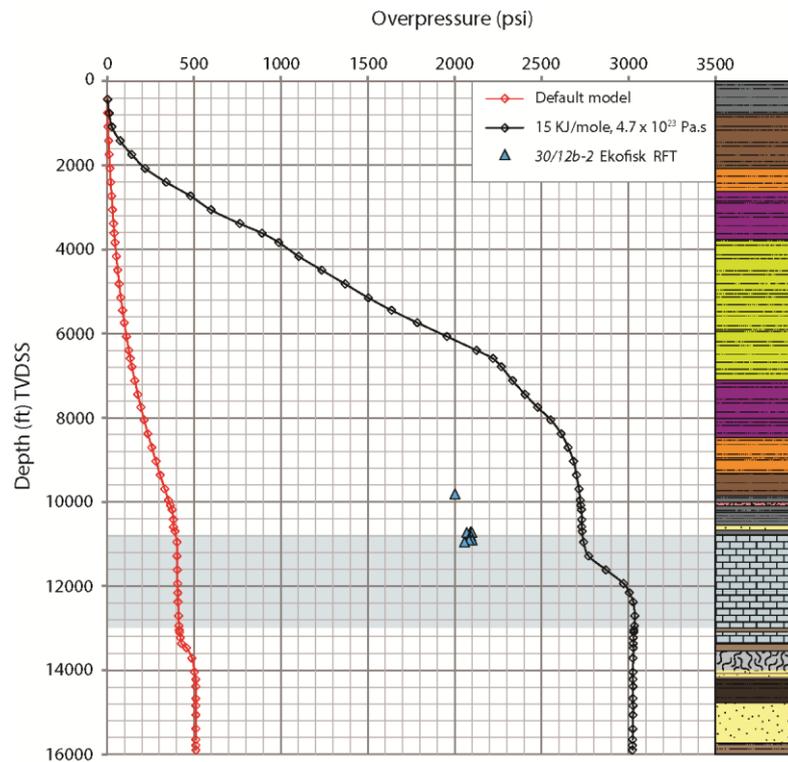
Figure 7.8 - Overpressure versus depth plot showing overpressure profiles generated during 1D modelling of UK 30/11b-3 using default lithologies (red) and the adapted lithologies described in *section 7.1.4* (black) to populate the model. Direct pore pressure measurements collected from the Ekofisk Formation in neighbouring well UK 30/12b-2 are shown for comparison purposes. Direct pore pressure measurements recorded within the Jurassic Fulmar Sandstone Member of the modelled well are not shown in the figure due to scale; however, overpressures of approximately 5915 psi (40.8 MPa) were calculated between depths of 14946 ft (4560 m) and 15077 ft (4600 m) TVDSS.

MPa) lower than those generated via the 1D model at the same depth. Similarly, modelled overpressures of 2732 psi (18.8 MPa) are generated in the Mey Sandstone Member situated at depths of 10600 ft (3230 m) TVDSS within UK 30/11b-3, whereas the Mey overpressure distribution maps presented in **Figures 5.3** suggest that overpressure magnitudes within the sandstone member should be approximately 530 psi (3.7 MPa) lower.

Modelled chalk porosity decreases from top to base down hole from 16 % at the top of the Chalk at 10800 ft (3290 m) TVDSS down to a minimum of 4 % around 13000 ft (3960 m) TVDSS. These porosities match reasonably well with the log-derived porosity profile through the Chalk, although modelled porosities are considered to be

191

too low towards the base of the Chalk where differences of up to 4% between the observed and modelled values occur. Higher observed porosities of around 8 % towards the base of the Chalk are likely to indicate higher magnitudes of overpressure encountered within this section of the well, which are not captured in the 1D model. Modelled overpressures can be seen to step up rather rapidly through the Chalk from 2742 psi (18.9 MPa) at a depth of 11000 ft (3353 m) TVDSS in the Ekofisk Formation, up to 3035 psi (20.9 MPa) at a depth of 12940 ft (3944 m) TVDSS towards the base of the Hod Formation. A small pressure transition zone of 257 psi (1.8 MPa) is encountered largely within the Tor Formation of the Chalk Group, over a vertical distance of approximately 1550 ft (473 m) between depths of 11286 ft (3440 m) TVDSS and 12383 ft (3774 m) TVDSS. Below this transition zone, overpressure magnitudes remain relatively constant through to the total drilled depth of the well.

In the model, overpressure magnitudes of 3027 psi (20.9 MPa) are generated within the Jurassic Fulmar Sandstone Formation. These magnitudes are approximately 2888 psi (19.9 MPa) lower than the overpressures calculated from direct RFT pore pressure measurements recorded within the Fulmar Sandstone Formation of UK 30/11b-3, where magnitudes of 5915 psi (40.8 MPa) are encountered. This discrepancy between modelled and observed magnitudes of overpressure is not surprising because the effects of hydrocarbon maturation are not included within the model, so overpressures due to hydrocarbon generation and oil to gas cracking have not been simulated

7.1.6. Discussion of results

The 1D modelling results presented in **Figures 7.7** and **7.8** can be seen to slightly overestimate magnitudes of overpressure towards the base of the Tertiary mudstone sequence and considerably underestimate magnitudes developed within the pre-Cretaceous strata, specifically the Fulmar Sandstone Formation (**Figure 7.3**).

One of the major limitations encountered during 1D modelling is the inability to simulate mass transfer and fluid flow in any direction other than vertically. Consequently, lateral fluid drainage encountered within the Palaeogene sandstone members cannot be simulated in the 1D model of UK 30/11b-3, which explains why modelled overpressures within the Mey Sandstone Member are so much greater than

those observed in surrounding wells. Since Palaeocene overpressure is overestimated by approximately 600 psi (4.1 MPa) within the model, it is assumed that at least this level of overpressure is bled off by lateral drainage through the Mey Sandstone Member. The higher than expected modelled porosities of around 46 % to 54 % found between depths of 3000 ft (915 m) to 6800 ft (2073 m) TVDSS (**Figure 7.7**) may represent an interval where excess overpressure has developed within the Tertiary mudstone sequence. Since this interval contains the highest modelled clay fraction of 80 %, higher magnitudes of generated overpressure are expected via disequilibrium compaction, considering the input porosity and permeability relationships used. In UK 30/11b-3, it is likely that the 600 psi (4.1 MPa) excess overpressure is sourced from this interval of the well above the Mey Sandstone Member.

The 1D model of UK 30/11b-3 only simulates overpressures generated by disequilibrium compaction. Although this mechanism of overpressure generation proves to be adequate for the post-Chalk strata, it is not sufficient through the pre-Cretaceous, where overpressure magnitudes are underestimated by approximately 2888 psi (19.9 MPa). As previously mentioned, this underestimate in the modelled overpressure is thought to be primarily due to the lack of simulation of hydrocarbon maturation in the Kimmeridge Clay Formation, meaning there is no overpressure development via gas generation or oil cracking to gas. It is also likely that some of the underestimate is associated with the lack of chemical compaction simulated within the pre-Cretaceous strata as well as the lack of overpressure generation by sediments below the well total depth, the latter being another limitation of 1D modelling. The overpressure generated through disequilibrium compaction alone is approximately half the calculated overpressure within the Fulmar Sandstone Formation. This difference is somewhat larger than was suggested by Cavanagh *et al.* (1996) and Swarbrick *et al.* (2005), whose modelling work found disequilibrium compaction to account for nearly 75 % and 70 % of Late Jurassic overpressures, respectively. The exact magnitude of overpressure generated via hydrocarbon maturation within UK 30/11b-3 remains unknown, as do the effects of chemical compaction within the pre-Cretaceous section.

The parameters selected to model the chalk lithology were deemed to be satisfactory, producing reasonable matches to the present day chalk porosities and permeabilities. Towards the base of the Chalk Group, the deficit in modelled porosity compared to log-derived porosity may indicate that the true overpressure in this part of

the Chalk is greater than that modelled. The small transition zone of only 257 psi (1.8 MPa) developed within the chalk separates the highly overpressured pre-Cretaceous from the overlying and lower overpressured Tertiary and Quaternary strata. When the 1D model was run using other values for chemical compaction parameters, a larger transition zone through the entire Chalk sequence could be developed, resulting in higher overpressure magnitudes of up to 5020 psi (34.6 MPa) simulated within the Jurassic Fulmar section. However the simulated values of chalk porosity and permeability were compromised, as they became exceptionally small and unrealistic. Overpressures simulated within the Upper Chalk Ekofisk Formation are approximately 710 psi (4.9 MPa) greater than those which were mapped by Dennis *et al*. (2005, Fig. 3), perhaps indicating that some of this excess overpressure is fed into the laterally draining Palaeogene system above.

Overall the 1D model shows that disequilibrium compaction, as a sole mechanism of overpressure generation, is sufficient to generate the magnitudes of overpressure observed within the Tertiary and Quaternary strata, plus up to 600 psi (4.1 MPa) excess overpressure generated within the Tertiary and Quaternary mudstones, above the Mey Sandstone Member. It is assumed that such excess Tertiary pressures source the laterally draining Palaeogene sandstone system, but this cannot be simulated within a 1D model. The massive underestimation of overpressure generated within the pre-Cretaceous and Chalk sections shows that other overpressure generating mechanisms are in operation within this section of the well, such as gas generation and chemical compaction or unloading mechanisms, as was previously suggested for the Central North Sea region (Darby *et al*., 1998; Swarbrick *et al*., 2000; Daniel, 2001; Swarbrick *et al*., 2005). The 1D model indicates that up to 49 % of the measured overpressure within the pre-Cretaceous section is unaccounted for. Since the effects of hydrocarbon maturation were not simulated within the model, the precise magnitudes of overpressure generated via gas generation remain unknown. The Upper Chalk section is thought to be satisfactorily modelled owing to the realistic values of porosity and permeability simulated; however, as with the Tertiary section, overpressure magnitudes are thought to be overestimated. An excess of approximately 710 psi (4.9 MPa) exists in comparison to the measured overpressures of Dennis *et al*. (2005) and consequently it is assumed that this magnitude of overpressure may be leaking off into the laterally draining Mey Sandstone Member above. If this is the case then it can be seen that a

larger magnitude of fluid is sourced into the Palaeogene sandstone system from below than above. Towards the base of the Chalk Group, modelled porosities are lower than log-derived porosities, suggesting higher levels of overpressure may actually exist in this part of the Chalk than those modelled. Such discrepancies in the Chalk Group, i.e. lower and higher overpressure magnitudes in the upper and lower parts, respectively, indicate that a larger transition zone across the group may actually occur than is produced by the model.

7.2. 3D basin modelling

Following on from 1D modelling, attempts were made at producing a simple 3D model of the Central North Sea study region using the PetroMod basin modelling software at the Exploration and New Business department of Maersk Oil UK, Aberdeen. The 3D modelling work was carried out towards the latter stages of the project and it is unfortunate that a large amount of calibration was still needed to better refine the model. Despite this, some useful conclusions can still be drawn from the results obtained. The main focus of modelling was on the laterally draining Palaeogene sandstone units and the relative amounts of fluids entering the system, as well as the source of such fluids.

The geometric framework of the model consisted of eight regional seismic horizons, including the seabed, top Nordland Group, top Hordaland Group, top Balder Formation representing the top Palaeocene, top Chalk Group, top Lower Cretaceous, top Jurassic and base Kimmeridge Clay Formation. This basic framework is shown in **Figure 7.9** along with the absolute ages (in Ma) of each interval. Coverage of the 3D model is shown in **Figure 7.1**, encapsulating a large proportion of the north-western study region. Although the lateral distribution of each Palaeocene sandstone member across the study region was known from the previously generated distribution maps presented in **Chapter 2**, the regional tops and bottoms of each Palaeocene fan sandstone member were not. Consequently, assigning lithological facies to the Palaeocene section of the model was complicated. Well analysis performed across the basin led to the development of a simple framework whereby the Palaeocene section was divided into four layers. The Mey and Maureen sands, assumed to be hydraulically connected were modelled as a single combined unit. The first and third layers of the Palaeocene model each comprised 40 % of the entire Palaeocene thickness and were selected to represent

195

	Name	Color	Deposition Age from [Ma]	Deposition Age to [Ma]	Erosion Age from [Ma]	Erosion Age to [Ma]	Max. Time Step Duration [Ma]	Facies 1
7	Nordland Gp		12.00	0.00	0.00	0.00	10.00	FACIES
6	Hordland Gp		54.00	17.00	0.00	0.00	10.00	FACIES
5	Palaeocene		62.00	54.00	0.00	0.00	10.00	FACIES
4	Chalk Gp		98.90	62.00	0.00	0.00	10.00	FACIES
3	Lower Cretaceous		136.50	98.90	0.00	0.00	10.00	FACIES
2	Jurassic		151.00	137.20	0.00	0.00	10.00	FACIES
1	07SBLF_BKimm		154.10	151.00	0.00	0.00	10.00	FACIES

Figure 7.9 - Table showing the input geometric framework of the 3D model comprising seven seismic horizons along with absolute ages.

the Forties Sandstone Member and combined Mey/Maureen sandstone members, respectively (**Figure 7.10**). The second and fourth layers each comprised 10 % of the entire Palaeocene thickness, and formed intervening layers of shale between the adjacent sandstone members and underlying Chalk Formation. Since the model did not cover the far northern area of the basin where the Palaeocene sandstone members combine, a small area of sandstone was included in the second layer, providing a flow pathway for fluids (**Figure 7.10** and **Figure 7.11**). Post-Balder sandstone members such as the Tay and Grid sandstone members were not included within the model.

The adapted chalk porosity-depth relationship of Mallon and Swarbrick (2002) and the porosity-permeability relationship of Mallon (2000) were used to populate the model (see *section 7.1.4.2*). Unlike the 1D modelling, chemical compaction was not simulated within the chalk lithology. The porosity-effective stress and porosity-permeability relationships of Yang and Aplin (2000, 2004) were used to simulate all mudrock lithologies. Since regional variations in the clay fraction, both vertically and laterally across the basin, remained unknown, it was assumed that all mudrocks were of 60 % clay fraction. This value for the clay fraction within the Jurassic strata is almost certainly too high, but was adopted within the early stages of 3D modelling as an initial value, and was never changed because it proved impossible to model sufficient overpressure in the Jurassic. Petromod default lithological parameters were used to simulate all sandstones contained within the model. The effects of hydrocarbon maturation were not simulated within the model and consequently all overpressures generated in the 3D model result from disequilibrium compaction only.
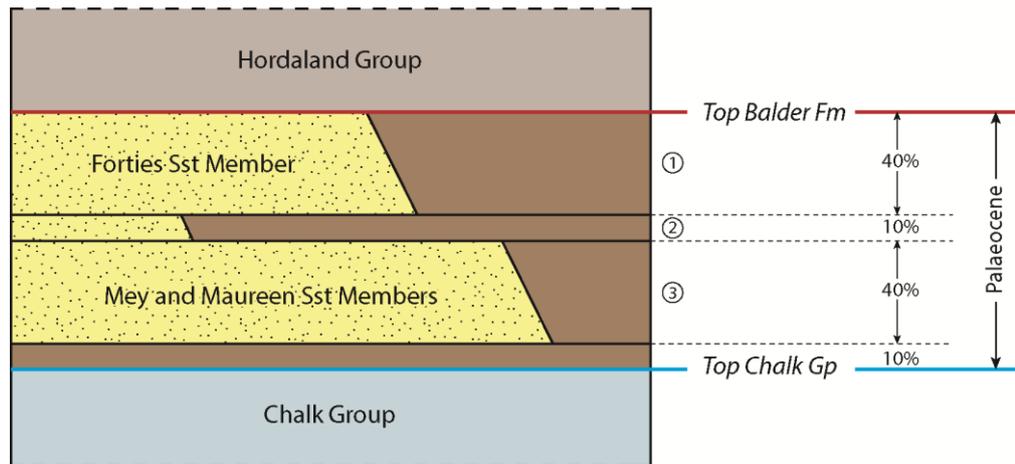
Figure 7.10 - The Palaeocene section of the well was divided into four separate layers with relative thickness values of 40%, 10%, 40% and 10%, in order to simulate the thickness and vertical distribution of the Forties and combined Mey/Maureen sandstone members. The fourth layer consisted entirely of mudrock. The lateral distribution of each sandstone layer across the modelled area is shown in **Figure 7.11**.

The model was run using a horizontal cell size of 4 km x 4 km and a maximum cell thickness of 400 m. Such values produced a coarse grid with fairly low resolution, as can be seen in **Figure 7.11**. These values were selected to be used during the early stages of 3D modelling in order to increase the speed of simulation runs.

7.2.1. 3D modelling result

The results of the 3D basin modelling within the Palaeogene are presented in **Table 7.2** and **Figure 7.12**. Comparisons between modelled overpressures and those calculated from direct measurements, or inferred from the overpressure distribution maps presented in **Chapter 5**, are shown in **Table 7.2** for selected wells.

For the majority of the basin, it can be seen that modelled overpressures largely underestimate those which are observed within the Palaeogene sandstone members. Towards the south-eastern areas of the Palaeogene fan sands, maximum overpressures in excess of 1100 psi (7.6 MPa) and 2500 psi (17.2 MPa) were calculated within the Forties and Mey/Maureen sandstone members, respectively. Those values are much greater than the maximum overpressures of 653 psi (4.5 MPa) and 725 psi (5.0 MPa) simulated by the 3D model. Specific values in wells UK 30/13-5 and NO 1/6-4, show
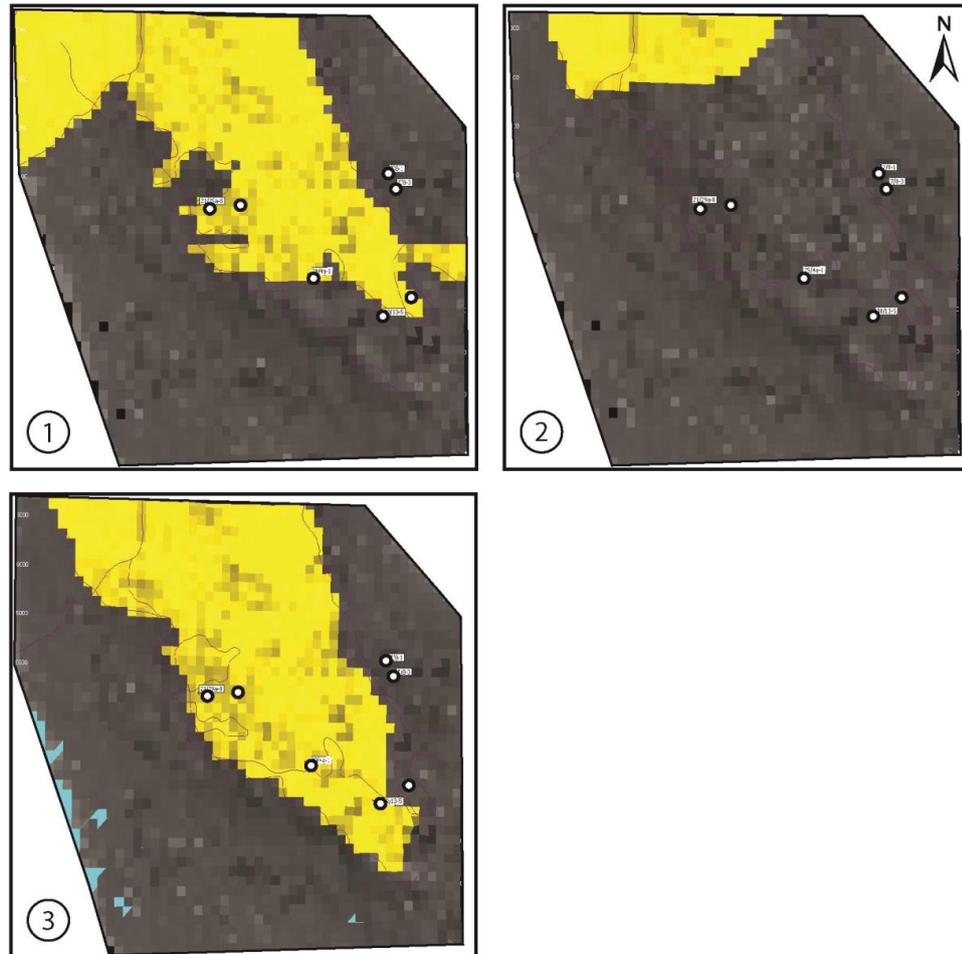
Figure 7.11 - Sandstone distributions used for each of the three Palaeocene layers, as shown in **Figure 7.10**. The resolution of each layer is low owing to the run parameters used, with horizontal cell dimensions of 4 km x 4 km and maximum cell thickness of 400 m.

overpressure magnitudes within the Mey and Forties sandstones members to be similarly underestimated by approximately 1800 psi (12.4 MPa) and 600 psi (4.1 MPa), respectively. These large underestimates of overpressure within the Palaeocene strata may be attributed to the limitations of the 3D model (see *section 7.2.2*).

Assuming that overpressure generation via disequilibrium compaction is effectively simulated by the 3D model, the lower magnitudes of overpressure modelled within the Palaeogene, in comparison to those generated within the 1D model (*section 7.1.5*), result from the simulated lateral drainage of fluids along the Palaeogene sandstones members. The large underestimate of overpressure within the Tertiary and Quaternary mudstones of the 3D model, appear to indicate that insufficient overpressure

198
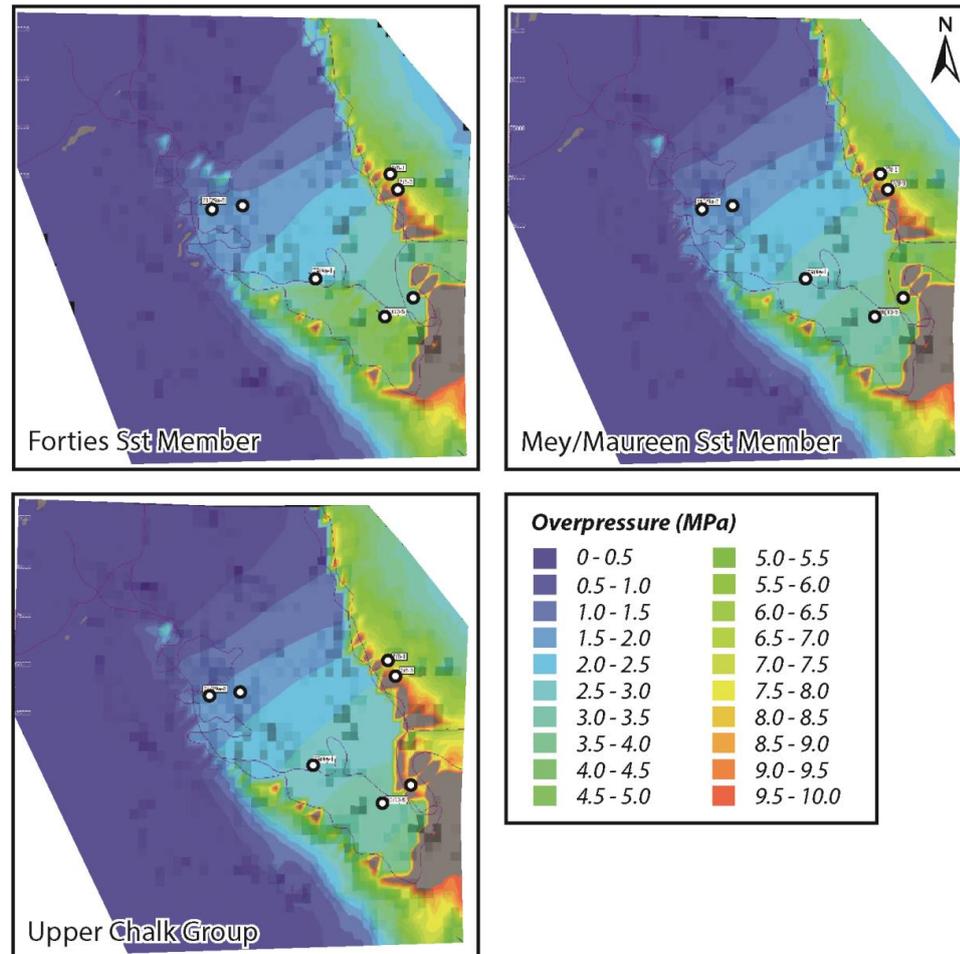
Figure 7.12 - Results of 3D modelling in map view for three major horizons: the Forties Sandstone Member, the Mey/Maureen Sandstone Member and the Upper Chalk Group.

is generated within the Tertiary and Quaternary mudstone sequence by disequilibrium compaction, to source the rate of lateral drainage within the Palaeogene system as well as generate the observed present-day magnitudes of overpressure.

The 3D model captures lateral drainage of fluids from the SE towards the NW within the Forties and combined Mey/Maureen sandstone members, as well as within the underlying Chalk Group (**Figure 7.12**). Although this direction of drainage within the Forties and combined Mey/Maureen sandstone members is largely in agreement with the overpressure distribution maps presented in **Chapter 5** (**Figures 5.1, 5.3** and **5.4**), it can be seen that drainage towards the western margin of the basin has not been simulated by the model. This is likely to explain why the magnitudes of overpressure

Well Name	Horizon	Modelled overpressure [psi]	Observed or inferred overpressure [psi]
UK 21/29a-8	Forties Sandstone	226	46
UK 21/29a-8	Lista Formation	223	-
UK 21/29a-8	Chalk Group	232	-
UK 22/21-3	Forties Sandstone	239	61
UK 22/21-3	Mey Sandstone	255	60
UK 22/21-3	Chalk Group	267	-
UK 29/4a-1	Forties Sandstone	328	327
UK 29/4a-1	Maureen Sandstone	387	1919
UK 29/4a-1	Chalk Group	395	725
UK 30/13-5	Sele Formation	692	-
UK 30/13-5	Mey Sandstone	476	*2300-2400*
UK 30/13-5	Chalk Group	480	*2465*
NO 1/6-4	Forties Sandstone	500	*> 1100*
NO 1/6-4	Lista Formation	709	-
NO 1/6-4	Chalk Group	1197	1813
NO 7/8-1	Sele Formation	1015	2170
NO 7/8-1	Lista Formation	1067	2031
NO 7/8-1	Chalk Group	1080	-
NO 7/8-3	Sele Formation	1155	-
NO 7/8-3	Lista Formation	1115	-
NO 7/8-3	Chalk Group	1232	-

Table 7.2 - Magnitudes of Palaeogene and Chalk overpressure generated via the 3D model in selected wells across the basin. For several of these wells, calculated values of overpressure derived from direct pore pressure measurements or inferred from the pressure distribution maps presented in **Chapter 5**, are shown for comparison with the modelled results. Chalk overpressures are inferred from the overpressure distribution map of Dennis *et al* (2005). Well locations are shown in **Figure 7.1**.

modelled within the Palaeogene sandstone members towards the western basin margin are overestimated. In UK wells 21/29a-8 and 22/21-3 overpressure magnitudes within the Forties and Mey/Maureen sandstone members are overestimated by an average of 185 psi (1.3 MPa). In UK 29/04a-1 the magnitude of overpressure within the Maureen Sandstone Member is underestimated by approximately 1530 psi (10.6 MPa), although overpressure within the Forties Sandstone Member is correctly matched at around 330 psi (2.3 MPa). This well matched overpressure within the Forties sandstone of UK 29/04a-1 is thought to be coincidental since, in this area of the basin, westwards

drainage has only been mapped within the Forties Sandstone Member and not within the underlying Mey and Maureen sands.

Modelled Chalk overpressures consistently underestimate those inferred from the overpressure map of Dennis *et al.* (2005) shown in **Figure 5.23**. Once again, this most likely relates to the limitations of the 3D model and in particular the fact that chemical compaction was not simulated within the chalk lithology. In UK well 29/04a-1 and Norwegian well 1/6-4, modelled Chalk overpressures are underestimated by 330 psi (2.3 MPa) and 616 psi (4.3 MPa) respectively. In UK well 30/15-5, this underestimate is exceptionally large being 1985 psi (13.7 MPa). It is suspected that the large underestimate in UK 30/13-5 results from vertical fluid drainage out from the Chalk into the immediately overlying Mey/Maureen Sandstone Member. In contrast, modelled chalk overpressures are thought to be closer to those observed in NO well 1/6-4, since vertical fluid drainage is not as easily facilitated out from the Chalk in an area of the basin where there are no overlying Mey/Maureen sands. Although the Forties Sandstone Member is present in and around NO 1/6-4, it is separated from the overlying Chalk by a thick section of Lista Formation mud. Overpressures modelled within the Chalk Group are consistently higher than those modelled within the directly overlying Palaeogene strata as might be expected for the basin.

The pattern of lateral drainage within the chalk is reflective of the overlying Palaeogene sands. This pattern was noted by Dennis *et al.* (2005) who attributed it to vertical bleed-off of fluids from the chalk into the overlying Palaeogene laterally draining sands. Water vectors generated by the 3D model within the Chalk, support this idea of Dennis *et al.* (2005) showing fluid flow to be everywhere vertically upwards out of the Chalk into the overlying Palaeogene strata, with no evidence of lateral flow within the Chalk unit itself. Realistically the vertical drainage through the Upper Chalk Group may not be as excessive as the model appears to show, taking into consideration the low resolution of the model and large cell thickness of 400m.

The highest magnitudes of overpressure are simulated towards the south and south-eastern areas of the basin where the Palaeogene sandstone members are absent, which is in agreement with the overpressure distribution maps. However, even within the mudstone formations, overpressure magnitudes are largely underestimated, e.g. within Norwegian well 7/8-1 the Sele and Lista formation overpressures are

underestimated by 1155 psi (8.0 MPa) and 964 psi (6.7 MPa), respectively. Where the overlying Mey/Maureen and Forties sandstone members are present above the Chalk and Lista Formations, it can be seen that the overpressures are lower than in those areas where no overlying Mey/Maureen and Forties sands are present (**Figure 7.12**). Similarly, where the Sele Formation muds overly the Mey/Maureen sandstone member, overpressures appear lower than in those areas of the Sele Formation where there are no underlying sands. Such patterns imply vertical drainage of fluids out from the underlying Chalk and Lista Formation muds vertically upwards, and indeed vertical drainage of fluids downwards in the case of the Sele Formation into the underlying Mey/Maureen sandstone member. UK well 30/13-5, recorded within this area of the basin beyond the extent of the Forties Sandstone Member, shows that overpressures within the Sele Formation exceed those within the underlying Mey/Maureen Sandstone Member by approximately 216 psi (1.5 MPa), indicating that fluids may indeed drain vertically downwards into the underlying Mey/Maureen laterally draining system.

Vertically, the largest magnitudes of overpressure, in excess of 1450 psi (10 MPa), are generated below the Chalk Group (**Figure 7.13**). Water vectors generated by the model indicate greater flow upwards into the Palaeogene sandstones than downwards from the overlying Tertiary and Quaternary mudstones.

7.2.2. Limitations

There are several limitations to the 3D model, which are ultimately responsible for the low magnitudes of overpressure generated. The lack of hydrocarbon maturation simulated within the Kimmeridge Clay Formation and the lack of chemical compaction simulated within the Chalk and pre-Cretaceous sediment are thought to be the most significant limitations to the 3D model, since both are large contributors to overpressure generation within the Central North Sea.

The geometry used to represent the Palaeocene section of the 3D model does not realistically model the variations in thickness and lithology within individual Palaeogene sandstone members. A significant limitation of the 3D model is that the thickness and quantity of sandstone within the Palaeocene cannot be accurately modelled. Considering that the sandstone thickness and quality decreases with
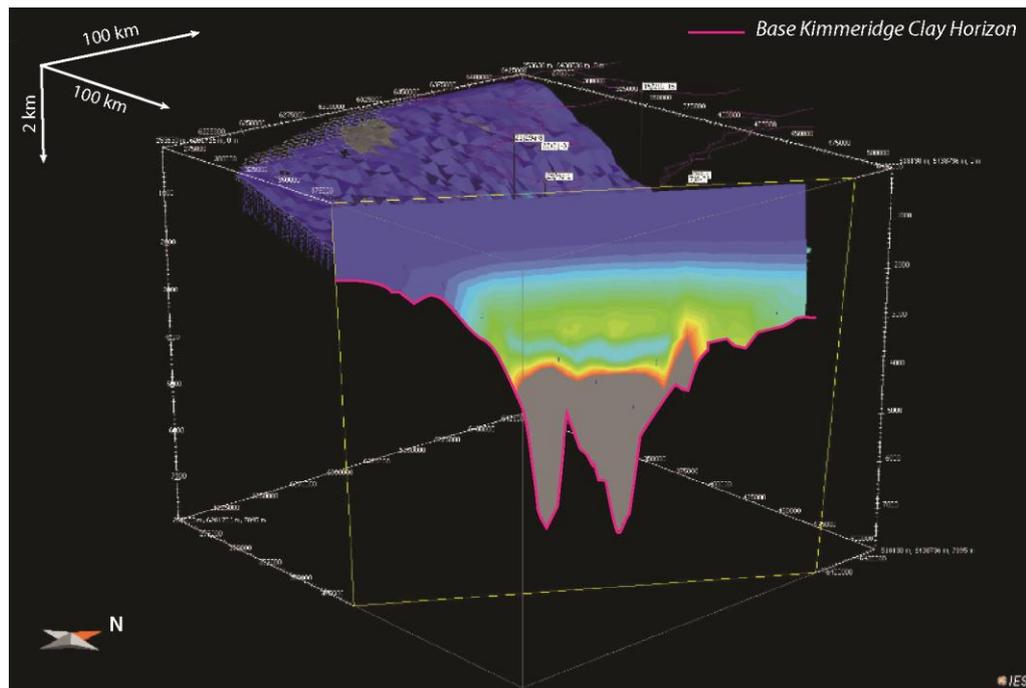
Figure 7.13 - Cross-section through the 3D model, showing the large pressure decrease towards the Palaeogene sandstone members. Below these sands, overpressure magnitudes can be seen to rapidly increase downwards into the Post-Cretaceous section where magnitudes of overpressure exceed 1450 psi (10MPa). See **Figure 7.12** for overpressure colour key and position of cross-section.

increasing distance from the sediment source, it can be seen that the 3D model exaggerates the degree and thickness of sandstone in these distal areas, which will consequently increase the levels of fluids flowing through the Palaeogene system. A second limitation relating to the geometry of the model is the lack of overpressure generation by sediments below the base Kimmeridge Clay Formation, which is the selected base of the 3D model.

Another limitation to the model is that a consistent clay fraction of 60 % was used to simulate all of the mudstones within the model comprising the Tertiary and Quaternary sequence as well as the pre-Cretaceous sediments. It was previously shown during 1D modelling that the porosity and permeability relationships of mudstones vary according to clay fraction and consequently, this could have a profound effect on the magnitudes of overpressure generated by disequilibrium compaction within the 3D model, particularly within the Tertiary strata where clay fractions within UK 30/11b-3 were seen to range between 40-80 %. Accurately assessing the clay fraction distribution

203

across a 3D volume of the Tertiary and Quaternary strata however, would pose several difficulties. The clay fraction of 60 % is considered to be too high to realistically represent the pre-Cretaceous mudstones. Swarbrick *et al.* (2005) used a clay fraction of 40 % to simulate the pre-Cretaceous mudstones, and this value was previously used in the 1D modelling of UK 30/11b-3 (*section 7.1*). The effects of modelling pre-Cretaceous mudstones using a higher clay content are thought to be minimal, since the parameters selected for higher clay contents mean that they should produce higher magnitudes of overpressure, within the already well underestimated Pre-Cretaceous strata.

7.2.3. Discussion of results

The 3D model provides a simple first attempt at assessing the predominant source of fluids that feed the laterally draining Palaeocene sandstone members. The results of the model show that disequilibrium compaction is insufficient at generating the observed magnitudes of overpressure within the Palaeogene sequence, when lateral drainage within the Palaeocene sandstones is simulated. This contrasts to the results of 1D modelling, whereby disequilibrium compaction produced approximately 600 psi (4.1 MPa) excess overpressure within the Mey Sandstone Member, which was thought to be related to the lack of lateral drainage simulated within a 1D model. Considering that across most of its volume, the 3D model underestimates Palaeocene overpressures by 600 psi (4.1 MPa) to 1800 psi (12.4 MPa), it can be crudely assumed that between 1200 psi (8.3 MPa) and 2400 psi (16.6 MPa) overpressure, at least, is lost into the laterally draining system.

Although the magnitudes of overpressure generated for the entire 3D model are grossly underestimated, the model can still provide indications as to where the majority of fluids entering into the Palaeocene system are coming from. Water vectors generated by the model indicate that most of the water entering into the Palaeocene system is sourced from the underlying Chalk and pre-Cretaceous sediments below, as opposed to the overlying Tertiary mudstones. In addition, the water vectors show that fluid flow out from the chalk is everywhere vertically upwards, and no-where can lateral drainage within the chalk itself be seen.

Palaeocene overpressures were overestimated towards the western margin of the basin, where it was apparent that lateral drainage towards the Western Shelf had not been simulated. Had such drainage been simulated, it is likely that overpressures would have been underestimated as is the case for the remainder of the fan sands.

The maps generated by the 3D model presented in **Figure 7.12**, show the Chalk Group and lower permeability muds, belonging to the Sele and Lista formations, to be better drained and of lower overpressure, where there are overlying and underlying Palaeocene sandstone members. This is in agreement with what was similarly observed and discussed in **Chapter 5** (*section 5.3.1*) whereby Palaeogene sandstone members are found to be of greatest overpressure where there are no underlying or overlying sandstones. Overpressures within the lower permeability muds and chalk exceed 1450 psi (10 MPa) in areas where there are no surrounding Palaeocene sands.

Magnitudes of overpressure within the 3D model were massively underestimated, reflecting the limitations of the 3D model which include; the unrealistic geometric framework, use of a single clay content lithology to populate the 'Tertiary and Quaternary' and Pre-Cretaceous mudstone sequences, lack of overpressure generation by sediments below the base of the 3D model, lack of hydrocarbon generation within the Kimmeridge Clay and lack of chemical compaction simulated within the Chalk and Pre-Cretaceous strata. The latter two limitations are thought to cause the largest decrease in the total overpressure generated. Had more overpressure been generated within the deeper regions of the 3D model, vertically upwards fluid flow may have better sourced drainage within the Palaeocene strata and overpressure generated may have been more reflective of the present day distributions. Much further calibration was required by the 3D model in order to receive more quantitative results, regarding fluid flow and source of the fluids.

205

8 | Conclusions and future work

"Though the road's been rocky it sure feels good to me" Bob Marley (1945-1981) [Jamaican singer-songwriter and musician]

8. Conclusions and future work

In this chapter the primary findings of the thesis are brought together and the main conclusions drawn from the research are discussed with reference to the objectives of the thesis which were laid out in **Chapter 1** (*section 1.3*). Suggestions for future research and areas for improvement are also made towards the end of this chapter.

8.1. Pathways for lateral drainage and hydrocarbon migration within the Palaeogene strata

The present-day overpressure distributions within the Palaeogene strata of the Central North Sea Basin have been examined on a regional scale. The lateral overpressure distribution maps created for each of the Palaeocene and Eocene reservoir sandstone members are presented in **Chapter 5**. From these maps, it was found that each of the reservoir sandstone members, with the exception of the Grid Sandstone Member, was laterally draining, providing lateral migration pathways for formation waters and hydrocarbons alike.

For the Maureen, Mey and Forties sandstone members the predominant direction of fluid flow is from SE to the NW, as had been previously documented by Lindberg *et al*. (1980), Cayley (1987), Holm (1998) and O'Connor *et al.* (2008). Fluids are likely to escape from the Palaeocene basinal sandstone system through shelfal sands belonging to the Dornoch and Mousa formations, in the area of the Moray Firth, around UK quadrants 14 and the western part of UK quadrant 15.

New areas of drainage were identified along the western margin of the basin, with lateral drainage of fluids to the west observed in the Mey and Forties sandstone members, in and around UK quadrants 21, 28 and 29. Such fluid flow reflects the westerly derived fan systems which were active during deposition of the Mey and Forties sandstone members (Reynolds, 1994; Hempton *et al.*, 2005; Kilhams *et al.*, 2012). Westerly drainage appears to be best established within the Forties Sandstone Member, possibly enhanced by vertical fluid flow between the Forties and overlying Cromarty and Tay sandstone members. Fluid drainage within the Cromarty and Tay

sandstone members is laterally westwards and south-westwards, where fluids are likely to drain into the adjacent shelfal sands belonging to the Dornoch and Mousa formations, up slope in UK quadrants 20 and 27, outside the study region.

Pressures within the Grid Sandstone Member are predominantly near-hydrostatic, with an area of higher overpressure, up to 50 psi (0.35 MPa) located around UK block 16/26, in the area of the Alba and Chestnut fields. Patterns of lateral drainage could not be established within the Grid Sandstone Member, and it is likely that the area of slightly higher Grid sandstone overpressure is associated with vertical drainage.

8.2. Pathways for vertical drainage and hydrocarbon migration within the Palaeogene strata

Several areas of vertical drainage are recognised between the Palaeogene sandstone members. In the NW of the study region, around UK quadrants 15, 16, 21 and the northern area of UK quadrant 22, overpressures within each Palaeogene sandstone member are for the most part near-hydrostatic, suggesting that the sandstones are in good hydraulic communication with the seafloor. Small vertical differences in overpressure between sands in this area suggest that the sands are hydraulically well-connected, which is consistent with the thickening of the sandstone members towards the NW.

Vertical overpressure differences calculated in **Chapter 5** indicate that the Mey and Maureen sandstone members are in hydraulic connection across most of their distributions, including the SE of the basin, where the sandstones thin and decrease in quality (Hempton *et al.*, 2005). Consequently, it is assumed that the Maureen and Mey sandstone members act as a single hydraulic unit on a regional scale, which is more convenient for the purposes of basin modelling.

Towards the SE of the area of sandstone distribution, where both the Forties and underlying Mey sandstone members are present, vertical connectivity is best established surrounding salt diapir structures, such as seen around the Machar (UK 23/26) and Merganser (UK 22/30) fields. In UK quadrant 29, a large pressure transition zone exists

between the Forties and Mey/Maureen sands, indicating that there is no vertical fluid migration between the sandstones in this area.

Vertical drainage is widespread between the Forties and overlying Cromarty sandstone members since these sands are commonly in direct contact with one another or, otherwise, are separated by a relatively thin interval of Sele Formation mudrock, on average 50 ft (15 m) TVD thick. Distortion of the Forties overpressure contours around the southern part of UK quadrant 22, corresponding crudely with the distribution of overlying Cromarty sands, further supports the inference of vertical drainage between the Forties and Cromarty sandstone members.

Areas of direct contact between the Tay and underlying Cromarty or Forties sandstone members are rare. On average, the intervening mudrocks are 100 ft (30 m) TVD thick, and yet the sandstone members still appear to be well connected hydraulically. Vertical connectivity between the Tay and underlying sands is, again, best established around salt diapir structures, where it is thought fluid flow is facilitated via the associated fault and fracture systems. Salt diapir structures are thought to facilitate vertical fluid drainage between sandstone members across the entire basin, with hydrocarbon columns commonly seen to extend across multiple reservoir units around such structures, as can be seen at the Gannet F, Gannet D, Banff, Machar and Merganser fields (Banner *et al*., 1992; Kloosterman *et al*., 2003; Evans *et al*., 1999).

Pressure data cannot be used directly to indicate vertical fluid flow along injected sands, although it is likely that injectites do provide conduits for fluid flow, especially around the southern parts of UK quadrants 16 and 21 and the northern parts of UK quadrants 28 and 29, where sandstone remobilisation has been well documented (Hurst *et al*., 2005; Huuse *et al*., 2005; Murphy and Wood, 2011). Where the Grid Sandstone Member is present, it can be seen that the member is largely in hydraulic connectivity with the underlying Forties or Mey sandstone members, despite being separated by more than 850 ft (260 m) TVD of Horda and Balder formation mudstones. Considering that the Caran Sandstone Unit may be of a completely injected origin (Huuse *et al*., 2003; Murphy and Wood, 2011), it is probable that fluid flow is facilitated between the Eocene and Palaeocene sandstones via remobilised sands in this part of the basin.

Along the western graben margin, vertical fluid flow may be facilitated by: areas of direct contact between sands, which may be enhanced by areas of compensational stacking between sands such as seen at the Bittern Field; salt diapir structures; remobilised sands; and non-sealing graben-bounding faults. Graben-bounding faults facilitate fluid flow at the Catcher Field in UK block 28/09, where hydrocarbons are shared between the Tay and Cromarty reservoir sands. Vertical migration of hydrocarbons along deep-rooted faults in this area of the basin may explain why oils of better than expected quality and lower biodegradation were found in Catcher, owing to the shorter migration distance and potentially late placement. Future exploration may prove to be successful further southwards along the western graben margin, extending into UK blocks 28/14 and 28/15, where it is likely more Tay and Cromarty reservoir sands are present, deposited against graben-bounding faults.

8.3. Areas of the basin with the potential for hydrodynamic trapping

Greater tilting of hydrocarbon-water contacts occurs where overpressure gradients are larger, for fixed densities of hydrocarbon and water within the reservoir (see *section 5.3.2*). Areas with the greatest potential for hydrodynamic trapping are not directly identifiable without detailed maps of reservoir structure. Consequently, areas of the basin where the lateral overpressure gradients are highest were identified, since it is in these areas that the effects on estimating total reserves in place are likely to be greatest.

UK quadrants 29 and 30 are the areas within the Mey and Maureen sandstone members where hydrodynamic tilting is likely to be greatest, with estimated tilts of 9° and 14° on the assumed oil-water contacts. For the Forties Sandstone Member, UK quadrant 23 has the greatest magnitudes of hydrodynamic tilting, with tilts of 5° calculated for oil-water contacts. These areas would provide good candidates for hydrodynamic trapping. In some areas of the basin, the predicted level of tilting may act to discourage exploration, since the reservoir structural dips are not high enough to contain the hydrocarbons. Such an area is observed within UK block 23/27, where an oil-water contact tilt of 23° was calculated for the Mey Sandstone Member.

Identification of hydrodynamic traps needs to be done on a local scale rather than on a regional scale because of the need for structural closure given the

hydrodynamic tilt. In the Cromarty and Tay sandstone members, where small lateral overpressure gradients are observed, tilts on oil-water contacts may still prove to be significant where the quality of the oil is lower. Oils ranging between 15° API and 25° API could generate hydrocarbon-water tilts of around 0.5° and 1.5° for the observed lateral overpressure gradients in these sandstone members, which may increase levels of estimated oil significantly within subtle traps.

8.4. Relative contributions from Tertiary and Mesozoic strata into the presently draining Palaeocene sands.

At the present day, larger contributions of fluid enter the laterally draining Palaeogene sands from the underlying Mesozoic strata than from the overlying Tertiary strata. This has been determined largely from comparison of overpressure distributions within individual sandstone members, in addition to simple analysis via basin modelling.

Using rare pressure measurements recorded within the Nordland Group and Lark Formation mudrocks, it was shown in **Chapter 6** that top overpressure is likely to develop at relatively shallow depths of around 1000 m across the basin, in agreement with the depth suggested by Leonard (1993) and O'Connor and Swarbrick (2008).Other pressure measurements discussed in **Chapter 6** further show that overpressures calculated within the Tertiary mudrocks overlying and adjacent to the Palaeogene sandstone members are generally greater than those recorded within the fan sands themselves. The largest magnitudes of mudrock overpressure were recorded towards the SE of the study region, where the sandstone members thin distally or are completely absent. Smaller overpressure magnitudes are recorded within intraformational mudrocks in the NE area of the study region, where the sandstone members thicken. Such data indicate that the Tertiary mudrocks are likely to source some of the fluids entering into the Palaeogene sandstone system, although estimates of the actual fluid quantities cannot be made reliably without accurate information on mudrock permeabilities.

It was noted in **Chapter 5** that overpressure decreases vertically between Palaeogene sandstone members, with the greatest magnitudes of overpressure encountered within the deepest Maureen Sandstone Member and the lowest magnitudes within the Eocene Tay and Grid sandstone members. It is suggested that overpressure magnitudes within the Forties Sandstone Member are smaller than those in the Maureen

and Mey sands, since these underlying sands effectively 'buffer' the Forties from vertical fluid input from the underlying Chalk below. This explains why, within each Palaeocene sandstone member, the greatest magnitudes of overpressure are encountered where no underlying Palaeogene sandstone members are present: e.g., magnitudes in excess of 1100 psi (7.58 MPa) are encountered within the Forties Sandstone Member of Norwegian quadrants 1 and 2, and magnitudes in excess of 2500 psi (17.2 MPa) are encountered within the Mey Sandstone Member of UK block 30/13, suggesting larger fluid input from the underlying Mesozoic sediments in these areas.

Similar results were observed in the 3D basin modelling of **Chapter 7**, which showed that the Chalk Group and lower permeability muds belonging to the Sele and Lista formations are better drained (lower overpressure) where there are overlying or underlying Palaeocene sandstone members, indicating drainage of the surrounding sediments into the Palaeogene system. Water flow vectors generated by the 3D modelling further indicate that most of the water entering into the Palaeocene system is sourced from the underlying Chalk and pre-Cretaceous sediments below, as opposed to the overlying Tertiary mudstones.

8.5. Suggested future work

The largest area in need of future work concerns the 3D regional basin modelling. Several improvements could have been made to the 3D basin model presented in **Chapter 7**, most notably by including hydrocarbon maturation within the Kimmeridge Clay Formation and simulating the effects of chemical compaction within the Chalk and pre-Cretaceous sediments. Including such processes in the model would have greatly increased the magnitudes of overpressure generated and enabled better calibration of the modelled data to the measured values of pressure recorded within individual wells.

A better understanding of clay fraction distribution, both laterally and vertically, through the Tertiary and Quaternary claystone sequence would have improved the lithological parameters of the 3D basin model by more realistically simulating the magnitudes of overpressure generated in this sequence.

Such improvements in the 3D basin model would most certainly enable better quantification of fluids entering into and exiting out of the Palaeogene system, as well

as providing an understanding of where fluids are sourced within the basin, both at the present day and throughout the basin's history.

Other areas identified for future work concern the limitations of regional studies. When working on a regional scale, detail is often compromised. Consequently, there is always room for improvement to better the detail of regional research. For example, newly obtained Palaeogene pressure data could be continually added to the pressure database to improve the contouring of the overpressure distribution maps. Of greatest interest would be pressure data collected from within the Grid Sandstone Member, where no pattern of later drainage could be established and it appears as if water may be flowing vertically downwards out from the Brodie Sandstone Unit, around the Alba and Chestnut fields.

Detailed seismic mapping of the top Palaeocene and Eocene sandstone members would enable better assessment of the possible locations for hydrodynamic traps, since calculated tilts of hydrocarbon-water contacts could be compared against the structural dip of the reservoir in question, to assess whether or not hydrodynamic trapping is feasible, and to estimate trap volumes for hydrocarbons of given density. Mapped seismic horizons of reservoir tops could additionally be used to improve basin modelling. Use of such seismic horizons would have greatly improved the geometric framework of the 3D basin model documented in **Chapter 7**.

9 | References

"I've had a wonderful time, but this wasn't it" Groucho
Marx (1895-1977) [American comedian and film star]

9. References

A

Ahmadi, Z. M., Sawyers, M., Kenyon-Roberts, S., Stanworth, C. W., Kugler, K.A., Kristensen, J. and Fugelli, E. M. G. 2003. Palaeocene. *In:* Evans, D., Graham, C., Armour, A. and Bathurst, P. (eds) *The Millennium Atlas: petroleum geology of the Central and Northern North Sea.* The Geological Society London, p. 235-259

Alnes, J. R. and Lilburn, R. A. 1998. Mechanisms for generating overpressure in sedimentary basins: a reevaluation: discussion. *AAPG Bulletin,* v. 82, no. 12, p. 2266-2269.

Anderton, R. 1993. Sedimentation and basin evolution in the Palaeogene of the Northern North Sea and Faroes-Shetland basins. *In:* Parker, J. R. (ed) *Petroleum Geology of the Northwest Europe: Proceedings of the 4th Conference*, The Geological Society, London, p. 31.

Anderton, R. 2000. Tertiary events: the North Atlantic plume and Alpine pulses. *In:* Woodcock, N. and Strachan, R. (eds) *Geological History of Britain and Ireland,* Blackwell Science, Oxford, p. 374-391.

Archie, G. 1942. The electrical resistivity log as an aid in determining some reservoir characteristics. *Transactions of the AIME*, v. 146, p. 54-62.

Armstrong, L. A., Have, A. T. and Johnson, H. D. 1987. The geology of the Gannet Fields, Central North Sea, UK sector. *In*: Brooks, J. and Glennie, K. W. (eds) *Petroleum Geology of North West Europe: Proceedings of the 3rd Conference*. Graham & Trotman, London, p. 533-548.

B

Banner, J. A., Chatellier, J. Y., Feurer, J. R. and Neuhaus, D. 1992. Guillemot D: a successful appraisal through alternative interpretation. *In:* Hardman, R. F. P. (ed) *Exploration Britain: Geological Insights for the Next Decade,* Geological Society Special Publication, v. 67, p. 129-149.

Barker, C. 1972. Aquathermal pressuring - role of temperature in development of abnormal-pressure zones. *AAPG Bulletin*, v. 56, no. 10, p. 2068-2071.

Barker, C. 1990. Calculated volume and pressure changes during the thermal cracking of oil and gas in reservoirs. *AAPG Bulletin,* v. 74, no. 8, p. 1254-1261.

Barnard, P. C. and Bastow, M. A. 1991. Hydrocarbon generation, migration, alteration, entrapment and mixing in the Central and Northern North Sea. *In*: England, W. A. and Fleet, A. J. (eds) *Petroleum Migration*. Geological Society, London, Special Publication, No. 59, p. 167-190.

Bartholomew, I. D., Peters, J. M. and Powell, C. M. 1993. Regional structural evolution of the North Sea: oblique slip and the reactivation of basement lineaments. *In*: Parker, J. R. (ed) *Petroleum Geology of the Northwest Europe: Proceedings of the 4th Conference*, The Geological Society, London, p. 1109-1122.

Birch, P. and Haynes, J. 2003. The Pierce Field, Blocks 23/22a, 23/27, UK North Sea. *In*: Gluyas, J. G. and Hichens, H. M. (eds) *United Kingdom Oil and Gas Fields, Commemorative Millennium Volume,* The Geological Society, London, Memoir No. 20, p. 647-659.

Bjørlykke, K. 1993. Fluid flow in sedimentary basins. *Sedimentary Geology*, v. 86, p. 137-158.

Bjørlykke, K. 2006. Effects of compaction processes on stresses, faults, and fluid flow in sedimentary basins: examples from the Norwegian margin. *In:* Buiter, S. J. H. and Schreurs, G. (eds) *Analogue and Numerical Modelling of Crustal-Scale Processes.* Geological Society, London, Special Publications, v. 253, p. 359-379.

Boles, J. R. and Franks, S. G. 1979. Clay diagenesis in Wilcox sandstones of southwest Texas: implications of smectite diagenesis on sandstone cementation. *Journal of Sedimentary Petrology,* v. 49, no. 1, p. 55-70.

Bowers, G. 2002. Detecting high overpressures. *The Leading Edge*, v. 21, p. 174-177.

Bredhoeft, J. D., Djevanshir, R. D. and Belitz, K. R. 1988. Lateral fluid flow in a compacting sand-shale sequence: South Caspian Basin. *AAPG Bulletin*, v. 72, p. 416-424.

Brookes, N. 2012. Application for production licence in part of block 1/6, APA 2012. *Maersk Proprietary Confidential Report*, Figure 2.14.

Bujak, J. and Mudge, D. 1994. A high-resolution North Sea Eocene dinocyst zonation. *Journal of the Geological Society*, v. 151, p. 449-462.

Burhig, C. 1989. Geopressured Jurassic reservoirs in the Viking Graben: modelling and geological significance. *Marine and Petroleum Geology*, v. 6, p. 31-48

Byerlee, J. 1993. Model for episodic flow of high-pressure water in fault zones before earthquakes. *Geology*, v. 21, p. 303-306.

C

Cavanagh, A., Couples, G., Darby, D., and Haszeldine, R. S. 1996. Overpressure and seals in the North Sea; a model approach. *Annual Meeting Abstracts AAPG/SEPM*, v. 5, p. 24-25.

Cayley, G. T. 1987. Hydrocarbon migration in the central North Sea. *In*: Brooks, J. and Glennie, K. W. (eds) *Petroleum Geology of North West Europe: Proceedings of the 3rd Conference*. Graham & Trotman, London, p. 549-555.

Cornford, C., 1994, Mandal-Ekofisk (!) petroleum system in the Central Graben of the North Sea. *In:* L.B. Magoon and W.G. Dow (eds) *The Petroleum System- from Source to Trap: AAPG Memoir*, v. 60, p. 537-571.

D

Daniel, R. B. 2001. Pressure prediction for a Central Graben wildcat well, UK North Sea. *Marine and Petroleum Geology,* v. 18, p. 235-250.

Darby, D., Haszeldine, S., and Couples, G. D. 1996. Pressure cells and pressure seals in the UK Central Graben. *Marine and Petroleum Geology,* v. 13, no. 8, p. 865 878.

Darby, D., Haszeldine, R. S., and Couples, G. D. 1998. Central North Sea overpressures: insights into fluid flow from one- and two-dimensional basin modelling. *In:* Düppenbecker, S. J. and Iliffe, J. E. (eds) *Basin Modelling: Practice and Progress.* Geological Society, London, Special Publications, v. 141, p. 95-107.

Darby, D. and Funnell, R. H. 2001. Overpressure associated with a convergent plate margin: East Coast Basin, New Zealand. *Petroleum Geoscience*, v. 7, p. 291-299.

Davis, D. M., Suppe, J. and Dahlen, F. A. 1983. Mechanics of fold-and-thrust belts and accretionary wedges. *Journal Geophysical Research,* v. 88, p. 1153-1172.

Davis, C., Haughton, P., McCaffrey, W., Scott, E., Hogg, N. and Kitching, D. 2009. Character and distribution of hybrid sediment gravity flow deposits from the outer Forties Fan, Palaeocene - Central North Sea, UKCS. *Marine and Petroleum Geology*, v. 26, p. 1919-1939.

Davison, I., Alsop, I., Birch, P., Elders, C., Evans, N., Nicholson, H., Rorison, P., Wade, D., Woodward, J. and Yound, M. 2000. Geometry and late-stage structural evolution of Central Graben salt diapirs, North Sea. *Marine and Petroleum Geology,* v. 17, p. 499-522.

Davison, I. 2004. Bathymetric control on Palaeocene gravity flows around salt domes in the Central Graben, North Sea. Presented at the GCSSEPM Foundation 24th Annual Research Conference 'Salt-Sediment Interactions and Hydrocarbon Prospectivity: Concepts, Applications, and Case Studies for the 21st Century", December 5–8, 2004, Houston Texas, p. 1031-1044.

Deegan, C. E. and Scull, B. J. 1977. A standard lithostratigraphic nomenclature for the Central and Northern North Sea. Report of the Institute of Geological Sciences, No 77/25, *Bulletin of the Norwegian Petroleum Directorate*, no. 1, p. 31-39.

Deming, D. 1994. Factors necessary to define a pressure seal. *AAPG Bulletin,* v. 78, p. 1005-1009.

Den Hartog Jager, D., Giles, M. R. and Griffiths, G. R. 1993. Evolution of Palaeogene submarine fans of the North Sea in space and time. *In*: Parker, J. R. (ed)

Petroleum Geology of the Northwest Europe: Proceedings of the 4ᵗʰ Conference, The Geological Society, London, p. 59-71.

Dennis, H., Baillie, J., Holt, T. and Wessel-Berg, D. 1998. Hydrodynamic activity and tilted oil-water contacts in the North Sea. NPF Conference, Haugesund, September 1998.

Dennis, H., Baillie, J., Holt, T. and Wessel-Berg, D. 2000. Hydrodynamic activity and tilted oil-water contacts in the North Sea. *In*: Ofstad, K. Kittilsen, J. E. and Alexander-Marrack, P. (eds) *Improving the Exploration Process by Learning from the Past.* NPF Special Publications, v. 9, p. 171–185.

Dennis, H., Bergmo, P. and Holt, T. 2005. Tilted oil-water contacts: modelling the effects of aquifer heterogeneity. *In:* Dore, A. G. and Vining, B. A. (eds) *Petroleum Geology: North-West Europe and Global Perspectives: Proceedings of the 6ᵗʰ Petroleum Geology Conference*. Geological Society, London, p. 145–158.

D' Heur, M. 1992. Cod Fields - Norwegian Sector Central Graben, North Sea. *In:* Foster, N. H. and Beaumont, E. A. 1992. *Structural Traps VI: Treatise of Petroleum Geology Atlas of Oil and Gas Fields*. American Association of Petroleum Geologists. p. 153-173.

Department of Energy and Climate change. 2012. Well Data. [online] Available at: <https://www.og.decc.gov.uk/pls/wons/wdep0100.qryWell> [Accessed 01 September 2012]

Duranti, D., Hurst, A., Bell, C., Groves, S., and Hanson, R. 2002. Injected and remobilized Eocene sandstones from the Alba Field, UKCS: core and wireline log characteristics. *Petroleum Geoscience,* v. 8, p. 99-107.

Duranti, D. and Hurst, A. 2004. Fluidization and injection in the deep-water sandstones of the Eocene Alba Formation (UK North Sea). *Sedimentology,* v. 51, p. 503-529.

E

Ecclestone-Brown, P. 2002. Mudstone Porosity and Clay fraction in overpressured basins. *Durham PhD thesis.* Durham University.

Eriksen, S. H., Andersen, J. H. Grist, M., Stoker, S. and Brzozowska, J. 2003. Oil and gas resources. *In:* Evans, D., Graham, C., Armour, A. and Bathurst, P. (eds) *The Millennium Atlas: Petroleum Geology of the Central and Northern North Sea*. The Geological Society London, p. 345-358.

Erratt, D., Thomas, G.M. and Wall, G.R.T. 1999. The evolution of the Central North Sea Rift. *In:* Fleet, A.J. and Boldt, S.A.R. (eds) *Petroleum Geology of Northwest Europe: Proceedings of the 5th Conference,* The Geological Society, London, p. 63-82.

Evans, N., Rorison, P. and Sykes, G. 1999. Banff Field, UK Central Graben – evaluation of a steeply dipping, fractured chalk reservoir. *In*: Fleet, A. J. and Boldy, S. A. R. (eds) *Petroleum Geology of the Northwest Europe: Proceedings of the 5th Conference*, The Geological Society, London, p. 975-988.

Evans, D., Graham, C., Armour, A. and Bathurst, P. (eds) 2003. T*he Millennium Atlas: Petroleum Geology of the Central and Northern North Sea*. The Geological Society of London. 989 p.

F

Fisher, M. J. and Mudge, D. C. 1990. Triassic. *In:* Glennie, K. W. (ed) *Introduction to the Petroleum Geology of the North Sea* (third edition), Blackwell Scientific Publications, Oxford, p. 191-218.

Fisher, A. T. and Zwart, G. 1996. Relation between permeability and effective stress along a plate-boundary fault, Barbados accretionary complex. *Geology,* v. 24, p. 307-310.

Fraser, S. I., Robinson, A. M., Johnson, H. D., Underhill, J. R., Kadolsky, D. G. A., Connell, R., Johannessed, P., and Ravnâs, R. 2002. Upper Jurassic *In:* Evans, D., Graham, C., Armour, A. and Bathurst, P. (eds) *The Millennium Atlas:*

Petroleum Geology of the Central and Northern North Sea. The Geological Society London, p. 157-189.

Fyfe, A., Gregersen, U., Jordt, H., Rundberg, Y., Eidvin, T., Evans, D., Stewart, D., Hovland, M. and Andresen, P. 2003. Oligocene to Holocene. *In:* Evans, D., Graham, C., Armour, A. and Bathurst, P. (eds) *The Millennium Atlas: Petroleum Geology of the Central and Northern North Sea.* The Geological Society London, p. 631-662.

G

Gaarenstroom, L., Tromp, R. A. J., Jong, de. M. C. and Brandenburg. A. M. 1993. Overpressures in the Central North Sea: implications for trap integrity and drilling safety. *In*: Parker, J. R. (ed) *Petroleum Geology of the Northwest Europe: Proceedings of the 4th Conference.* Geological Society, London, p. 1305-1313.

Galloway, W. E., Garber, J. L., Liu, X., and Sloan, B. J. 1993. Sequence stratigraphic and depositional framework of the Cenozoic fill, Central and Northern North Sea Basin. *In:* Parker, J. R. (ed) *Petroleum Geology of the Northwest Europe: Proceedings of the 4th Conference.* Geological Society, London, p. 33-43.

Gatliff, R. W. Richards, P. C., Smith, K., Graham, C. C., McCormac, M., Smith, N. J. P., Long, D., Cameron, T. D. J., Evans, D., Stevenson, A. G., Bulat, J. and Ritchie, J. D. 1994. United Kingdom offshore regional report: the geology of the central North Sea. *London: HMSO for the British Geological Survey.*

Geological Survey of Denmark and Greenland (GEUS). 2012. Well Data (Deep wells) - Danish. [online] Available at: http://www.geus.dk/geuspage-uk.htm [Accessed 01 September 2012]

Giles, M. R., Indrelid, S. L., Kusznir, N. J., Loopik, A., Muijerink, J. A., Dijkstra, P., Hiedug, W., Toth, J., Willis, M., Rutten, K., Elsinga, B., Huysse, P., Riviere, P., Burgisser, H. and Rowley, E. 1999. Charge and overpressure modelling in the North Sea: multi-dimensional modelling and uncertainty analysis. *In:* Fleet, A. J. and Boldy, S. A. R. (eds) *Petroleum Geology of Northwest Europe: Proceedings of the 5th Conference.* Geological Society, London, p. 1313-1324.

Glennie, K. W. 1990. Outline of North Sea history and structural framework. *In:* Glennie, K. W. (ed) *Introduction to the petroleum geology of the North Sea, third edition.* Blackwell Scientific Publications, Oxford, p. 34-77.

Gluyas, J. G. and Hichens, H. M. 2003. *United Kingdom Oil and Gas Fields Commemorative Millennium Volume.* Geological Society Memoir No. 20, The Geological Society, London.

Goulty, N. R. 2008. Geomechanics of polygonal fault systems: a review. *Petroleum Geoscience*, v. 14, p. 389-397.

Goulty, N. R. 2012. Properties of polygonal fault systems – fluid flow, aligned arrays and simple shear. *74th EAGE Conference and Exhibition*, Extended Abstracts, Z041.

Gradstein, F. M., Kristiansen, I. L., Loemo, L. and Kaminiski, M. A. 1992. Cenozoic foraminiferal and dinoflagellate cyst biostratigraphy of the central North Sea. *Micropaleontology,* v. 38, p. 101-137.

Grosjean, Y., Bois, M., DePazzis, L. and Burrus, J. 1994. Evaluation and detection of overpressures in a deltaic basin: the Sisi Field case history, offshore Mahakam, Kutei Basin, Indonesia. *AAPG Bulletin*, v. 78, p.1143.

Gyllenhammar, C. F. 2003. A critical review of currently available pore pressure methods and their input parameters: glaciations and compaction of North Sea sediments. *Durham PhD thesis.* Durham University. Available at Durham E-Theses Online: http://etheses.dur.ac.uk/4090/.

H

Hansen, S. 1996. A compaction trend for Cretaceous and Tertiary shales on the Norwegian Shelf based on sonic transit times. *Petroleum Geoscience*, v. 2, p. 159-166.

Hansom, J. and Lee, M. K. 2005. Effects of hydrocarbon generation, basal heat flow and sediment compaction on overpressure development: a numerical study. *Petroleum Geoscience,* v. 11, p. 353-360.

Hempton, M., Marshall, J., Sadler, S., Hogg, N., Charles, R. and Harvey, C. 2005. Turbidite reservoirs of the Sele Formation, Central North Sea: geological challenges for improving production. *In*: Dore, A. G. and Vining, B. A. (eds) *Petroleum Geology: North-West Europe and Global Perspectives – Proceedings of the 6th Petroleum Geology Conference*. Geological Society, London, p. 449-459.

Hermanrud, C 1993. Basin modelling techniques - an overview. *In:* Doré, A. J. (ed) *Basin Modelling: Advances and Applications*. NPF Special Publication, v. 3, p. 1-34.

Hodgson, N. A., Farnsworth, J. and Fraser, A. J. 1992. Salt-related tectonics, sedimentation and hydrocarbon plays in the Central Graben, North Sea, UKCS. *In:* Hardman, R. F. P (ed). *Exploration Britain: Geological insights for the next decade* .Geological Society, London, Special Publication, No. 67, p. 31-63.

Holm, G.M. 1998. Distribution and origin of overpressure in the Central Graben of the North Sea. *In*: Law, B.E., Ulmishek, G.F. and Slavin, V.I. (eds) *Abnormal Pressure in Hydrocarbon Environments*, AAPG Memoir, v. 70, p. 123-144.

Hower, J., Eslinger, E. V., Hower, M. E. and Perry, E. A. 1976. Mechanism of burial metamorphism of argillaceous sediment: 1. Mineralogical and chemical evidence. *Geological Society of American Bulletin,* v. 87, no. 5, p. 725-737.

Hubbert, M.K. 1953. Entrapment of petroleum under hydrodynamic conditions. *AAPG Bulletin,* v. 37, p. 1954-2026.

Hunt, J. M. 1990. Generation and Migration of Petroleum from abnormally pressured fluid compartments, *AAPG Bulletin*, v. 74, p. 1-12.

Hurst, A., Cartwright, J., Huuse, M., Jonk, R., Schwab, A., Duranti, D. and Cronin, B. 2003. Significance of large-scale sand injectites as long-term fluid conduits: evidence from seismic data. *Geofluids,* v. 3, p. 263-274.

Hurst, A., Cartwright, J. A., Duranti, D., Huuse, M. and Nelson, M. 2005. Sand injectites: an emerging global play in deep-water clastic environments. *In:* Doré, A. G. and Vining, B. A. (eds) *Petroleum Geology: North-West Europe*

and Global Perspectives – Proceedings of the 6th Petroleum Geology Conference. Geological Society, London, p. 133-144.

Huuse, M., Duranti, D., Guargena, C. G., Prat, P., Holm, K., Steinsland, N., Cronin, B. T., Hurst, A., and Cartwright, J. 2003. Sandstone intrusions: detection and significance for exploration and production. *First Break*, v. 1, p. 15-24

Huuse, M., Cartwright, J. A., Gras, R. and Hurst, A. 2005. Kilometre-scale sandstone intrusions in the Eocene of the Outer Moray Firth (UK North Sea): migration paths, reservoirs and potential drilling hazards. *In:* Doré, A. G. and Vining, B. A. (eds) *Petroleum Geology: North-West Europe and Global Perspectives – Proceedings of the 6th Petroleum Geology Conference.* Geological Society, London, p. 1577-1594.

I

Ireland, T., Joseph, J., Colley, N., Reigner, P., and Richardson, S. 1992. The MDT tool: a wireline testing breakthrough. *Oilfield Review,* April, p. 58-65.

J

Jennette, D. C., Garfield, T. R., Mohrig, D. C. and Cayley, G. T. 2000. The interaction of shelf accommodation, sediment supply and sea level in controlling the facies, architecture and sequence stacking patterns of the Tay and Forties/Sele basin floor fans, Central North Sea. Presented at the GCSSEPM Foundation 20th Annual Research Conference: Deep-Water Reservoirs of the World, December 3−6, 2000.

Jones, E., Jones, R., Ebdon, C., Ewen, D., Milner, P., Plunkett, J., Hudson, G. and Slater, P. 2003. Eocene. *In:* Evans, D., Graham, C., Armour, A. and Bathurst, P. (eds) *The Millennium Atlas: Petroleum Geology of the Central and Northern North Sea.* The Geological Society London, p. 261-277.

Jordt, H., Faleide, J. I., Bjorlykke, K. and Ibrahil, M. T. 1995. Cenozoic sequence stratigraphy of the central and northern North Sea Basin: tectonic development, sediment distribution and provenance areas. *Marine and Petroleum Geology,* v. 12, no. 8, p. 845-879.

Jowett, E. C., Cathles III, L. M. and Davis, B. W. 1993. Predicting depths of gypsum dehydration in evaporitic sedimentary basins. *AAPG Bulletin,* v. 77, no. 3, p. 402-413.

Joy, A. M. 1996. Controls on Eocene sedimentation in the central North Sea Basin: results of a basinwide correlation study. *In*: Knox, R. W. O'B., Corfield, R. M. and Dunay, R. E. (eds) *Correlation of the Early Paleogene in Northwest Europe,* Geological Society, London, Special Publication, No. 101, p. 79-90.

K

Kessler, L. G., Zang, R. D., Englehorn, J. A. and Eger, J. D. 1980. Stratigraphy and sedimentology of a Paleocene submarine fan complex, Cod field, Norwegian North Sea. *In:* Sedimentation of the North Sea reservoir rocks: Norsk Petroleumsforening, Article VIII, p. 19.

Kilhams, B., Hartley, A., Huuse, M. and Davis, C. 2012. Characterizing the Paleocene turbidites of the North Sea: the Mey Sandstone Member, Lista Formation, UK Central Graben. *Petroleum Geoscience*, v. 18, p. 337-354.

King, C. 1989. Cenozoic of the North Sea. *In:* Jenkins, D. G. and Murray, J. W. (eds) *Stratigraphic Atlas of Fossil Foraminifera,* p. 418-489.

Kloosterman, H. J., Kelly, R. S., Stammeijer, J., Hartung, M., van Waarde, J. and Chajecki, C. 2003. Successful application of time-lapse seismic data in Shell Expro's Gannet Fields, Central North Sea, UKCS. *Petroleum Geoscience,* v. 9, p. 25-34.

Knox, R. W. O' B. and Holloway, S. 1992. Paleogene of the Central and Northern North Sea. *In*: Knox, R. W. O' B. and Cordey, W. G. (eds) *Lithostratigraphic Nomenclature of the UK North Sea*, v. 1, British Geological Survey.

Knox, R. W. O' B. and Morton, A. C. 1988. The record of early Tertiary N Atlantic volcanism in sediments of the North Sea Basin. *In:* Morton, A. C. and Parson, L. M. (eds) *Early Tertiary Volcanism and the opening of the NE Atlantic,* Geological Society Special Publication, v. 39, p. 407-419.

Kooi, H. 1997. Insufficiency of compaction disequilibrium as the sole cause of high pore fluid pressures in pre-Cenozoic sediments. *Basin Research*, v. 9, p. 227-241.

Koša, E. 2007. Differential subsidence driving the formation of mounded stratigraphy in deep-water sediments; Palaeocene, central North Sea. *Marine and Petroleum Geology,* v. 24, p. 632-652.

Kubala, M., Bastow, M., Thompson, S., Scotchman, I. and Oygard, K. 2003. Geothermal regime, petroleum generation and migration. *In:* Evans, D., Graham, C., Armour, A. and Bathurst, P. (eds) *The Millennium Atlas: Petroleum Geology of the Central and Northern North Sea*. The Geological Society London, p. 289-315.

L

Lahann, R. W. 2002. Impact of smectite diagenesis on compaction modeling and compaction equilibrium. *In*: Huffman, A. R. and Bowers, G. L. (eds) *Pressure Regimes in Sedimentary Basins and their Prediction*, AAPG Memoir, v. 76, p. 61-72.

Lahann, R. W. and Swarbrick, R. E. 2011. Overpressure generation by load transfer following shale framework weakening due to smectite diagenesis. *Geofluids*, v. 11, p. 362-375.

Law, B.E. and Spencer, C. W. 1998. Abnormal pressures in hydrocarbon environments. *In:* Law, B.E., Ulmishek, G.F. and Slavin, V.I. (eds) *Abnormal Pressure in Hydrocarbon Environments*, AAPG Memoir, v. 70, p. 1-11.

Leonard, R. C. 1993. Distribution of sub-surface pressure in the Norwegian Central Graben and applications for exploration. *In*: Parker, J. R. (ed) *Petroleum Geology of the Northwest Europe: Proceedings of the 4th Conference*. Geological Society, London, p. 1295–1303.

Lindberg, P., Riise, R., and Fertl, W.H. 1980. Occurrence and distribution of overpressures in the Northern North Sea area. 55th Annual Fall Technical Conference for the Society of Petroleum Engineers of AIME, 21-24 September 1980, Dallas, Texas.

Liu, X. and Galloway, W. E. 1997. Quantitative Determination of Tertiary sediment supply to the North Sea Basin. *AAPG Bulletin,* v. 81, p. 1482-1509.

Longeran, L. and Cartwright, J. A. 1999. Polygonal Faults and their influence on deep water sandstone reservoir geometries, Alba Field, United Kingdom Central North Sea. *AAPG Bulletin*, v. 83, no. 3, p. 410-432.

Luo, X. and Vasseur, G. 1992. Contributions of compaction and aquathermal pressuring to geopressure and the influence of environmental conditions. *AAPG Bulletin*, v. 76, no. 10, p. 1550-1559.

M

Macleod, E. J. and Casey, S. J. 1994. The Forties Field. *In*: Warren, E. A. and Smalley, P. C (eds.) *North Sea Formation Waters Atlas*. Geological Society, London, Memoir No. 15, p. 34-35.

Mallon, A. J. 2000. A new compaction curve for chalk. *GeoPOP Monthly Reports*. Phase 2, v.3, chapter 2, unpublished report.

Mallon, A. J. and Swarbrick, R. E. 2002. A compaction trend for non-reservoir North Sea Chalk. *Marine and Petroleum Geology*, v. 19, p. 527-539.

Mallon, A. J. and Swarbrick, R. E. 2008. How should permeability be measured in fine grained lithologies? Evidence from the chalk. *Geofluids,* v. 8, p. 35-45.

Mallon, A. J., Swarbrick, R. E. and Katsube, T. J. 2005. Permeability of fine-grained rocks: new evidence from chalks. *Geology*, v. 33, no. 1, p. 21-24.

Magara, K. 1978. The significance of the expulsion of water in oil-phase primary migration. *Bulletin of Canadian Petroleum Geology*, v. 26, p. 123-131.

Marcussen, Ø, Maast, T. E., Mondol, N. H., Jahren, J. and Bjørlykke, K. 2010. Changes in physical properties of a reservoir sandstone as a function of burial depth – The Etive Formation, northern North Sea. *Marine and Petroleum Geology*, v. 27, p. 1725-1735.

Marine, I. W. and Fritz, S. J. 1981. Osmotic model to explain anomalous hydraulic heads. *Water Resources Research,* v. 17, p. 73-82.

Mason, P. C., Burwood, R. and Myke, B. 1995. The reservoir geochemistry and petroleum charging histories of Palaeogene reservoired fields in the Outer Witch Ground Graben. *In:* Cubitt, J. M. and England, W. A. (eds) *The*

Geochemisty of Reservoirs. Geological Society, London, Special Publication, No. 86, p. 281-301.

Mattingly, G. A. and Bretthauer, H. H. 1992. A Middle Eocene Deep Water Channel System in the UK North Sea. *In:* Halbouty, M. T. (ed) *Giant oil and gas fields of the decade 1978-1988.* American Association of Petroleum Geologists, Special Publication, v. 54, p. 297-305.

McCormick, D. and Leisham, M. 2004. The Bittern Field: topographic control of an Eocene aged "channel-fill" turbidite reservoir in the UK Central North Sea. *Search and Discovery*, Article #20016.

Meissner, F. F. 1978. Petroleum geology of the Bakken Formation, Williston Basin, North Dakota and Montana. *In: The economic geology of the Williston basin; Montana, North Dakota, South Dakota, Saskatchewan, Manitoba*. 24th Annual Conference, Williston Basin Symposium, Montana Geological Society, p. 207-227.

Molyneux, S., Cartwright, J. and Lonergan, L. 2002. Conical sandstone injection structures imaged by 3D seismic in the central North Sea, UK. *First Break,* v. 20, no. 6, p. 383-393.

Morton, A., Hallsworth, C. and Chalton, B. 2004. Garnet compositions in Scottish and Norwegian basement terrains: a framework for interpretation of North Sea sandstone provenance. *Marine and Petroleum Geology,* v. 21, p. 393-410.

Moss, B., Barson, D., Rakhit, K., Dennis, H. and Swarbrick, R. 2003. Formation pore pressures and formation waters. *In*: Evans, D., Graham, C., Armour, A. and Bathurst, P. (eds) *The Millennium Atlas: Petroleum Geology of the Central and Northern North Sea*. Geological Society, London, p. 317-329.

Mouchet, J. P. and Mitchell, A. 1989. *Abnormal Pressures while Drilling*. Manuels Techniques Elf Aquitaine, v. 2, 264 p.

Mudge, D. C. and Bujak, J. P. 1994. Eocene stratigraphy of the North Sea basin. *Marine and Petroleum Geology,* v. 11, no. 2, p. 166-181.

Mudge, D. C. and Bujak, J. P. 1996*a*. Palaeocene biostratigraphy and sequence stratigraphy of the UK Central North Sea. *Marine and Petroleum Geology,* v. 13, p. 295-312.

Mudge, D. C. and Bujak, J. P. 1996*b*. An integrated stratigraphy for the Paleocene and Eocene of the North Sea. *In*: Knox, R. W. O'B., Corfield, R. M. and Dunay, R. E. (eds) *Correlation of the Early Paleogene in Northwest Europe, Geological Society Special Publication,* v. 101, p. 91-113.

Mudge, D. C and Copestake, P. 1992a. Revised Lower Palaeogene lithostratigraphy for the Outer Moray Firth, North Sea. *Marine and Petroleum Geology*, v. 9, p. 53-69.

Mudge, D. C. and Copestake, P. 1992b. Lower Palaeogene stratigraphy of the Northern North Sea. *Marine and Petroleum Geology*, v. 9, p. 287-301.

Murphy, S. D. and Wood, P. H. 2011. Palaeogene remobilized sandstones of the Central North Sea – implications for hydrocarbon migration. *First Break,* v. 29, no. 12, p. 45-55.

N

Nadin, P. A. and Kusznir, N. J. 1995. Palaeocene uplift and Eocene subsidence in the northern North Sea Basin from 2D forward and reverse stratigraphic modelling. *Journal of the Geological Society,* v. 152, p. 833-848.

Neuzil, C. E. 1995. Abnormal pressures as hydrodynamic phenomena. *American Journal of Science,* v. 295, p. 742-786.

Newton, S. K. and Flanagan, K. P. 1993. The Alba Field: evolution of the depositional model. *In*: Parker, J. R. (ed) *Petroleum Geology of the Northwest Europe: Proceedings of the 4th Conference*. Geological Society, London, p. 161-171.

Norwegian Petroleum Directorate Factpages. 2012. Factpages - Wellbore Exploration. [online] Available at: http://factpages.npd.no/factpages/default.aspx [Accessed 01 September 2012].

O

O' Connor, S. A. and Swarbrick, R. E. 2008. Pressure regression, fluid drainage and hydrodynamically controlled fluid contact in the North Sea, Lower Cretaceous, Britannia Sandstone Formation. *Petroleum Geoscience,* v. 14, p. 115-126.

O' Connor, S., Swarbrick, R. and Jones, D. 2008. Where has all the pressure gone? Evidence from pressure reversals and hydrodynamic flow. *First Break*, v. 26, p. 55-61.

O' Connor, S. J. and Walker, D. 1993. Palaeocene reservoirs of the Everest trend. *In*: Parker, J. R. (ed) *Petroleum Geology of the Northwest Europe: Proceedings of the 4th Conference*, The Geological Society, London, p. 145-160.

Osborne, M. J. and Swarbrick, R. E. 1997. Mechanisms for generating overpressure in sedimentary basins: a reevaluation. *AAPG Bulletin,* v. 81, no. 6, p. 1023-1041.

Osborne, M. J. and Swarbrick, R. E. 1999. Diagenesis in North Sea HPHT clastic reservoirs - consequences for porosity and overpressure prediction. *Marine and Petroleum Geology,* v. 16, p. 337-353.

P

Peltonen, C., Marcussen, O., Bjorlykke, K. and Jahren, J. 2009. Clay mineral diagenesis and quartz cementation in mudstones: the effects of smectite to illite reaction on rock properties. *Marine and Petroleum Geology*, v. 26, p. 887-898.

Powell, A. J. 1992. Dinoflagellate cysts from the Tertiary system. *In:* Powell, A. J. (ed) *A stratigraphic index of Dinoflagellate series,* British Micropalaeontological Society Publication Series, London, p. 155-251.

R

Raiga-Clemenceau, J., Martin, J. P. and Nicoletis, S. 1988. The concept of acoustic formation factor for more accurate porosity determination from sonic transit time data. *The Log Analyst*, v. 29, p. 54-59.

Ramdhan, A. M. 2010. Overpressure and compaction in the lower Kutai basin, Indonesia. *Durham PhD thesis.* Durham University. Available at Durham E-Theses Online: http://etheses.dur.ac.uk/402/.

Ramm, M. 1992. Porosity-depth trends in reservoir sandstones: theoretical models related to Jurassic sandstones offshore Norway. *Marine and Petroleum Geology*, v. 9, p. 553-567.

Reynolds, T. 1994. Quantitative analysis of submarine fans in the Tertiary of the North Sea Basin. *Marine and Petroleum Geology,* v. 11, no. 2, p. 202-207.

Robertson, J., Goulty, N. R. and Swarbrick, R. E. 2013. Overpressure distributions in Palaeogene reservoirs of the UK Central North Sea and implications for lateral and vertical fluid flow. *Petroleum Geoscience*, v. 19, p. 223-236.

S

Schmidt, G. W. 1973. Interstitial water compositon and geochemisty of deep Gulf Coast shales and sandstones. *AAPG* Bulletin, v. 57, p. 321-337.

Schneider, F. and Hay, S. 2001. Compaction model for quartzose sandstones application to the Garn Formation, Haltenbanken, Mid-Norwegian Continental Shelf. *Marine and Petroleum Geology*, v. 18, p. 833-848.

Schneider, F., Potdevin, J. L., Wolf, S. and Faille, I. 1996. Mechanical and chemical compaction model for sedimentary basin simulators. *Tectonophysics*, v. 263, p. 307-317.

Schröder, T. 1992. A Palynological Zonation for the Paleocene of the North Sea Basin. *Journal of Micropalaeontology*, v. 11, p. 113-126.

Scott, E. D., Gelin, F., Jolley, S. J., Leenaarts, E., Sadler, S. P. and Elsinger, R. J. 2010. Sedimentological control of fluid flow in deep marine turbidite reservoirs: Pierce Field, UK Central North Sea. *In:* Jolley, S. J., Fischer, Q. J. Ainsworth, R. B., Vrolijk, P. J. and Delisle, S. (eds) *Reservoir Compartmentalization*, Geological Society, London, Special Publications, v. 347, p. 113-132.

Surlyk, F., Dons, T., Clausen, C. K. and Higham, J. 2003. Upper Cretaceous. *In*: Evans, D., Graham, C., Armour, A. and Bathurst, P. (eds) *The Millennium Atlas: Petroleum Geology of the Central and Northern North Sea.* The Geological Society London, p. 235-259.

Swarbrick, R.E. and Osborne, M.J. 1998. Mechanisms that generate abnormal pressures: an overview. *In:* Law, B.E., Ulmishek, G.F. and Slavin, V.I. (eds) *Abnormal Pressure in Hydrocarbon Environments*, AAPG Memoir, v. 70, p. 13-34.

Swarbrick, R. E., Lahann, R. E., O'Connor, S. A. and Mallon, A. J. 2010. Role of Chalk in development of deep overpressures in the Central North Sea. *In*: Vining, B. A. and Pickering, S. C. (eds) *Petroleum Geology from Mature Basins to New Frontiers: Proceedings of the 7th Conference*, v. 1, p. 493-507.

Swarbrick, R. E., Osborne, M. J., Grunberger, D., Yardley, G. S., Macleod, G., Aplin, A. C., Larter, S. R., Knight, I. and Auld, H. A. 2000. Intergrated study of the Judy Field (Block 30/7a) - an overpressured Central North Sea oil/gas field. *Marine and Petroleum Geology,* v. 17, p. 993-1010.

Swarbrick, R. E., Osborne, M. J. and Yardley, G. S. 2002. Comparison of overpressure magnitude resulting from the main generating mechanisms. *In*: Huffman, A. R. and Bowers, G. L. (eds) *Pressure Regimes in Sedimentary Basins and their Prediction*, AAPG Memoir, v. 76, p. 1-12.

Swarbrick, R. E., Lee, K., Lahann, R., Thomas, S. and Hardy, N. 2004. North Sea Central Graben Pressure Study, 1, GeoPressure Technology and IHS Energy.

Swarbrick, R.E., Seldon, B., and Mallon, A. J. 2005. Modelling the Central North Sea pressure history. *In:* Dore, A. J. and Vinning, B. A. (eds) *Petroleum Geology: North-West Europe and Global Perspectives – Proceedings of the 6th Petroleum Geology Conference,* p. 1237-1245.

Szarawarska, E., Huuse, M., Hurst, A., De Boer, W., Lu, L., Molyneux, S. and Rawlinson, P. 2010. Three-dimensional seismic characterisation of large-scale sandstone intrusions in the lower Palaeogene of the North Sea: completely injected vs. in situ remobilised sand bodies. *Basin Research*, v. 22, p. 517-532.

T

Terzaghi, K. 1943. *Theoretical Soil Mechanics*. Wiley, New York. 510 p.

Tingay, M. R. P., Hillis, R. R., Swarbrick, R. E., Morley, C. K. and Razak Damit, A. 2007. 'Vertically transferred' overpressures in Brunei: Evidence for a new mechanism for the formation of high-magnitude overpressure. *Geology*, v. 35, no. 11, p. 1023-1026.

Tingay, M. R. P., Morley, C. K., Laird, A., Limpornpipat, O., Krisadasima, K., Pabchanda, S., Macintyre, H. R. 2013. Evidence for overpressure generation by kerogen-to-gas maturation in the Northern Malay Basin. *AAPG Bulletin.* First published online 18 Feb 2013, http://dx.doi.org/10.1306/09041212032

Tissot, B. P., Pelet, R., and Ungerer, P. H. 1987. Thermal history of sedimentary basins, maturation indices and kinetics of oil and gas generation. *AAPG Bulletin,* v. 71, no. 12, p. 1445-1466.

U

Underhill, J. R. and Partington, M. A. 1993. Jurassic thermal doming and deflation in the North Sea: implications of the sequence stratigraphic evidence. *In*: Parker, J. R. (ed) *Petroleum Geology of the Northwest Europe: Proceedings of the 4th Conference*, The Geological Society, London, p. 337-345.

Ungerer, P., Behar, E. and Discamps, D. 1983. Tentative calculation of the overall volume expansion of organic matter during hydrocarbon genesis from geochemistry data: implications for primary migration. *In:* Bjorøy, M., Albrecht, P., Cornford, C., de Groot, K., Eglinton, G., Galimov, E., et al. (eds) *Advances in Organic Geochemistry.* John Wiley, p. 129-135.

V

Van Ruth, P., Hillis, R., Tingate, P. and Swarbrick, R. 2003. The origin of overpressure in 'old' sedimentary basins: an example from the Cooper Basin, Australia. *Geofluids,* v. 3, p. 125-131.

Vella, M., Veneruso, T., Lefoll, P., McEvoy, P. and Reiss, A. 1992. The nuts and bolts of well testing. *Oilfield Review,* April, p. 14-27.

W

Warren, E. A. and Smalley, P. C. 1993. The chemical composition of North Sea formation waters: a review of their heterogeneity and potential applications. *In*: Parker, J. R. (ed) *Petroleum Geology of Northwest Europe: Proceedings of the 4th Conference*. Geological Society, London, p. 1347-1352.

Warren, E. A. and Smalley, P. C. (eds). 1994. North Sea Formation Waters Atlas. *Geological Society Memoir*, No. 15.

Whyatt, M., Bowen, J. M. and Rhodes, D. N. 1992. The Nelson Field: a successful application of a development geoseismic model in North Sea exploration. *In:* Hardman, R. F. P. (ed) *Exploration Britain: Geological Insights for the Next Decade,* Geological Society, London, Special Publication, No. 67, p. 283-305.

Wills, J. M. 1991. The Forties Field, Block 21/10, 22/6a, UK North Sea. *In:* Abbotts, I. L. (ed) *United Kingdom Oil and Gas Fields, 25 Years Commemorative Volume,* Geological Society, London, Memoir No. 14, p. 301-308.

Wyllie, M. R. J., Gregory, A. R. and Gardner, G. H. F. 1958. An experimental investigation of factors affecting elastic wave velocities in porous media. *Geophysics*, v. 29, no. 1, p. 459-493.

Y

Yang, Y. and Aplin, A. C. 2000. Permeability-void ratio relationships of muds and mudstones. *GeoPOP Monthly Reports.* Phase 2, v.4, chapter 5, unpublished report.

Yang, Y. and Aplin, A. C. 2004. Definition and practical application of mudstone porosity-effective stress relationships. *Petroleum Geoscience*, v. 10, no. 2, p. 153-162.

Yang, Y., Aplin, A. C. and Larter, S. R. 2004. Quantitative assessment of mudstone lithology using geophysical wireline logs and artificial neural networks. *Petroleum Geoscience*, v. 10, no. 2, p. 141-151.

Yardley, G. S. and Swarbrick, R. E. 2000. Lateral transfer: a source of additional overpressure? *Marine and Petroleum Geology*, v. 17, p. 523-537.

Appendix

Hydrocarbon Accumulations | **A**

Appendix A - Hydrocarbon accumulations organised by Palaeogene reservoir interval

A brief description of play fairway, trap type and play risk is provided for each of the Palaeogene sandstone members present within the Central North Sea study region. This is accompanied by several tables, in which all of the presently known hydrocarbon occurrences for each of the Palaeogene reservoir intervals are listed, along with details such as 'hydrocarbon type', 'reservoir interval/s', 'discovery date' and 'production date' (if necessary). Additionally, 'hydrocarbon trap type' and 'oil gravity (API)' are provided where known. **Figure A.3** (**A** to **F**) shows the locations of these hydrocarbon accumulations, with the additional details being provided in the accompanying tables.

Maureen Sandstone Member

Considering its vast extent across the basin, there are relatively few hydrocarbon accumulations within the Maureen Sandstone Member (**Figure A.3.A**). As the deepest of the Palaeogene sequence fans, the sandstone member is for most of its area, overlain by younger Mey/ Heimdal and Forties sands, which appear to pose a potential topseal risk for accumulating hydrocarbons. The vast majority of Maureen hydrocarbon occurrences are generally restricted along the eastern margin of the fan, where the distally thinning sandstone reaches its basinal limit (i.e. shale-out). Hydrocarbons in this area are located in stratigraphic pinch-out traps, as observed in the Arran South, Fleming, Everest and Sleipner Øst fields. In fields such as Maureen, Mabel and Fleming, where there is an absence of any overlying Palaeocene or Eocene sands, the Maureen Sandstone forms the sole reservoir unit, indicating sufficient topseal presence in these areas.

The relatively few hydrocarbon accumulations within central areas of the Maureen sandstone distribution are salt-piercement traps (i.e. at Banff, Machar and Merganser). In these fields, the Maureen sand does not form the primary reservoir interval since hydrocarbon columns are sufficiently long that oil and gas are present across multiple reservoirs units.

236

Where oil is present within the Maureen Sandstone reservoir, gravities typically range from 36° to 56° API and thus it is of sufficiently high quality. Risk of biodegradation to Maureen hydrocarbons is unlikely within the study area, as the sandstone member is situated everywhere at depths greater than 1700 m (6000 ft) which is taken within this report as an approximate critical depth above which biodegradation may occur (see **Chapter 2**).

Mey/ Heimdal Sandstone Member

Hydrocarbon accumulations within the Mey Sandstone Member are generally restricted to two areas, in the northeast and southeast of the fan distribution (**Figure C.3.B**), where the overlying Forties Sandstone Member is absent and, consequently, there is no risk to the Mey/Heimdal topseal.

The majority of Mey/Heimdal hydrocarbon accumulations are situated within UK quadrant 16 and the eastern part of UK quadrant 15. In this area, accumulations consist predominantly of light oil with gravities in the range of 32° to 44° API. Traps typically comprise anticlinal structures with simple four-way dip closure, such as seen at the Balmoral, Blenheim and Cyrus fields. A few stratigraphic traps have also been found in this area, such as seen at the MacCulloch and Brenda fields.

In the south-eastern area, within UK quadrant 30, there are smaller accumulations of oil, gas and condensate such as Stella, Julia, Joanne, Flyndre and Orion. The Balmoral Sandstone Unit is the reservoir interval for these fields, thinning distally south-eastwards into Lista Formation shales. The Andrew Sandstone Unit is not present in this area of the basin. Traps of this south-eastern area are once again anticlinal, associated with underlying salt and fault structures.

The relatively few hydrocarbon accumulations found in the middle of the Mey sandstone distribution, at Gannet D, Merganser and Machar; are salt-piercement traps. In these areas, hydrocarbon columns are sufficiently long that oil and gas are present across multiple reservoirs intervals. At Merganser and Machar, these intervals comprise the Forties, Mey and Maureen reservoirs. In the case of the Gannet D field, where the Forties Sandstone Member is not present, reservoirs intervals comprise the Tay and Mey sandstones.

237

Along the eastern margin of Mey fan distribution, stratigraphic trapping is common, as observed at the Everest and Sleipner Øst fields. Where the Balmoral Tuffite Unit is present in the northern areas of the study region, it may act as a topseal for hydrocarbon accumulations within the older Andrew Sandstone Unit. Such a scenario is observed in the Rubie oilfield of UK block 15/28. Risk of biodegradation to Mey hydrocarbons is unlikely within the study area, as the sandstone member is largely situated at depths greater than 1700 m, which is approximately the critical depth above which biodegradation may occur (**Chapter 2**). There is a potential risk of biodegradation where the Mey is buried at depths less than 1700 m and temperatures are likely to be less than 60°C, around the western margin of the basin in UK blocks 21/11, 21/16, 21/17 and 21/22. Up to the present, no hydrocarbon accumulations have been found in this area of the Mey.

<u>Forties Sandstone Member</u>

The majority of hydrocarbon accumulations within the Palaeogene system are found within the Forties Sandstone Member (**Figure C.3.C**). As the youngest of the extensive Palaeocene fan sands, a vast area of the Forties is covered by the thick sequence of overlying shales and consequently the reservoir does not suffer from the topseal problems which are characteristic of the underlying Maureen and Mey sandstone members. Where the overlying, albeit less extensive Eocene Cromarty and Tay sandstones are present, there is topseal risk for the underlying Forties Sandstone Member, as shown by the shared hydrocarbon accumulations across the Forties, Cromarty and Tay reservoirs at the Bittern, Gannet B and Gannet F fields. Such examples highlight the poor sealing capacity of the intra-formational Sele and Horda mudstones in this area of the basin. It is not known whether this poor sealing capacity results from properties of the mudstones themselves or via remobilised sandstone features which may facilitate fluid flow.

Several types of trapping are present within the Forties play fairway, from the major hydrocarbon accumulations of Forties, Nelson, Montrose and Arbroath, which are anticlinal traps formed above the underlying structural feature of the Forties-Montrose High, through to the stratigraphic traps formed along the eastern lateral margins of the Forties fan, such as seen at the Everest and Arran (South) fields. Salt piercement fields

are present around UK quadrants 22, 23 and 29, as seen at Banff, Monan, Machar, Merganser, Arran (North), Kyle, Fram, Starling and Pierce. It is not uncommon for hydrocarbon columns to be shared across multiple reservoir intervals in these salt-piercement traps such as is observed at Banff, Pierce, Merganser, Machar and Kyle. Several fields are associated with salt-induced anticlinal trapping, such as the Lomond, Mungo, Cod and Gannet fields (B, C, E and F).

The quality of oil within the Forties reservoir is variable, with oil gravities ranging from 20° to 54° API. Heavy (low API) oils are typically found along the Western Platform area, around the Gannet fields in UK quadrant 21, where the Forties Sandstone Member gradually shallows. Biodegradation of hydrocarbons may be considered a risk along the western parts of UK quad 15 and within UK blocks 21/22 and 21/23, where the Forties sand is buried at depths shallower than 1700 m and temperatures are expected to be less than 60°C, enabling bacterial growth. Across the remainder of the study area, biodegradation is not considered a risk, where the Forties sands are consistently buried at depths greater than 1700 m.

Cromarty Sandstone Member

Relatively few hydrocarbon accumulations have been found in the Cromarty Sandstone Member to date (**Figure C.3.D**). The majority of known hydrocarbon accumulations are located around the southern areas of UK quadrants 21 and 22 and the northern areas of UK quadrants 28 and 29, within discrete Cromarty channels which have been fed into the basin from along the Western Platform. These relatively thin Cromarty sands play host reservoir to fields such as Gannet B, Gannet D, Gannet F, Curlew A, Bittern and the newly discovered Catcher Field.

The predominant trap style for Cromarty hydrocarbons is above salt-induced anticlines and recorded oil gravities range from 30° to 43° API. Many of the known Cromarty accumulations share the same hydrocarbon column across multiple reservoirs, suggesting there is good connectivity between sandstones in this area of the basin. At the Catcher Field, Cromarty and Tay sands are juxtaposed against each other across a non-sealing basin margin fault. Whereas at the Bittern Field, Forties and Cromarty sands are juxtaposed against each other, as a result of differential compaction. Within

the Gannet F Field, a common oil gradient is present across the Forties, Cromarty and Tay sands, with suspected migration of oil into this anticlinal salt-induced structure along faults and fractures associated with active salt diapirism, or potentially along areas where sands are in direct contact with each other. Distribution of Cromarty sands still remains relatively unknown, particularly further southwards, where it is highly likely there may be more Cromarty channels entering the basin along the western margin. Consequently, the Cromarty remains an attractive target for further exploration.

Risk of biodegradation to Cromarty hydrocarbons may be an issue where the sands are shallowest within the western areas of UK quadrants 15 and 21, as well as around UK blocks 28/09 and UK 28/10. In these parts of the basin, Cromarty sands are at burial depths of only ~ 1200 m, and temperatures are estimated to be ~ 40°C.

Oil accumulations at the McEnroe discovery and Rubie Field in UK quadrant 15 indicate that oil quality may be variable, with heavy Cromarty oils of 13.9° API gravity recorded at McEnroe and relatively light Cromarty oils of 41° API gravity recorded at Rubie. Hydrocarbons trapped within the Cromarty reservoir of UK quad 28 are found to be of higher quality, with less biodegradation than was expected. Oil of approximately 30° API is recorded at the Catcher Field. This may suggest shorter hydrocarbon migration routes into the Cromarty sands in this area of the basin.

Tay Sandstone Member

The Tay Sandstone Member is the most successful of the Eocene sandstone plays in the Central North Sea region (**Figure C.3.E**). Where the Tay Sandstone Member is present, towards the west of the basin, it is the shallowest of the Palaeogene sands and is overlain by a thick sequence of Horda mudstones. Consequently, the reservoir does not suffer from any topseal problems and hydrocarbons are unlikely to migrate (escape) vertically into the overlying sediments.

The vast majority of hydrocarbon accumulations within the Tay comprise oil, with only the Gannet D Field containing gas/condensate. Several trap styles are present, with salt-induced anticlinal structures common within UK quadrant 21 at the Gannet and Guillemot fields. Stratigraphic trapping is also common within thinner Tay channels, such as seen at the Fyne, Dandy and Pilot fields (UK quadrant 21). The

majority of known accumulations are situated along the slope margin of the Western Platform where Tay channels are fed into the deeper basin.

Oil gravities range from 14° to 43° API across the Tay sandstone, with a notable decrease in oil quality towards the west, where the sand shallows. Biodegradation of hydrocarbons proves to be the greatest risk to Tay oil producibility. Heavy, low API, partly biodegraded oils are recorded at the Elke (UK 28/03), Narwhal (UK 28/02) and Pilot (UK 21/27) fields, where the top Tay is situated at depths of around 3000 ft (914 m). Risk of biodegradation is also expected further south in UK block 28/09, where the Tay depth is 1070-1370 m). Although the recent discoveries of Catcher, Varadero and Burgman shown some signs of biodegradation, they are of a slightly higher quality than might be expected, with API gravities in the range 24-30° API.

Grid Sandstone Member

The only known hydrocarbon accumulations that have been found in the Grid Sandstone Member (**Figure C.3.F**) are the Alba field in UK quadrant 16 and the Chestnut and Brimmond fields in UK quadrant 22. All accumulations contain oil only. Classification of the Eocene Grid sands is complex, as are the mechanisms for trapping hydrocarbons within them. Each of the known accumulations within the Central North Sea region incorporates some element of stratigraphic trapping. Topseal risk for the Grid Sandstone Member is relatively low as it is the youngest, and consequently shallowest, of all the Palaeogene sands in the study region, and is overlain by a thick sequence of Horda mudstones. Biodegradation and water washing remain the largest risk to hydrocarbon accumulations within the Grid play, with sands being buried at depths less than 1700 m across most of their distribution, as seen in UK quadrant 15 and the western half of UK quadrant 16.

Maureen hydrocarbon occurrences (see Figure A.3.A):

Field Name	Location	H/C Type	Reservoir(s)	Trap Type	Discovery Date	Production Date	Oil gravity (API)
Arran South (Phyllis)	UK 23/16	O/G	Maureen, Forties	Stratigraphic - pinch-out	Mar-85	-	-
Banff	UK 22/27, UK 29/02	O	Maureen, Mey, Forties	Salt piercement	Oct-91	Sep-96	38°
Everest	UK 22/09, UK 22/10	G/C	Maureen, Mey, Forties	Stratigraphic - pinch-out	Mar-82	May 1993	-
Fleming	UK 16/25, UK 22/05	G/C	Maureen	Stratigraphic - pinch-out	Sep-82	Oct-97	48°- 56°
Mabel	UK 16/29	O	Maureen	Anticlinal	Feb-75	-	-
Machar	UK 23/26	O	Ekofisk Chalk, Maureen, Forties	Salt piercement	Apr-76	Jun-94	40°
Maureen	UK 16/29	O	Maureen	Anticlinal - salt induced	Feb-73	Sep-93	36°
Merganser	UK 22/25, UK 22/30	G/C	Maureen, Mey, Forties	Salt piercement	Jun-95	Dec-06	-
Moira	UK 16/29	O	Maureen, Mey	Anticlinal - salt induced	May-88	Aug-90	42°
Sleipner Øst	NO 15/09	G/C	Maureen, Heimdal	Stratigraphic - pinch-out	Jul-81	Oct-93	-

Mey and Heimdal hydrocarbon occurrences (see Figure A.3.B):

Field Name	Location	H/C Type	Reservoir(s)	Trap Type	Discovery Date	Production Date	Oil gravity (API)
Andrew	UK 16/27, UK 16/28	O/G	Mey	Anticlinal - salt induced	Jun-74	Jun-96	40°
Arundal	UK 16/23	O	Mey	-	Sep-00	Jan-12	-

Balmoral	UK 16/21	O	Mey	Anticlinal	Aug-75	Nov-86	39.3°
Banff	UK 22/27, UK 29/02	O	Maureen, Mey, Forties	Salt piercement	Oct-91	Sep-96	38°
Beauly	UK 16/21	O	Mey	Anticlinal	Dec-98	Feb-01	36.8
Bladon	UK 16/21	O	Mey	Anticlinal	Nov-96	Sep-97	44.3°
Blair (Glamis)	UK 16/21	O	Mey	Anticlinal	Jun-83	Mar-90	36.5°
Blenheim	UK 15/25, UK 16/21	O	Mey	Anticlinal	Nov-90	Mar-95	39°
Brenda	UK 15/25, UK 16/21	O	Mey	Stratigraphic (?)	Jul-90	Jun-07	39°
Bughley	UK 16/22	O	Mey	-	Dec-05	Jul-10	-
Cyrus	UK 16/28	O	Mey	Anticlinal	Oct-79	Apr-90	36°
Donan (Dumbarton)	UK 15/20	O	Mey	Anticlinal	May-87	Mar-92	39°
Everest	UK 22/09, UK 22/10	G/C	Maureen, Mey, Forties	Stratigraphic - pinch-out	Mar-82	May-93	-
Farragon	UK 16/28, UK 16/23	O/G	Mey	Anticlinal	Apr-03	Nov-05	35°
Flyndre	UK 30/14	O	Mey	Anticlinal	Aug-89	May-11	40°
Gannet D	UK 22/21	O	Mey, Cromarty, Tay	Anticlinal - salt induced	Aug-87	Oct-92	43°
Joanne	UK 30/07, UK 30/12	O	Ekofisk/Tor Chalk, Mey	Anticlinal - salt induced	May-81	Oct-95	39°
Julia	UK 30/07	O/G	Mey	-	Aug-91	-	-
Lochranza	UK 15/20	O	Mey	Anticlinal	Sep-92	Jan-10	41°
MacCulloch	UK 15/24	O	Mey	Structural/ stratigraphic	Mar-90	Aug-97	32°- 37°
Maria	UK 15/18	O/G	Mey	-	Feb-08	-	-
Merganser	UK 22/25, UK 22/30	G/C	Maureen, Mey, Forties	Salt piercement	Jun-95	Dec-06	-
Moira	UK 16/29	O	Maureen, Mey	Anticlinal - salt induced	May-88	Aug-90	42°
Murray	UK 15/26	O	Mey	Anticlinal	Dec-73	-	29.3°
Nicol	UK 15/25	O	Mey	-	Nov-88	Jun-07	-
Orion	UK 30/18	O/G	Mey	Anticlinal - salt induced	Sep-71	Sep-99	44°

Parliament (Caledonia)	UK 16/26	O	Mey	-	Oct-93	Feb-03	-
Pierce	UK 23/22, UK 23/27	O	Mey, Forties	Salt piercement	Mar-76	Feb-99	38°
Rubie	UK 15/28	O	Mey, Cromarty	Anticlinal	Mar-85	May-99	41°
Siri	Den 5604/16, Den 5604/20, Den 5605/13	O	Heimdal	Structural/ stratigraphic	Dec-95	Mar-99	35°
Sleipner Øst	NO 15/09	G/C	Maureen, Heimdal	Stratigraphic - pinch-out	Jul-81	Oct-93	-
Stella	UK 30/06	G/C	Ekofisk Chalk (oil), Mey	Anticlinal	Apr-84	-	-
West Blair	UK 16/21	O	Mey	-	Sep-89	-	-
Yeoman	UK 15/18	O/G	Mey	-	Aug-05	-	-

Forties hydrocarbon occurrences (see Figure A.3.C):

Field Name	Location	H/C Type	Reservoir(s)	Trap Type	Discovery Date	Production Date	Oil gravity (API)
Arbroath	UK 22/17, UK 22/18	O	Forties	Anticlinal	Dec-69	Apr-90	38°
Arkwright	UK 22/23	O	Forties	Anticlinal	Apr-90	Nov-96	40°
Banff	UK 22/27, UK 29/02	O	Maureen, Mey, Forties	Salt piercement	Oct-91	Sep-96	38°
Arran North (Barbara)	UK 23/16	G/C	Forties	Salt piercement	May-02	Oct-12	-

Arran South (Phyllis)	UK 23/16	O/G	Maureen, Forties	Stratigraphic - pinch-out	Mar-85	-	-
Bittern	UK 29/1	O	Forties, Cromarty	Anticlinal	Jul-96	Apr-00	39°
Blane	UK 30/3, NO 1/02	O	Forties	-	Nov-89	Sep-07	-
Brechin	UK 22/23	O	Forties	-	Jun-87	Jun-05	-
Callanish	UK 15/29, UK 21/04	O	Forties	-	Dec-99	Jul-08	-
Cod	NO 7/11	G/C	Forties	Anticlinal - salt induced	May-69	Dec-77	54°
Everest	UK 22/09, UK 22/10	G/C	Maureen, Mey, Forties	Stratigraphic - pinch-out	Mar-82	May-93	-
Forties	UK 21/10, UK 22/06	O	Forties	Anticlinal	Nov-70	Sep-75	37°
Fram	UK 29/03	G	Forties	Salt piercement	Oct-99	-	-
Gannet B	UK 21/25	G/C	Forties, Cromarty, Tay	Anticlinal - salt induced (salt piercement)	Sep-79	Nov-92	-
Gannet C	UK 21/30	O	Forties	Anticlinal - salt induced (salt piercement)	Sep-82	Dec-92	38°
Gannet E	UK 21/30	O	Forties	Anticlinal - salt induced	Jun-82	Jan-98	20°
Gannet F	UK 21/30	O	Forties, Cromarty, Tay	Anticlinal - salt induced	Mar-69	Jun-97	35°
Kyle	UK 29/02	G/C	Forties	Salt piercement	Aug-93	Apr-01	38°
Lomond	UK 23/21	G/C	Forties	Anticlinal - salt induced	May-72	Jun-93	53°
Machar	UK 23/26	O	Ekofisk Chalk, Maureen, Forties	Salt piercement	Apr-76	Jun-94	40°
Merganser	UK 22/25, UK 22/30	G/C	Maureen, Mey, Forties	Salt piercement	Jun-95	Dec-06	-
Mirren	UK 22/25	O	Forties	-	Jan-93	Nov-02	-
Monan	UK 22/20	O	Forties	Salt piercement	Dec-90	Sep-98	41°
Montrose	UK 22/17, UK 22/18	O	Forties	Anticlinal	Nov-71	Jun-76	38.5°
Mungo	UK 22/20, UK 23/16	G/C	Forties	Anticlinal - salt induced	May-89	Jul-98	39°

Nelson	UK 22/06, UK 22/07, UK 22/11, UK 22/12	O	Forties	Anticlinal	Mar-88	Feb-94	40°
Oselvar	NO 1/03	G	Forties	-	Jun-91	Apr-12	-
Peach	UK 30/07, UK 30/08	G/C	Forties	Structural/ stratigraphic	Feb-85	-	-
Pierce	UK 23/22, UK 23/27	O	Mey, Forties	Salt piercement	Mar-76	Feb-99	38°
Ptarmigan	UK 15/29	O	Forties	Anticlinal	Sep-94	-	43°
Scoter	UK 22/30, UK 23/26	G	Forties	-	Nov-89	Mar-04	-
Shelley	UK 22/02, UK 22/03	O	Forties	-	Feb-84	Aug-09	31°
Starling	UK 29/03	G	Forties	-	Jan-79	Jan-08	-
UK 15/18 (Area 6)	UK 15/18	O	Forties	-	Jun-86	-	-
UK 15/21 (Area 45)	UK 15/21	O	Forties	-	Jan-92	-	-
UK 30/01 (Area 7)	UK 30/01	O	Forties	-	May-88	-	-
UK 30/02 (Area 2)	UK 30/02	G/C	Forties	-	May-91	-	-

Cromarty hydrocarbon occurrences (see Figure A.3.D):

Field Name	Location	H/C Type	Reservoir(s)	Trap Type	Discovery Date	Production Date	Oil gravity (API)
Bittern	UK 29/01	O	Forties, Cromarty	Anticlinal	Jul-96	Apr-00	39°
Catcher	UK 28/09	O	Cromarty, Tay	Anticlinal	Jun-10	-	30°
Curlew A	UK 29/07	O	Cromarty	Anticlinal - salt induced	Oct-77	Nov-97	30°
Gannet B	UK 21/25	G/C	Forties, Cromarty, Tay	Anticlinal - salt induced (salt piercement)	Sep-79	Nov-92	-

Gannet D	UK 22/21	O	Mey, Cromarty, Tay	Anticlinal - salt induced	Aug-87	Oct-92	43°
Gannet F	UK 21/30	O	Forties, Cromarty, Tay	Anticlinal - salt induced	Mar-69	Jun-97	35°
McEnroe	UK 15/26	O	Cromarty	Stratigraphic	Dec-73	-	13.9°
Rubie	UK 15/28	O	Mey, Cromarty	Anticlinal	Mar-85	May-99	41°
UK 29/04 (Area 1)	UK 29/04	O	Cromarty	-	May-84	-	-
UK 29/09 (Area 1)	UK 29/09	G/C	Cromarty	-	May-83	-	-

Tay hydrocarbon occurrence (see Figure A.3.E):

Field Name	Location	H/C Type	Reservoir(s)	Trap Type	Discovery Date	Production Date	Oil gravity (API)
Burgman	UK 28/09	O	Tay	Anticlinal	Mar-11	-	24°
Catcher	UK 28/09	O	Cromarty, Tay	Anticlinal	Jun-10	-	30°
Dandy	UK 21/28	O	Tay	Stratigraphic - pinch-out	Jan-87	-	23°
Elke	UK 28/03	O	Tay	-	Nov-00	-	16°
Fyne	UK 21/28	O	Tay	Stratigraphic	Jan-87	-	25°- 26°
Gannet A	UK 21/25, UK 22/21	O/G	Tay	Anticlinal - salt induced/ Stratigraphic - pinch-out	Jan-75	Oct-92	40.5°
Gannet B	UK 21/25	G/C	Forties, Cromarty, Tay	Anticlinal - salt induced (salt piercement)	Sep-79	Nov-92	-
Gannet D	UK 22/21	O	Mey, Cromarty, Tay	Anticlinal - salt induced	Aug-87	Oct-92	43°
Gannet F	UK 21/30	O	Forties, Cromarty, Tay	Anticlinal - salt induced	Mar-69	Jun-97	35°

Guillemot NW	UK 21/24	O	Tay	-	Aug-85	May-00	35°- 38°
Guillemot W	UK 21/24, UK 21/25, UK 21/29, UK 21/30	O	Tay	Anticlinal - salt induced/ Stratigraphic	Feb-83	Apr-00	35°- 38°
Kate	UK 22/23, UK 22/28	O	Tay	-	Sep-87	-	-
Madoes	UK 22/23, UK 22/28	O	Tay	-	Sep-87	Dec-02	-
Milburn	UK 22/22	O	Tay	-	Dec-96	-	-
Narwhal	UK 28/02	O	Tay	-	Dec-93	-	14°
Pict	UK 21/23	O	Tay	Anticlinal	Jan-82	Jun-05	-
Pilot	UK 21/27	O	Tay	Stratigraphic	Nov-89	-	14°- 18°
Riddon	UK 21/29	O	Tay	-	Apr-91	-	24°
Saxon	UK 21/23	O/G	Tay	-	Jan-05	Nov-07	-
Scavaig	UK 21/29	O	Tay	-	Apr-91	-	27°
UK 21/30 (Area 12)	UK 21/30	O	Tay	-	Sep-84	-	30°
UK 21/30 (Area 17)	UK 21/30	O	Tay	-	Sep-90	-	-
Varadero	UK 28/09	O	Tay	Anticlinal	Dec-10	-	26°

Grid hydrocarbon occurrences (see Figure A.3.F):

Field Name	Location	H/C Type	Reservoir(s)	Trap Type	Discovery Date	Production Date	Oil gravity (API)
Brimmond	UK 22/06	O	Grid(Caran)	Anticlinal/ stratigraphic	Jan-85	Oct-96	23.9°

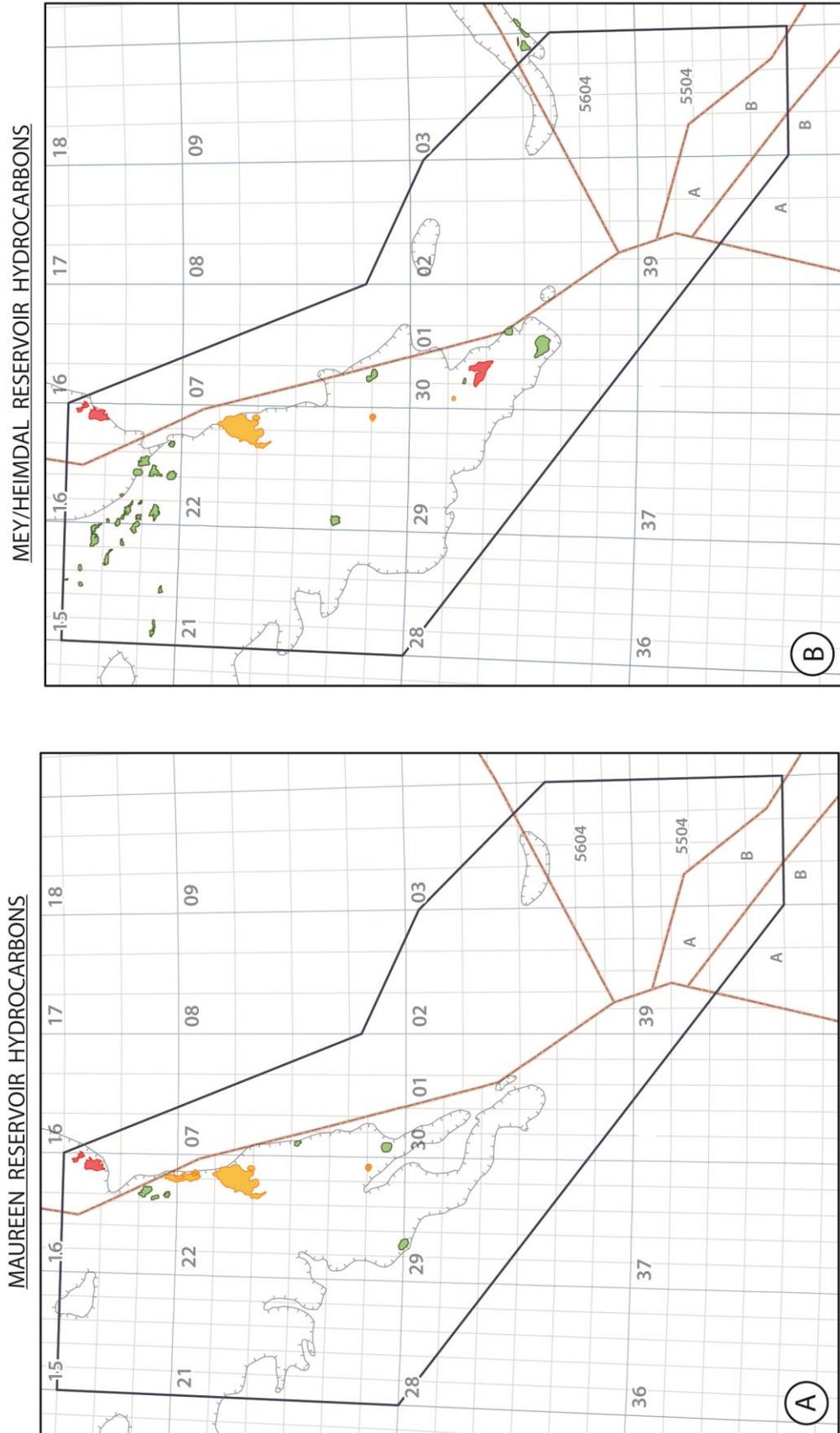| Alba | UK 16/26 | O | Grid (Brodie) | Stratigraphic | Dec-84 | Jan-94 | 19° |
| Chestnut | UK 22/02 | O | Grid (Brodie) | Anticlinal/ stratigraphic | Oct-86 | Sep-08 | 30° |

Figure A.1 - Hydrocarbon accumulations within the **A)** Maureen Sandstone Member and **B)** Mey/Heimdal Sandstone Member
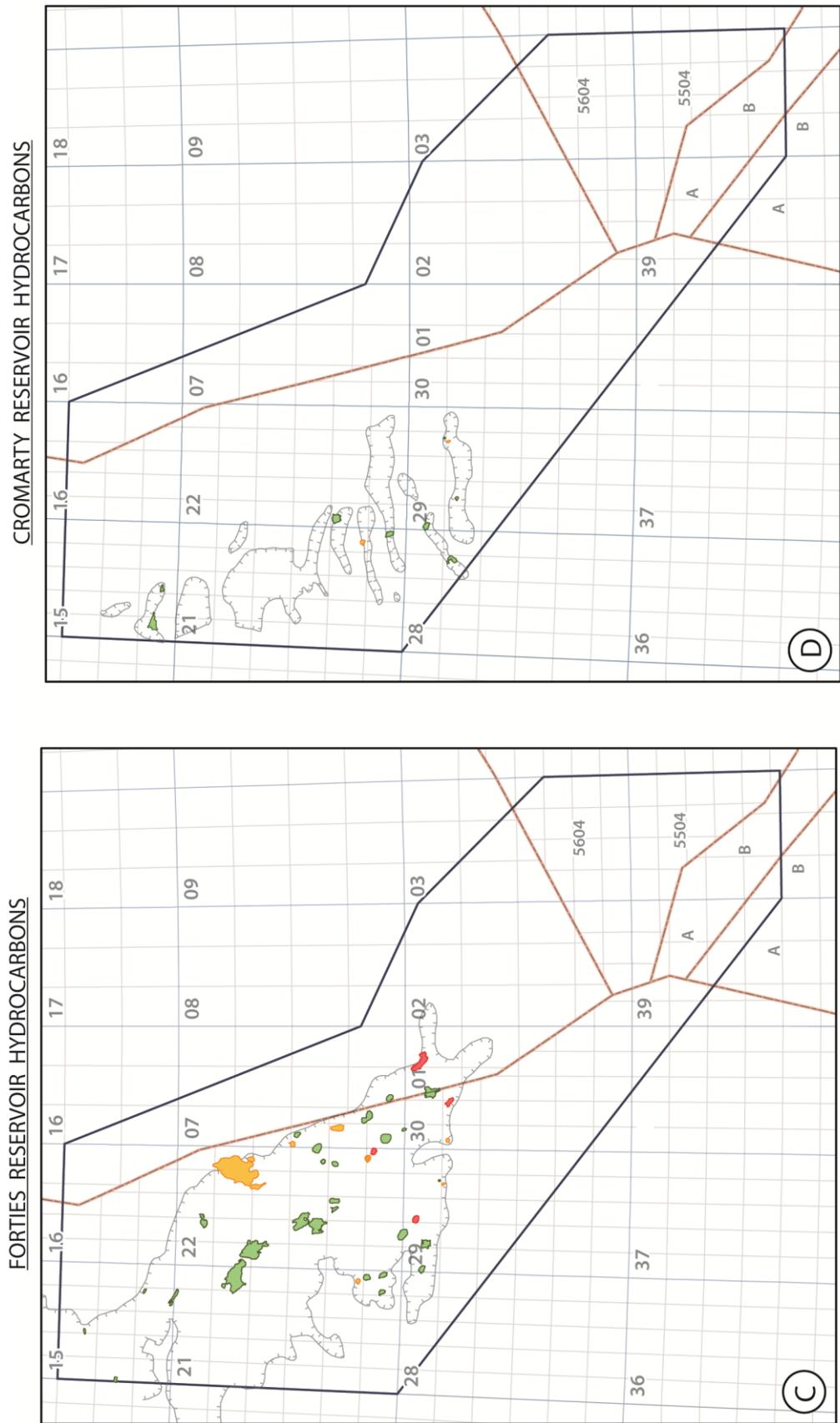
Figure A.3 - Hydrocarbon accumulations within the **C)** Forties Sandstone Member and **D)** Cromarty Sandstone Member
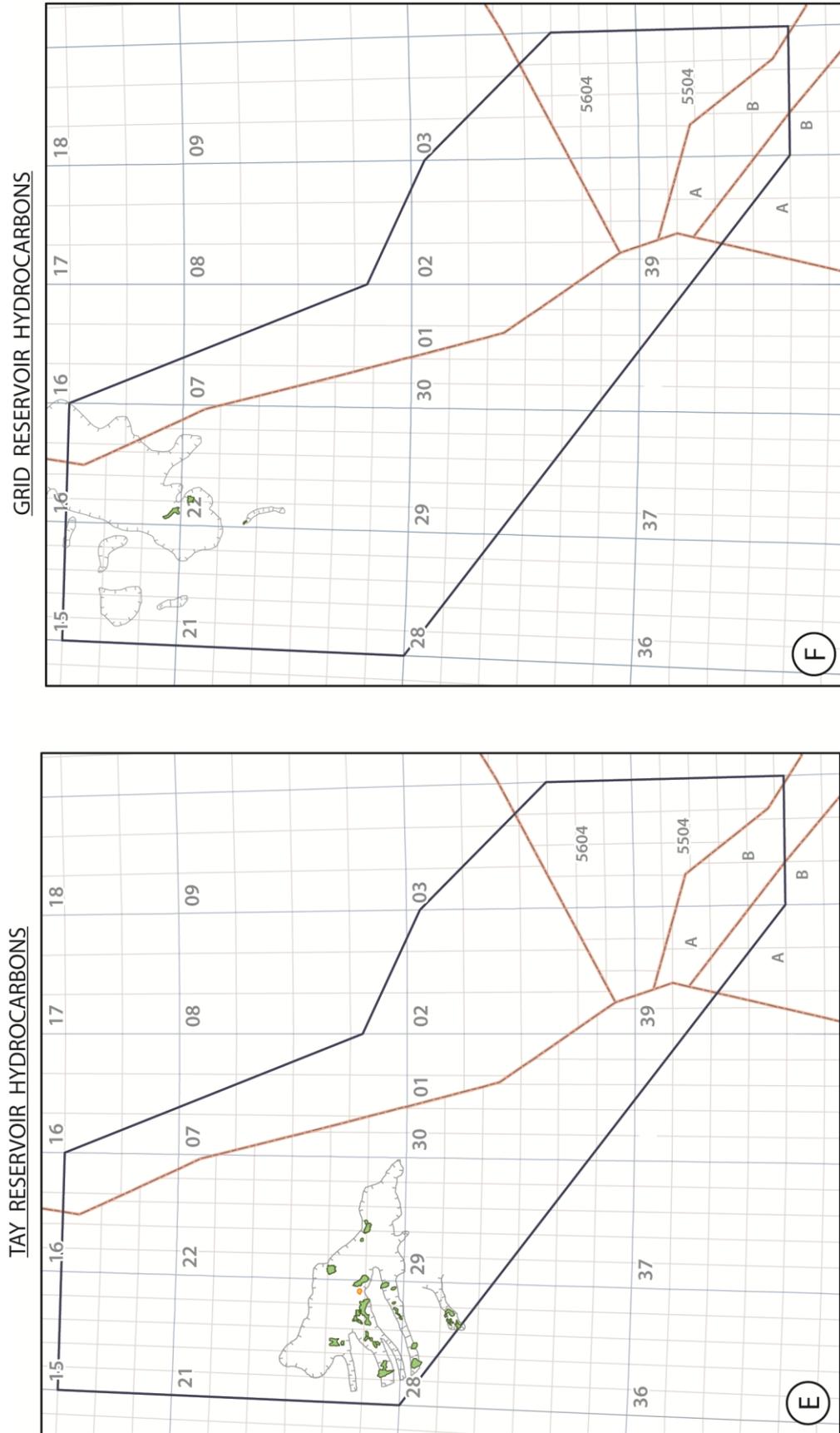
Figure A.3 - Hydrocarbon accumulations within the **E)** Tay Sandstone Member and **F)** Grid Sandstone Member